

# **Transcriptional regulation of smooth muscle cell differentiation in the murine ureter**

Von der Naturwissenschaftlichen Fakultät der  
Gottfried Wilhelm Leibniz Universität Hannover

zur Erlangung des Grades  
Doktorin der Naturwissenschaften (Dr. rer. nat.)

genehmigte Dissertation

von

Jennifer Kurz, M.Sc.

2021

**Referent:** Prof. Dr. rer. nat. Andreas Kispert

**Korreferentin:** Prof. Dr. rer. nat. Rita Gerardy-Schahn

**Tag der Promotion:** 05.10.2021



Hannover Medical School



Angefertigt am

Institut für Molekularbiologie

der Medizinischen Hochschule Hannover

unter der Betreuung von

Prof. Dr. rer. nat. Andreas Kispert

# **Meiner Familie**



## **Erklärung zur kumulativen Dissertation von Jennifer Kurz (geboren am 24.04.1989 in Schwäbisch Hall)**

Diese kumulative Dissertation basiert auf folgendem veröffentlichten Fachartikel und bisher unveröffentlichten Manuskripten:

1. **Jennifer Kurz**, Anna-Carina Weiss, Hauke Thiesler, Timo H. Lüdtkke, Herbert Hildebrandt, Joerg Heineke, Stephen A. Duncan, Mark-Oliver Trowe and Andreas Kispert. "GATA6 is a critical factor for *Myocd* expression in the visceral smooth muscle cell differentiation program of the murine ureter". Manuscript in preparation

2. Anna-Carina Weiss, Tobias Bohnenpoll, **Jennifer Kurz**, Patrick Blank, Rannar Airik, Timo H Lüdtkke, Marc-Jens Kleppa, Lena Deuper, Marina Kaiser, Tamrat M Mamo, Rui Costa, Thomas von Hahn, Mark-Oliver Trowe and Andreas Kispert. "Delayed onset of smooth muscle cell differentiation leads to hydroureter formation in mice with conditional loss of the zinc finger transcription factor gene *Gata2* in the ureteric mesenchyme". *Journal of Pathology* 248 (4). John Wiley and Sons Ltd: 452–63. doi:10.1002/path.5270.

3. Anna-Carina Weiss\*, **Jennifer Kurz\***, Hauke Thiesler, Jaskiran Kaur, Lena Deuper, Irina Wojahn, Fairouz Qasrawi, Herbert Hildebrandt, Mark-Oliver Trowe and Andreas Kispert. "Notch signaling is a novel regulator of visceral smooth muscle cell differentiation in the murine ureter". Submitted to Development

\*Contributed equally to this work

In **Artikel 1** habe ich alle Abbildungen (Abb.) (mit Ausnahme von Teilen von Abb.1A, Abb. 2A,B,D, Teilen von 2E, Teilen von Abb. 6D und Teilen von Abb. S8 und Abb. S9) experimentell und graphisch erstellt. Für die Abb. 6A,B;C und F habe ich das Material gesammelt und die RNA isoliert. Die. Das inhaltliche Konzept des Projekts wurde von Andreas Kispert und mir gemeinsam erarbeitet. Das Manuskript wurde von Andreas Kispert und mir gemeinsam geschrieben. Andreas Kispert hat das Projekt finanziert.

In **Artikel 2** habe ich die Abb. 5D experimentell und graphisch dargestellt. Das inhaltliche Konzept des Projekts wurde von Andreas Kispert und Anna-Carina Weiss

erarbeitet. Das Manuskript wurde von Andreas Kispert und Anna-Carina Weiss geschrieben. Andreas Kispert hat das Projekt finanziert.

In **Artikel 3** habe ich die Abb. 3A-C, Abb. 4C-F und Abb.6A habe experimentell und graphisch erstellt. Abb. 6B habe ich graphisch erstellt. Für Abb. 2I und teilweise für Abb. 5E, Abb. 6C,D das Material gesammelt und die RNA isoliert. Das inhaltliche Konzept des Projekts wurde von Andreas Kispert, Anna-Carina Weiss und mir gemeinsam erarbeitet. Das Manuskript wurde von Andreas Kispert, Anna-Carina Weiss und mir gemeinsam geschrieben. Andreas Kispert hat das Projekt finanziert.

## Abstract

The murine ureters are a pair of slender tubes that mediate by peristaltic contractions the efficient transport of urine from the renal pelvis to the bladder. Smooth muscle cells (SMCs) account for this activity. They arise together with their surrounding fibrocytes from a common pool of mesenchymal precursors. Proliferation, patterning and SMC differentiation of this ureteric mesenchyme (UM) depends on SHH and WNT signals from an adjacent epithelial primordium, the distal ureteric bud, and on BMP4 signaling within the UM. Retinoic acid (RA) from the ureteric epithelium (UE) and the UM inhibits ureteric SMC differentiation. How these signaling pathways interact with each other and with which transcription factors they cooperate to orchestrate SMC differentiation in the murine ureter is poorly understood.

The aim of this thesis was to characterize the role of two zinc-finger transcription factors, GATA2 and GATA6, and the Notch signaling pathway in the development of the UM in the mouse.

Expression of both *Gata2* and *Gata6* was found to be restricted to the undifferentiated UM. While *Gata2* expression depends on RA signaling, *Gata6* is controlled by BMP4 signaling. Mice with a conditional loss of *Gata6* in the UM showed dilatation of the ureter and renal pelvis at birth and at postnatal stages. SMC differentiation and peristaltic activity was severely delayed and reduced. Molecular profiling revealed reduced expression of the transcriptional driver of SMC differentiation, *Myocd*.

Mice with conditional loss of *Gata2* in the UM displayed severe hydroureter formation due to reduced ureteric SMC investment at birth. SMC differentiation was delayed but ureters regained peristaltic activity when relieved of urine pressure in explant cultures. Molecular analysis identified increased RA signaling as one factor contributing to the delay in SMC differentiation.

Notch signaling components were expressed in the UM and UE. Conditional deletion of the unique Notch signaling mediator *Rbpj* in the UM resulted in one-day delay of *Myocd* expression and SMC differentiation, but did not lead to morphological changes around birth. At postnatal stages, reduction of a group of late genes including *Tnnt2*, *Ckm*, *Pcp4* and *Pcp4l1* in the mutant led to hydroureter formation.

This thesis identified three novel regulators of SMC differentiation in the murine ureter. GATA2, GATA6 and Notch signaling act in different molecular subprograms, but they all affect the activation of the key regulator of SMC differentiation, *Myocd*.

**Keywords: Ureter, SMC differentiation, GATA6, GATA2, Notch signaling**

## Zusammenfassung

Die Ureteren sind paarig angelegte schlanke Röhren, die den Urin vom Nierenbecken in die Blase transportieren. Dies wird durch kontraktile Glattmuskelzellen ermöglicht, die peristaltische Wellen erzeugen. Glattmuskelzellen entstehen zusammen mit umgebenden Fibrozyten aus einem gemeinsamem Pool mesenchymaler Vorläufer. Die Proliferation, Musterung und Differenzierung dieses Uretermesenchyms (UM) hängt von SHH- und WNT-Signalen aus dem Epithel der benachbarten Ureterknospe und von BMP4-Signalen im UM ab. Retinsäure (RS) aus dem Uretherepithel (UE) und UM, hemmt die Glattmuskeldifferenzierung. Wie diese Signalwege miteinander interagieren und mit welchen Transkriptionsfaktoren sie kooperieren, um die Differenzierung von Glattmuskelzellen zu induzieren, ist noch wenig verstanden.

Das Ziel dieser Arbeit war die Rolle zweier Zinkfinger-Transkriptionsfaktoren (GATA6, und GATA2) und des Notch-Signalwegs in der Entwicklung des UM zu analysieren.

*Gata2* und *Gata6* sind beide im undifferenzierten UM exprimiert. Dabei hängt die Expression von *Gata2* vom RS-Signalweg ab, die von *Gata6* vom BMP4-Signalweg. Mäuse mit einem konditionellen Verlust von *Gata6* im UM wiesen pränatal und auch postnatal eine Hydroureternephrose auf. Die Glattmuskeldifferenzierung und die Kontraktion des Ureters war verzögert und reduziert. Molekulare Analysen zeigten eine reduzierte Expression des Regulators der Glattmuskeldifferenzierung, *Myocd*.

Mäuse mit einem konditionellen Verlust von *Gata2* im UM entwickelten ebenfalls kurz vor der Geburt aufgrund verzögerter und reduzierter Expression von Glattmuskelgenen einen Hydroureter. Die Ureteren kontrahierten in Explantat-Kulturen ohne Urinlast weitestgehend normal. Molekulare Analysen identifizierten erhöhte RS-Mengen als einen Grund für die verzögerte Glattmuskeldifferenzierung.

Notch-Signalwegkomponenten sind im UE und im UM exprimiert. Der konditionelle Verlust des Mediators des Notch-Signalwegs *Rbpj* im UM resultierte in einer Verzögerung der *Myocd* Expression und Glattmuskeldifferenzierung von einem Tag. Postnatal führt die reduzierte Expression von späten Glattmuskelgenen (u.a. *Tnnt2*, *Ckm*, *Pcp4*, *Pcp4l1*) zur Bildung dilatierter Ureteren.

In dieser Arbeit wurden drei neue Regulatoren der Glattmuskeldifferenzierung identifiziert. Obwohl GATA2, GATA6 und der Notch-Signalweg verschiedene molekulare Unterprogramme regulieren, spielen sie alle eine wichtige Rolle als Aktivatoren der Expression von *Myocd*, des Hauptregulators der Glattmuskeldifferenzierung.

**Schlagwörter: Ureter, Glattmuskeldifferenzierung, GATA6, GATA2, Notch-Signalweg**

# Table of contents

<b>Anfertigungsstätte und Betreuung</b>	<b>I</b>
<b>Widmung</b>	<b>II</b>
<b>Erklärung zur kumulativen Dissertation</b>	<b>III</b>
<b>Abstract</b>	<b>V</b>
<b>Zusammenfassung</b>	<b>VI</b>
<b>Table of contents</b>	<b>VII</b>
<b>Introduction</b>	<b>1</b>
<b>Visceral and vascular smooth muscle cells (SMCs)</b>	<b>1</b>
The structure and function of the murine ureter	3
<b>Embryonic development of the murine ureter</b>	<b>4</b>
<b>Molecular regulation of SMC differentiation in the murine ureter</b>	<b>5</b>
<b>GATA transcription factors as regulators of ureteric SMC differentiation</b>	<b>7</b>
<b>The Notch signaling pathway</b>	<b>8</b>
<b>Aim of the thesis</b>	<b>10</b>
<b>Part 1 - GATA6 in SMC differentiation</b>	<b>12</b>
<b>Part 2 - GATA2 in SMC differentiation</b>	<b>64</b>
<b>Part 3 - Notch signaling in SMC differentiation</b>	<b>109</b>
<b>Concluding remarks</b>	<b>169</b>
<b>References</b>	<b>173</b>
<b>Appendix</b>	<b>181</b>
<b>Acknowledgement</b>	<b>VIII</b>
<b>Curriculum vitae</b>	<b>IX</b>
<b>List of publications</b>	<b>X</b>

## Introduction

### Visceral and vascular smooth muscle cells (SMCs)

SMCs are found in the walls of many hollow organs where they provide structural support and contractile activity. SMCs are spindle-shaped, uni-nucleated and not striated. In contrast to skeletal muscle cells, they do not harbor sarcomeres, but a network of thin, thick and intermediate filaments. Multiple thin filaments surround every thick filament. These filaments consist of actin and myosin proteins. The thin filaments are connected by dense bodies, which are interconnected by intermediate filaments. The intermediate filaments connect the dense bodies also to integrins in the cell membrane and are composed of vimentin and desmin. Upon stimulation, the thin and thick filaments contract, pulling the dense bodies closer to each other. Consequently, also the plasma membrane is pulled and the cells get smaller and the whole cell contracts uniformly [1]. Inflow of Calcium ions from the sarcoplasmic reticulum and binding to calmodulin initiates SMC contractions [2]. The contractions are involuntary controlled and regulated by parasympathetic nerves of the autonomic nervous system, hormones and possibly locally released signals from the adjacent epithelium or endothelium. SMCs can be activated as a single or multi-unit. Single unit SMCs are found in the gastrointestinal tract (e.g. stomach and intestine) and the urogenital tract (e.g. bladder, uterus, ureter) as well as in small arteries and veins. Here, only a few cells of the SM are innervated by the same neuron, but the cells are interconnected to neighboring cells through gap junctions, leading to rhythmic and simultaneous contractions. Single unit SMCs show myogenic activity; an input of the nervous system is not necessary. Multi-unit SMCs are less common and located in the eye, in the *tunica media* of large arteries, in the skin and in bronchioles. Every cell of the SM is innervated by a neuron, they are structurally independent of each other and contract individually.

Within the body, the location distinguishes vascular from visceral SMCs. Vascular SMCs are located in the *tunica media* of blood vessels whereas visceral SMCs cover the mesenchymal walls of hollow organs like the intestine, stomach, uterus, bladder and ureter. Vascular SMCs are necessary for the stabilization of blood vessels and the contraction and regulation of blood pressure, flow and vessel tone [3]. They originate from multiple different embryonic tissues [4],[5]. Lineage-tracing studies revealed that neural crest cells (NCCs) migrate and differentiate into SMCs of the branchial arch

arteries [6]. NCCs also give rise to SMCs of the ascending aorta, the aortic arch, the common carotid arteries, the right subclavian artery and the ductus arteriosus [7]–[9], whereas the descending aorta has progenitors from the somites [9],[10]. Cells of the secondary heart field give rise to the SMCs of the base of the aorta and the pulmonary trunk whereas proepicardial cells undergo an epithelial-to-mesenchymal transition to give rise to progenitors of the coronary arteries [11]–[14]. Lastly, peritoneal (mesothelial) cells contribute to blood vessels of the mesenteries and the gut [15]. Visceral SMCs are necessary for the unidirectional transport in tubular organs. Thereby, luminal content such as food or urine is transported by peristaltic waves through the digestive tract (stomach and intestine) and urinary tract (ureter, bladder), respectively. Visceral SMCs derive from the intermediate mesoderm (SMCs of the ureter and bladder) and the lateral plate mesoderm (SMCs of the stomach and intestine) [16],[17].

The differentiation of almost all SMCs is regulated by serum response factor (SRF). This ubiquitously expressed DNA-binding protein self-dimerizes and binds to the highly conserved CA<sub>n</sub>G-box (CC(A/T)<sub>6</sub>GG), which is found in promoters of almost all SMC-specific genes [18]. Loss or reduction of SRF leads to defects in differentiation, migration and proliferation of vascular as well as visceral SMCs [19]. SRF alone is a weak activator of CA<sub>n</sub>G-box-dependent genes and relies on interactions with coactivators and/or corepressors. The most important coactivators of SMC-specific gene expression are Myocardin (MYOCD) and Myocardin-related transcription factors (MRTFs). MYOCD and MRTFs do not have a DNA binding domain and directly interact with SRF to activate SMC-specific gene expression. MYOCD is specifically expressed in SMCs, whereas expression of MRTFs is more widespread in embryonic and adult tissues [20],[21]. Loss of *Myocd* leads to a complete lack of vascular SMCs and death at around embryonic day (E)10.5 [22].

Interestingly, activation of *Myocd* expression is mediated by different signals in the vascular and visceral context, reflecting different input from adjacent endothelial and epithelial primordia. In vascular SMCs, TGF $\beta$ -signaling regulates SMC differentiation through SMAD2 and 3 [23] and this is facilitated, at least for SMAD3, by direct interaction with SRF [24]. Platelet-derived growth factor (PDGF)-BB has been implicated in repression of vascular SMC differentiation [25],[26]. NOTCH signaling is also involved in vascular SMC differentiation and will be discussed later. In the visceral context, Sonic hedgehog (SHH) has been implicated in the regulation of SMC differentiation in the gut, the bladder and the lung [27]–[29]. Bone morphogenetic protein (BMP)4 and

WNT signaling have a role in mediating SMC formation in the lung [30],[31]. In the bladder, WNT signaling is also suggested to play a role in SMC differentiation [32],[33].

## The structure and function of the murine ureter

SMCs are a critical component of the ureters, a pair of straight tubes that connect the renal pelvises with the bladder. The kidneys produce urine by filtration of blood in their nephrons. The urine is collected in the collecting duct system in the papilla of the kidney and accumulates in the renal pelvis. The ureters then propel by peristaltic contractions of their SMCs the urine into the bladder, where it is temporally stored before expulsion occurs to the outside via the urethra [34].

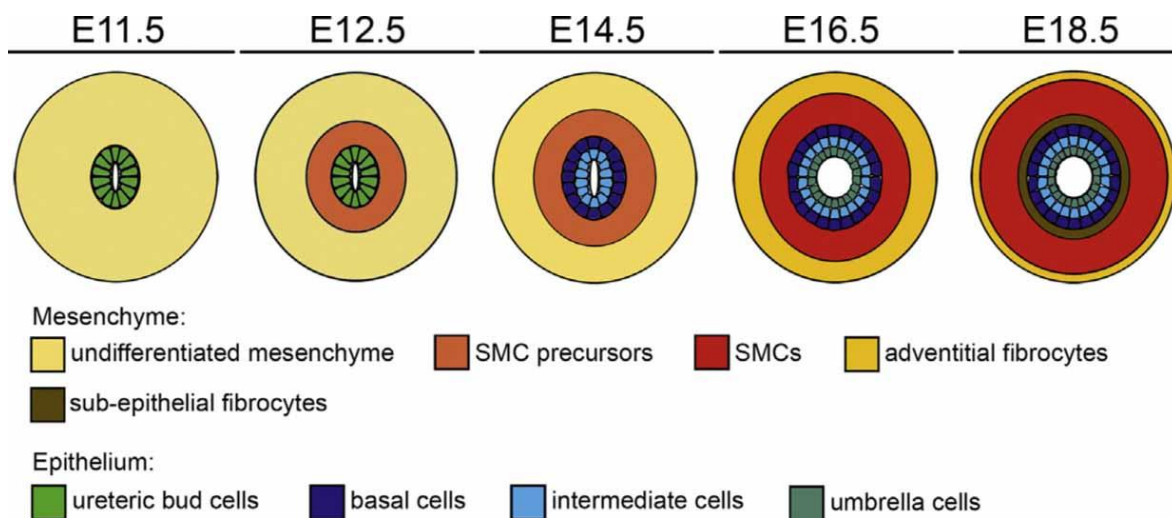
Ureteric SMCs are rhomboid-shaped cells that lie densely packed in the *tunica muscularis* in the mesenchymal wall of this organ. They are ensheathed on the outside by the *tunica adventitia*, fibroelastic material with tangentially organized fibrocytes, which anchors the whole tube to the body wall. On the inside lies the *lamina propria*, a loosely organized tissue with fibrocytes and an abundant extracellular matrix that connects the mesenchymal compartment to the highly specialized inner epithelial tissue, the urothelium.

The urothelium has a three-tiered organization with a layer of basal (B) cells, one or two intermediate (I) cell layers and a superficial (S) cell layer. Together, these epithelial cells provide a flexible but tight barrier between the urine in the ureter lumen and the interstitial space.

Coordinated unidirectional SMC contraction is triggered by special pacemaker cells in the pelvis-kidney junction (PKJ) which respond to increased hydrostatic pressure in the renal pelvis [35]. Lack or functional insufficiency of SMCs in the ureter can damage the integrity of the upper urinary system. Urine accumulation leads to dilatation of the ureter (hydroureter) and renal pelvis (hydronephrosis), a condition that can culminate in destruction of the kidney parenchyma [36]. Congenital forms of this and other anomalies of the kidney and urinary tract (CAKUT) occur in 3-6:1000 live births and present the most common cause of end-stage renal disease in children [37], [38]. Only parts of the mutations that underlie ureteric SMC differentiation defects and CAKUT in humans have been identified. The need to further understand these congenital defects on one side, and the suitability for genetic and pharmacological manipulation on the



other side, define the murine ureter as a relevant and highly appropriate model to decipher the molecular network regulating SMC differentiation in the development of a visceral organ.



**Figure 1: Graphical representation of mesenchymal and epithelial differentiation in embryonic development of the ureter.**

At E11.5, the ureter consists of ureteric bud cells surrounded by an undifferentiated mesenchyme. Mesenchymal cells directly adjacent to the ureteric bud transit to an enlarged shape at E12.5. These SMC progenitors start to differentiate at E14.5 into SMCs and underlying sub-epithelial fibrocytes. The outer mesenchymal cells differentiate into fibroblasts. The epithelium starts to differentiate also at E14.5, first into I-cells and later into S- and B-cells. Modified from Bohnenpoll et al., 2014 [36].

## Embryonic development of the murine ureter

The development of the ureter starts together with that of the kidney at E10.5 at the level of the future hindlimbs with an outgrowth of an epithelial diverticulum from the nephric duct (ND) into the surrounding metanephric mesenchyme. The proximal part of this ureteric bud undergoes multiple branching events to form a ureteric tree that matures into the collecting duct system of the kidney. The distal part of the ureteric bud elongates, separates from the ND and integrates into the bladder wall by apoptotic events. It further differentiates into the urothelium of the ureter [17].

The mesenchymal coat of the ureter including the SMCs derives from a T-box transcription factor gene *Tbx18* positive fibroblast-like cell population that surrounds the distal stalk of the ureteric bud starting from E11.5 [36]. The mesenchymal progenitors that lie in direct vicinity to the epithelium undergo a morphological transition to a rhomboid, densely packed shape at E12.5. These cells start to express the SMC regulatory gene *Myocd* at E14.5, and structural SMC genes at E15.5 in a proximal to distal wave.

Some of the innermost *Myocd*-positive cells leave the SMC program after E15.5 and become fibroblasts of the *lamina propria*. The other SMC progenitors differentiate into terminal SMCs to ensure peristaltic activity of the ureter with the onset of urine production in the kidney at E16.5. The outermost cells of the ureteric mesenchyme (UM) maintain their fibroblastic fate and differentiate into the fibroblasts of the *tunica adventitia*. The ureteric bud epithelium (UE) is initially one-layered and starts to stratify and differentiate into I-cells at E14.5. At E15.5 to E16.5, the cells on the luminal side differentiate into S-cells; B-cell differentiation starts at E16.5 [39] (Figure 1).

### **Molecular regulation of SMC differentiation in the murine ureter**

The differentiation of Tbx18+ mesenchymal progenitors into SMCs is controlled by a complex interplay of signals that originate both from the UE and UM. The most important epithelial signal is SHH, a member of the hedgehog (HH) protein family. *Shh* is expressed starting from E11.5 throughout development in the UE and activates its receptor *Patched 1 (Ptch1)* in the adjacent UM in a paracrine fashion. Global or conditional deletion of *Shh* from the UE leads to reduced mesenchymal proliferation, delayed SMC differentiation and consequently results in hydroureter formation [38],[39]. *Bone morphogenetic protein 4 (Bmp4)* is a member of the transforming growth factor- $\beta$  (TGF- $\beta$ ) superfamily that is expressed under the control of SHH signaling in the UM from E11.5 to E14.5 [38],[40],[41],[42]. Homozygous *Bmp4* null mutant mice are embryonic lethal between E6.5 and E10 due to defects in mesoderm formation and gastrulation [45]. Analysis of heterozygous *Bmp4* null mutant mice revealed that *Bmp4* is necessary to regulate the site of ureter budding on the ND, for ureter growth and elongation, and for SMC formation [41],[44]. Conditional deletion of *Bmp4* from the UM resulted in hydroureteronephrosis and showed that *Bmp4* is necessary for proliferation and differentiation in the UM. Further pharmacological loss- and gain-of-function experiments revealed that UM proliferation is mediated by AKT kinase while differentiation of SMCs depends on the combined activities of AKT, P38 and SMAD1/5/9 downstream of BMP4 [44].

Another pathway important for SMC differentiation in the UM is canonical WNT signaling. Two WNT ligand genes, *Wnt7b* and *Wnt9b*, and one receptor gene, *Frizzled1 (Fzd1)* show specific expression in the ureter. *Wnt7b* and *Wnt9b* are coexpressed in the UE from E11.5 to E14.5. *Wnt7b* expression is maintained during embryonic development, whereas *Wnt9b* is downregulated after E14.5. *Fzd1* is expressed in the UM

from E11.5 to E18.5. Conditional deletion and overexpression of *Ctnnb1* ( $\beta$ -catenin), the unique intracellular mediator of the canonical WNT pathway, in the UM revealed that paracrine WNT signals from the UE to the UM are important to induce SMC precursor differentiation and proliferation [47], [48]. Further analysis identified the two closely related T-box transcription factor genes *Tbx2* and *Tbx3* as targets of WNT signaling in the UM. Both genes are expressed in the UE and the inner layer of the UM from E12.5 throughout embryonic development. The conditional deletion of both genes from the UM showed that *Tbx2* and *Tbx3* promote SMC differentiation by maintaining BMP4 and WNT signaling in the inner layer of the UM [47].

Another pathway important for SMC differentiation in the ureter is retinoic acid (RA) signaling. RA is synthesized in the UE and UM at E11.5 but RA signaling persists until E14.5. Pharmacological pathway activation and inhibition experiments showed that RA signaling is necessary for UM expansion by inhibiting SMC differentiation [50].

Deeper insight into the regulation of SMC differentiation was obtained by investigating the role of SHH signaling in the UM using the unique HH transducer *Smoothed* (*Smo*) [51]. Conditional deletion and overexpression of *Smo* in the UM not only confirmed previous results that SHH signaling is required for proliferation and SMC differentiation of the inner ring of the UM, but also identified *Forkhead-Box-Protein F1* (*Foxf1*) as a downstream target of *Shh*. *Foxf1* is expressed at E14.5 in the UM, expression at later stages has not been investigated so far. Misexpression of a dominant negative version of *Foxf1* in the UM led to failure to activate *Myocd* expression [50],[51]. Additional pharmacological inhibition experiments of *Shh* with re-installment of *Foxf1* in the UM confirmed that *Foxf1* acts downstream of SHH signaling and upstream of and together with *Bmp4* to regulate SMC differentiation by activating *Myocd* expression. Interestingly, SHH signaling is not sufficient to induce *Foxf1* and *Myocd* expression in the outer ring of the UM, indicating cooperation with additional signaling pathways in this program [53].

Multiple transcription factors including *Tbx18*, *Sox9*, *Tshz3* and *Id2* are required downstream of these signaling pathways in the regulation of SMC differentiation [54]–[56]. Although a lot of research has been done on the regulation of SMC differentiation both in the ureter and other visceral organs, there are still many open questions with respect to molecular circuits that regulate this program. What other inputs does *Foxf1* have? Why is *Myocd* expression exactly expressed at E14.5 in the proximal inner layer of the

UM? What other transcription factors and pathways are involved in the regulation of this cell differentiation program?

## **GATA transcription factors as regulators of ureteric SMC differentiation**

GATA proteins are members of a small family of evolutionary conserved zinc finger transcription factors that exert crucial roles in fate decisions and tissue morphogenesis during embryonic development. They have been especially noted for relevance in regulating progenitor differentiation and lineage specification. The name of the GATA family was given after the consensus DNA-binding sequence (A/T)GATA(A/G). The family members have two highly conserved zinc finger domains that recognize the GATA-binding site, a less conserved N- and C-terminal region and a nuclear localization signal (NLS) in common. Transcriptional activation modules are found in the N-terminal region and differ between the family members. The GATA family can be divided into two subgroups. GATA1, GATA2 and GATA3 are regulators of the hematopoietic lineage, whereas GATA4, GATA5 and GATA6 are regulators of the mesodermal and endodermal lineages [57].

Previous work showed that the family member GATA2 plays an important role in the development of the urinary system. *Gata2* expression was detected in the mesenchyme surrounding the ND at E10.5. Later at E12.5, expression was found in the mesenchyme surrounding the ND but also in the UE and UM. In adults, expression was seen in all derivatives of the ND and in the collecting duct system of the kidney [58]. *Gata2* regulates *aquaporin 2 (Aqp2)* expression and is thereby involved in the regulation of water homeostasis by the kidney [59]. *Gata2*-null embryos die around E10.5 from severe hematopoietic defects [60]. *Gata2*-deficient mice with transgenic *Gata2* expression survived until birth and exhibited megaureter formation and hydronephrosis due to a failed distal ureter-bladder connection [61]. This defect was traced to a rostral shift of the ureter budding site, most likely by reduced *Bmp4* signaling [60],[61]. The functional significance of *Gata2* expression in the UM had not yet been investigated. *Gata6* null mice are embryonic lethal between E5.5 and E7.5 due to defects in visceral endoderm formation [64],[65]. Interestingly, GATA6 is highly expressed in vascular SMCs in embryonic and postnatal development [66]; upon mitogen stimulation its expression is rapidly downregulated. Overexpression in proliferating vascular SMCs led

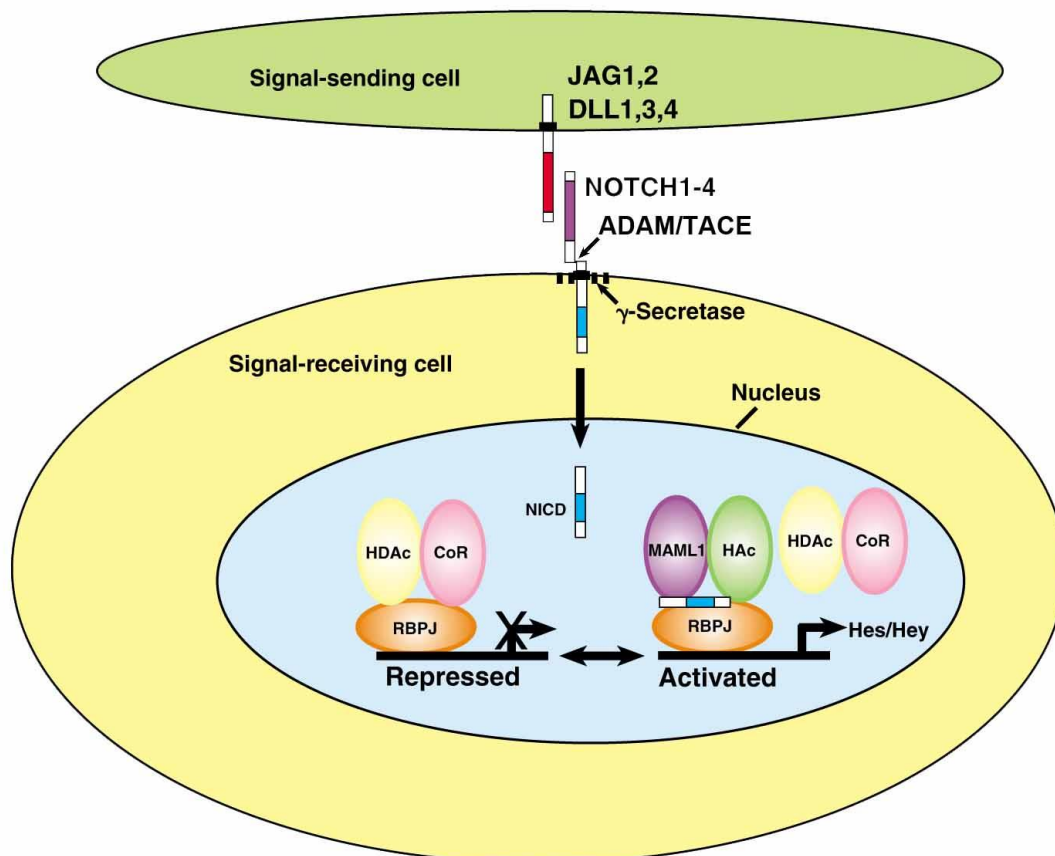
to cell cycle arrest, indicating that GATA6 is involved in the maintenance of the quiescent state of these cells [65],[66]. Additionally, GATA6 modulates the activity of the SRF-*Myocd* complex [69]. Furthermore, GATA6 promotes SMC differentiation in the great vessels by directing activation of *Myocd* and *Jagged1* (*Jag1*) [70]. GATA6 is also expressed in visceral SMCs, except for the ones populating the gastrointestinal tract and uterus [66]. In the human bladder GATA6 mediates SMC differentiation by directly regulating  $\alpha$ -smooth muscle actin ( $\alpha$ -SMA) in primary SMC culture [71]. Lastly, it was shown that the specific deletion of *Gata6* in adrenocortical progenitors impairs adrenal development [70],[71]. The role of *Gata6* in visceral SMC development in the ureter has not yet been addressed.

## The Notch signaling pathway

Notch signaling is an evolutionary highly conserved intercellular communication pathway that regulates a multitude of developmental processes such as proliferation, stem cell maintenance and differentiation during embryonic development and adult homeostasis in a variety of tissues. In mammals four Notch receptors (NOTCH1-4) and five ligands (Delta-like (DLL1,3,4) and Jagged (JAG1,2)) are known. All of the receptors and ligands are type I transmembrane proteins with large extracellular domains that consist of epidermal growth factor-like (EGF) repeats [74]. Transactivation of a receptor by binding of a ligand to the extracellular domain leads to a conformational change, exposing a cleavage site (S2) for metalloproteases of the ADAM/TACE family [75], [76]. Proteolytic cleavage at S2 and further cleavage by the  $\gamma$ -secretase complex leads to the release of the intracellular domain of the Notch receptor (NICD) [77], [78]. NICD translocates into the nucleus where it binds together with other cofactors to the DNA-binding protein recombination signal-binding protein for immunoglobulin kappa J (RBPJ). This complex activates expression of target genes including *hairy and enhancer of split* (*Hes*) and *Hairy/enhancer-of-split related with YRPW motif* (*Hey*) proteins which act as transcriptional repressors [79], [80] (Figure 2).

Vascular SMCs and their progenitors express NOTCH1-3 receptors while the neighboring endothelial cells express the ligands JAG1 and DLL1 and DLL4. Endothelial JAG1 activates NOTCH3 expression in neighboring SMCs [82]. The differentiation of vascular SMCs which are derived from NCCs, the second heart field or the pro-epicardium is positively regulated by NOTCH signaling [83],[84]. Here, JAG1 is the important NOTCH ligand and NOTCH2 and NOTCH3 the important receptors in the activation of

early SMC genes [84]–[87]. Moreover, it was shown that NOTCH signaling regulates and synergizes with PDGFRB and TGFB signaling in regulating vascular SMC differentiation [88]–[90]. Thereby, NICD and SMAD2/3 directly interact to regulate SMC genes [91]. The functional significance of NOTCH signaling in visceral SMC differentiation has not yet been experimentally addressed.



**Figure 2: The NOTCH signaling pathway**

Binding of a ligand (JAG1,2, DLL1,3,4) to a receptor (NOTCH1-4) leads to transactivation and a conformational change. Proteolytic cleavage of S2 by metalloproteases of the ADAM/TACE family and subsequent cleavage at S3 by the  $\gamma$ -secretase complex leads to the release of the intracellular domain of the NOTCH receptor (NICD). NICD translocates into the nucleus and binds together with other cofactors to RBPJ to activate target gene expression such as *Hes/Hey* genes. Modified from Gidley et al., 2007 [81].

## Aim of the thesis

Previous work characterized a number of signals and transcription factor activities that are crucial for SMC differentiation in the ureter. How these signals and factors interact to activate expression of *Myocd* and SMC structural genes in a temporally precise manner is not known. Moreover, the known signals are not sufficient to activate the SMC program in the ureter, suggesting the existence of additional signals that impinge on *Myocd* expression in the development of this organ. In this thesis, the importance of the GATA transcription factors, GATA2 and GATA6, and of the NOTCH signaling pathway in ureteric SMC differentiation shall be investigated.

In a first project, the functional significance of GATA6 in ureteric SMC development shall be examined. GATA6 is implicated in SMC differentiation of the vasculature making it an interesting candidate for regulation of visceral SMC development. Initial experiments performed in our group with conditionally-deleted (*Tbx18<sup>cre</sup>-mediated*) *Gata6* (*Gata6cKO*) mutant mice revealed hydroureter formation and reduced SMC markers at the endpoint of embryonic development. In this thesis, the temporal and spatial expression of GATA6/*Gata6* during embryonic ureter development using RNA *in-situ* hybridization and immunofluorescence analyses shall be performed. The regulation by signaling pathways known to be involved in SMC development in the ureter shall also be analyzed using conditional knockout mutants and pharmacological gain- and loss-of-function experiments for components of the different pathways. The morphological, histological, molecular and cellular changes at the different time points shall be analyzed in *Gata6cKO* mutant ureters. The functionality of the mutant ureter shall be investigated in *ex vivo* cultures screening for peristaltic activity. The underlying molecular changes in the *Gata6*-deficient mutant ureters shall be explored by unbiased transcriptional profiling. Subsequent validation shall be done using RNA *in situ* hybridization and real-time quantitative PCR (qRT-PCR) analyses. Additional pharmacological and functional genomic analyses shall be performed to get deeper insight into the molecular mechanism of GATA6 function.

The second project shall investigate the importance of *Gata2* in SMC development of the ureter. In our group, the *Tbx18<sup>cre</sup>-mediated* conditional deletion of *Gata2* (*Gata2cKO*) resulted in hydroureter formation in prenatal mutant embryos; molecular analysis identified increased RA signaling in the UM. In this thesis, pharmacological gain- and loss-of-function studies shall be performed to investigate the contribution of RA signaling to the phenotypic changes of *Gata2cKO* mutant ureters.

NOTCH signaling has been investigated in vascular SMC differentiation for years, but the role in visceral SMC differentiation is completely unclear and shall be investigated in a third project. In conditional *Rbpj* mutants (again obtained by using the *Tbx18<sup>cre</sup>*-driver line), our group found delayed onset of SMC differentiation markers. In this thesis, the functional relevance of this delay will be investigated using *ex vivo* cultures and monitoring the peristaltic activity at different time points of embryonic SMC development. In addition, pharmacological loss-of-function studies using the NOTCH signaling inhibitor DAPT and RT-qPCR analyses will be performed.

Together, this thesis shall identify novel transcription factor and signaling activities involved in the regulation of SMC differentiation in the ureter, and hence, provide a more highly resolved image of the molecular circuits driving visceral SMC differentiation in general.



## Part 1- GATA6 in SMC differentiation

GATA6 is a critical factor for *Myocd* expression in the visceral smooth muscle cell differentiation program of the murine ureter

**Jennifer Kurz<sup>1</sup>, Anna-Carina Weiss<sup>1</sup>, Hauke Thiesler<sup>2</sup>, Timo H. Lüttke<sup>1</sup>, Herbert Hildebrandt<sup>2</sup>, Joerg Heineke<sup>3</sup>, Stephen A. Duncan<sup>4</sup>, Mark-Oliver Trowe<sup>1</sup> and Andreas Kispert<sup>1,\*</sup>**

<sup>1</sup>Institut für Molekularbiologie, Medizinische Hochschule Hannover, Hannover, Germany

<sup>2</sup>Institut für Klinische Biochemie, Medizinische Hochschule Hannover, Hannover, Germany

<sup>3</sup>Abteilung für Kardiovaskuläre Physiologie, European Center for Angioscience, Medizinische Fakultät Mannheim, Universität Heidelberg, Mannheim, Germany.

<sup>4</sup>Department of Regenerative Medicine and Cell Biology, Medical University of South Carolina, Charleston, SC, United States of America

\*Address correspondence to: Andreas Kispert, Medizinische Hochschule Hannover, Institut für Molekularbiologie, OE5250, Carl-Neuberg-Str. 1, 30625 Hannover, Germany. Phone: +49 511 5324017, Fax: +49 511 5324283, E-mail: kispert.andreas@mh-hannover.de

Short title: Gata6 in ureter development

Key words: ureter, smooth muscle cell, differentiation, mesenchyme, *Myocd*

**Type of authorship:** First author

**Type of article:** Research article

**Share of the work:** 75%

**Contribution to the publication:** performed experiments, analyzed data, prepared Figures, assisted in writing the manuscript

**Journal:** -

**Impact factor:** -

**Number of citations:** -

**Date of publication:** manuscript in preparation

**DOI:** -

## **Abstract**

Smooth muscle cells (SMCs) are a critical component of the mesenchymal wall of the ureter since they account by means of their contractile activity for the efficient removal of the urine from the renal pelvis to the bladder. Here, we show that the zinc-finger transcription factor gene *Gata6* is expressed in mesenchymal precursors of ureteric SMCs under the control of BMP4 signaling. Mice with a conditional loss of *Gata6* in these precursors exhibit a delayed onset and reduced level of SMC differentiation and compromised peristaltic activity, as well as dilatation of the ureter and renal pelvis (hydroureteronephrosis) at birth and at postnatal stages. Molecular profiling revealed a delayed and reduced expression of the myogenic driver gene *Myocd* but the activation of signaling pathways and transcription factors previously implicated in activation of the visceral SMC program in the ureter, was unchanged. Our work suggests that GATA6 controls ureteric SMC differentiation as a pioneer factor for *Myocd* activation.

## Introduction

In mammals, efficient removal of the urine from the kidneys to the outside relies on the peristaltic activity of a pair of tubular organs, the ureters. Structural basis of the contractile behavior of these straight tubes are smooth muscle cells (SMCs) that form concentric layers in the outer mesenchymal wall. In the mouse, SMCs arise together with ensheathing fibrocytes in a precisely orchestrated manner from a homogenous pool of mesenchymal progenitors. This pool surrounds the distal aspect of the ureteric bud, an epithelial outgrowth of the nephric duct, at embryonic day (E)11.5. At E12.5, the mesenchymal cells adjacent to the ureteric epithelium (UE) transit from a slender fibroblastic to an enlarged rhomboid shape. At E14.5, they start to express *Myocd*, the key regulator of SMC differentiation (Wang and Olson, 2004). Cells in the vicinity of the UE become devoid of *Myocd* expression and differentiate from E16.5 onwards into fibrocytes of the *lamina propria*. The ones further away maintain *Myocd* expression and activate in a stepwise fashion expression of different SMC structural genes until E18.5. As a consequence, they form a functional *tunica muscularis* that engages in peristaltic activity shortly after onset of urine production in the fetal kidney at E16.5. The cells in the outer region of the ureteric mesenchyme (UM) differentiate into fibrocytes of the *tunica adventitia*, which anchors the ureter in the posterior body wall (Bohnenpoll et al., 2017a; Bohnenpoll and Kispert, 2014).

Failure to activate the SMC differentiation program in the fetal ureter is detrimental to the integrity of the upper urinary system, i.e. the ureters and kidneys (Bohnenpoll et al., 2017c; Trowe et al., 2012). The urine is no longer propelled to the bladder and therefore accumulates in the ureter and renal pelvis, driving dilatation of these structures finally resulting in destruction of the renal parenchyma. Importantly, ureter dilatations are frequently observed in human newborns and in most cases, initial dilatation recedes over time. However, in some cases the condition remains unresolved manifesting in severe uro- and nephropathy (Chiodini et al., 2019; Ek et al., 2007; Herthelius et al., 2020).

A combination of embryological and genetic analyses in the mouse uncovered an interconnected system of signals and transcription factor activities that impinges on the proliferation, patterning and subsequent differentiation of the UM into SMCs and fibroblasts (Bohnenpoll and Kispert, 2014). Sonic hedgehog (SHH) originating from the UE prevents apoptosis in the outer UM, and induces proliferation and SMC differentiation of mesenchymal cells adjacent to the UE. In the latter cells, SHH signaling is required

for expression of the transcription factor gene *Foxf1* which, in turn, induces the gene encoding the signaling molecule BMP4, and synergizes in an unknown fashion with BMP4 on *Myocd* expression and SMC differentiation (Bohnenpoll et al., 2017c; Mamo et al., 2017; Yu et al., 2002). WNTs from the UE activate the T-box transcription factors TBX2 and TBX3 to confine the adventitial fate to the outer UM (Aydogdu et al., 2018; Trowe et al., 2012). This may aid in directing the inner UM to the SMC differentiation pathway. Retinoic acid (RA) emanating from the UM and/or the UE delays SMC differentiation possibly by counteracting WNT signaling (Bohnenpoll et al., 2017b).

The GATA transcription factors are a highly conserved family of zinc finger proteins that mediate tissue-specific gene expression. In mammals there are six family members that based on structure and function were assigned to two subfamilies (Tremblay et al., 2018). We have previously shown that GATA2, a member of the GATA1,2,3 subfamily acts at least partly as a feed-back inhibitor of RA signaling to time the activation of *Myocd*, hence, of SMC differentiation in ureter development (Weiss et al., 2019). Here, we set out to study the functional significance of GATA6, a member of the GATA4,5,6 subfamily, in this process. Of note, GATA6 has been implicated in patterning and differentiation of cardiac neural crest cells into vascular SMCs (Kodo K, 2009; Lepore et al., 2006; Losa et al., 2017) as well as the maintenance of the quiescent phenotype of these cells (Mano et al., 1999a; Perlman et al., 1998; Tremblay et al., 2018). GATA6 is also expressed in bladder SMCs but an *in vivo* requirement for the differentiation of these or other visceral SMCs has not been reported.

We demonstrate here that *Gata6* is expressed in the undifferentiated UM and that its conditional loss from this tissue leads to hydroureteronephrosis in fetal and adult mice. Further molecular analyses suggest that GATA6 activates *Myocd* expression and thereby assures timely activation of the SMC differentiation program in the ureter.

## Results

### ***Gata6* expression in the undifferentiated UM depends on BMP4 signaling**

To obtain a detailed profile of *Gata6* expression in the development of the ureter, we performed RNA *in situ* hybridization on whole kidney/ureter rudiments as well as on proximal ureter sections of E11.5 to E18.5 wildtype mouse embryos. Strong *Gata6* expression was found in the entire UM at E11.5 and E12.5. At E14.5 and E16.5, expression at much reduced levels was confined to the inner region of the UM (Fig. 1A,B). GATA6 protein expression recapitulated the pattern of *Gata6* mRNA in this organ. The protein was confined to the nucleus at all analyzed stages (Fig. 1C).

To determine whether *Gata6* expression depends on one of the signaling systems involved in UM development, we analyzed mutants in which key cellular signaling components were conditionally deleted. We used a *Tbx18<sup>cre</sup>* line, which mediates recombination in the entire UM starting from E11.5 (Airik et al., 2010; Bohnenpoll et al., 2013), and floxed alleles of the unique mediator of SHH signaling, *Smo* (Long et al., 2001), of canonical WNT signaling, *Ctnnb1* (Brault et al., 2001), and of *Bmp4* (Kulesa and Hogan, 2002), as previously reported (Bohnenpoll et al., 2017c; Mamo et al., 2017; Trowe et al., 2012). Loss of *Smo* and *Ctnnb1* had no effect on *Gata6* expression in the UM at E12.5. In contrast, *Gata6* expression was strongly reduced in this region in *Tbx18<sup>cre/+</sup>;**Bmp4<sup>fl/fl</sup>* embryos (Fig. 1D). Moreover, in E11.5 kidney rudiments cultured for 18 h with 10 µg/ml of the BMP antagonist NOGGIN (Zimmerman et al., 1996) *Gata6* expression was very weak in the UM whereas application of 100 ng/ml BMP4 resulted in enhanced and ectopic *Gata6* expression in the renal stroma. Application of 1 µM RA or 1 µM of the pan-RA receptor (RAR) antagonist BMS493 (Chazaud et al., 2003) did not affect *Gata6* expression in this culture system (Fig. 1E). We conclude that expression of *Gata6* in the undifferentiated UM depends on BMP4 signaling.

### **Loss of *Gata6* in the UM leads to prenatal hydronephrosis formation**

Development of *Gata6* null embryos arrests during gastrulation as a consequence of defects in extraembryonic endoderm function (Koutsourakis et al., 1999; Morrissey et al., 1998). We therefore used a conditional gene inactivation approach with a floxed allele of *Gata6* and our *Tbx18<sup>cre</sup>* line to analyze *Gata6* function specifically in the UM (Airik et al., 2010; Sodhi et al., 2006). The tissue-specific inactivation of *Gata6* in *Tbx18<sup>cre/+</sup>;**Gata6<sup>fl/fl</sup>* (*Gata6*CKO) ureters was confirmed by severe down-regulation of *Gata6* mRNA in the UM at E11.5 and of GATA6 protein at E12.5 (Fig. S1). In matings

of *Tbx18<sup>cre/+</sup>;Gata6<sup>fl/+</sup>* males with *Gata6<sup>fl/fl</sup>* females, *Gata6cKO* embryos were recovered at the expected ratio at E18.5 and all other analyzed stages (Fig. S2A). The external appearance of E18.5 mutant embryos was normal, but their urogenital system was frequently (80%, n=49) and sex-independently characterized by dilatation of the ureter with the proximal aspect being more affected. The severity of this phenotypic defect ranged from weak unilateral to strong bilateral hydroureter (Fig. 2A, Fig. S2B,C). Testis and epididymis were invariably laterally tethered to the kidney (cryptorchidism); the adrenals were drastically reduced in size (Fig. 2A). The latter phenotype is likely to relate to the reported requirement of *Gata6* in adrenogonadal progenitors (Tevosian et al., 2015) in which *Tbx18<sup>cre</sup>* also mediates recombination (Hafner et al., 2015). In *Tbx18<sup>cre/+</sup>;Gata6<sup>fl/+</sup>* littermates, the adrenals appeared unchanged, the testis was descended but weak hydroureter formation occurred in 72% of the cases (n=32) (Fig. S2B,C) indicating a certain degree of haploinsufficiency.

Histological analysis showed that in E18.5 *Gata6cKO* embryos, hydroureter was associated with a dilation of the renal pelvis and a weak reduction of the renal papilla (Fig. 2B). To exclude that ureter dilatation is caused or contributed by physical obstruction along the ureter and/or of the vesico-ureteric junction, we injected ink into the renal pelvis and observed its flow upon mild hydrostatic pressure. In all mutants, the ink drained smoothly into the bladder indicating that functional rather than physical obstruction underlies hydroureteronephrosis (Fig. 2C). To further test this hypothesis, we analyzed proximal ureter sections of E18.5 *Gata6cKO* embryos for presence of SMCs. Markers of this differentiated cell type (*ACTA2*, *TAGLN*, *Tagln*, *Tnnt2*, *Myh11*) were severely down-regulated, as was *Aldh1a2*, a marker for fibroblasts of the inner *lamina propria*. Markers for adventitial fibrocytes (*Dpt*, *Fbln2*) were still expressed in the outer loose mesenchyme, albeit more weakly (Fig. 2D,E). Mesenchymal defects did not affect cyto-differentiation of the urothelium as revealed by normal expression of KRT5,  $\Delta$ NP63, and UPK1B which combinatorially mark B-cells (KRT5<sup>+</sup> $\Delta$ NP63<sup>+</sup>UPK1B<sup>-</sup>), I-cells (KRT5<sup>-</sup> $\Delta$ NP63<sup>+</sup>UPK1B<sup>+</sup>) and S-cells (KRT5<sup>-</sup> $\Delta$ NP63<sup>-</sup>UPK1B<sup>+</sup>) (Bohnenpoll et al., 2017a) (Fig. 2F). Since increased hydrostatic pressure affects cyto-differentiation in the mesenchymal compartment, we also analyzed weakly dilated proximal ureters and non-dilated distal ureters. Expression of SMC markers was also reduced in these settings but the degree of reduction varied from very strong (*Tnnt2*, *ACTA2*, *TAGLN*) to moderate (*Tagln*, *Myh11*). Fibrocyte and epithelial cyto-differentiation was unaffected

(Fig. S3,S4). We conclude that SMC differentiation is reduced in E18.5 *Gata6cKO* ureters and that pressure-mediated dilatation aggravates the effect.

### ***Gata6cKO* mice do not resolve hydroureter in adolescence**

Since hydroureter formation is frequently observed in newborn babies but often resolves for unknown reasons (Dudley et al., 1997), we wondered whether the dilative nephro-/uropathy in *Gata6cKO* mice persists into postnatal (P) stages. To answer this question, we analyzed urogenital systems of *Gata6cKO* mice at P21, when the animals still showed a normal external appearance and behavior. We found undescended testes, a strongly dilated ureter and pelvis, absence of the renal papilla and a severe reduction of the renal parenchyma (Fig. 3A-C). Expression of SMC markers was strongly reduced whereas urothelial differentiation appeared unaffected (Fig. 3D-J). This shows that hydroureter-nephrosis progresses after birth in an untamed fashion in *Gata6cKO* animals.

### ***Gata6* is required for timely activation of the SMC program**

To define both the onset as well as the progression of urogenital malformations in *Gata6cKO* embryos, we analyzed urogenital systems at E14.5 to E16.5, i.e. shortly before and after onset of urine production in the kidney. On the morphological level, the mutant was distinguished by adrenal hypoplasia starting from E14.5, and by hydroureter formation and absent testicular descent at E16.5 (Fig. 4A). Histological staining of proximal ureter sections revealed a less condensed inner mesenchymal layer compared to the control at E15.5, and a strongly dilated ureter at E16.5 (Fig. 4B). In control embryos, expression of *Myh11* started robustly at E14.5, of *Tagln*, *Tnnt2* and *ACTA2* at E15.5 in the UM. In *Gata6cKO* ureters, expression of SMC structural genes/proteins occurred at dramatically reduced levels at all stages analyzed (Fig. 4C,D). In contrast, expression profiles of markers for the *lamina propria* (*Aldh1a2*) and the *tunica adventitia* (*Dpt*, *Fbln2*, *Col1a2*) were unchanged (Fig. S5). Expression of the epithelial cyto-differentiation markers  $\Delta$ NP63, UPK1B and KRT5 occurred normally, but expression of  $\Delta$ NP63 (at E14.5 and E15.5) and of UPK1B (E15.5) was weaker, and stratification was delayed in *Gata6cKO* ureters (Fig. 4E).

The TUNEL assay did not detect apoptotic bodies in the mutant UM at E12.5 and E14.5 (Fig. S6A). Moreover, cell proliferation as studied by the BrdU incorporation assay was not changed in the mesenchymal and epithelial compartments of the mutant ureter at

either stage (Fig. S6B,C; Table S1). Hence, GATA6 is critically required to initiate the SMC program but does not affect survival, proliferation and patterning of the UM.

### **Peristalsis and SMC differentiation occur in a delayed and reduced fashion in *Gata6cKO* ureters**

Although SMC differentiation was dramatically reduced in *Gata6cKO* ureters at E14.5 and E15.5, the program may be compromised from E16.5 onwards by pressure-induced ureter dilatation. To analyze ureter development in absence of urine load, we explanted ureters at E14.5, i.e. prior to urine formation, and cultured them for 8 days, monitoring daily for morphological changes and peristaltic activity. In the control, peristaltic movements started after two days and reached their frequency peak after 6 days. In *Gata6cKO* ureters, contractions started very weakly only after 4 days, exhibited approximately half of the wildtype frequency after 6 days, but reached the control levels after 8 days of culture (Fig. 5A,B; Table S2). The contraction intensity was strongly decreased at day 4 at the proximal, medial and distal positions analyzed, but reached control levels at the following days except proximally where it continued to be significantly reduced (Fig. 5C; Table S3). After 6 days of culture, expression of *Myh11* appeared normal; *Tagln/TAGLN* and *ACTA2* expression was weakly and *Tnnt2* was strongly reduced in the proximal ureter region (Fig. 5D).

Dilated ureters of E18.5 *Gata6cKO* embryos regained frequent peristaltic contractions after 2 to 4 days after explantation (Fig. 5E,F; Table S4). Contraction intensity was strongly decreased at day 0 and 2 of culture but after 4 and 6 days control levels were observed medially. At the proximal and distal position, the contraction intensity remained strongly and weakly reduced, respectively (Fig. 5G, Table S5). At day 6 of culture, expression of SMC markers appeared unaffected (*Myh11*), weakly (*Tagln/TAGLN*, *ACTA2*) and strongly reduced (*Tnnt2*) (Fig. 5H). These data show that expression of most SMC structural genes/proteins is delayed but not permanently lost in *Gata6cKO* ureters, and that SMC differentiation and peristaltic activity can be partly recovered in *ex vivo* culture conditions even after a dilatation has occurred.

### ***Myocd* expression is decreased in *Gata6cKO* ureters**

To identify in an unbiased fashion molecular changes that may cause delayed and reduced SMC differentiation in *Gata6cKO* ureters, we performed microarray-based gene expression profiling of E14.5 *Gata6cKO* and control ureters. Using an intensity



threshold of 100 and fold changes of at least 2 in the two individual arrays, we detected 61 genes with reduced and 57 genes with increased expression in mutant ureters (Fig. 6A-C; Table S6, S7).

Functional annotation using the DAVID software tool (Huang et al., 2009) revealed an enrichment of gene ontology (GO) terms related to “neuron” in the pool of upregulated genes (Table S8) but RNA *in situ* hybridization did not detect changes of expression of selected candidate genes (*Cartpt*, *Nefm*, *Phox2b*, *Hand2*) in E14.5 *Gata6cKO* ureters (Fig. S7A). Interestingly, two genes relating to RA synthesis, *Aldh1a3* (+5.5) and *Aldh1a2* (+2.2) belonged to the top-upregulated genes. Targets of RA signaling in the UM (Bohnenpoll et al., 2017b), including *Wt1* (+2.4), *Ecm1* (+1.6) were also increased (Fig. 6B, Table S8). RNA *in situ* hybridization confirmed increased expression of *Aldh1a2* and *Wt1* in the outer UM, of *Aldh1a3* in the UE, and of *Ecm1* in the inner UM of *Gata6cKO* ureters at E14.5. However, the direct target of RA signaling, *Rarb* (Mendelsohn et al., 1991), appeared unchanged in the UM (Fig. 6D).

Functional annotation revealed an enrichment of GO terms related to “epithelial differentiation” in the pool of downregulated genes (Table S9). Genes associated with these terms included the S-cell markers *Upk1b* (-4.3), *Upk2* (-3.2), *Upk1a* (-3.0), the regulator of S-cell differentiation, *Grl3* (-2.3) (Yu et al., 2009), and the regulator of epithelial stratification *Trp63* (-2.5) (Weiss et al., 2013). *In situ* hybridization was not sensitive enough to detect expression changes of these candidate genes in mutant ureters (Fig. S7B). The list of downregulated genes also included *Car3* (-3.2) and the WNT antagonist *Shisa2* (-3.1) two genes previously shown to be expressed in the UM (Airik et al., 2010; Aydogdu et al., 2018), and most notably *Myocd* (-2.8), the master regulator of SMC differentiation (Wang and Olson, 2004). RNA *in situ* hybridization confirmed reduced expression of *Car3* and *Shisa2* in the UM of E14.5 *Gata6cKO* embryos; *Myocd* expression was almost absent (Fig. 6E).

*Myocd* expression and SMC differentiation in the developing ureter depends on a number of signaling pathways and transcription factor activities (Bohnenpoll and Kispert, 2014). Our microarray and *in situ* hybridization analyses did not detect changes in expression of *Shh*, and of the direct target genes of SHH signaling, *Ptch1* and *Gli1* (Bohnenpoll et al., 2017c; Ingham and McMahon, 2001); of *Wnt7b* and *Wnt9b*, and of *Axin2*, direct target of this pathway (Jho et al., 2002; Trowe et al., 2012); of *Bmp4*, (Bohnenpoll et al., 2017c) and the direct targets of its activity, *Id2* and *Id4* (Hollnagel et al., 1999; Mamo et al., 2017), and of the transcription factor genes *Foxf1* (Bohnenpoll

et al., 2017c), *Gata2* (Weiss et al., 2019), *Sox9* (Airik et al., 2010), *Tbx18* (Airik et al., 2006), *Tcf21* (Airik et al., 2006), *Tshz3* (Caubit et al., 2008), *Tbx2/TBX2* and *Tbx3/TBX3* (Aydogdu et al., 2018) in *Gata6cKO* ureters at E14.5 (Fig. S8, S9).

RT-PCR analysis confirmed that *Myocd* expression was strongly reduced in E14.5 *Gata6cKO* ureters whereas expression of *Foxf1*, activator of *Myocd* expression, of the WNT target gene *Axin2*, the BMP4 target *Id2*, and of the mesenchymal RA target, *Rarb* was unchanged (Fig. 6F, Table S10).

Expression of *Myocd* remained strongly reduced at E15.5 and E16.5. In E18.5 ureters and in E18.5 ureter explants cultured for 6 days *Myocd* expression was weakly reduced, indicating that *Myocd* expression is regained to a significant degree after E16.5 (Fig. G).

Hence, *Gata6* is required for activation of *Myocd* expression at E14.5 independent from transcription factors and signaling activities previously implicated in the regulation of this gene.

### **Enhanced RA signaling does not account for the peristalsis defects of *Gata6cKO* ureters**

Although our assays did not detect increased expression of the direct RA target gene *Rarb* in the UM, increased expression of RA synthesizing enzymes and some RA dependent genes may point to a functional implication of enhanced RA signaling in the delayed onset of SMC differentiation as previously reported (Bohnenpoll et al., 2017b; Weiss et al., 2019). We therefore tested whether reduction of RA signaling ameliorates the peristaltic changes of *Gata6cKO* ureters. Treatment of control E13.5 ureter explants with the pan-RAR antagonist BMS493 (1  $\mu$ M) did not affect the onset of contractions but lowered the contraction frequency from day 4 onwards. In *Gata6cKO* ureters, BMS493 treatment further delayed the peristaltic onset and reduced the contraction frequency (Fig. S10; Table S11). We conclude that increased RA signaling does not contribute in a major fashion to the delayed onset of SMC differentiation and peristaltic activity in *Gata6cKO* ureters.

### ***Gata2* and *Gata6* do not cooperate in SMC differentiation in the developing ureter**

We recently reported that in mice with conditional loss of *Gata2* in the UM, SMC differentiation was delayed and RA signaling was increased (Weiss et al., 2019). Given the phenotypic similarities, we wondered whether GATA2 and GATA6 would cooperate in

ureteric SMC differentiation. We tested this by generating mice compound heterozygous for *Gata2* and *Gata6*. Urogenital systems of *Tbx18<sup>cre/+</sup>;Gata2<sup>fl/+</sup>;Gata6<sup>fl/+</sup>* embryos neither exhibited enhanced ureter dilatation nor did they present cryptorchidism compared to *Tbx18<sup>cre/+</sup>;Gata2<sup>fl/+</sup>* and *Tbx18<sup>cre/+</sup>;Gata6<sup>fl/+</sup>* embryos indicating that *Gata2* and *Gata6* control different molecular programs (Fig. S11).

## Discussion

Here, we identified GATA6 as a novel regulator of visceral SMC differentiation in the ureter. Our findings indicate that GATA6 acts downstream of BMP4 as an activator of *Myocd* expression. Our work confirms that a delayed and reduced onset of SMC differentiation results in ureter dilatation at birth, and that relief from the resulting hydrostatic pressure may aid in regaining ureter peristalsis.

### ***Gata6* is a novel regulator of visceral SMC differentiation**

Previous work described expression of *Gata6* in various progenitor populations during murine development including the visceral endoderm, the (pre-)cardiac mesoderm, the neural crest, and the endoderm of the primitive gut tube including the bronchial tree but also in mature SMCs of the aorta, large arteries and the bladder. These studies also mentioned *Gata6* expression in the urogenital ridge at E13.5 but did not further analyze expression during urinary tract development (Freyer et al., 2015; Morrisey et al., 1996; Nemer and Nemer, 2003). Our work characterized the undifferentiated UM as an additional expression domain of *Gata6*/GATA6 in mouse development. We found downregulation of *Gata6*/GATA6 expression with onset of mesenchymal cyto-differentiation in the ureter which contrasts with the pattern in the adjacent bladder primordium where *Gata6* expression is maintained into adult stages (Freyer et al., 2015; Morrisey et al., 1996).

The conditional loss of *Gata6* in the UM did not affect survival, proliferation and patterning of these progenitors but led to failure to activate the SMC program in the fetal ureter. This finding is in line with previous reports that *Gata6* is critical for lineage specification and early differentiation of progenitors of various endodermal, mesodermal and ectodermal sources (Morrisey et al., 1998; Tevosian et al., 2015; Zhao et al., 2008; Zhao et al., 2005) (for a review see (Tremblay et al., 2018)).

Our study stresses the significance of *Gata6* and its related family members (*Gata4*, *Gata5*) as regulators of muscle cell differentiation. While the role of *Gata6* (in combination with *Gata4*) in early differentiation of cardiomyocytes has been appreciated for long (Zhao et al., 2008), the role in vascular and especially in visceral SMC differentiation has remained less clear. Some *in vitro* studies initially suggested that GATA6 induces and maintains the contractile phenotype of vascular SMCs (Abe et al., 2003; Mano et al., 1999b; Wada et al., 2002), while others questioned such a role (Lepore et

al., 2005; Yin and Herring, 2005 ). However, recent *in vivo* loss- and gain-of-function studies provided compelling evidence that *Gata6* is both required and sufficient for the differentiation of cardiac neural crest cells into SMCs that surround the large vessels of the cardiac outflow tract (Losa et al., 2017).

Knockdown of endogenous *GATA6* in primary human bladder SMCs led to decreased mRNA levels of some SMC structural genes suggesting a role in maintaining the differentiated phenotype of these visceral SMCs (Kanematsu et al., 2007). However, to our knowledge, an *in vivo* requirement for *Gata6* in the establishment or maintenance of the SMC phenotype in the bladder has not been reported.

It is important to note that *Gata6* expression has not been observed during visceral SMC development of the respiratory system, the urethra and the gastrointestinal tract (Morrisey et al., 1996). Moreover, a role of *Gata6* has not been reported for vascular SMCs that do not derive from neural crest cells such as epicardium-derived coronary SMCs. We cannot exclude that low levels of expression of *Gata6* or of other *Gata* family members has escaped detection and/or that redundancy of several *Gata* genes has precluded functional insights. However, it is also conceivable that *Gata6* acts only in some of the SMC differentiation programs during embryonic development. This is in line with the finding that both vascular and visceral SMCs arise from a multitude of progenitors, and that diverse signals from adjacent epithelial and endothelia primordia but also from within the SMC progenitors are implicated in activation of the SMC differentiation program (Donadon and Santoro, 2021; Mack, 2011).

Our *in vivo* and *ex vivo* experiments have shown that BMP4 signaling is both required and sufficient for *Gata6* expression in the UM. Given the findings that *Gata4* and *Gata6* are coexpressed in many mesodermal and endodermal progenitors, that BMP4 is upstream of *Gata4* in the precardiac mesoderm {Schultheiss, 1997 #445}, endoderm (Rossi et al., 2001), lateral plate mesoderm (Rojas et al., 2005), and that neural crest cell induction requires BMP4 signaling (Baker and Bronner-Fraser, 1997), it is tempting to speculate that BMP4 signaling regulated expression of *Gata6* (and/or *Gata4*) defines a critical axis in the differentiation of both cardiomyocytes and a subset of vascular and visceral SMCs.

### ***Gata6* is required for activation of *Myocd* expression in the UM**

Our molecular characterization of *Gata6cKO* ureters revealed a dramatic reduction of *Myocd* expression in the fetal ureter. MYOCD acts a transcriptional coactivator that

complexes with the DNA-binding protein serum response factor (SRF) in the activation of genes that harbor binding sites for SRF, so called CArG boxes in their promoters (Norman et al., 1988; Sun et al., 2006; Wang et al., 2001; Wang and Olson, 2004). Given the fact that *Myocd* is required for SMC differentiation, downregulation of *Myocd* expression is the likely cause for SMC differentiation and peristalsis defects in *Gata6cKO* ureters.

Since *Myocd* is sufficient to induce SMC differentiation when ectopically expressed (van Tuyn et al., 2005; Wang et al., 2003), temporal and spatial control of *Myocd* expression underlies the regionalized programs of visceral and vascular SMC differentiation. As mentioned above, activation of *Myocd*, hence, of the SMC program occurs as response to a multitude of signals that are released from endothelial and epithelial primordia as well as from signals secreted from the SMC progenitors (Donadon and Santoro, 2021; Mack, 2011). In the murine ureter, SHH and WNTs have been characterized as epithelial signals from the ureteric bud that maintain UM proliferation and induce *Myocd* expression and SMC differentiation. SMO-dependent SHH signaling and CTNNB1-dependent WNT signaling induce and maintain, respectively, BMP4 expression in the UM. In turn, BMP4 is required for UM proliferation, *Myocd* expression and SMC differentiation (Bohnenpoll et al., 2017c; Mamo et al., 2017; Trowe et al., 2012). Importantly, we did neither detect changes in expression of *Shh*, *Wnt* and *Bmp4* ligand genes nor alterations in their signaling activities in the UM of *Gata6cKO* ureters. Furthermore, we found unaltered expression of transcription factors that impinge on *Myocd* expression downstream of the activity of these signaling pathways in the UM. These data show that all known positive molecular inputs on *Myocd* expression in the UM are unaffected by loss of *Gata6*. This is notable since several studies suggested that *Gata6* acts as a regulator of *Bmp4* expression in some developmental settings (2014; Nemer and Nemer, 2003; Peterkin et al., 2003; Zeng and Childs, 2012).

Our *Gata6cKO* analysis detected increased expression of RA synthesizing enzymes in the early ureter, and slight increase in some RA dependent genes in the UM. Pharmacological inhibition of RA signaling did not alleviate the SMC defects but increased them, making it unlikely that RA, which is known to inhibit SMC differentiation in the UM (Bohnenpoll et al., 2017b), represents a significant factor for the lack of *Myocd* activation in *Gata6cKO* UM. Increased RA signaling may, however, contribute to the

slight delay in epithelial stratification and differentiation, and/or occurrence of a neuronal expression profile in the mutant ureter as suggested by some studies (Bohnenpoll et al., 2017b; Lakard et al., 2007; Sidell and Horn, 1985)

Based on these results, we hypothesize that GATA6 acts as a direct transcriptional activator of *Myocd* expression in the UM. This assumption gets indirect but strong support from a recent report stating that *Gata6* is required and sufficient for *Myocd* expression in cardiac neural crest cells, and that it occupies a binding site in the *Myocd* locus (Losa et al., 2017).

*Myocd* expression and SMC differentiation occurred in *Gata6cKO* ureters at E18.5 and at later stages in *ex vivo* cultures. This was associated with a significantly improved peristaltic activity. Hence, *Gata6* is not absolutely required to establish the SMC lineage, but shifts the onset of *Myocd* expression and SMC differentiation to earlier stages to cope with onset of urine production in the fetal kidney. Given the expression of *Gata6* in the undifferentiated UM, normal activation of *Foxf1* on which *Myocd* expression crucially depends, and recent reports on the molecular function of GATA6 as a pioneer factor (Sharma et al., 2020), we deem it likely that GATA6 opens chromatin in and around the *Myocd* locus and that FOXF1 subsequently activates *Myocd* expression as a lineage determining factor. In the absence of *Gata6* FOXF1 expression may gradually increase to levels sufficient to activate *Myocd* albeit with a strong delay and at reduced levels.

Interestingly, with the exception of *Tnnt2* all of the SMC structural genes evaluated returned to normal expression levels in extended *ex vivo* cultures of *Gata6cKO* explants. Since GATA6 binds and transactivates a cardiac specific enhancer element in the closely related *Tnnc1* gene (Morrissey et al., 1996), it is conceivable that *Tnnt2* presents an additional direct target of GATA6 activity in the UM.

### ***Gata2* and *Gata6* genes regulate distinct subprograms of ureteric SMC differentiation**

We have recently reported that *Gata2* is expressed in the UM and that its conditional loss leads to a delayed onset of SMC differentiation, ureter dilatation in fetal life and hydroureteronephrosis after birth (Weiss et al., 2019). Given the coexpression of *Gata6* with *Gata2* in the UM, and the strong similarity of phenotypic changes of the upper urinary tract upon individual loss in the UM, it appears possible that *Gata2* and *Gata6* act in a common pathway for *Myocd* activation. However, our analyses have shown

that the two genes are differentially regulated (*Gata6* depends on BMP4, *Gata2* on RA signaling), and that the loss of either gene in the UM leads to greatly differing molecular changes at E14.5. While GATA2, at least partially, acts as a feed-back inhibitor for RA signaling (Weiss et al., 2019), deregulation of RA signalling is irrelevant for the SMC defects in *Gata6cKO* ureters, and direct regulation of *Myocd* seems likely. Moreover, we did not find genetic interaction when combining loss-of-function alleles of both genes. Last but not least, GATA2 and GATA6 belong to different subfamilies whose members preferentially interact with themselves (Tremblay et al., 2018)

Similar to *Gata2*-deficient ureters, *Gata6cKO* ureters regained considerable peristaltic performance when relieved from urinary pressure in an *ex vivo* culture setting. While this confirms that increased hydrostatic pressure exacerbates the SMC defects *in vivo*, it highlights that a temporary artificial bypass *in vivo* may provide an opportunity to the mesenchymal coat to (re-)differentiate contractile SMCs and regain peristaltic activity. Irrespective of future therapeutic options for congenital forms of hydroureter formation in human patients, *Gata6* and *Gata2* are candidates to include in mutational screens for monogenetic causes of these disease entities.



## Material and methods

### Mouse work

Mice for conditional inactivation of *Gata6* (*Gata6<sup>tm2.1Sad</sup>*, synonym: *Gata6<sup>fl/fl</sup>*) (Sodhi et al., 2006) were obtained from Jörg Heineke (previously Medizinische Hochschule Hannover, now Medical Faculty Mannheim, Germany) after permission from Steve Duncan (Medical University of South Carolina, Charleston, SC, USA); mice for conditional inactivation of bone morphogenetic protein 4 (*Bmp4*) (Kulesa and Hogan, 2002) were received from Rolf Zeller (University of Basel, Switzerland) after permission from Brigid Hogan (Duke University Medical Center, Durham, NC, USA). Rolf Kemler (Max-Planck-Institute for Immunobiology and Epigenetics, Freiburg/Germany) provided mice for conditional inactivation of catenin, beta (*Ctnnb1*) (*Ctnnb1<sup>tm2Kem</sup>*, synonym: *Ctnnb1<sup>fl</sup>*) (Brault et al., 2001). Mice for conditional inactivation of smoothened (*Smo*) (*Smo<sup>tm2Amc</sup>*, synonyms: *Smo<sup>fl</sup>*, JAX #004526) (Long et al., 2001) were purchased from the Jackson lab (JAX #004526, Bar Harbor, Maine, USA). The cre driver line *Tbx18<sup>tm4(cre)Akis</sup>* (synonym: *Tbx18<sup>cre</sup>*) was previously generated in the lab (Airik et al., 2010).

All mouse lines were maintained on an NMRI outbred background. NMRI wild-type embryos were used for expression analysis. Embryos for phenotypic analyses were derived from matings of males double heterozygous for *Tbx18<sup>cre</sup>* line and the floxed loss-of-function allele with females homozygous for the same floxed loss-of-function allele. Littermates without the *Tbx18<sup>cre</sup>* allele were used as controls. For timed pregnancies, vaginal plugs were checked on the morning after mating; noon was taken as E0.5. Embryos and urogenital systems were dissected in PBS. Specimens were fixed in 4% PFA/PBS, transferred to methanol and stored at -20°C prior to further processing. PCR genotyping was performed on genomic DNA prepared from yolk sacs or liver biopsies. The experiments were approved by the local Institutional Animal Care and Research Advisory Committee and permitted by the Lower Saxony State Office for Consumer Protection and Food Safety (reference number 42500/1H).

### Organ cultures

Ureters were dissected from the embryo, explanted on 0.4 µm polyester membrane Transwell supports (#3450, Corning Inc., Lowell, MA, USA) and cultured at the air-liquid interface with DMEM/F12 supplemented with 1% of concentrated stocks of Penicillin/Streptomycin, sodium pyruvate, glutamax, non-essential amino acids

(#21331020, #15140122, #11360070, #35050038, #11140035, Thermo Fisher Scientific, Waltham, MA, USA) and 10% FCS (S0115, Biochrom, Berlin, Germany) or IST-G (insulin-transferrin-selenium, #41400045, Thermo Fisher Scientific, Waltham, MA, USA) (only in experiment Fig. S10). Recombinant mouse BMP4 (5020-BP, R&D Systems, Minneapolis, MN, USA) was dissolved in 4 mM HCl to a final concentration of 100 ng/ml. The BMP4 inhibitor NOGGIN (#ZO3205, Biozol/GenScript, Piscataway Township, NJ, USA) was dissolved in water to 10 µg/ml. BMS493 (#3509, Tocris Bioscience, Minneapolis, MN, USA) or RA (#0695, Tocris) were dissolved in DMSO and added to the medium at a final concentration of 1 µM. The culture medium was replaced every second day. Contra-lateral kidneys were used as controls. For video documentation, the cultures were acclimatized to room conditions and then imaged in a bright field channel for 1 min with a frame rate of 5 per second. Measurement of the contractions per minute and the peristaltic intensity was done either manually or via computational Fiji Multi-Kymograph analysis (Schindelin et al., 2012). Therefore, the length of the ureter was subdivided into 25 ( $\hat{=}$  proximal level), 50 ( $\hat{=}$  medial level) or 75 ( $\hat{=}$  distal level) percentiles. One contraction was set to 100 frames representing 20 sec in real time. Kymograph grey values were divided by the maximum grey value and ratios were plotted with Microsoft Excel (Microsoft Corp., Redmond, WA, USA).

### **Histological analysis**

Embryos and urogenital systems were embedded in paraffin and sectioned to 5 µm. Hematoxylin and eosin staining was performed according to standard procedures. Ink injection experiments were performed as described (Airik et al., 2006).

### **RNA *in situ* hybridization analysis**

Section *in situ* hybridization on 10 µm paraffin sections was performed as previously described (Moorman et al., 2001). Whole mount *in situ* hybridization of whole kidney rudiments or kidney cultures followed a standard procedure with digoxigenin-labeled antisense riboprobes (Wilkinson and Nieto, 1993).

### **Reverse transcription-quantitative polymerase chain reaction (RT-qPCR)**

Total RNA was isolated from 3 pools of 10 ureters each of E14.5 control and *Gata6cKO* embryos using TRIzol (#15596-018, Thermo Fisher Scientific). cDNA was synthesized from 2.5 µg total RNA applying RevertAid H Minus reverse transcriptase (#EP0452,

Thermo Fisher Scientific) as described (Thiesler et al., 2021). The NCBI tool Primer3 version 4.1 was used to design specific primers (Table S12). RT-quantitative (q)PCR was performed in 10  $\mu$ l 1:2 diluted BIO SyGreen Lo-ROX mix (PCR Biosystems, London, UK) with 400 nM primers and 1 ng/ $\mu$ l cDNA applying a QuantStudio3 PCR system fluorometric thermal cycler (Thermo Fisher Scientific). Each of the three biological replicates represents the average of four technical replicates. Data were processed by QuantStudio data analysis software (version 1.5.1, Thermo Fisher Scientific) using the comparative threshold cycle ( $\Delta\Delta C_T$ ) method with *Gapdh* (Werneburg et al., 2015) and *Ppia* as reference genes.

### **Microarray analysis**

Two pools of 10 E14.5 ureters each from male and female control and *Gata6cKO* embryos were collected. Total RNA was extracted using peqGOLD RNAPure (product #732-3312, order #30-1010, PeqLab Biotechnologie GmbH, Erlangen, Germany) and subsequently sent to the Research Core Unit Transcriptomics of Hannover Medical School where RNA was Cy3-labeled and hybridized to Agilent Whole Mouse Genome Oligo v2 (4x44K) microarrays (G4846A, Agilent Technologies Inc., Santa Clara, CA, USA). To identify differentially expressed genes, normalized expression data was filtered using Excel (Microsoft Corp., Redmond, WA, USA) based on an intensity threshold of 100 and a more than 1.9 fold change in all pools. Microarray data have been submitted to Gene Expression Omnibus (GEO, <http://www.ncbi.nlm.nih.gov/geo/>) (GSE174614).

### **Immunofluorescent detection of antigens**

For immunofluorescent stainings 5  $\mu$ m paraffin sections were stained as previously described (Bohnenpoll et al., 2017a). Primary antibodies and dilutions were used as follows: goat-anti-GATA6 (1:50, AF1700, R&D Systems, Minneapolis, MN, USA) or rabbit-anti-GATA6 (1:200, #5851, Cell Signaling Technology Europe B.V., Frankfurt, Germany), mouse-anti-ACTA2 (1:500, A5228, Sigma-Aldrich, St. Louis, MO, USA), rabbit-anti-TAGLN (1:200, ab14106, Abcam, Cambridge, UK), rabbit-anti- $\Delta$ NP63 (1:250, 619001, BioLegend, San Diego, CA, USA), rabbit-anti-KRT5 (1:250, PRB-160P, BioLegend), mouse-anti-UPK1B (1:200, WH0007348M, Sigma-Aldrich, St. Louis, MO, USA), rabbit-anti-TBX2 (1:200, 07-318, Merck Millipore, Darmstadt, Germany) and goat-anti-TBX3 (1:500, sc-31656, Santa Cruz Biotechnology, Inc., Santa

Cruz, CA, USA). Goat-anti-rabbit Alexa488 (1:250, A11034, Invitrogen, Invitrogen, Carlsbad, CA, USA), donkey-anti-mouse Alexa488 (1:250, A21202, Invitrogen), goat-anti-mouse Alexa555 (1:500, A21422, Invitrogen), biotinylated goat-anti-rabbit (1:200, 111065033, Dianova, Hamburg, Germany) and biotinylated donkey-anti-goat (1:200, 705-065-003, Dianova) were used as secondary antibodies. For amplification of the antibodies the TSA Tetramethylrhodamine Amplification Kit (1:100, NEL701001KT, PerkinElmer, Waltham, MA, USA) was used. After antigen retrieval (#H-3300, Antigen Unmasking Solution, Vector Laboratories, Burlingame, CA, USA; 15 minutes, 100°C), labeling of primary antibodies was performed over night at 4°C. Labeling of secondary antibodies was performed for 1 h at RT in blocking solution.

### **Cell proliferation and apoptosis assays**

Cell proliferation rates were investigated by the detection of incorporated BrdU on 5 µm paraffin sections according to published protocols (Bussen et al., 2004). For the analysis 12 sections per specimen (n=3) and genotype of the proximal ureter were stained. The BrdU-labeling index was defined as the number of BrdU-positive nuclei relative to the total number of nuclei as detected by counterstaining of nuclei with 4',6-diamidino-2-phenylindole (DAPI, # 6335.1, Carl Roth, Karlsruhe, Germany) in histologically defined compartments of the ureter. Apoptosis in tissues was assessed by the TUNEL assay using the ApopTag Plus Fluorescein *In Situ* Apoptosis Detection Kit (S7111, Merck KGaA, Darmstadt, Germany) on 5-µm paraffin sections.

### **Statistics**

For statistical analysis the two-tailed Student's t-test was performed and the data were expressed as mean ± standard deviation. For relative analyses wildtype values were set to 1. Differences were considered significant with a P-value below 0.05 (p<0.05, \*), highly significant (p≤0.005, \*\*) and extremely significant (p≤ 0.0005, \*\*\*).

### **Image documentation**

Sections and organ cultures were photographed using a DM5000 microscope (Leica Camera, Wetzlar, Germany) with Leica DFC300FX digital camera or a Leica DM6000 microscope with Leica DFC350FX digital camera. Urogenital systems were documented using a Leica M420 microscope with a Fujix HC-300Z digital camera (Fujifilm Holdings, Minato/Tokyo, Japan). Whole mount *in situ* hybridizations of cultured kidney

rudiments were documented using a Leica Z6 APO microscope with Leica DFC420C digital camera. Figures were prepared with Adobe Photoshop CS3 and CS4 (Adobe, San Jose, CA, USA).

### **Acknowledgments**

We thank Rolf Kemler, Rolf Zeller and Brigid Hogan for mice, Swagata Goswami for help, Rita Gerardy-Schahn for providing lab space, and the Research Core Unit Transcriptomics of Hannover Medical School for microarray analysis.

### **Competing interests statement**

No competing interests declared.

### **Funding**

This work was supported by grants from the Deutsche Forschungsgemeinschaft (DFG KI728/7-2 and 9-2) to A.K.

### **Data availability**

Microarray data have been deposited in Gene Expression Omnibus under accession number GSE174614.

## References

- Abe, M., Hasegawa, K., Wada, H., Morimoto, T., Yanazume, T., Kawamura, T., Hirai, M., Furukawa, Y. and Kita, T.** (2003). GATA-6 is involved in PPAR $\gamma$ -mediated activation of differentiated phenotype in human vascular smooth muscle cells. *Arterioscler Thromb Vasc Biol* **23**, 404-410.
- Airik, R., Bussen, M., Singh, M. K., Petry, M. and Kispert, A.** (2006). Tbx18 regulates the development of the ureteral mesenchyme. *J Clin Invest* **116**, 663-674.
- Airik, R., Trowe, M. O., Foik, A., Farin, H. F., Petry, M., Schuster-Gossler, K., Schweizer, M., Scherer, G., Kist, R. and Kispert, A.** (2010). Hydroureteronephrosis due to loss of Sox9-regulated smooth muscle cell differentiation of the ureteric mesenchyme. *Hum Mol Genet* **19**, 4918-4929.
- Aydogdu, N., Rudat, C., Trowe, M. O., Kaiser, M., Ludtke, T. H., Taketo, M. M., Christoffels, V. M., Moon, A. and Kispert, A.** (2018). TBX2 and TBX3 act downstream of canonical WNT signaling in patterning and differentiation of the mouse ureteric mesenchyme. *Development* **145**, dev171827.
- Baker, C. V. and Bronner-Fraser, M.** (1997). The origins of the neural crest. Part I: embryonic induction. *Mech Dev* **69**, 3-11.
- Bohnenpoll, T., Bettenhausen, E., Weiss, A. C., Foik, A. B., Trowe, M. O., Blank, P., Airik, R. and Kispert, A.** (2013). Tbx18 expression demarcates multipotent precursor populations in the developing urogenital system but is exclusively required within the ureteric mesenchymal lineage to suppress a renal stromal fate. *Dev Biol* **380**, 25-36.
- Bohnenpoll, T., Feraric, S., Nattkemper, M., Weiss, A. C., Rudat, C., Meuser, M., Trowe, M. O. and Kispert, A.** (2017a). Diversification of Cell Lineages in Ureter Development. *J Am Soc Nephrol* **28**, 1792-1801.
- Bohnenpoll, T. and Kispert, A.** (2014). Ureter growth and differentiation. *Semin Cell Dev Biol* **36C**, 21-30.
- Bohnenpoll, T., Weiss, A. C., Labuhn, M., Ludtke, T. H., Trowe, M. O. and Kispert, A.** (2017b). Retinoic acid signaling maintains epithelial and mesenchymal progenitors in the developing mouse ureter. *Sci Rep* **7**, 14803.
- Bohnenpoll, T., Wittern, A. B., Mamo, T. M., Weiss, A. C., Rudat, C., Kleppa, M. J., Schuster-Gossler, K., Wojahn, I., Ludtke, T. H., Trowe, M. O. et al.** (2017c). A SHH-FOXF1-BMP4 signaling axis regulating growth and differentiation of epithelial and mesenchymal tissues in ureter development. *PLoS Genet* **13**, e1006951.
- Brault, V., Moore, R., Kutsch, S., Ishibashi, M., Rowitch, D. H., McMahon, A. P., Sommer, L., Boussadia, O. and Kemler, R.** (2001). Inactivation of the beta-catenin gene by Wnt1-Cre-mediated deletion results in dramatic brain malformation and failure of craniofacial development. *Development* **128**, 1253-1264.
- Bussen, M., Petry, M., Schuster-Gossler, K., Leitges, M., Gossler, A. and Kispert, A.** (2004). The T-box transcription factor Tbx18 maintains the separation of anterior and posterior somite compartments. *Genes Dev* **18**, 1209-1221.
- Caubit, X., Lye, C. M., Martin, E., Core, N., Long, D. A., Vola, C., Jenkins, D., Garratt, A. N., Skaer, H., Woolf, A. S. et al.** (2008). Teashirt 3 is necessary for ureteral smooth muscle differentiation downstream of SHH and BMP4. *Development* **135**, 3301-3310.
- Chazaud, C., Dolle, P., Rossant, J. and Mollard, R.** (2003). Retinoic acid signaling regulates murine bronchial tubule formation. *Mech Dev* **120**, 691-700.
- Chiodini, B., Ghassemi, M., Khelif, K. and Ismaili, K.** (2019). Clinical Outcome of Children With Antenatally Diagnosed Hydronephrosis. *Front Pediatr* **7**, 103.
- Donadon, M. and Santoro, M. M.** (2021). The origin and mechanisms of smooth muscle cell development in vertebrates. *Development* **148**, dev197384.
- Dudley, J. A., Haworth, J. M., McGraw, M. E., Frank, J. D. and Tizard, E. J.** (1997). Clinical relevance and implications of antenatal hydronephrosis. *Arch Dis Child Fetal Neonatal Ed* **76**, F31-34.
- Ek, S., Lidfeldt, K. J. and Varricio, L.** (2007). Fetal hydronephrosis; prevalence, natural history and postnatal consequences in an unselected population. *Acta Obstet Gynecol Scand* **86**, 1463-1466.

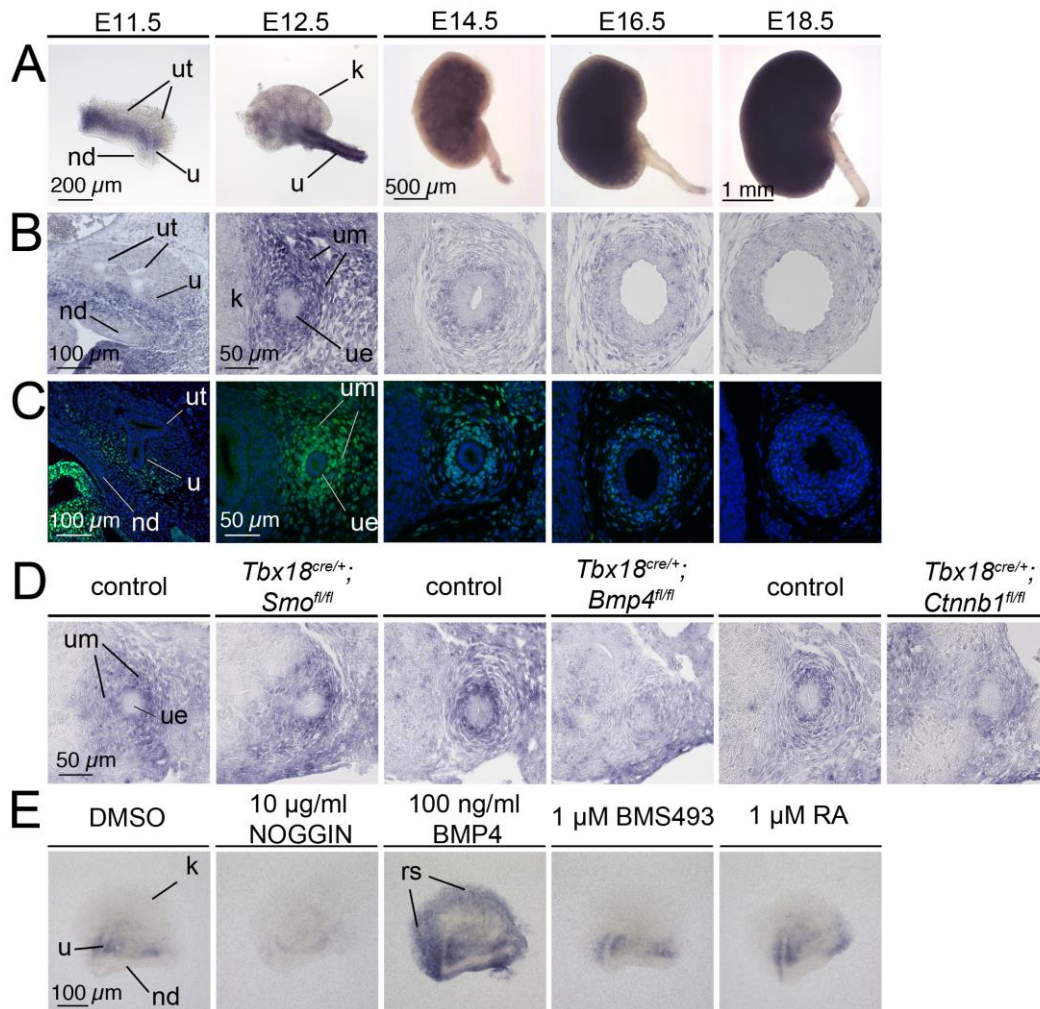
- Freyer, L., Schröter, C., Saiz, N., Schrode, N., Nowotschin, S., Martinez-Arias, A. and Hadjantonakis, A. K.** (2015). A loss-of-function and H2B-Venus transcriptional reporter allele for *Gata6* in mice. *BMC Dev Biol* **15**, 38.
- Hafner, R., Bohnenpoll, T., Rudat, C., Schultheiss, T. M. and Kispert, A.** (2015). *Fgfr2* is required for the expansion of the early adrenocortical primordium. *Mol Cell Endocrinol* **413**, 168-177.
- Herthelius, M., Axelsson, R. and Lidefelt, K. J.** (2020). Antenatally detected urinary tract dilatation: a 12-15-year follow-up. *Pediatr Nephrol* **35**, 2129-2135.
- Hollnagel, A., Oehlmann, V., Heymer, J., Ruther, U. and Nordheim, A.** (1999). *Id* genes are direct targets of bone morphogenetic protein induction in embryonic stem cells. *J Biol Chem* **274**, 19838-19845.
- Huang da, W., Sherman, B. T. and Lempicki, R. A.** (2009). Systematic and integrative analysis of large gene lists using DAVID bioinformatics resources. *Nat Protoc* **4**, 44-57.
- Ingham, P. W. and McMahon, A. P.** (2001). Hedgehog signaling in animal development: paradigms and principles. *Genes Dev* **15**, 3059-3087.
- Jho, E. H., Zhang, T., Domon, C., Joo, C. K., Freund, J. N. and Costantini, F.** (2002). Wnt/beta-catenin/Tcf signaling induces the transcription of *Axin2*, a negative regulator of the signaling pathway. *Mol Cell Biol* **22**, 1172-1183.
- Kanematsu, A., Ramachandran, A. and Adam, R. M.** (2007). GATA-6 mediates human bladder smooth muscle differentiation: involvement of a novel enhancer element in regulating alpha-smooth muscle actin gene expression. *Am J Physiol Cell Physiol* **293**, C1093-1102.
- Kodo K, N. T., Furutani M, Arai S, Yamamura E, Joo K, Takahashi T, Matsuoka R, Yamagishi H.** (2009). GATA6 mutations cause human cardiac outflow tract defects by disrupting semaphorin-plexin signaling. *Proc Natl Acad Sci US*. **106**, 13933-13938.
- Koutsourakis, M., Langeveld, A., Patient, R., Beddington, R. and Grosveld, F.** (1999). The transcription factor GATA6 is essential for early extraembryonic development. *Development* **126**, 723-732.
- Kulesa, H. and Hogan, B. L.** (2002). Generation of a loxP flanked *bmp4loxP-lacZ* allele marked by conditional lacZ expression. *Genesis* **32**, 66-68.
- Lakard, S., Lesniewska, Michel, G., Lakard, B., Morrand-Villeneuve, N. and Versaux-Botteri, C.** (2007). In vitro induction of differentiation by retinoic acid in an immortalized olfactory neuronal cell line. *Acta Histochem* **109**, 111-121.
- Lepore, J., Cappola, T. P., Mericko, P. A., Morrissey, E. E. and Parmacek, M. S.** (2005). GATA-6 regulates genes promoting synthetic functions in vascular smooth muscle cells. *Arterioscler Thromb Vasc Biol* **25**, 309-314.
- Lepore, J. J., Merick, o. P. A., Cheng, L., Lu, M. M., Morrissey, E. E. and Parmacek, M. S.** (2006). GATA-6 regulates semaphorin 3C and is required in cardiac neural crest for cardiovascular morphogenesis. *J Clin Invest* **116**, 929-939.
- Long, F., Zhang, X. M., Karp, S., Yang, Y. and McMahon, A. P.** (2001). Genetic manipulation of hedgehog signaling in the endochondral skeleton reveals a direct role in the regulation of chondrocyte proliferation. *Development* **128**, 5099-5108.
- Losa, M., Latorre, V., Andrabi, M., Ladam, F., Sagerström, C., Novoa, A., P., Z., Bridoux, L., Hanley, N. A., Mallo, M. and Bobola, N.** (2017). A tissue-specific, *Gata6*-driven transcriptional program instructs remodeling of the mature arterial tree. *Elife* **6**, e31362.
- Mack, C. P.** (2011). Signaling mechanisms that regulate smooth muscle cell differentiation. *Arterioscler Thromb Vasc Biol* **31**, 1495-1505.
- Mamo, T. M., Wittern, A. B., Kleppa, M. J., Bohnenpoll, T., Weiss, A. C. and Kispert, A.** (2017). BMP4 uses several different effector pathways to regulate proliferation and differentiation in the epithelial and mesenchymal tissue compartments of the developing mouse ureter. *Hum Mol Genet* **26**, 3553-3563.
- Mano, T., Luo, Z., Malendowicz, S. L., Evans, T. and Walsh, K.** (1999a). Reversal of GATA-6 downregulation promotes smooth muscle differentiation and inhibits intimal hyperplasia in balloon-injured rat carotid artery. *Circ Res* **84**, 647-654.

- Mano, T., Luo, Z., Malendowicz, S. L., Evans, T. and Walsh, K.** (1999b). Reversal of GATA-6 downregulation promotes smooth muscle differentiation and inhibits intimal hyperplasia in balloon-injured rat carotid artery. *Circ Res* **84**, 647-654.
- Mendelsohn, C., Ruberte, E., LeMeur, M., Morriss-Kay, G. and Chambon, P.** (1991). Developmental analysis of the retinoic acid-inducible RAR-beta 2 promoter in transgenic animals. *Development* **113**, 723-734.
- Moorman, A. F., Houweling, A. C., de Boer, P. A. and Christoffels, V. M.** (2001). Sensitive nonradioactive detection of mRNA in tissue sections: novel application of the whole-mount in situ hybridization protocol. *J Histochem Cytochem* **49**, 1-8.
- Morrisey, E. E., Ip, H. S., Lu, M. M. and Parmacek, M. S.** (1996). GATA-6: a zinc finger transcription factor that is expressed in multiple cell lineages derived from lateral mesoderm. *Dev Biol* **177**, 309-322.
- Morrisey, E. E., Tang, Z., Sigrist, K., Lu, M. M., Jiang, F., Ip, H. S. and Parmacek, M. S.** (1998). GATA6 regulates HNF4 and is required for differentiation of visceral endoderm in the mouse embryo. *Genes Dev* **12**, 3579-3590.
- Nemer, G. and Nemer, M.** (2003). Transcriptional activation of BMP-4 and regulation of mammalian organogenesis by GATA-4 and -6. *Dev Biol* **254**, 131-148.
- Norman, C., Runswick, M., Pollock, R. and Treisman, R.** (1988). Isolation and properties of cDNA clones encoding SRF, a transcription factor that binds to the c-fos serum response element. *Cell* **55**, 989-1003.
- Perlman, H., Suzuki, E., Simonson, M., Smith, R. C. and Walsh, K.** (1998). GATA-6 induces p21(Cip1) expression and G1 cell cycle arrest. *J Biol Chem* **273**, 13713-13718.
- Peterkin, T., Gibson, A. and Patient, R.** (2003). GATA-6 maintains BMP-4 and Nkx2 expression during cardiomyocyte precursor maturation. *EMBO J* **22**, 4260-4273.
- Rojas, A., De Val, S., Heidt, A. B., Xu, S. M., Bristow, J. and Black, B. L.** (2005). Gata4 expression in lateral mesoderm is downstream of BMP4 and is activated directly by Forkhead and GATA transcription factors through a distal enhancer element. *Development* **132**, 3405-3417.
- Rossi, J. M., Dunn, N. R., Hogan, B. L. and Zaret, K. S.** (2001). Distinct mesodermal signals, including BMPs from the septum transversum mesenchyme, are required in combination for hepatogenesis from the endoderm. *Genes Dev* **15**, 1998-2009.
- Schindelin, J., Arganda-Carreras, I., Frise, E., Kaynig, V., Longair, M., Pietzsch, T., Preibisch, S., Rueden, C., Saalfeld, S., Schmid, B. et al.** (2012). Fiji: an open-source platform for biological-image analysis. *Nat Methods* **9**, 676-682.
- Sharma, A., Wasson, L. K., Willcox, J. A., Morton, S. U., Gorham, J. M., DeLaughter, D. M., Neyazi, M., Schmid, M., Agarwal, R., Jang, M. Y. et al.** (2020). GATA6 mutations in hiPSCs inform mechanisms for maldevelopment of the heart, pancreas, and diaphragm. *Elife* **9**, e53278.
- Sidell, N. and Horn, R.** (1985). Properties of human neuroblastoma cells following induction by retinoic acid. *Prog Clin Biol Res* **175**, 39-53.
- Sodhi, C. P., Li, J. and Duncan, S. A.** (2006). Generation of mice harbouring a conditional loss-of-function allele of Gata6. *BMC Dev Biol* **6**, 19.
- Sun, Q., Chen, G., Streb, J. W., Long, X., Yang, Y., Stoeckert, C. J., Jr. and Miano, J. M.** (2006). Defining the mammalian CARGome. *Genome Res* **16**, 197-207.
- Tevosian, S. G., Jimenez, E., Hatch, H. M., Jiang, T., Morse, D. A., Fox, S. C. and Padua, M. B.** (2015). Adrenal Development in Mice Requires GATA4 and GATA6 Transcription Factors. *Endocrinology* **156**, 2503-2517.
- Thiesler, H., Beimdiek, J. and Hildebrandt, H.** (2021). Polysialic acid and Siglec-E orchestrate negative feedback regulation of microglia activation. *Cell Mol Life Sci* **78**, 1637-1653.
- Tremblay, M., Sanchez-Ferras, O. and Bouchard, M.** (2018). GATA transcription factors in development and disease. *Development* **145**, dev164384.
- Trowe, M. O., Airik, R., Weiss, A. C., Farin, H. F., Foik, A. B., Bettenhausen, E., Schuster-Gossler, K., Taketo, M. M. and Kispert, A.** (2012). Canonical Wnt signaling regulates smooth muscle precursor development in the mouse ureter. *Development* **139**, 3099-3108.

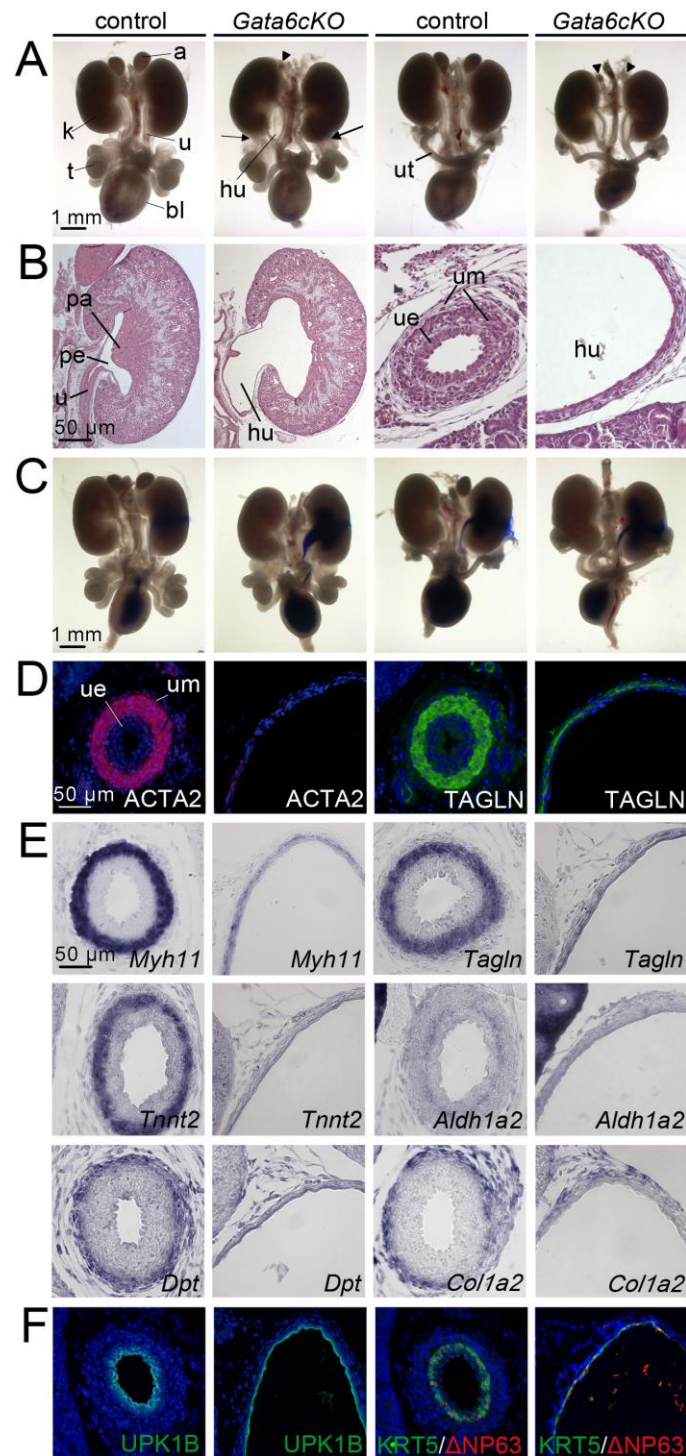


- van Tuyn, J., Knaän-Shanzer, S., van de Watering, M. J., de Graaf, M., van der Laarse, A., Schalijs, M. J., van der Wall, E. E. and de Vries, A. A. (2005). Activation of cardiac and smooth muscle-specific genes in primary human cells after forced expression of human myocardin. *Cardiovasc Res* **67**, 245-255.
- Wada, H., Hasegawa, K., Morimoto, T., Kakita, T., Yanazume, T., Abe, M. and Sasayama, S. (2002). Calcineurin-GATA-6 pathway is involved in smooth muscle-specific transcription. *J Cell Biol* **156**, 983-991.
- Wang, D., Chang, P. S., Wang, Z., Sutherland, L., Richardson, J. A., Small, E., Krieg, P. A. and Olson, E. N. (2001). Activation of cardiac gene expression by myocardin, a transcriptional cofactor for serum response factor. *Cell* **105**, 851-862.
- Wang, D. Z. and Olson, E. N. (2004). Control of smooth muscle development by the myocardin family of transcriptional coactivators. *Curr Opin Genet Dev* **14**, 558-566.
- Wang, Z., Wang, D. Z., Pipes, G. C. and Olson, E. N. (2003). Myocardin is a master regulator of smooth muscle gene expression. *Proc Natl Acad Sci USA* **100**, 7129-7134.
- Weiss, A. C., Bohnenpoll, T., Kurz, J., Blank, P., Airik, R., Ludtke, T. H., Kleppa, M. J., Deuper, L., Kaiser, M., Mamo, T. M. et al. (2019). Delayed onset of smooth muscle cell differentiation leads to hydronephrosis formation in mice with conditional loss of the zinc finger transcription factor gene *Gata2* in the ureteric mesenchyme. *J Pathol* **248**, 452-463.
- Weiss, R. M., Guo, S., Shan, A., Shi, H., Romano, R. A., S., S., L.G., C. and Guo, J. K. (2013). *Brg1* determines urothelial cell fate during ureter development. *J Am Soc Nephrol* **24**, 618-626.
- Werneburg, S., Buettner, F. F., Mühlhoff, M. and Hildebrandt, H. (2015). Polysialic acid modification of the synaptic cell adhesion molecule SynCAM 1 in human embryonic stem cell-derived oligodendrocyte precursor cells. *Stem Cell Res* **14**, 339-346.
- Whissell, G., Montagni, E., Martinelli, P., Hernando-Momblona, X., Sevillano, M., Jung, P., Cortina, C., Calon, A., Abuli, A. et al. (2014). The transcription factor GATA6 enables self-renewal of colon adenoma stem cells by repressing BMP gene expression. *Nat Cell Biol* **16**, 695-707.
- Wilkinson, D. G. and Nieto, M. A. (1993). Detection of messenger RNA by in situ hybridization to tissue sections and whole mounts. *Methods Enzymol* **225**, 361-373.
- Yin, F. and Herring, B. P. (2005). GATA-6 can act as a positive or negative regulator of smooth muscle-specific gene expression. *J Biol Chem* **280**, 4745-4752.
- Yu, J., Carroll, T. J. and McMahon, A. P. (2002). Sonic hedgehog regulates proliferation and differentiation of mesenchymal cells in the mouse metanephric kidney. *Development* **129**, 5301-5312.
- Yu, Z., Mannik, J., Soto, A., Lin, K. K. and Andersen, B. (2009). The epidermal differentiation-associated Grainyhead gene *Get1/Grhl3* also regulates urothelial differentiation. *EMBO J* **28**, 1890-1903.
- Zeng, L. and Childs, S. J. (2012). The smooth muscle microRNA miR-145 regulates gut epithelial development via a paracrine mechanism. *Dev Biol* **367**, 178-186.
- Zhao, R., Watt, A. J., Battle, M. A., Li, J., Bondow, B. J. and Duncan, S. A. (2008). Loss of both GATA4 and GATA6 blocks cardiac myocyte differentiation and results in acardia in mice. *Dev Biol* **317**, 614-619.
- Zhao, R., Watt, A. J., Li, J., Luebke-Wheeler, J., Morrissey, E. E. and Duncan, S. A. (2005). GATA6 is essential for embryonic development of the liver but dispensable for early heart formation. *Mol Cell Biol* **25**, 2622-2631.
- Zimmerman, L. B., De Jesus-Escobar, J. M. and Harland, R. M. (1996). The Spemann organizer signal noggin binds and inactivates bone morphogenetic protein 4. *Cell* **86**, 599-606.

## Figures/Figure legends

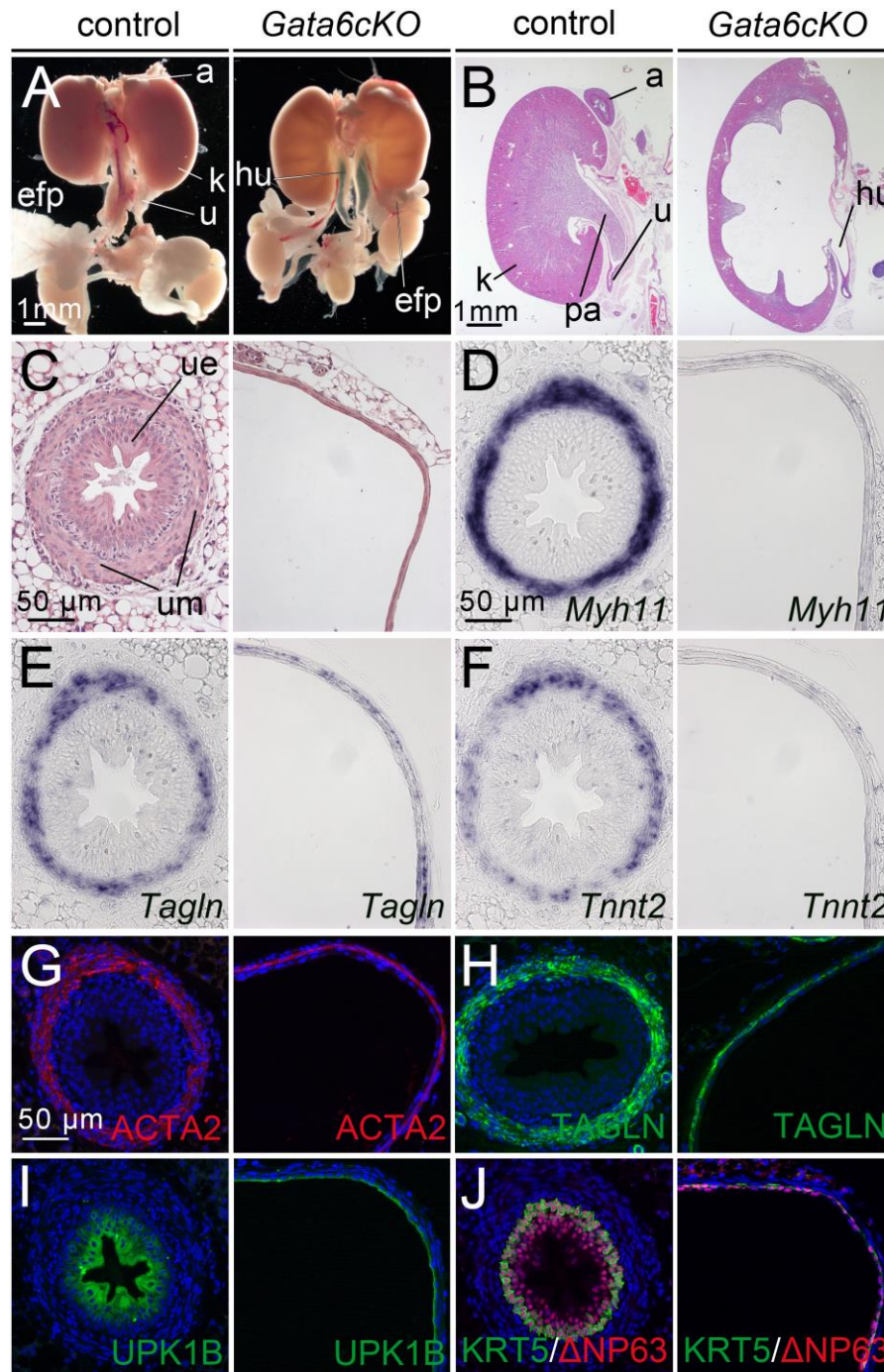


**Fig. 1. *Gata6* expression in the undifferentiated mesenchyme of the developing ureter depends on BMP4.** (A,B) RNA *in situ* hybridization analysis of *Gata6* expression in whole kidneys and ureters (A), and on sections of the metanephros (E11.5) and of the proximal ureter region (B) derived from E12.5 to E18.5 wildtype embryos. (C) Immunofluorescence analysis of the GATA6 protein on sections of the metanephros region (E11.5) and of the proximal ureter region of E12.5 to E18.5 wildtype embryos. Nuclei are counterstained with DAPI. (D) RNA *in situ* hybridization analysis of *Gata6* expression on transverse sections through the posterior trunk region of E12.5 control embryos, of embryos with loss of *Ctnnb1*-dependent WNT signaling (*Tbx18<sup>cre/+</sup>; Ctnnb1<sup>fl/fl</sup>*), with loss of SHH/SMO signaling (*Tbx18<sup>cre/+</sup>; Smo<sup>fl/fl</sup>*), and loss of *Bmp4* (*Tbx18<sup>cre/+</sup>; Bmp4<sup>fl/fl</sup>*) in the UM. (E) RNA *in situ* hybridization of *Gata6* expression in E11.5 ureter/kidney explants grown for 18 h with DMSO (control), 10  $\mu$ g/ml of the BMP4 antagonist NOGGIN, 100 ng/ml BMP4, 1  $\mu$ M of the pan-RAR inhibitor BMS493, and 1  $\mu$ M RA. At least three ( $n \geq 3$ ) independent specimens were analyzed for each assay. k, kidney; nd, nephric duct; rs, renal stroma; u, ureter; ue, ureteric epithelium; um, ureteric mesenchyme; ut, ureteric tip.

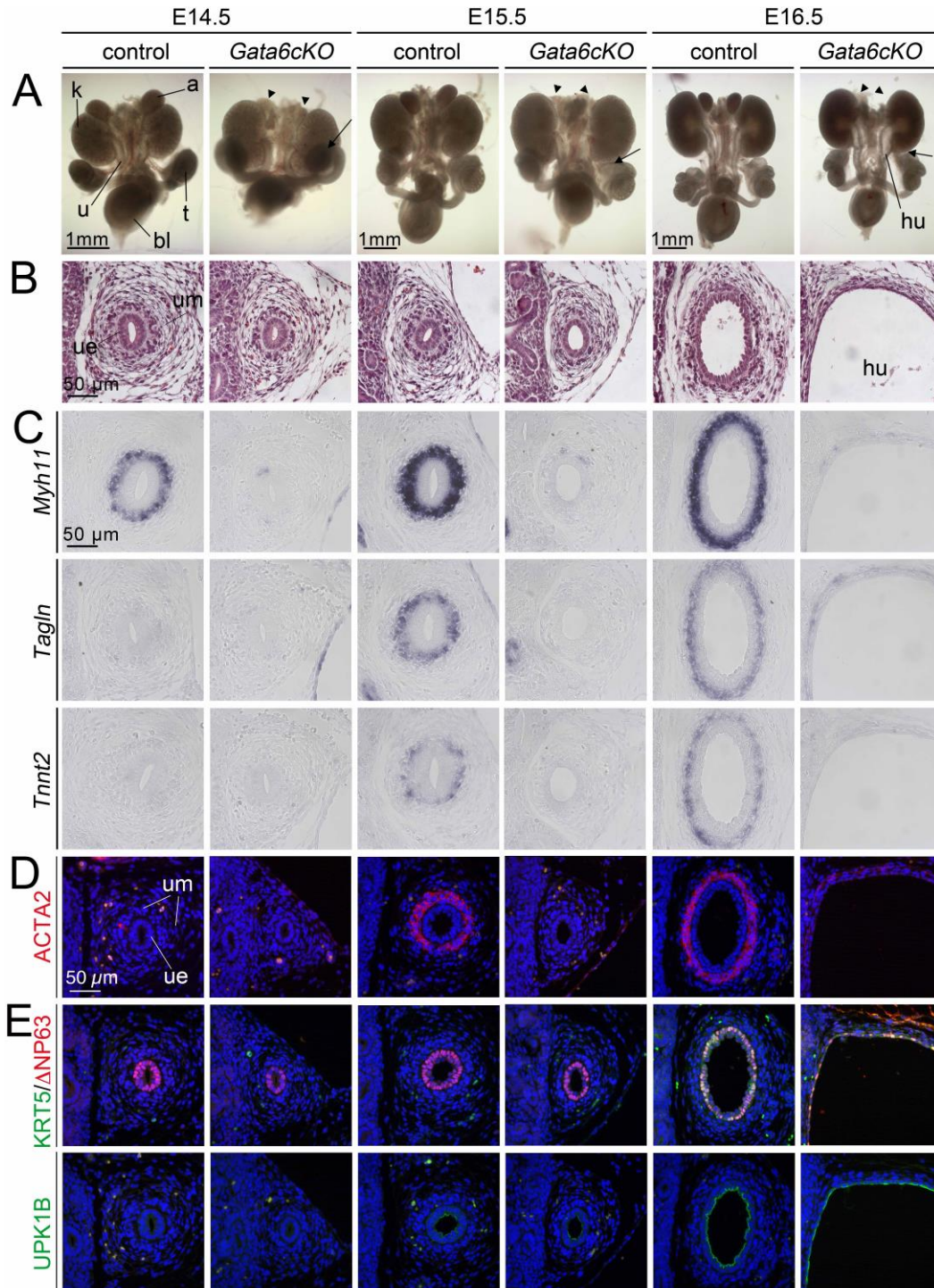


**Fig. 2. *Gata6cKO* embryos develop severe hydroureter due to functional insufficiency of the UM at E18.5.** (A) Morphology of whole urogenital systems of male (column 1 and 2) and female embryos (column 3 and 4). Arrows point to the attachment of the epididymal fat pad to the kidney, arrowheads point to hypoplastic adrenals in the mutant (control n=65; *Gata6cKO* n=49). (B) Hematoxylin and eosin staining on sagittal kidney sections (column 1 and 2) and transverse sections of the proximal ureter (column 3 and 4); n=3 for each genotype. (C) Analysis of physical obstruction along the ureter and the vesico-ureteric junction by ink injection into the renal pelvis (control n=6; *Gata6cKO* n=5). (D-F) Cyto-differentiation of the UM (D,E) and of the urothelium (F) as shown by immunofluorescence (D,F) and by section RNA *in situ* hybridization analysis (E) of markers. n>=3 for each marker per genotype. a, adrenal; bl, bladder; hu, hydroureter; k, kidney; pa, papilla; pe, pelvis; u, ureter; ue, ureteric epithelium; um, ureteric mesenchyme; ut, uterus; t, testis.



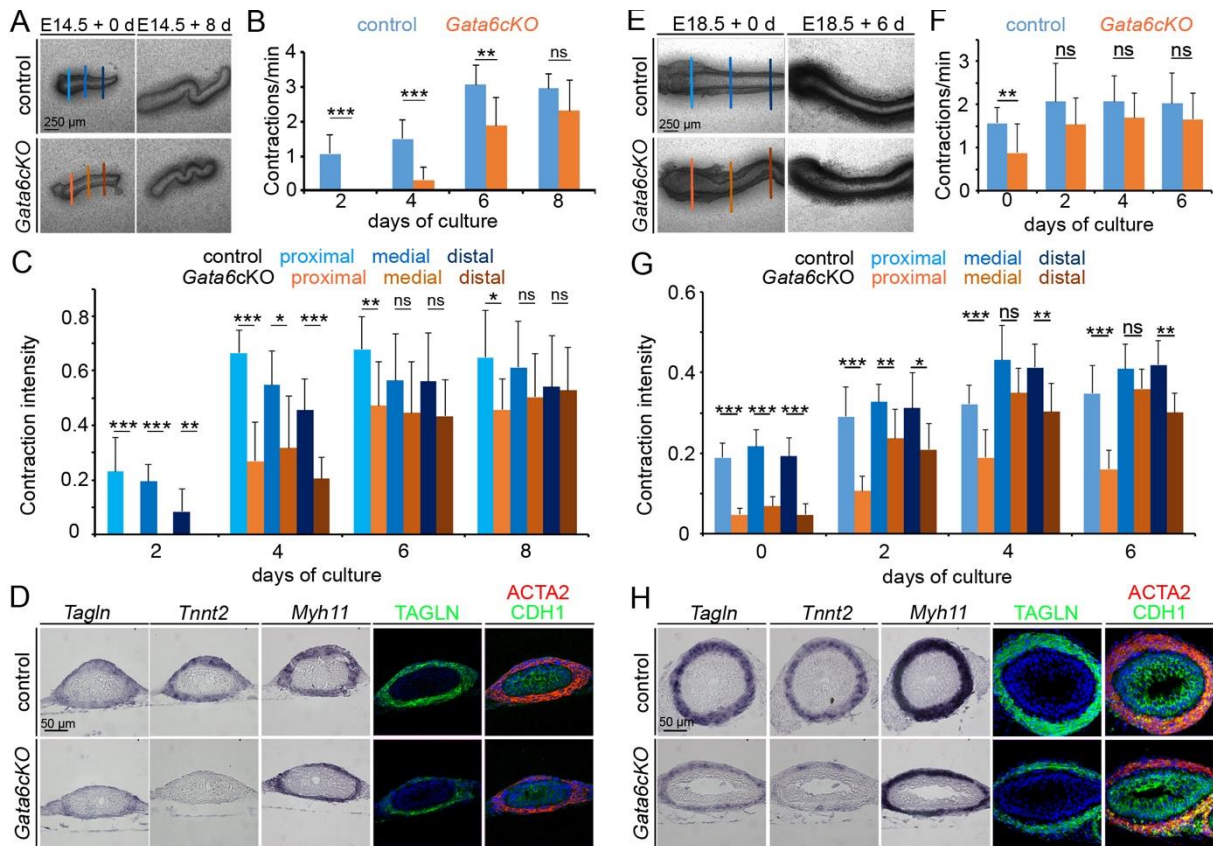


**Fig. 3. *Gata6cKO* mice exhibit severe hydronephrosis at P21.** (A) Morphology of whole urogenital systems of male mice (control  $n=7$ , mutant  $n=8$ ). Note the attachment of the epididymal fat pad to the kidney, lack of adrenals and hydronephrosis (hu) in the mutant. (B,C) Hematoxylin and eosin staining on sagittal kidney sections (B) and transverse sections of the proximal ureter (C). (D-G) Analysis of expression of SMC markers on transverse sections of the proximal ureter region by *in situ* hybridization (D-F) and by immunofluorescence (G) reveals reduced SMC differentiation in the mutant. (H,I) Analysis of urothelial differentiation by (co-)immunofluorescent detection the B-cell marker KRT5 and the I-cell marker DNP63 (H) and the S-cell marker UPK1B (I). (G-I) Nuclei are counterstained with DAPI. At least three ( $n \geq 3$ ) independent specimens were analyzed for each assay (B-I). a, adrenal; hu, hydronephrosis; efp, epididymal fat pad; k, kidney; pa, papilla; u, ureter; ue, ureteric epithelium; um, ureteric mesenchyme.

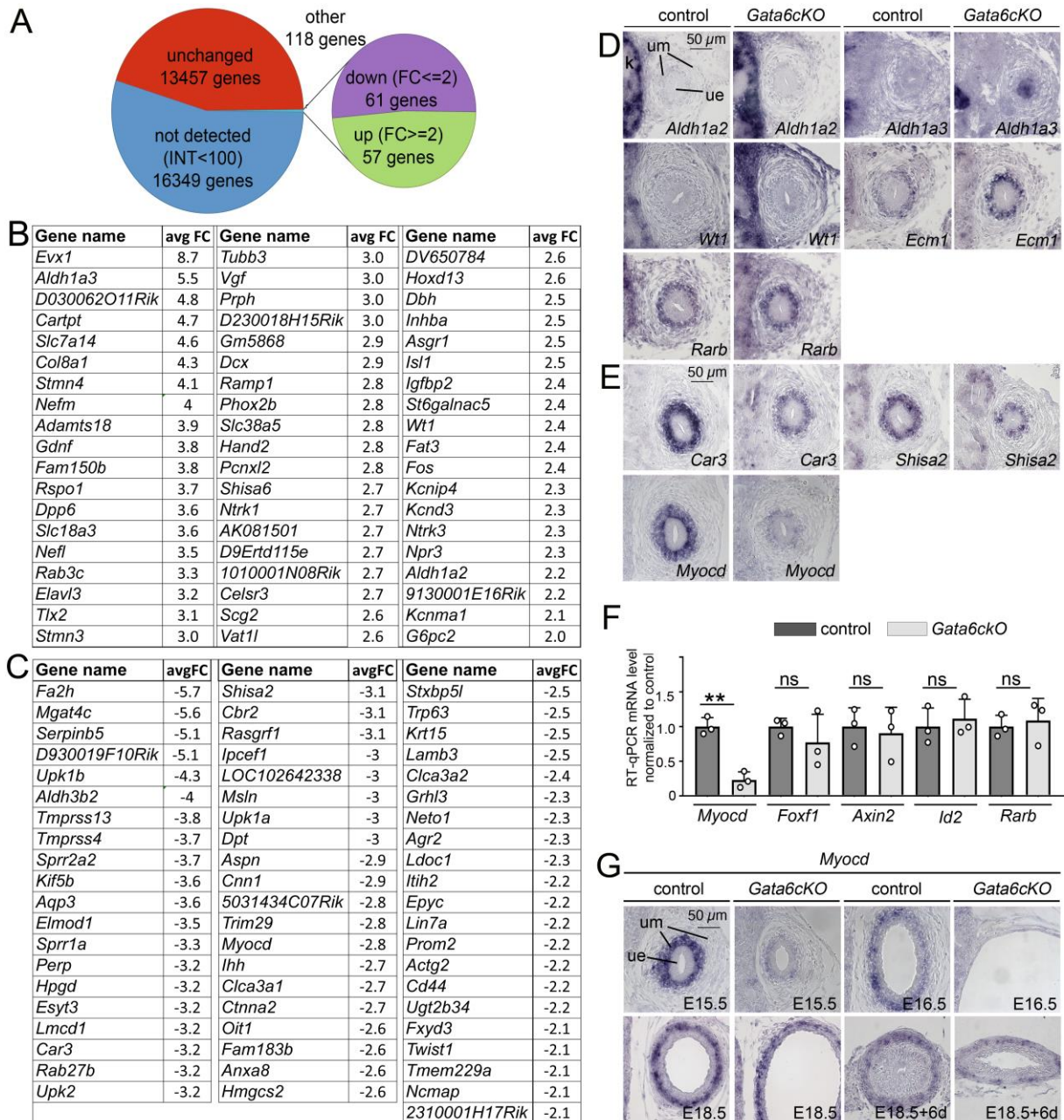


**Fig. 4. SMC differentiation is not initiated in *Gata6cKO* ureters at E14.5 to E16.5.** (A) Morphology of whole urogenital systems of male embryos. Arrowheads mark hypoplastic adrenals, arrows point to undescended testes (E14.5: control n=6, *Gata6cKO* n=7, E15.5: control n=6, *Gata6cKO* n=5, E16.5: control n=24, *Gata6cKO* n=7). (B) Hematoxylin and eosin staining on transverse sections of the proximal ureter shows hydronephrotic ureter formation at E16.5, i.e. shortly after onset of urine production in the kidney. (C,D) Expression analysis of SMC markers by RNA *in situ* hybridization on proximal ureter sections (C) and by immunofluorescence (D). (E) Cytodifferentiation of the urothelium as shown by immunofluorescence for KRT5, DNP63 and UPK1B. Nuclei are counterstained with DAPI (D,E). n>=3, each genotype and assay (B-E). a, adrenal gland; bl, bladder; hu, hydronephrotic ureter; k, kidney; ue, ureteric mesenchyme; um, ureteric mesenchyme.



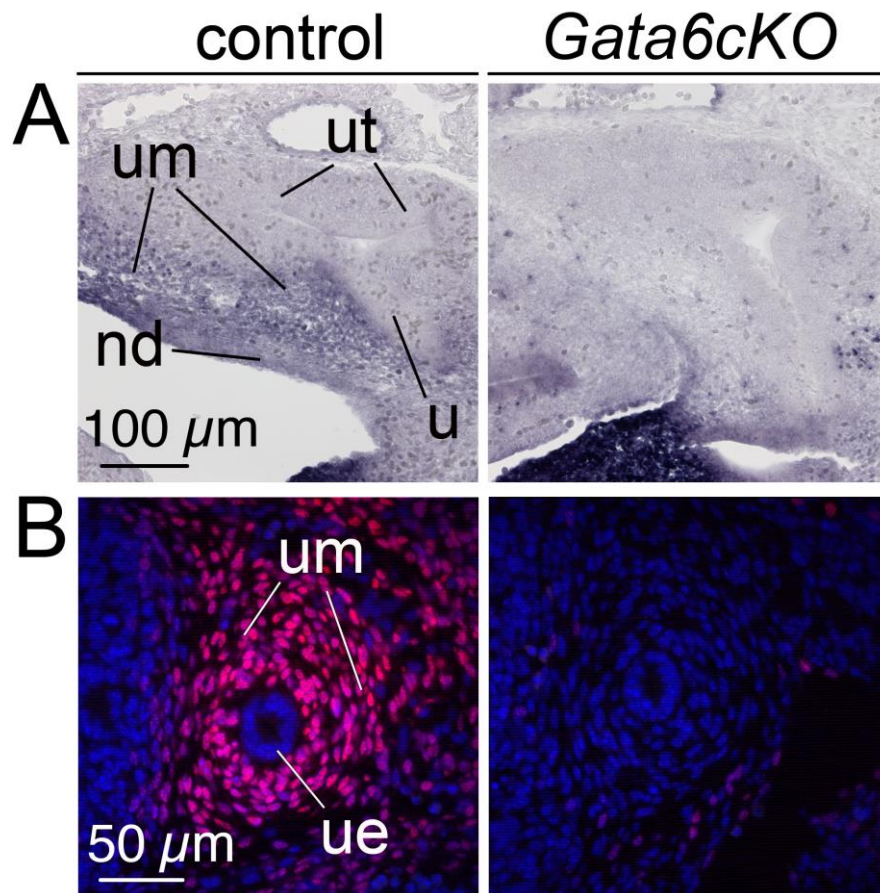


**Fig. 5. Peristaltic activity and SMC differentiation are regained in *Gata6cKO* ureters in absence of hydrostatic pressure.** (A) E14.5 ureters were explanted and grown for 8 days in culture. Vertical lines indicate proximal, medial, and distal ureter levels. Morphology and peristaltic activity was monitored every second day using video-microscopy. (B) Statistical analysis of peristaltic activity (expressed as contractions per min) of control (n=8) and mutant ureters (n=8). Bar graphs display mean±sd. Differences were considered significant with a P-value below 0.05 ( $p < 0.05$ , \*), highly significant ( $p \leq 0.005$ , \*\*) and extremely significant ( $p \leq 0.0005$ , \*\*\*), two-tailed Student's *t*-test. For source data and statistics see Table S2. (C) Analysis of contraction intensity measured at proximal, medial and distal levels of E14.5 ureters. Significance levels are as in (B). For source data and statistics see Table S3. (D) Analysis of SMC differentiation of the UM by RNA *in situ* hybridization and immunofluorescence of markers on sections of explants of E14.5 ureters grown for 6 days in culture.  $n \geq 3$ , each genotype and probe. (E) E18.5 ureters were explanted and grown for 6 days in culture. Vertical lines indicate proximal, medial, and distal ureter levels. (F) Statistical analysis of peristaltic activity (expressed as contractions per min) of control (n=8) and mutant ureters (n=11). Bar graphs display mean±sd. Significance levels are as in (B). For source data and statistics see Table S4. (G) Analysis of contraction intensity measured at proximal, medial and distal levels of E18.5 ureters. Significance levels are as in (B). For source data and statistics see Table S5. (H) Analysis of SMC differentiation of the UM by RNA *in situ* hybridization and immunofluorescence of markers on sections of explants of E18.5 ureters grown for 6 days in culture.  $n \geq 3$ , each genotype and probe.



**Fig. 6. Expression of *Myocd* is delayed and reduced in *Gata6cKO* ureters.** (A) Pie chart summarizing the results from the microarray analysis of E14.5 control and *Gata6cKO* ureters. (B,C) List of 57 genes with increased expression ( $FC \geq 2.0$ ) (B) and list of 61 genes with decreased expression ( $FC \leq -2.0$ ) (C) in the microarray analysis of E14.5 *Gata6cKO* ureters. (D,E) RNA *in situ* hybridization analysis on sections of the proximal ureter at E14.5 for genes encoding components and targets of RA signaling (D), and for microarray candidates (E). (F) RT-qPCR results of expression of selected genes in three independent total RNA pools of E14.5 control and *Gata6cKO* ureters. Differences were considered non-significant (ns) with a P-value  $> 0.05$ ; significant (\*)  $p \leq 0.05$ , highly significant (\*\*)  $p \leq 0.01$ ; two-tailed Student's t-test. For values and statistics see Table S10. (G) RNA *in situ* hybridization analysis of *Myocd* expression on sections of the proximal ureter at E15.5, E16.5, E18.5, and of ureters explanted at E18.5 and cultured for 6 days. k, kidney; ue, ureteric epithelium; um, ureteric mesenchyme.

## Supplemental Figures




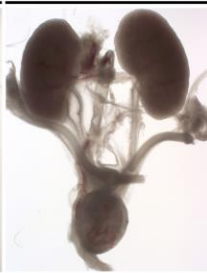



**Fig. S1. The *Tbx18<sup>cre</sup>* driver line mediates conditional deletion of *Gata6* in the UM.** (A) *In situ* hybridization analysis of *Gata6* expression on sagittal sections of the metanephros of E11.5 wildtype and *Gata6cKO* (*Tbx18<sup>cre/+</sup>;Gata6<sup>fl/fl</sup>*) embryos using a probe against exon2, which is floxed in the *Gata6<sup>fl</sup>* allele. (B) Immunofluorescence analysis of GATA6 protein on proximal sections of the ureter at E12.5.  $n \geq 3$  each assay and genotype. nd, nephric duct; ue, ureteric epithelium; um, ureteric mesenchyme; ut, ureteric tip; u, ureter.



**A**

Genotype	<i>Tbx18</i> <sup>+/+</sup> ; <i>Gata6</i> <sup>fl/+</sup>	<i>Tbx18</i> <sup>+/+</sup> ; <i>Gata6</i> <sup>fl/fl</sup>	<i>Tbx18</i> <sup>cre/+</sup> ; <i>Gata6</i> <sup>fl/+</sup>	<i>Tbx18</i> <sup>cre/+</sup> ; <i>Gata6</i> <sup>fl/fl</sup>
(expected %)	(25%)	(25%)	(25%)	(25%)
E11.5, n=94	26 (28%)	25 (27%)	21 (22%)	22 (23%)
E12.5, n=896	220 (25%)	206 (23%)	251 (28%)	219 (24%)
E14.5, n=575	132 (23%)	139 (24%)	151 (26%)	153 (27%)
E15.5, n=95	31 (33%)	19 (20%)	19 (20%)	26 (27%)
E16.5, n=102	33 (32%)	22 (22%)	24 (23%)	23 (23%)
E18.5, n=205	57 (28%)	45 (22%)	48 (23%)	55 (27%)

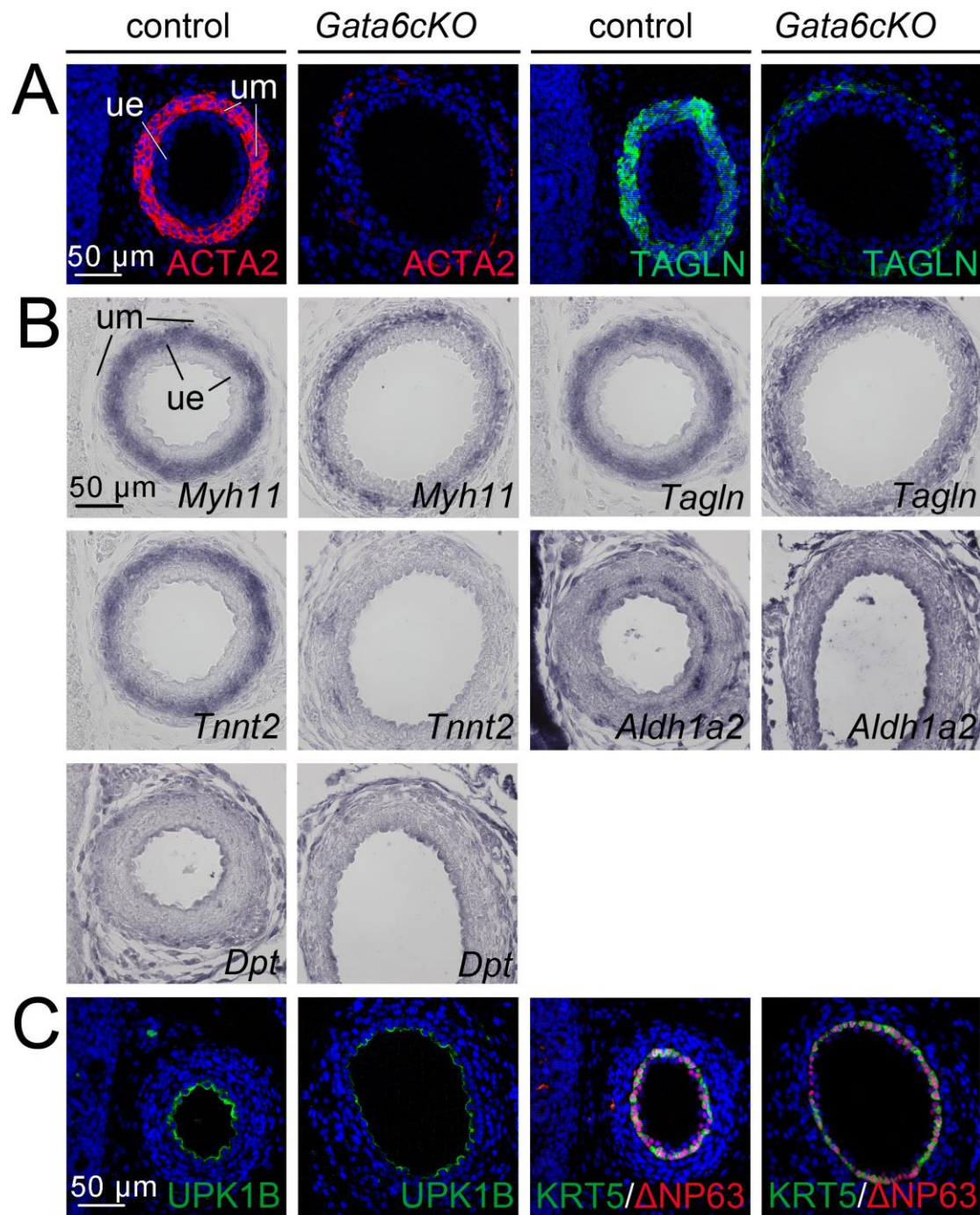
**B**

normal	unilateral weak hu	unilateral strong hu	bilateral weak hu	bilateral strong hu
				

**C**

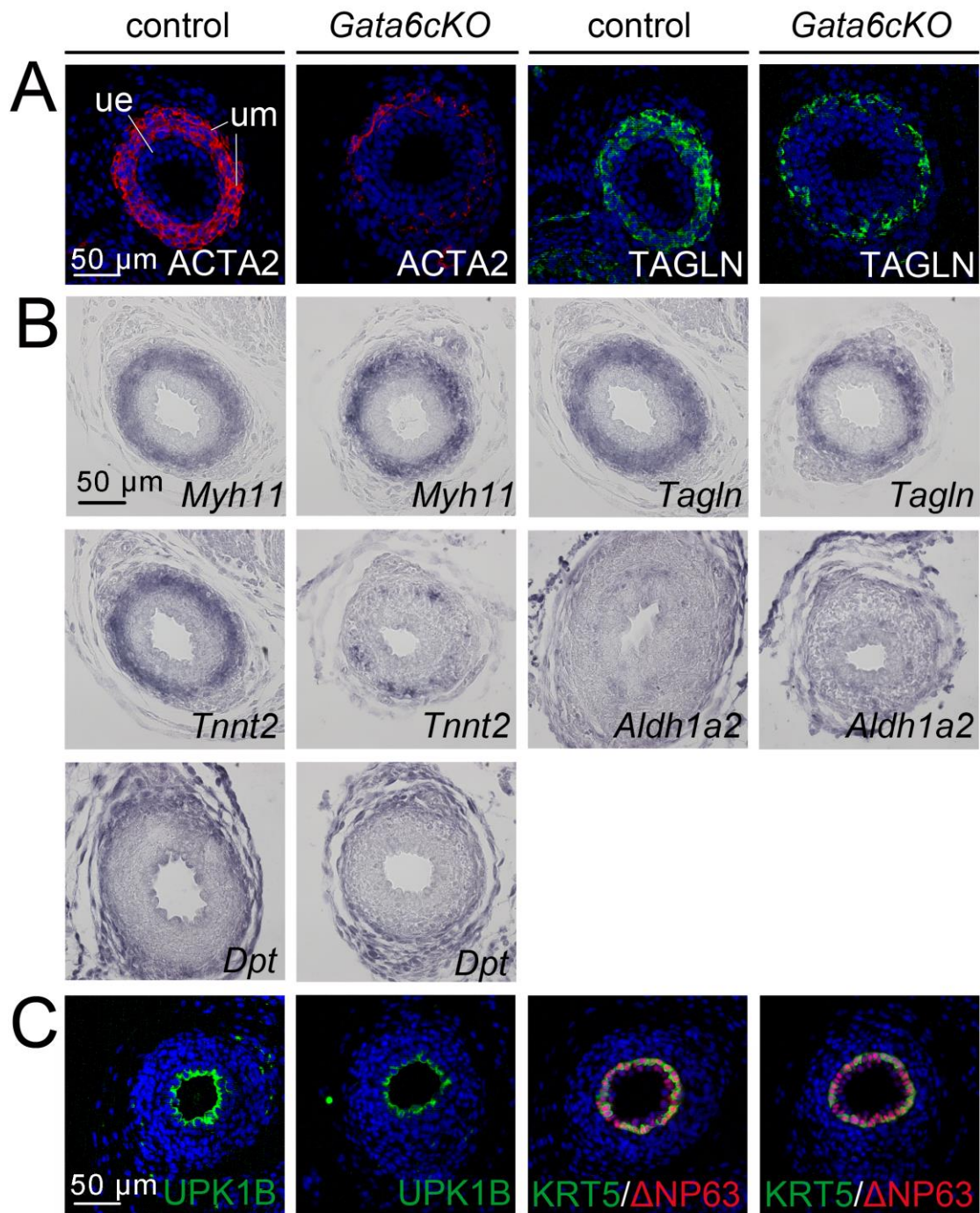
Genotype	Control	<i>Tbx18</i> <sup>cre/+</sup> ; <i>Gata6</i> <sup>fl/+</sup>	<i>Tbx18</i> <sup>cre/+</sup> ; <i>Gata6</i> <sup>fl/fl</sup>
normal	59 (91%)	9 (28%)	10 (20%)
unilateral weak hydronephrosis	4 (6%)	9 (28%)	7 (14%)
unilateral strong hydronephrosis	0	3 (9%)	4 (8%)
bilateral weak hydronephrosis	2 (3%)	11 (35%)	15 (31%)
bilateral strong hydronephrosis	0	0	13 (27%)
total number	65	32	49

**Fig. S2. *Gata6cKO* embryos are viable and display ureter dilatation of variable severity at E18.5.** (A) Distribution of genotypes in litters of matings of *Tbx18*<sup>cre/+</sup>;*Gata6*<sup>fl/+</sup> males with *Gata6*<sup>fl/fl</sup> females at the indicated stages. Shown are the stages, the number of embryos, the expected and obtained frequency of the indicated genotypes. (B) Morphology of whole urogenital systems of E18.5 *Gata6cKO* embryos displaying different grades of hydronephrosis (hu) used for classification in the Table shown in (C). (C) Distribution of ureter dilatations of different severity in *Tbx18*<sup>cre/+</sup>;*Gata6*<sup>fl/+</sup> and *Tbx18*<sup>cre/+</sup>;*Gata6*<sup>fl/fl</sup> embryos at E18.5.

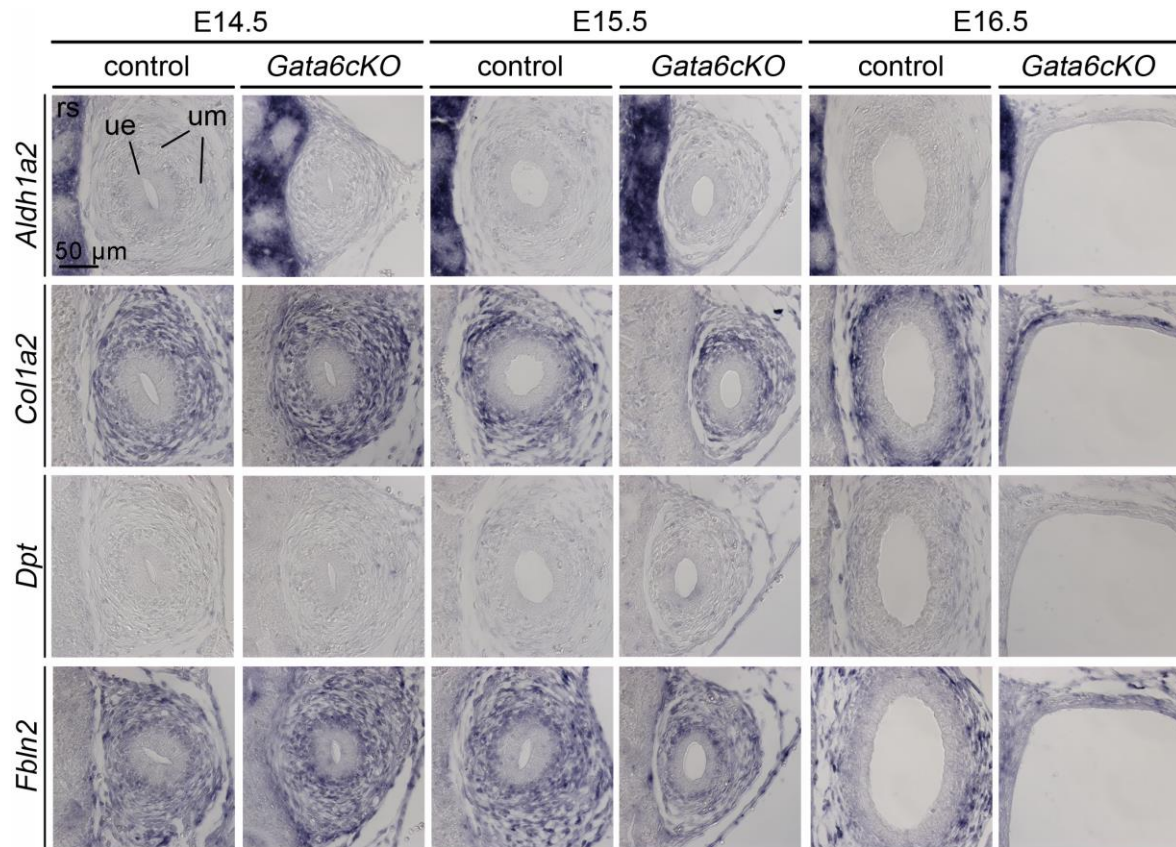


**Fig. S3. Weak proximal hydroureter is associated with reduced expression of SMC markers in *Gata6cKO* embryos at E18.5.** (A) Immunofluorescence of the SMC markers ACTA2 and TAGLN and (B) RNA *in situ* hybridization analysis of SMC genes (*Tagln*, *Tnnt2*, *Myh11*), of the lamina propria marker *Aldh1a2*, and of the tunica adventitia marker *Dpt* on transverse sections of the proximal ureter. (C) Analysis of urothelial differentiation by immunofluorescent detection of the B-cell marker KRT5, the I-cell marker  $\Delta$ NP63 and the S-cell marker UPK1B on proximal ureter sections. Nuclei are counterstained with DAPI (blue, in A and C). ue, ureteric epithelium; um, ureteric mesenchyme.



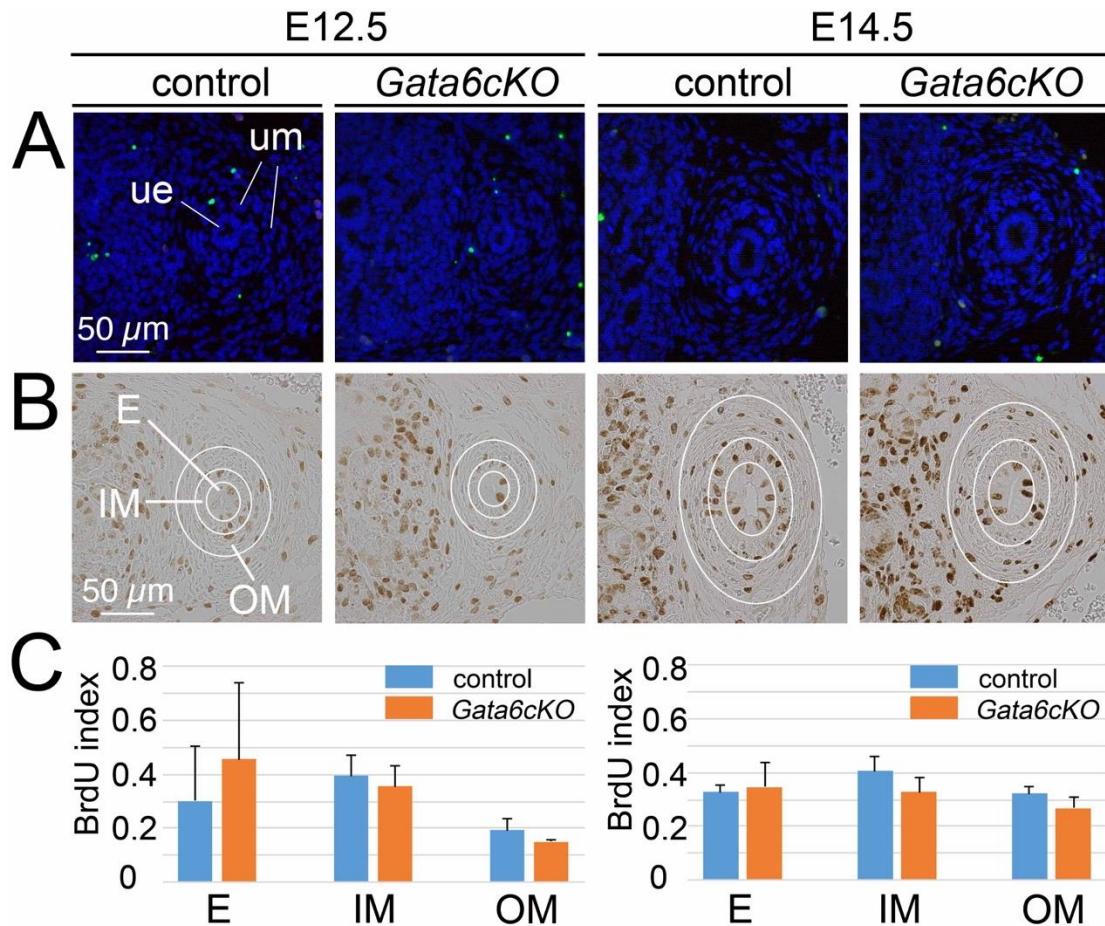


**Fig. S4. Expression of SMC markers is partly reduced in distal ureters in *Gata6cKO* embryos at E18.5.** (A) Immunofluorescence of the SMC markers ACTA2 and TAGLN and (B) RNA *in situ* hybridization analysis of SMC genes (*Tagln*, *Tnnt2*, *Myh11*), of the lamina propria marker *Aldh1a2*, and of the tunica adventitia marker *Dpt* on transverse sections of the proximal ureter. (C) Analysis of urothelial differentiation by immunofluorescent detection of the B-cell marker KRT5, the I-cell marker  $\Delta$ NP63 and the S-cell marker UPK1B on proximal ureter sections. Nuclei are counter-stained with DAPI (blue, in A and C). ue, ureteric epithelium; um, ureteric mesenchyme.

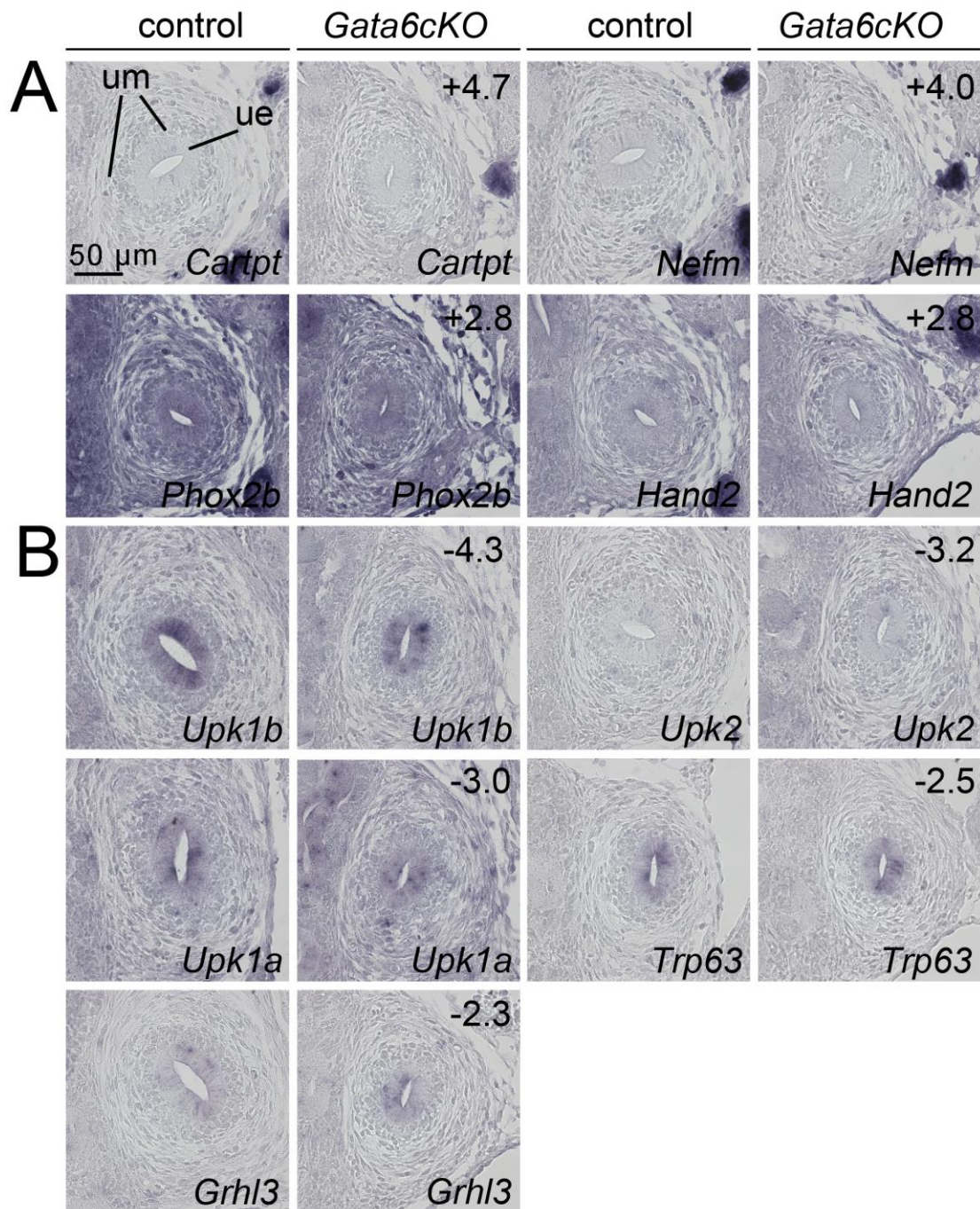


**Fig. S5. Differentiation of fibrocytes is unchanged in *Gata6cKO* ureters at E14.5 to E16.5.** Shown are RNA *in situ* hybridization analyses on sections of the proximal ureter at E14.5, E15.5 and E16.5 of control and *Gata6cKO* embryos for the *lamina propria* marker *Aldh1a2* and the *tunica adventitia* markers *Col1a2*, *Dpt*, *Fbln2*. rs, renal stroma; ue, ureteric epithelium; um, ureteric mesenchyme.



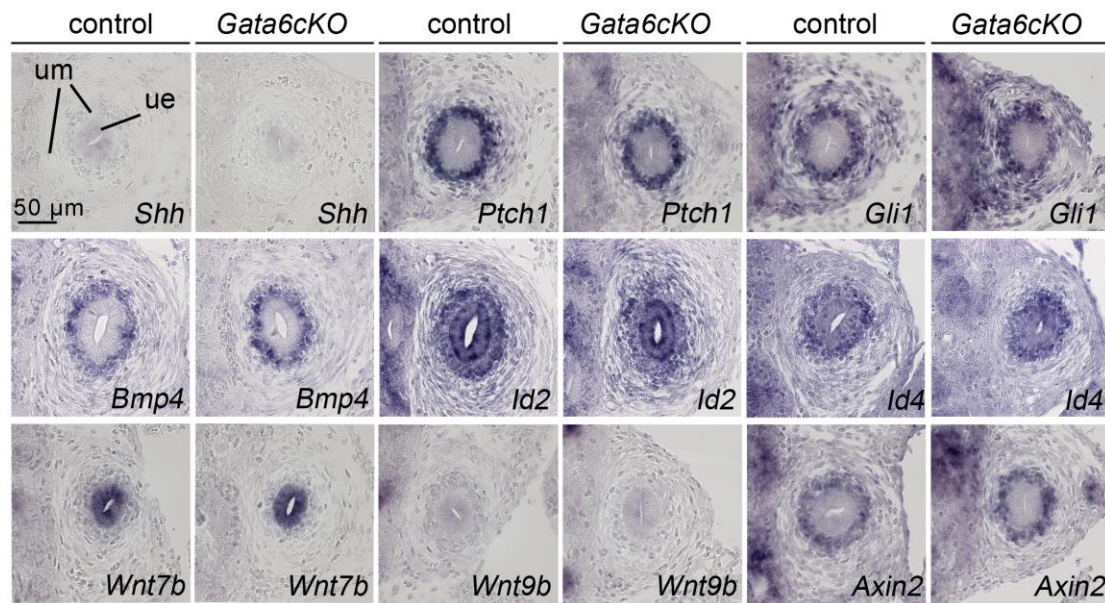


**Fig. S6. Proliferation and apoptosis are not affected in *Gata6cKO* embryos at E12.5 and E14.5.** (A) Immunofluorescent analysis of apoptosis (green) by the TUNEL assay on proximal ureter sections. Nuclei are counterstained with DAPI (blue). ue, ureteric epithelium; um, ureteric mesenchyme. (B) Immunohistochemical detection of BrdU on proximal ureter sections. White circles demarcate the ureteric epithelium (E), the inner and outer mesenchymal cell populations (IM and OM). (C) Quantification of BrdU-positive cells in E12.5 control (n=3) versus mutant (n=3) ureters. Values are displayed as mean  $\pm$  sd. All values are ns, *i.e.*  $P > 0.05$ ; two-tailed Student's t-test. For source data and statistics see Table S1.

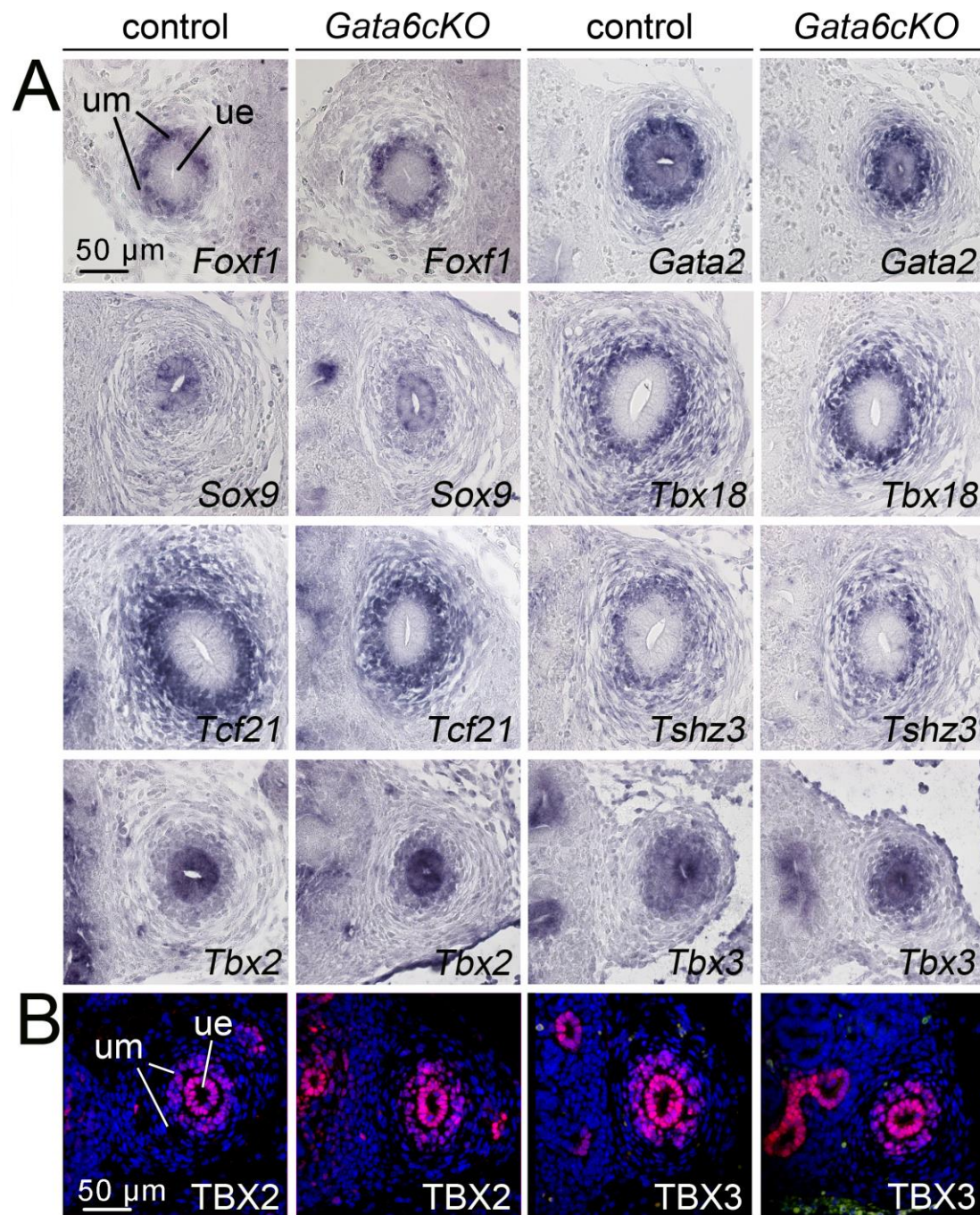


**Fig. S7. RNA *in situ* hybridization analysis of genes with altered expression in microarrays of E14.5 *Gata6cKO* ureters.** (A,B) Shown are RNA *in situ* hybridization analyses of proximal ureter sections of control and *Gata6cKO* embryos for genes with increased expression (A) and genes with decreased expression (B) in *Gata6cKO* microarrays. Probes, genotypes and fold changes in the microarray are as indicated.  $n \geq 3$ , all probes. ue, ureteric epithelium; um, ureteric mesenchyme.



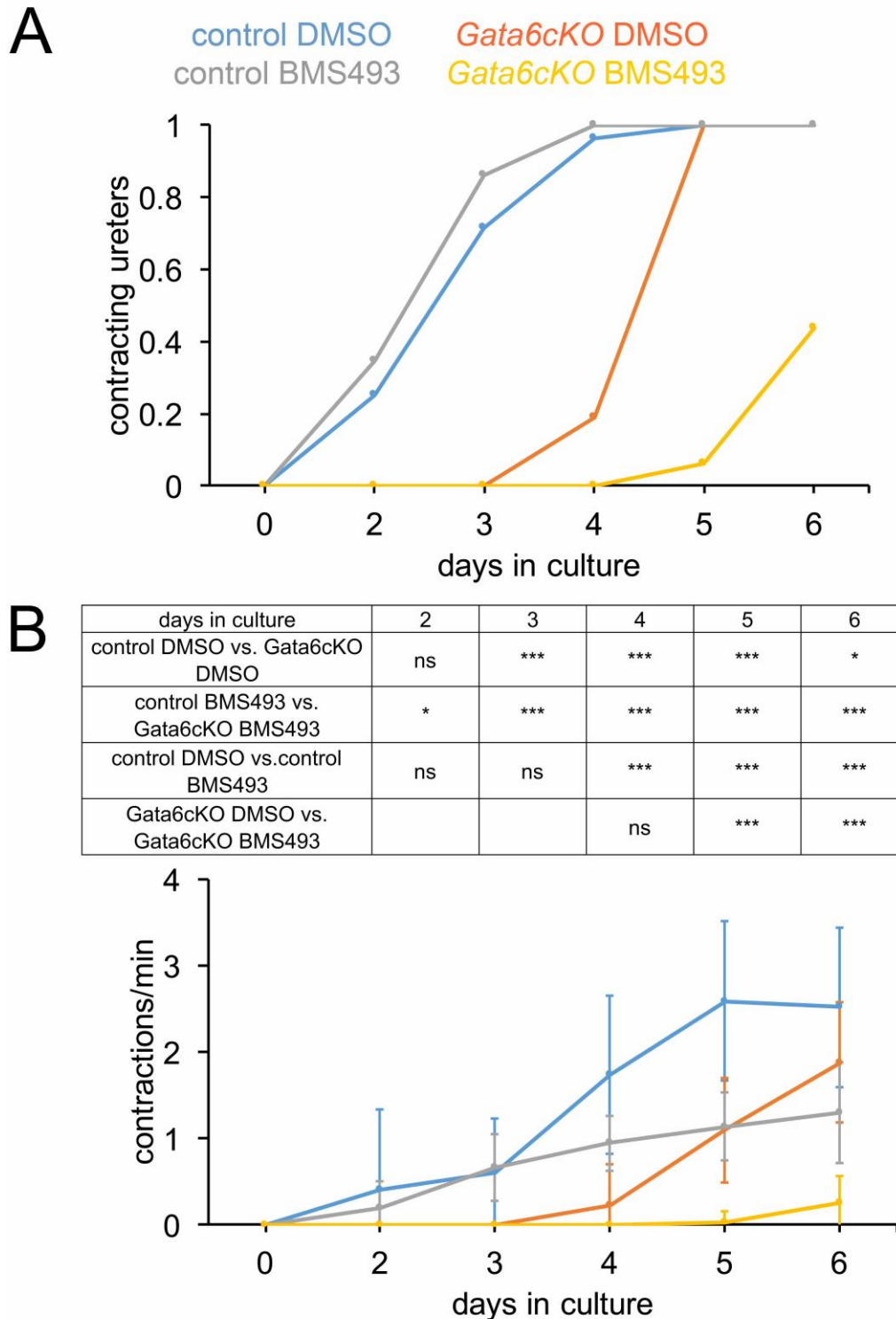


**Fig. S8. Signaling pathways relevant for SMC differentiation are unchanged in their activity/expression in *Gata6cKO* ureters at E14.5.** Shown are RNA *in situ* hybridization analyses on sections of the proximal ureter of E14.5 control and *Gata6cKO* embryos of *Shh*, and the targets of SHH signaling, *Ptch1* and *Gli1*; of *Wnt7b* and *Wnt9b*, and the WNT target gene *Axin2*; of *Bmp4*, and its target genes *Id2* and *Id4*.  $n \geq 3$  each marker, each genotype. ue, ureteric epithelium; um, ureteric mesenchyme.

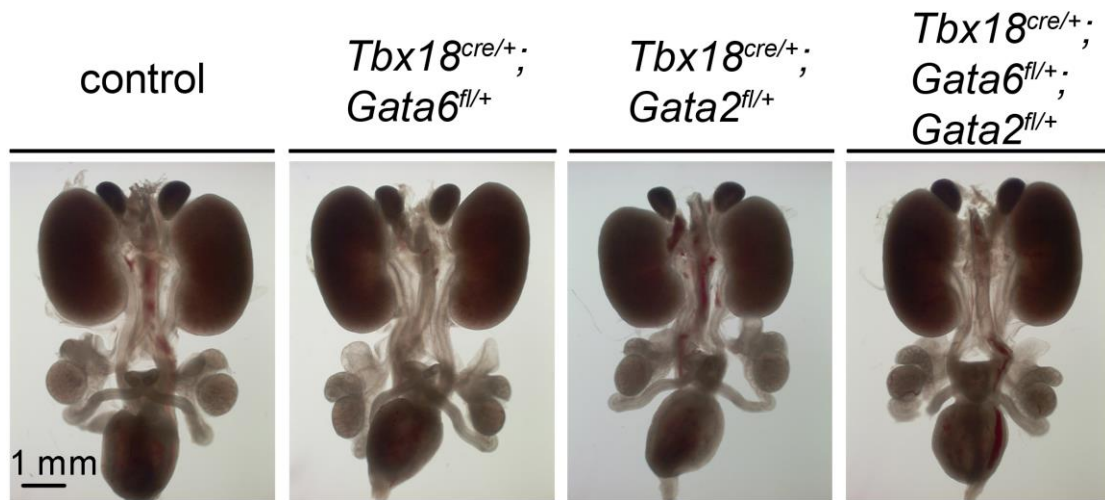


**Fig. S9. Transcription factors relevant for SMC differentiation are unchanged in their expression in *Gata6cKO* ureters at E14.5.** (A) RNA *in situ* hybridization analysis for expression of *Foxf1*, *Gata2*, *Sox9*, *Tbx18*, *Tcf21*, *Tshz3*, *Tbx2*, *Tbx3* and (B) immunofluorescence analysis of TBX2 and TBX3 on sections of the proximal ureter at E14.5 of control and *Gata6cKO* embryos. Nuclei are counterstained with DAPI (B).  $n \geq 3$  each marker, each genotype. ue, ureteric epithelium; um, ureteric mesenchyme.





**Fig. S10. Reduction of RA signaling does not rescue peristalsis defects in *Gata6cKO* ureters.** Kidney rudiments from E13.5 control and *Gata6cKO* embryos were explanted and cultured for 6 days in the presence of DMSO (control) or 1  $\mu$ M of the RA signaling inhibitor BMS493. Peristalsis was monitored daily in 1-min intervals. (A) Percentage of ureters that show peristaltic activity at the individual days during the culture period. (B) Statistical analysis of peristaltic activity (expressed as contractions per min) of control DMSO-treated (n=28), control BMS493-treated (n=29), mutant DMSO-treated (n=16) and mutant BMS493-treated (n=16) ureters. Bar graphs display mean  $\pm$ sd. Differences were considered significant with a P-value below 0.05 ( $p < 0.05$ , \*), highly significant ( $p \leq 0.005$ , \*\*) and extremely significant ( $p \leq 0.0005$ , \*\*\*); two-tailed Student's *t*-test. For source data and statistics see Table S11.



**Fig. S11. *Gata2* and *Gata6* do not interact in SMC differentiation in the developing ureter.** Morphological analysis of whole urogenital systems of control (n=20),  $Tbx18^{cre/+}; Gata6^{fl/+}$  (n=14),  $Tbx18^{cre/+}; Gata2^{fl/+}$  (n=3) and  $Tbx18^{cre/+}; Gata2^{fl/+}; Gata6^{fl/+}$  (n=20) embryos at E18.5.

## Supplementary tables

<b>E12.5</b>	<b>E</b>	<b>IM</b>	<b>OM</b>
<b>control (n=3)</b>	0.30±0.2	0.39±0.08	0.19±0.04
<b><i>Gata6cKO</i> (n=3)</b>	0.45±0.28	0.36±0.08	0.15±0.004
<b>t-Test</b>	0,4921988	0,569572	0,2624481
<b>E14.5</b>	<b>E</b>	<b>IM</b>	<b>OM</b>
<b>control (n=3)</b>	0.33±0.02	0.40±0.05	0.32±0.03
<b><i>Gata6cKO</i> (n=3)</b>	0.35±0.09	0.33±0.06	0.27±0.04
<b>t-Test</b>	0,7711156	0,1628705	0,1590087

**Table S1. Statistical evaluation of the BrdU incorporation assay in E12.5 and E14.5 control and *Gata6cKO* ureters.** E, epithelium; IM, inner layer of the ureteric mesenchyme; OM, outer layer of the ureteric mesenchyme.

	<b>2 days</b>	<b>4 days</b>	<b>6 days</b>	<b>8 days</b>
<b>control (n=8)</b>	1.06±0.6	1.50±0.6	3.06±0.6	2.97±0.4
<b><i>Gata6cKO</i> (n=8)</b>	0	0.31±0.37	1.88±0.8	2.31±0.9
<b>t-Test</b>	0,0001047	0,0002122	0,0046121	0,0775856

**Table S2. Statistics of the peristaltic frequency of explant cultures of E14.5 control and *Gata6cKO* ureters.**

	<b>2 days</b>	<b>4 days</b>	<b>6 days</b>	<b>8 days</b>
<b>control proximal (n=8)</b>	0.23±0.13	0.67±0.08	0.68±0.12	0.65±0.17
<b><i>Gata6cKO</i> proximal (n=8)</b>	0	0.27±0.14	0.47±0.16	0.46±0.11
<b>t-Test proximal</b>	0,0001357	4,86E-01	0,0112539	0,019402
<b>control medial (n=8)</b>	0.19±0.06	0.55±0.12	0.56±0.17	0.61±0.17
<b><i>Gata6cKO</i> medial (n=8)</b>	0	0.32±0.19	0.45±0.19	0.50±0.16
<b>t-Test medial</b>	5,04E-02	0,033822	0,2046569	0,2110983
<b>control distal (n=8)</b>	0.08±0.08	0.46±0.11	0.56±0.18	0.54±0.19
<b><i>Gata6cKO</i> distal (n=8)</b>	0	0.21±0.08	0.43±0.13	0.53±0.16
<b>t-Test distal</b>	0,0144015	0,0013368	0,1245349	0,8857825

**Table S3. Statistics of the peristaltic intensity of explant cultures of E14.5 control and *Gata6cKO* ureters.**

	<b>0 days</b>	<b>2 days</b>	<b>4 days</b>	<b>6 days</b>
<b>control (n=11)</b>	1.57±0.4	2.07±0.9	2.07±0.6	2.02±0.7
<b><i>Gata6cKO</i> (n=8)</b>	0.88±0.7	1.53±0.6	1.69±0.6	1.66±0.6
<b>t-Test</b>	0,0069488	0,1609758	0,176243	0,2452143

**Table S4. Statistics of the peristaltic frequency of explant cultures of E18.5 control and *Gata6cKO* ureters.**

	<b>0 days</b>	<b>2 days</b>	<b>4 days</b>	<b>6 days</b>
<b>control proximal (n=11)</b>	0.19±0.04	0.29±0.07	0.32±0.05	0.35±0.07
<b><i>Gata6cKO</i> proximal(n=8)</b>	0.05±0.02	0.11±0.04	0.19±0.07	0.16±0.05
<b>t-Test proximal</b>	8,72E-04	0,0001466	0,0007625	0,0001286
<b>control medial (n=11)</b>	0.22±0.04	0.33±0.04	0.43±0.09	0.41±0.06
<b><i>Gata6cKO</i> medial (n=8)</b>	0.07±0.02	0.24±0.07	0.35±0.06	0.36±0.05
<b>t-Test medial</b>	5,68E-02	0,0093293	0,0823311	0,200487
<b>control distal (n=11)</b>	0.19±0.05	0.31±0.09	0.41±0.06	0.42±0.06
<b><i>Gata6cKO</i> distal (n=8)</b>	0.05±0.03	0.21±0.06	0.30±0.07	0.30±0.05
<b>t-Test distal</b>	2,26E-01	0,0428714	0,0064858	0,0020696

**Table S5. Statistics of the peristaltic intensity of explant cultures of E18.5 control and *Gata6cKO* ureters.**

GeneName	control 1	mutant 1	control 2	mutant 2	FC1	FC2	avgFC
<i>Evx1</i>	19	149	19	178	7,9	9,5	8,7
<i>Aldh1a3</i>	336	1730	362	2117	5,2	5,9	5,5
<i>D030062O11Rik</i>	31	145	29	144	4,6	5,0	4,8
<i>Cartpt</i>	301	1249	236	1228	4,1	5,2	4,7
<i>Slc7a14</i>	27	108	20	101	4,0	5,2	4,6
<i>Col8a1</i>	74	289	50	241	3,9	4,8	4,3
<i>Stmn4</i>	311	1157	241	1066	3,7	4,4	4,1
<i>Nefm</i>	199	829	212	805	4,2	3,8	4,0
<i>Adamts18</i>	195	584	162	771	3,0	4,8	3,9
<i>Gdnf</i>	105	348	76	326	3,3	4,3	3,8
<i>Fam150b</i>	49	220	77	241	4,5	3,1	3,8
<i>Rspo1</i>	158	496	82	350	3,1	4,3	3,7
<i>Dpp6</i>	34	119	37	137	3,5	3,7	3,6
<i>Slc18a3</i>	58	228	63	199	3,9	3,2	3,6
<i>Nefl</i>	515	1725	421	1536	3,4	3,6	3,5
<i>Rab3c</i>	69	209	59	213	3,0	3,6	3,3
<i>Elavl3</i>	131	326	98	379	2,5	3,9	3,2
<i>Tlx2</i>	456	1192	305	1089	2,6	3,6	3,1
<i>Stmn3</i>	265	695	206	709	2,6	3,4	3,0
<i>Tubb3</i>	191	533	173	565	2,8	3,3	3,0
<i>Vgf</i>	55	163	46	141	3,0	3,0	3,0
<i>Prph</i>	110	326	106	319	3,0	3,0	3,0
<i>D230018H15Rik</i>	194	518	164	542	2,7	3,3	3,0
<i>Gm5868</i>	100	270	83	263	2,7	3,2	2,9
<i>Dcx</i>	157	321	100	369	2,0	3,7	2,9
<i>Ramp1</i>	67	143	52	182	2,1	3,5	2,8
<i>Phox2b</i>	428	958	284	967	2,2	3,4	2,8
<i>Slc38a5</i>	1053	2370	819	2715	2,3	3,3	2,8
<i>Hand2</i>	269	600	166	551	2,2	3,3	2,8
<i>Pcnx12</i>	59	136	51	164	2,3	3,2	2,8
<i>Shisa6</i>	51	125	34	102	2,5	3,0	2,7
<i>Ntrk1</i>	62	186	77	189	3,0	2,4	2,7
<i>AK081501</i>	132	362	165	442	2,7	2,7	2,7
<i>D9Ert115e</i>	126	310	123	357	2,5	2,9	2,7
<i>1010001N08Rik</i>	1331	3098	1308	3954	2,3	3,0	2,7
<i>Celsr3</i>	191	407	130	415	2,1	3,2	2,7
<i>Scg2</i>	52	111	33	101	2,1	3,1	2,6
<i>Vat1l</i>	668	1425	502	1505	2,1	3,0	2,6
<i>DV650784</i>	52	121	46	129	2,3	2,8	2,6
<i>Hoxd13</i>	293	809	358	842	2,8	2,4	2,6
<i>Dbh</i>	1117	2778	920	2351	2,5	2,6	2,5
<i>Inhba</i>	656	1509	635	1703	2,3	2,7	2,5
<i>Asgr1</i>	124	349	143	305	2,8	2,1	2,5
<i>Isl1</i>	386	947	354	875	2,5	2,5	2,5
<i>Igfbp2</i>	3000	7363	2981	7101	2,5	2,4	2,4
<i>St6galnac5</i>	45	115	48	107	2,6	2,2	2,4
<i>Wt1</i>	2502	5899	2110	5071	2,4	2,4	2,4
<i>Fat3</i>	56	144	63	136	2,6	2,2	2,4
<i>Fos</i>	3432	8771	3084	6676	2,6	2,2	2,4
<i>Kcnip4</i>	164	414	150	324	2,5	2,2	2,3
<i>Kcnd3</i>	1026	2698	1197	2452	2,6	2,0	2,3
<i>Ntrk3</i>	111	252	106	251	2,3	2,4	2,3
<i>Npr3</i>	351	787	306	698	2,2	2,3	2,3
<i>Aldh1a2</i>	5265	11983	5952	13159	2,3	2,2	2,2
<i>9130001E16Rik</i>	84	184	98	222	2,2	2,3	2,2
<i>Kcnma1</i>	525	1051	515	1089	2,0	2,1	2,1
<i>G6pc2</i>	59	119	52	106	2,0	2,0	2,0

**Table S6. Genes with increased expression in microarrays of E14.5 Gata6KO ureters.** Shown are gene names, individual intensities of the two control and mutant samples and the individual and average fold change (avgFC).

## Part 1- GATA6 in SMC differentiation

GeneName	control 1	mutant 1	control 2	mutant 2	FC1	FC2	avgFC
<i>Fa2h</i>	316	49	208	41	-6,4	-5,1	-5,7
<i>Mgat4c</i>	142	27	118	20	-5,2	-6,0	-5,6
<i>Serpinb5</i>	220	38	125	28	-5,7	-4,5	-5,1
<i>D930019F10Rik</i>	218	40	185	39	-5,4	-4,7	-5,1
<i>Upk1b</i>	1542	317	1075	286	-4,9	-3,8	-4,3
<i>Aldh3b2</i>	211	47	134	39	-4,5	-3,5	-4,0
<i>Tmprss13</i>	312	79	182	48	-3,9	-3,8	-3,8
<i>Tmprss4</i>	117	30	101	28	-3,8	-3,6	-3,7
<i>Sprr2a2</i>	217	50	146	50	-4,4	-3,0	-3,7
<i>Kif5b</i>	322	105	343	81	-3,1	-4,2	-3,6
<i>Aqp3</i>	954	255	645	186	-3,7	-3,5	-3,6
<i>Elmod1</i>	272	80	254	72	-3,4	-3,5	-3,5
<i>Sprr1a</i>	2570	731	2171	702	-3,5	-3,1	-3,3
<i>Perp</i>	9314	2487	6239	2303	-3,7	-2,7	-3,2
<i>Hpgd</i>	1410	418	1243	408	-3,4	-3,1	-3,2
<i>Esy3</i>	181	71	238	62	-2,6	-3,8	-3,2
<i>Lmcd1</i>	1898	746	2398	631	-2,5	-3,8	-3,2
<i>Car3</i>	24909	7512	22020	7276	-3,3	-3,0	-3,2
<i>Rab27b</i>	2223	572	1342	548	-3,9	-2,4	-3,2
<i>Upk2</i>	474	165	383	111	-2,9	-3,4	-3,2
<i>Shisa2</i>	2655	894	3153	981	-3,0	-3,2	-3,1
<i>Cbr2</i>	443	138	207	71	-3,2	-2,9	-3,1
<i>Rasgrf1</i>	538	159	546	199	-3,4	-2,7	-3,1
<i>Ipcef1</i>	122	41	127	41	-3,0	-3,1	-3,0
<i>LOC102642338</i>	273	115	126	34	-2,4	-3,7	-3,0
<i>Msln</i>	2191	584	1590	707	-3,8	-2,2	-3,0
<i>Upk1a</i>	3475	1105	2719	955	-3,1	-2,8	-3,0
<i>Dpt</i>	241	82	183	60	-2,9	-3,0	-3,0
<i>Aspn</i>	732	242	550	200	-3,0	-2,8	-2,9
<i>Cnn1</i>	3631	1273	2113	740	-2,9	-2,9	-2,9
<i>5031434C07Rik</i>	176	63	209	76	-2,8	-2,8	-2,8
<i>Trim29</i>	469	148	360	152	-3,2	-2,4	-2,8
<i>Myocd</i>	562	233	805	260	-2,4	-3,1	-2,8
<i>Ihh</i>	1471	462	935	411	-3,2	-2,3	-2,7
<i>C1ca3a1</i>	746	257	690	271	-2,9	-2,5	-2,7
<i>Ctnna2</i>	105	46	145	48	-2,3	-3,0	-2,7
<i>Oit1</i>	354	136	322	122	-2,6	-2,6	-2,6
<i>Fam183b</i>	580	231	458	170	-2,5	-2,7	-2,6
<i>Anxa8</i>	5697	1878	3478	1625	-3,0	-2,1	-2,6
<i>Hmgcs2</i>	363	139	303	120	-2,6	-2,5	-2,6
<i>Stxbp5l</i>	159	68	178	66	-2,4	-2,7	-2,5
<i>Trp63</i>	1107	394	756	347	-2,8	-2,2	-2,5
<i>Krt15</i>	227	81	173	79	-2,8	-2,2	-2,5
<i>Lamb3</i>	1362	472	931	451	-2,9	-2,1	-2,5
<i>C1ca3a2</i>	513	222	531	214	-2,3	-2,5	-2,4
<i>Grhl3</i>	2495	1075	2075	898	-2,3	-2,3	-2,3
<i>Neto1</i>	419	200	488	194	-2,1	-2,5	-2,3
<i>Agr2</i>	153	76	141	55	-2,0	-2,5	-2,3
<i>Ldoc1</i>	1982	821	1235	592	-2,4	-2,1	-2,2
<i>Itih2</i>	213	99	223	98	-2,2	-2,3	-2,2
<i>Epyc</i>	134	62	133	59	-2,2	-2,3	-2,2
<i>Lin7a</i>	258	114	228	106	-2,3	-2,2	-2,2
<i>Prom2</i>	567	274	551	236	-2,1	-2,3	-2,2
<i>Actg2</i>	1592	726	943	429	-2,2	-2,2	-2,2
<i>Cd44</i>	130	60	126	58	-2,2	-2,2	-2,2
<i>Ugt2b34</i>	505	220	460	224	-2,3	-2,1	-2,2
<i>Fxyd3</i>	4632	2078	3533	1720	-2,2	-2,1	-2,1
<i>Twist1</i>	1728	830	1602	758	-2,1	-2,1	-2,1
<i>Tmem229a</i>	184	89	184	87	-2,1	-2,1	-2,1
<i>Ncmap</i>	524	254	489	236	-2,1	-2,1	-2,1
<i>2310001H17Rik</i>	236	113	189	94	-2,1	-2,0	-2,1

**Table S7. Genes with decreased expression in microarrays of E14.5 *Gata6*KO ureters.** Shown are gene names, individual intensities of the two control and mutant samples and the individual and average fold change (avgFC).

Part 1- GATA6 in SMC differentiation

Category	Term	Count	%	PValue	Genes	List Total	Pop Hits	Pop Total	Fold Enrichment	Bonferroni	Benjamini	FDR
GOTERM_CC_DIRECT	GO:0030424~axon	9	16.66666667	2.04E-06	PRPH, STMN3, NTRK1, STMN4, SLC18A3, DBH,	47	370	19662	10.17584819	1.96E-04	1.96E-04	0.002244
UP_KEYWORDS	Developmental protein	12	22.22222222	4.63E-06	NTRK3, PHOX2B, EVX1, FAT3, HAND2, NTRK1,	49	376	22680	5.690866511	5.00E-04	5.00E-04	0.005216703
GOTERM_CC_DIRECT	GO:0043005~neuron projection	9	16.66666667	5.20E-06	FOS, KCND3, STMN3, STMN4, SLC18A3, VGF,	47	420	19662	8.96443769	4.99E-04	2.49E-04	0.00572373
GOTERM_BP_DIRECT	GO:0048485~sympathetic nervous system development	4	7.407407407	1.16E-05	PHOX2B, HAND2, NTRK1, GDNF	49	17	18082	86.82833133	0.00664193	0.00664193	0.017067162
GOTERM_CC_DIRECT	GO:0043025~neuronal cell body	9	16.66666667	2.95E-05	KCNMA1, PRPH, KCND3, NTRK1, VGF, DBH,	47	534	19662	7.050681329	0.002830975	9.45E-04	0.032520215
UP_KEYWORDS	Glycoprotein	21	38.88888889	ADAMTS18, SLC38A5, CELSR3, NPR3, DBH,	49	3815	22680	2.547837484	0.004532842	0.002268995	0.002268995	0.047355309
GOTERM_BP_DIRECT	GO:0007275~multicellular organism development	12	22.22222222	6.20E-05	NTRK3, PHOX2B, EVX1, FAT3, HAND2, NTRK1,	49	1029	18082	4.303444993	0.034926033	0.017618217	0.091013571
INTERPRO	IPR006821~intermediate filament head, DNA-binding domain	3	5.555555556	1.06E-04	PRPH, NEFL, NEFM	48	7	20594	183.875	0.016234694	0.127418574	0.171418574
GOTERM_CC_DIRECT	GO:0030425~dendrite	8	14.81481481	1.32E-04	KCNMA1, KCND3, FAT3, NTRK1, DBH, DCX,	47	490	19662	6.830047764	0.012588143	0.003162002	0.145233431
GOTERM_CC_DIRECT	GO:0005883~neurofilament	3	5.555555556	1.91E-04	PRPH, NEFL, NEFM	47	9	19662	139.4468085	0.018148634	0.003656367	0.209090133
GOTERM_BP_DIRECT	GO:0001764~neuron migration	5	9.259259259	3.25E-04	NTRK3, PHOX2B, FAT3, CELSR3, DCX	49	124	18082	14.87985517	0.16975906	0.060129435	0.475366146
GOTERM_BP_DIRECT	GO:0030182~neuron differentiation	5	9.259259259	3.56E-04	PHOX2B, ALDH1A2, ISL1, GDNF, TUBB3	49	127	18082	14.52836253	0.184341485	0.049664192	0.520526528
UP_SEQ_FEATURE	region of interest:Linker 2	3	5.555555556	4.14E-04	PRPH, NEFL, NEFM	47	12	18012	95.80851064	0.092794607	0.031696539	0.531696539
GOTERM_BP_DIRECT	GO:0048484~enteric nervous system development	3	5.555555556	5.28E-04	PHOX2B, TLX2, GDNF	49	13	18082	85.15855573	0.261240478	0.058759473	0.772513521
UP_KEYWORDS	GO:0001077~transcriptional activator activity, RNA polymerase	6	11.11111111	6.98E-04	PHOX2B, FOS, HAND2, HOXD13, ISL1, WT1	47	270	17446	8.248699764	0.096316926	0.096316926	0.825754021
GOTERM_BP_DIRECT	II core promoter proximal region sequence-specific binding	5	9.259259259	8.15E-04	PHOX2B, EVX1, HOXD13, ISL1, TLX2	48	184	20594	11.65874094	0.117995392	0.060848996	0.973281284
GOTERM_CC_DIRECT	GO:0008076~voltage-gated potassium channel complex	4	7.407407407	8.37E-04	KCNMA1, KCND3, DPP6, KCNIP4	47	79	19662	21.1817937	0.07722156	0.013305404	0.917793376
UP_SEQ_FEATURE	disulfide bond	16	29.62962963	1.00E-03	NTRK3, ST6GALNAC5, ASGR1, INHBA, FAT3,	47	2510	18012	2.442926168	0.209437568	0.110864222	1.278261111
UP_SEQ_FEATURE	DNA-binding region:Homeobox	5	9.259259259	0.001134423	PHOX2B, EVX1, HOXD13, ISL1, TLX2	47	180	18012	10.64539007	0.234128386	0.085075359	1.44958957
GOTERM_MF_DIRECT	GO:0043565~sequence-specific DNA binding	8	14.81481481	0.001251091	PHOX2B, FOS, EVX1, HAND2, HOXD13, ISL1,	47	633	17446	4.691203657	0.16599994	0.086763963	1.475185585
GOTERM_BP_DIRECT	GO:0051412~response to corticosterone	3	5.555555556	0.001403147	NTRK3, FOS, NEFL	49	21	18082	52.71720117	0.552718814	0.125492701	2.039639016
UP_KEYWORDS	Disulfide bond	16	29.62962963	0.001449234	NTRK3, ST6GALNAC5, ASGR1, INHBA, FAT3,	49	3124	22680	2.370587159	0.144903011	0.050870719	1.619759889
UP_KEYWORDS	Homeobox	5	9.259259259	0.002887416	PHOX2B, EVX1, HOXD13, ISL1, TLX2	49	280	22680	8.265306122	0.268232192	0.075103097	3.203499438
GOTERM_BP_DIRECT	GO:0007399~nervous system development	6	11.11111111	0.003147521	NTRK3, FOS, NTRK1, ELAVL3, DCX, GDNF	49	377	18082	5.873003843	0.835751341	0.227446022	4.521239539
INTERPRO	IPR001356~Homeodomain	5	9.259259259	0.003354606	PHOX2B, EVX1, HOXD13, ISL1, TLX2	48	271	20594	3.039578067	0.158435487	0.350791352	3.950791352
GOTERM_CC_DIRECT	GO:0043235~receptor complex	4	7.407407407	0.003793256	NTRK3, NTRK1, RAMP1, GDNF	47	134	19662	12.4877739	0.305695725	0.050785721	4.099427749
GOTERM_BP_DIRECT	GO:0045944~positive regulation of transcription from RNA	9	16.66666667	0.004333132	ISL1, GDNF, WT1	49	995	18082	3.337873039	0.916947286	0.267311747	6.174503059
GOTERM_BP_DIRECT	polymerase II promoter	5	9.259259259	0.00501596	NTRK3, ALDH1A2, HAND2, ISL1, WT1	49	261	18082	7.069356478	0.943942521	0.273962112	7.114280629
UP_SEQ_FEATURE	glycosylation site:N-linked (GlcNAc...)	18	33.33333333	0.005073633	SLC38A5, ADAMTS18, CELSR3, NPR3, DBH,	47	3563	18012	1.936086897	0.697541468	0.258405569	6.336479048
GOTERM_BP_DIRECT	GO:0045105~intermediate filament polymerization or	2	3.703703704	0.005302247	NEFL, NEFM	49	2	18082	369.0204082	0.952464128	0.262601676	7.505744838
SMART	SM00389~HOX	5	9.259259259	0.005954855	PHOX2B, EVX1, HOXD13, ISL1, TLX2	30	266	10425	6.531954887	0.183779131	0.183779131	5.116841499
INTERPRO	IPR020777~Tyrosine-protein kinase, neurotrophic receptor	2	3.703703704	0.006831372	NTRK3, NTRK1	48	3	20594	286.0277778	0.652030725	0.2319575	7.894026899
KEGG_PATHWAY	mmu05014~Amyotrophic lateral sclerosis (ALS)	3	5.555555556	0.006859688	PRPH, NEFL, NEFM	20	51	7691	22.62058824	0.369462549	0.369462549	6.816310068
UP_SEQ_FEATURE	site:interaction with PLC-gamma-1	2	3.703703704	0.007642432	NTRK3, NTRK1	47	3	18012	255.4893617	0.835174768	0.302723965	9.397931011
UP_SEQ_FEATURE	site:interaction with SHC1	2	3.703703704	0.007642432	NTRK3, NTRK1	47	3	18012	255.4893617	0.835174768	0.302723965	9.397931011
INTERPRO	IPR009057~Homeodomain-like	5	9.259259259	0.007833448	PHOX2B, EVX1, HOXD13, ISL1, TLX2	48	345	20594	6.217995169	0.70213079	0.215116639	9.00267775
GOTERM_MF_DIRECT	GO:0005030~neurotrophin receptor activity	2	3.703703704	0.007889735	NTRK3, NTRK1	47	3	17446	247.4609929	0.682903293	0.318084476	8.974926509
GOTERM_BP_DIRECT	GO:0033693~neurofilament bundle assembly	2	3.703703704	0.007943037	NEFL, NEFM	49	3	18082	246.0136054	0.989637197	0.339931755	11.04492469
INTERPRO	IPR018039~intermediate filament protein, conserved site	3	5.555555556	0.008563456	PRPH, NEFL, NEFM	48	61	20594	21.10040984	0.734051171	0.198076365	9.180260813
UP_SEQ_FEATURE	signal peptide	16	29.62962963	0.008708089	SHISA6, INHBA, RSPO1, FAT3, NTRK1, CARPT1,	47	3124	18012	1.96278639	0.871953668	0.290049847	10.64162368
GOTERM_BP_DIRECT	GO:0043524~negative regulation of neuron apoptotic process	4	7.407407407	0.008787925	NTRK1, ISL1, NEFL, GDNF	49	160	18082	9.225510204	0.993640064	0.343923632	12.15032046
UP_KEYWORDS	Potassium channel	3	5.555555556	0.008884443	KCNMA1, KCND3, KCNIP4	49	67	22680	20.7249467	0.618562252	0.175321383	9.560213255
GOTERM_BP_DIRECT	GO:0010468~regulation of gene expression	5	9.259259259	0.00891704	PHOX2B, RSPO1, ISL1, GDNF, WT1	49	308	18082	5.990591042	0.994097511	0.326184234	12.31811537
UP_KEYWORDS	Signal	18	33.33333333	0.009395279	GDNF, NTRK3, SHISA6, INHBA, RSPO1, FAT3,	49	4543	22680	1.833904594	0.639219983	0.15626303	10.08370253

GOTERM_BP_DIRECT	GO:0050885~neuromuscular process controlling balance	3	5,555555556	0.010376549	KCNMA1, ALDH1A3, NEFL	49	58	18082	19,08726249	0.997463134	0.347481724	14,19419267
UP_SEQ_FEATURE	topological domain:Cytoplasmic	15	27,7777778	0.010471029	KCNMA1, SLC38A5, KCND3, CELSR3, NPR3, KCNMA1, G6PC2, NTRK3, SHISA6, ASGR1, DBH	47	2880	18012	1,996010638	0.915724624	0.297690293	12,66457483
GOTERM_BP_DIRECT	GO:0003266~regulation of secondary heart field cardioblast proliferation	2	3,703703704	0.010576963	HAND2, ISL1	49	4	18082	184,5102041	0.997741103	0.333817696	14,44886701
PIR_SUPERFAMILY	PIRSF002285~Op18/stathmin	2	3,703703704	0.011031338	STMN3, STMN4	6	4	1807	150,5833333	0.053953138	0.053953138	4,707938614
UP_KEYWORDS	Intermediate filament	3	5,555555556	0.011031833	PRPH, NEFL, NEFM	49	75	22680	18,51428571	0.698220459	0.157390586	11,74225477
GOTERM_MF_DIRECT	GO:0046982~protein heterodimerization activity	6	11,11111111	0.011040886	FOS, PRPH, INHBA, HAND2, NEFL, NEFM	47	514	17446	4,332974584	0.800078779	0.331325558	12,34853586
INTERPRO	IPR000956~Stathmin family	2	3,703703704	0.011360222	STMN3, STMN4	48	5	20594	171,6166667	0.827866918	0.22225404	12,80797486
GOTERM_BP_DIRECT	GO:0072659~protein localization to plasma membrane	3	5,555555556	0.01179104	DPPE, RAMP1, KCNIP4	49	62	18082	17,8558262	0.998882223	0.34608365	15,97665132
GOTERM_BP_DIRECT	GO:0043065~positive regulation of apoptotic process	5	9,259259259	0.011867096	KCNMA1, NTRK3, ALDH1A2, ALDH1A3, WT1	49	335	18082	5,507767286	0.998930448	0.331275586	16,07150785
UP_SEQ_FEATURE	region of interest:Coil 1B	3	5,555555556	0.012337458	PRPH, NEFL, NEFM	47	66	18012	17,41972921	0.945922451	0.305572158	14,76018479
UP_SEQ_FEATURE	region of interest:Coil 1A	3	5,555555556	0.012337458	PRPH, NEFL, NEFM	47	66	18012	17,41972921	0.945922451	0.305572158	14,76018479
UP_SEQ_FEATURE	region of interest:Linker 1	3	5,555555556	0.012337458	PRPH, NEFL, NEFM	47	66	18012	17,41972921	0.945922451	0.305572158	14,76018479
GOTERM_BP_DIRECT	GO:0003007~heart morphogenesis	3	5,555555556	0.0125283	ALDH1A2, HAND2, ISL1	49	64	18082	17,29783163	0.999271165	0.330575481	16,89196511
UP_SEQ_FEATURE	region of interest:Rod	3	5,555555556	0.012696579	PRPH, NEFL, NEFM	47	67	18012	17,15973325	0.950352108	0.283691524	15,15804328
INTERPRO	IPR001664~intermediate filament protein	3	5,555555556	0.013050841	PRPH, NEFL, NEFM	48	76	20594	16,93585526	0.8677498	0.223440848	14,57988608
UP_SEQ_FEATURE	region of interest:Head	3	5,555555556	0.013428439	PRPH, NEFL, NEFM	47	69	18012	16,66234968	0.958292013	0.272183457	15,96355004
UP_SEQ_FEATURE	region of interest:Tail	3	5,555555556	0.014178292	PRPH, NEFL, NEFM	47	71	18012	16,19298771	0.965116612	0.262926517	16,78154166
UP_SEQ_FEATURE	region of interest:Coil 2B	2	3,703703704	0.015227718	NEFL, NEFM	47	6	18012	127,7446809	0.972840812	0.259554555	17,91400231
UP_SEQ_FEATURE	region of interest:Coil 2A	2	3,703703704	0.015227718	NEFL, NEFM	47	6	18012	127,7446809	0.972840812	0.259554555	17,91400231
UP_KEYWORDS	Neurogenesis	4	7,407407407	0.01539391	NTRK3, NTRK1, ELAVL3, DCX	49	247	22680	7,495662233	0.8127780145	0.188956799	16,02772348
UP_KEYWORDS	Cleavage on pair of basic residues	4	7,407407407	0.01559612	INHBA, CARTPT, GDNF, SCG2	49	248	22680	7,465437788	0.816152524	0.171537081	16,18671164
GOTERM_BP_DIRECT	GO:0031133~regulation of axon diameter	2	3,703703704	0.015824287	NEFL, NEFM	49	6	18082	123,0068027	0.999892694	0.381861902	20,87148468
GOTERM_BP_DIRECT	GO:0002138~retinoic acid biosynthetic process	2	3,703703704	0.015824287	ALDH1A2, ALDH1A3	49	6	18082	123,0068027	0.999892694	0.381861902	20,87148468
GOTERM_BP_DIRECT	GO:0045110~intermediate filament bundle assembly	2	3,703703704	0.015824287	NEFL, NEFM	49	6	18082	123,0068027	0.999892694	0.381861902	20,87148468
SMART	SM01391:SM01391	3	5,555555556	0.01693278	PRPH, NEFL, NEFM	30	72	10425	14,47916667	0.440462363	0.251977516	13,94497042
GOTERM_MF_DIRECT	GO:0042803~protein homodimerization activity	7	12,96296296	0.01701289	KCNMA1, ASGR1, HAND2, ALDH1A3, NTRK1, domain:Cadherin 8	47	798	17446	3,256065696	0.924955605	0.404250548	19,1055254
UP_SEQ_FEATURE	domain:Cadherin 8	2	3,703703704	0.01774352	FAT3, CELSR3	47	7	18012	109,4954407	0.985111446	0.276480629	20,57123431
UP_SEQ_FEATURE	domain:Cadherin 9	2	3,703703704	0.01774352	FAT3, CELSR3	47	7	18012	109,4954407	0.985111446	0.276480629	20,57123431
UP_SEQ_FEATURE	GO:0005004~GPI-linked ephrin receptor activity	2	3,703703704	0.018314721	NTRK3, NTRK1	47	7	17446	106,0547112	0.931454271	0.360269976	19,70321669
GOTERM_BP_DIRECT	GO:0042490~mechanoreceptor differentiation	2	3,703703704	0.018437721	NTRK3, NTRK1	49	7	18082	105,4344023	0.999976615	0.41325865	23,8998987
GOTERM_BP_DIRECT	GO:1901166~neural crest cell migration involved in autonomic nervous system development	2	3,703703704	0.018437721	PHOX2B, GDNF	49	7	18082	105,4344023	0.999976615	0.41325865	23,8998987
GOTERM_BP_DIRECT	GO:0008285~negative regulation of cell proliferation	5	9,259259259	0.018692527	PHOX2B, ALDH1A2, INHBA, NTRK1, WT1	49	384	18082	4,804953231	0.999979848	0.40241943	24,18931195
GOTERM_CC_DIRECT	GO:0005576~extracellular region	10	18,51851852	0.018725337	ADAMTS18, INHBA, RSP01, CARTPT, IGFBP2, domain:Cadherin 7	47	1753	19662	2,386425702	0.837109332	0.202947322	18,79518627
GOTERM_MF_DIRECT	GO:0005267~potassium channel activity	3	5,555555556	0.018864866	KCNMA1, KCND3, KCNIP4	47	80	17446	13,91968085	0.996805391	0.32598653	20,23580282
UP_SEQ_FEATURE	domain:Cadherin 7	2	3,703703704	0.020253034	FAT3, CELSR3	47	8	18012	95,80851064	0.991838445	0.290682093	23,14258885
GOTERM_BP_DIRECT	GO:0006357~regulation of transcription from RNA polymerase II promoter	5	9,259259259	0.020840941	FOS, INHBA, ISL1, TLX2, WT1	49	397	18082	4,647612193	0.99999426	0.422218837	26,58905901
GOTERM_MF_DIRECT	GO:0001758~retinal dehydrogenase activity	2	3,703703704	0.020904177	ALDH1A2, ALDH1A3	47	8	17446	92,79787234	0.953263768	0.318121947	22,18192727
GOTERM_BP_DIRECT	GO:0048935~peripheral nervous system neuron development	2	3,703703704	0.021044436	HAND2, ISL1	49	8	18082	92,25510204	0.999994904	0.411321003	26,81256718
UP_KEYWORDS	Potassium transport	3	5,555555556	0.021600838	KCNMA1, KCND3, KCNIP4	49	107	22680	12,97730307	0.905433838	0.21009734	21,79924618
GOTERM_CC_DIRECT	GO:0005615~extracellular space	9	16,66666667	0.022083202	INHBA, RSP01, CARTPT, IGFBP2, VGF, DBH, IPRO02011~Tyrosine-kinase, receptor class II, conserved site	47	1504	19662	2,503366908	0.882785049	0.211950192	21,80382476
INTERPRO	IPRO02011~Tyrosine-kinase, receptor class II, conserved site	2	3,703703704	0.022594105	NTRK3, NTRK1	48	10	20594	85,80833333	0.970382875	0.323650097	23,97804103
GOTERM_MF_DIRECT	GO:0004028~3-chloroallyl aldehyde dehydrogenase activity	2	3,703703704	0.02348695	ALDH1A2, ALDH1A3	47	9	17446	82,48699764	0.968134742	0.318129443	24,58425741
GOTERM_BP_DIRECT	GO:0061032~visceral serous pericardium development	2	3,703703704	0.023644422	HAND2, WT1	49	9	18082	82,00453515	0.99999889	0.435201636	29,61390787
GOTERM_BP_DIRECT	GO:0061564~axon development	2	3,703703704	0.023644422	NEFL, NEFM	49	9	18082	82,00453515	0.99999889	0.435201636	29,61390787
GOTERM_BP_DIRECT	GO:0071805~potassium ion transmembrane transport	3	5,555555556	0.023827886	KCNMA1, KCND3, KCNIP4	49	90	18082	12,30068027	0.999999003	0.42462898	29,8079792
UP_KEYWORDS	Secreted	9	16,66666667	0.023967356	ADAMTS18, INHBA, RSP01, CARTPT, IGFBP2, Secreted	49	1685	22680	2,472123997	0.927197033	0.211940503	23,90283592
GOTERM_MF_DIRECT	GO:0005198~structural molecule activity	4	7,407407407	0.024210737	KCNMA1, PRPH, NEFL, NEFM	47	236	17446	6,291381176	0.971382933	0.299089588	25,24518554
GOTERM_BP_DIRECT	GO:0001525~angiogenesis	4	7,407407407	0.025493782	HAND2, COL8A1, RAMP1, SCG2	49	239	18082	6,176073777	0.999999625	0.433982103	31,54562225



Part 1- GATA6 in SMC differentiation

GOTERM_BP_DIRECT	GO:0031110~regulation of microtubule polymerization or depolymerization	2	3,703703704	0.026237319	STMN3, STMN4	49	10	18082	73,80408163	0.999999758	0.431212968	32,30817011
GOTERM_BP_DIRECT	GO:0060052~neurofilament cytoskeleton organization	2	3,703703704	0.026237319	NEFL, NEFM	49	10	18082	73,80408163	0.999999758	0.431212968	32,30817011
UP_KEYWORDS	Palmitate	4	7,407407407	0.026467585	KCNMA1, ASGR1, STMN3, STMN4	49	304	22680	6,090225564	0.944811959	0.214486328	26,06915798
UP_KEYWORDS	Potassium	3	5,555555556	0.026729338	KCNMA1, KCND3, KCNIP4	49	120	22680	11,57142857	0.946391668	0.201548322	26,29267277
UP_KEYWORDS	Phosphoprotein	24	44,44444444	0.027625216	KCNMA1, PRPH, KCND3, RAB3C, STMN3, STMN4, CELSR3, DBH, ISL1, SLC7A14, KCNIP4, SLC18A3, DBH	49	7617	22680	1,458391943	0.951466869	0.194331517	27,05302466
GOTERM_CC_DIRECT	GO:0007169~transmembrane receptor protein tyrosine kinase signaling pathway	3	5,555555556	0.028749172	KCNMA1, SLC18A3, DBH	47	113	19662	11,10638298	0.939212454	0.244244249	27,47821672
GOTERM_BP_DIRECT	GO:000555556	3	5,555555556	0.028962476	NTRK3, NTRK1, GDNF	49	100	18082	11,07061224	0.999999951	0.451982887	35,03585898
UP_KEYWORDS	Calcium	6	11,11111111	0.029948792	KCNMA1, ASGR1, FAT3, CELSR3, KCNIP4, SCG2	49	827	22680	3,358092935	0.962517948	0.196618998	28,99190878
GOTERM_CC_DIRECT	GO:0005882~intermediate filament	3	5,555555556	0.03064952	PRPH, NEFL, NEFM	47	117	19662	10,72667758	0.949631427	0.237895523	29,02583431
GOTERM_BP_DIRECT	GO:0007623~circadian rhythm	3	5,555555556	0.033359203	KCNMA1, NTRK3, NTRK1	49	108	18082	10,25056689	0.999999996	0.488484134	39,022169635
UP_KEYWORDS	Voltage-gated channel	3	5,555555556	0.033643084	KCNMA1, KCND3, KCNIP4	49	136	22680	10,21008403	0.975176878	0.206259528	31,97808246
GOTERM_BP_DIRECT	GO:0042574~retinal metabolic process	2	3,703703704	0.033976221	ALDH1A2, ALDH1A3	49	13	18082	56,77237049	0.999999997	0.483265683	39,78858672
GOTERM_BP_DIRECT	GO:0007019~microtubule depolymerization	2	3,703703704	0.036542447	STMN3, STMN4	49	14	18082	52,71720117	0.999999999	0.49746814	42,09388021
GOTERM_BP_DIRECT	GO:0031076~embryonic camera-type eye development	2	3,703703704	0.036542447	ALDH1A2, ALDH1A3	49	14	18082	52,71720117	0.999999999	0.49746814	42,09388021
GOTERM_BP_DIRECT	GO:0051493~regulation of cytoskeleton organization	2	3,703703704	0.039101998	STMN3, STMN4	49	15	18082	49,20272109	1	0.510429509	44,31103221
GOTERM_BP_DIRECT	GO:0048665~neuron fate specification	2	3,703703704	0.039101998	NTRK3, ISL1	49	15	18082	49,20272109	1	0.510429509	44,31103221
GOTERM_BP_DIRECT	GO:1901379~regulation of potassium ion transmembrane transport	2	3,703703704	0.039101998	DPP6, KCNIP4	49	15	18082	49,20272109	1	0.510429509	44,31103221
GOTERM_BP_DIRECT	GO:0042573~retinoic acid metabolic process	2	3,703703704	0.039101998	ALDH1A2, ALDH1A3	49	15	18082	49,20272109	1	0.510429509	44,31103221
INTERPRO	IPR016160A Aldehyde dehydrogenase, conserved site	2	3,703703704	0.040308959	ALDH1A2, ALDH1A3	48	18	20594	47,6712963	0.988228905	0.469330426	38,95521032
GOTERM_BP_DIRECT	GO:0045104~intermediate filament cytoskeleton organization	2	3,703703704	0.04165489	PRPH, NEFM	49	16	18082	46,12755102	1	0.522301879	46,44340816
GOTERM_BP_DIRECT	GO:0060009~Sertoli cell development	2	3,703703704	0.04165489	NTRK1, WTI	49	16	18082	46,12755102	1	0.522301879	46,44340816
GOTERM_BP_DIRECT	GO:0014032~neural crest cell development	2	3,703703704	0.044201141	ALDH1A2, HAND2	49	17	18082	8,717017516	1	0.533213903	48,49424515
GOTERM_BP_DIRECT	GO:0006813~potassium ion transport	3	5,555555556	0.044756914	KCNMA1, KCND3, KCNIP4	49	127	18082	8,717017516	1	0.527462608	48,93204307
UP_SEQ_FEATURE	glycosylation site-O-linked (GlcNAc)	7	12,96296296	0.046134128	NTRK3, SLC38A5, KCND3, NTRK1, SLC18A3,	47	1126	19662	2,600695363	0.989265501	0.314671988	40,56067043
GOTERM_CC_DIRECT	GO:0005887~integral component of plasma membrane	2	3,703703704	0.046870687	ALDH1A2, ALDH1A3	48	21	20594	40,86111111	0.999384283	0.489347377	43,77815176
INTERPRO	IPR016161A Aldehyde/histidinol dehydrogenase	2	3,703703704	0.046870687	ALDH1A2, ALDH1A3	48	21	20594	40,86111111	0.999384283	0.489347377	43,77815176
INTERPRO	IPR015590A Aldehyde dehydrogenase, N-terminal	2	3,703703704	0.046870687	ALDH1A2, ALDH1A3	48	21	20594	40,86111111	0.999384283	0.489347377	43,77815176
INTERPRO	IPR016163A Aldehyde dehydrogenase, C-terminal	2	3,703703704	0.046870687	ALDH1A2, ALDH1A3	48	21	20594	40,86111111	0.999384283	0.489347377	43,77815176
UP_KEYWORDS	Differentiation	5	9,259259259	0.047343896	NTRK3, HAND2, NTRK1, ELAVL3, DCX	49	646	22680	3,823485626	0.994689876	0.26517719	42,0810029
GOTERM_BP_DIRECT	GO:0042593~glucose homeostasis	3	5,555555556	0.048617014	VGF, DBH, GPCR2	49	133	18082	8,323768605	1	0.547634157	51,87939203
GOTERM_BP_DIRECT	GO:0005244~voltage-gated ion channel activity	3	5,555555556	0.048656355	KCNMA1, KCND3, KCNIP4	47	134	17446	8,310257225	0.999277353	0.481859158	44,6865621
GOTERM_MF_DIRECT	GO:0004029~aldehyde dehydrogenase (NAD) activity	2	3,703703704	0.048950851	ALDH1A2, ALDH1A3	47	19	17446	39,07278835	0.999309077	0.454720572	44,8894945
GOTERM_BP_DIRECT	GO:0034765~regulation of ion transmembrane transport	3	5,555555556	0.04929971	KCNMA1, KCND3, KCNIP4	49	135	18082	8,200453515	1	0.547610331	52,84389548
UP_KEYWORDS	DNA-binding	8	14,81481481	0.050518186	PHOX2B, FOS, EVX1, HAND2, HOXD13, ISL1,	49	1604	22680	2,308514428	0.996296961	0.267310605	44,21728886
GOTERM_BP_DIRECT	GO:0030539~male genitalia development	2	3,703703704	0.051800212	HOXD13, WTI	49	20	18082	36,90204082	1	0.551591218	54,18806993
GOTERM_BP_DIRECT	GO:0060324~face development	2	3,703703704	0.051800212	ALDH1A2, ALDH1A3	49	20	18082	36,90204082	1	0.551591218	54,18806993
GOTERM_BP_DIRECT	GO:0060384~innervation	2	3,703703704	0.051800212	NTRK1, ISL1	49	20	18082	36,90204082	1	0.551591218	54,18806993
GOTERM_BP_DIRECT	GO:0031175~neuron projection development	3	5,555555556	0.05259426	STMN3, STMN4, GDNF	49	139	18082	7,964469241	1	0.547873605	54,74789524
GOTERM_CC_DIRECT	GO:0030426~growth cone	3	5,555555556	0.053354261	STMN3, STMN4, NEFL	47	159	19662	7,893215576	0.994823949	0.332957151	45,33243525
GOTERM_MF_DIRECT	GO:0005515~protein binding	17	31,48148148	0.054722087	NTRK3, RSPH, HAND2, NTRK1, SLC18A3,	47	4092	17446	1,54209563	0.999714156	0.466180369	48,73128623
UP_SEQ_FEATURE	topological domain:Extracellular	11	20,37037037	0.0529166	KCNMA1, NTRK3, SHISA6, ASGR1, SLC38A5,	47	2256	18012	1,868605704	0.999998433	0.566803726	51,89173954
GOTERM_BP_DIRECT	GO:0031688~cellular response to extracellular stimulus	2	3,703703704	0.056833362	ASGR1, FOS	49	22	18082	33,54730983	1	0.567506816	57,63026219
GOTERM_CC_DIRECT	GO:0030667~secretory granule membrane	2	3,703703704	0.059118478	VGF, DBH	47	26	19662	32,18003273	0.997120254	0.341546216	48,88896447

UP_SEQ_FEATURE	site:Transition state stabilizer	2	3,703703704	0.059562549	ALDH1A2, ALDH1A3	47	24	18012	31,93617021	0.99999946	0.572116731	54.61580884
GOTERM_BP_DIRECT	GO:0042493~response to drug	4	7,407407407	0.060873954	FOS, INHBA, NTRK1, IGF1R2	49	339	18082	4,354223105	1	0.5842281196	60.21755976
GOTERM_BP_DIRECT	GO:0042572~retinol metabolic process	2	3,703703704	0.061840348	ALDH1A2, ALDH1A3	49	24	18082	30,75170068	1	0.581422697	60.81415628
GOTERM_CC_DIRECT	GO:0031410~cytoplasmic vesicle	5	9,259259259	0.063678025	NTRK1, SLC18A3, IGF1R2, VGF, DBH	47	646	19662	3,23792899	0.998193572	0.343671317	51.55173159
UP_SEQ_FEATURE	transmembrane region	17	31,48148148	0.064316262	DBH, SLC7A14, G6PC2, NTRK3, STEGALNACS, KCNMA1, SLC38A5, KCND3, CELSR3, NPR3,	47	432	18012	1,51089488	0.99999836	0.580169368	57.48011035
UP_KEYWORDS	Signal-anchor	4	7,407407407	0.065742128	STEGALNACS, ASGR1, DBH, DPP6	49	439	22680	4,217377156	0.999353735	0.320597909	53.49970697
GOTERM_MF_DIRECT	GO:0000978~RNA polymerase II core promoter proximal region sequence-specific DNA binding	4	7,407407407	0.068579614	PHOX2B, FOS, HOXD13, ISL1	47	359	17446	4,135838322	0.999966416	0.520886937	56.97600564
GOTERM_BP_DIRECT	GO:0035987~endodermal cell differentiation	2	3,703703704	0.069302063	INHBA, COL1A1	49	27	18082	27,33484505	1	0.615975905	65.14763245
INTERPRO	IPR002957~keratin, type I	2	3,703703704	0.070556809	PRPH, NFM	48	32	20594	26,81510417	0.999987226	0.608985158	58.42799011
UP_SEQ_FEATURE	domain:Cadherin 6	2	3,703703704	0.071527246	FAT3, CELSR3	47	29	18012	26,42993397	0.999999973	0.600648383	61.50815721
GOTERM_MF_DIRECT	GO:0005184~neuropeptide hormone activity	3	3,703703704	0.073764812	CARTPT, VGF	47	29	17446	25,99941306	0.999985052	0.523233573	59.73492769
GOTERM_BP_DIRECT	GO:0007268~chemical synaptic transmission	3	5,555555556	0.076367729	KCNMA1, SLC18A3, CARTPT	49	172	18082	6,436402468	1	0.644608592	68.8333928
GOTERM_BP_DIRECT	GO:0021983~pituitary gland development	2	3,703703704	0.076705658	ALDH1A2, ISL1	49	30	18082	24,60136054	1	0.638036412	69.00248349
GOTERM_BP_DIRECT	GO:0007568~aging	3	5,555555556	0.077113343	FOS, NTRK1, IGF1R2	49	173	18082	6,399197829	1	0.632081076	69.2125886
GOTERM_CC_DIRECT	GO:0048471~perinuclear region of cytoplasm	5	9,259259259	0.077723612	KCNMA1, ALDH1A2, INHBA, RAB3C, STMN3	47	692	19662	3,022690936	0.999576684	0.384587179	58.98136685
UP_SEQ_FEATURE	domain:EGF-like 4; calcium-binding	2	3,703703704	0.078634451	FAT3, CELSR3	47	32	18012	23,95212766	0.999999996	0.617989199	65.13115149
GOTERM_MF_DIRECT	GO:0016620~oxidoreductase activity, acting on the aldehyde or oxo group of donors, NAD or NADP as acceptor	2	3,703703704	0.081084699	ALDH1A2, ALDH1A3	47	32	17446	23,19946809	0.999995269	0.53528781	63.35443439
INTERPRO	IPR001839~Transforming growth factor-beta, C-terminal	2	3,703703704	0.081131849	INHBA, GDNF	48	37	20594	23,19144144	0.999997807	0.632978305	63.76026299
GOTERM_BP_DIRECT	GO:0048678~response to axon injury	2	3,703703704	0.081609318	NTRK3, NTRK1	49	32	18082	23,06377551	1	0.645799002	71.33280041
UP_KEYWORDS	Lipoprotein	5	9,259259259	0.082333092	KCNMA1, ASGR1, RAB3C, STMN3, STMN4	49	780	22680	2,967032967	0.999906677	0.37121904	61.99560886
GOTERM_BP_DIRECT	GO:0031016~pancreas development	2	3,703703704	0.084051575	ALDH1A2, ISL1	49	33	18082	22,36487322	1	0.649381117	72.43150596
GOTERM_BP_DIRECT	GO:0046777~protein autophosphorylation	3	5,555555556	0.084928148	NTRK3, NTRK1, DCX	49	183	18082	6,049514888	1	0.645789208	72.81618834
GOTERM_MF_DIRECT	GO:0015459~potassium channel regulator activity	2	3,703703704	0.085933153	DPP6, KCNIP4	47	34	17446	21,83479349	0.999997803	0.535308282	65.58512953
GOTERM_BP_DIRECT	GO:0015171~amino acid transmembrane transporter activity	2	3,703703704	0.085933153	SLC38A5, SLC7A14	47	34	17446	21,83479349	0.999997803	0.535308282	65.58512953
GOTERM_BP_DIRECT	GO:0019228~neuronal action potential	2	3,703703704	0.086487473	KCNMA1, DPP6	49	34	18082	21,70708283	1	0.645359566	73.48815974
GOTERM_BP_DIRECT	GO:0070374~positive regulation of ERK1 and ERK2 cascade	3	5,555555556	0.08891283	HAND2, NTRK1, FAMI50B	49	188	18082	5,88823535	1	0.648727678	74.50264477
GOTERM_BP_DIRECT	GO:0071173~cellular response to BMP stimulus	2	3,703703704	0.088917028	PHOX2B, KCND3	49	35	18082	21,08688047	1	0.641607019	74.50436906
GOTERM_BP_DIRECT	GO:0001707~mesoderm formation	2	3,703703704	0.088917028	INHBA, TLX2	49	35	18082	21,08688047	1	0.641607019	74.50436906
GOTERM_BP_DIRECT	GO:0010628~positive regulation of gene expression	4	7,407407407	0.089192577	NTRK3, ALDH1A2, INHBA, HAND2	49	399	18082	3,699452713	1	0.635793625	74.61730199
GOTERM_MF_DIRECT	GO:0017046~peptide hormone binding	2	3,703703704	0.090756578	INHBA, NPR3	47	36	17446	20,62174941	0.999989898	0.535328756	67.68027087
GOTERM_BP_DIRECT	GO:0048015~phosphatidylinositol-mediated signaling	2	3,703703704	0.091340255	NTRK1, NPR3	49	36	18082	20,50113379	1	0.638097612	75.48167985
KEGG_PATHWAY	mmu00350~Tyrosine metabolism	2	3,703703704	0.092176215	ALDH1A3, DBH	20	39	7691	19,72051282	0.998465014	0.960821107	62.91048843
SMART	SM00204~IGFB	2	3,703703704	0.093404075	INHBA, GDNF	30	35	10425	19,85714286	0.96385981	0.669379222	57.63323386
GOTERM_BP_DIRECT	GO:0001656~metanephros development	2	3,703703704	0.096167792	GDNF, WT1	49	38	18082	19,42212675	1	0.651249489	77.32549675

Table S8. Functional annotation by DAVID for genes with increased expression in the microarray of E14.5 *Gata6*CO ureters



gene	genotype	biological replicates			mean	standard deviation	normalized biological replicates			mean	standard deviation	Student's t-test-unpaired
		#1	#2	#3			#1	#2	#3			
<i>Myocd</i>	control	1	1,278	1,074	1,117333333	0,117556606	0,89498807	1,14379475	0,96121718	1	0,105211759	p = 0,0016
	<i>Gata6-cKO</i>	0,397	0,138	0,236	0,257	0,106773904	0,35531026	0,12350835	0,21121718	0,23001193	0,095561371	
<i>Foxf1</i>	control	1	1,258	1,214	1,157333333	0,112692305	0,8640553	1,08698157	1,04896313	1	0,097372383	p = 0,4025
	<i>Gata6-cKO</i>	1,419	0,52	0,742	0,893666667	0,38236312	1,22609447	0,44930876	0,64112903	0,77217742	0,330382879	
<i>Axin2</i>	control	1	1,749	1,466	1,405	0,308805224	0,71174377	1,24483986	1,04341637	1	0,219790197	p = 0,7354
	<i>Gata6-cKO</i>	1,722	0,691	1,395	1,269333333	0,430181615	1,22562278	0,49181495	0,99288256	0,9034401	0,306179085	
<i>Id2</i>	control	1	1,678	1,211	1,296333333	0,283292938	0,77140653	1,29442016	0,93417331	1	0,218534023	p = 0,6363
	<i>Gata6-cKO</i>	1,19	1,857	1,285	1,444	0,294599163	0,91797377	1,43250193	0,99125739	1,11391103	0,22725572	
<i>Rarb</i>	control	1	1,364	1,116	1,16	0,15182446	0,86206897	1,17586207	0,96206897	1	0,130883154	p = 0,6935
	<i>Gata6-cKO</i>	1,432	0,838	1,513	1,261	0,300928563	1,23448276	0,72241379	1,30431034	1,08706896	0,259421175	

Supplementary Table S10. qRT-PCR analysis of SMC gene expression in control and *Gata6-cKO* ureters at E14.5

	2 days	3 days	4 days	5 days	6 days
control , DMSO-treated (n=28)	0	0	0.22±0.5	1.09±0.6	1.88±0.7
control , BMS493-treated (n=29)	0.12±0.3	0.66±0.4	0.95±0.3	1.14±0.4	1.30±0.6
<i>Gata6cKO</i> , DMSO-treated (n=16)	0	0	0.22±0.5	1.09±0.6	1.88±0.7
<i>Gata6cKO</i> , BMS493-treated (n=16)	0	0	0	0.03±0.1	0.25±0.3
ttest DMSO-treated control vs. DMSO <i>Gata6cKO</i>	0.083995	0.000406	2,75E+07	8,25E-07	0.019571
ttest BMS493-treated control vs. BMS493 <i>Gata6cKO</i>	0.019476	2,10E-08	8,19E-15	8,69E-14	3,55E-08
ttest DMSO-treated control vs. BMS493-treated control	0.227755	0.727461	4,51E-05	2,23E-10	1,29E-07
ttest DMSO-treated <i>Gata6cKO</i> vs. BMS493-treated <i>Gata6cKO</i>	0	0	0.079459	1,49E-07	1,70E-09
Onset of peristaltic activity:					
	2 days	3 days	4 days	5 days	6 days
control , DMSO-treated (n=28)	7 (25%)	20 (71,4%)	27 (96,4%)	28 (100%)	28 (100%)
control , BMS493-treated (n=29)	10 (34,5%)	25 (86%)	29 (100%)	29 (100%)	29 (100%)
<i>Gata6cKO</i> , DMSO-treated (n=16)	0	0	3 (18,8%)	16 (100%)	16 (100%)
<i>Gata6cKO</i> , BMS493-treated (n=16)	0	0	0	1 (6,25%)	43,75 (100%)

Table S11. Statistics of the peristaltic frequency of explant cultures of E18.5 control and *Gata6cKO* ureters treated with the pan-RAR antagonist BMS493.

Gene	Forward primer	Reverse primer
<i>Axin2</i>	5'-GCAGAAGCCACACAGAGAGT-3'	5'-CACCTCTGCTGCCACAAAAC-3'
<i>Foxf1</i>	5'-CAAGGCATCCCTCGGTATCA-3'	5'-AGATCCTCCGCCTGTTGTATG-3'
<i>Gapdh</i>	5'-ATGACATCAAGAAGGTGGTG-3'	5'-CATACCAGGAAATGAGCTTG-3'
<i>Id2</i>	5'-CTGGACTCGCATCCACTATC-3'	5'-ATGCCTGCAAGGACAGGATG-3'
<i>Myocd</i>	5'-CACACCTCAAAGAACCAAATGAAC-3'	5'-TTTTGACAGGGGATAGAGGGG-3'
<i>Ppia</i>	5'-GATTCATGTGCCAGGGTGGT-3'	5'-GCCATTCAGTCTTGCCAGTG-3'
<i>Rarb</i>	5'-AGAAAACGACGACCCAGCAA-3'	5'-ATTACACGTTCCGCACCTTTC-3'

Supplementary Table S12. Primers for qRT-PCR analysis of gene expression.

## Part 2 – GATA2 in SMC differentiation

### Delayed onset of smooth muscle cell differentiation leads to hydronephrosis formation in mice with conditional loss of the zinc finger transcription factor gene *Gata2* in the ureteric mesenchyme

Anna-Carina Weiss<sup>1</sup>, Tobias Bohnenpoll<sup>1</sup>, Jennifer Kurz<sup>1</sup>, Patrick Blank<sup>1</sup>, Rannar Airik<sup>1</sup>, Timo H Lüdtkke<sup>1</sup>, Marc-Jens Kleppa<sup>1</sup>, Lena Deuper<sup>1</sup>, Marina Kaiser<sup>1</sup>, Tamrat M Mamo<sup>1</sup>, Rui Costa<sup>1,2</sup>, Thomas von Hahn<sup>1,2</sup>, Mark-Oliver Trowe<sup>1</sup> and Andreas Kispert<sup>1\*</sup>

<sup>1</sup> Institut für Molekularbiologie, Medizinische Hochschule Hannover, 30625 Hannover, Germany

<sup>2</sup> Klinik für Gastroenterologie, Hepatologie und Endokrinologie, Medizinische Hochschule Hannover, Hannover, Germany

\*Correspondence to: Andreas Kispert, Institut für Molekularbiologie, OE5250, Medizinische Hochschule Hannover, Carl-Neuberg-Str. 1, D-30625 Hannover, Germany. Phone: +49 511 5324017, Fax: +49 511 5324283, E-Mail: kispert.andreas@mh-hannover.de

**Type of authorship:** Co-author

**Type of article:** Research article

**Share of the work:** 15%

**Contribution to the publication:** performed experiments, analyzed data, prepared figures

**Journal:** Journal of pathology

**Impact factor:** 6.021


**Number of citations:** 2

**Date of publication:** 30.04.2019

**DOI:** 10.1002/path.5270

Reprinted with permission (see appendix)

## Delayed onset of smooth muscle cell differentiation leads to hydroureter formation in mice with conditional loss of the zinc finger transcription factor gene *Gata2* in the ureteric mesenchyme

Anna-Carina Weiss<sup>1</sup>, Tobias Bohnenpoll<sup>1</sup>, Jennifer Kurz<sup>1</sup>, Patrick Blank<sup>1</sup>, Rannar Airik<sup>1</sup>, Timo H Lütke<sup>1</sup>, Marc-Jens Kleppa<sup>1</sup>, Lena Deuper<sup>1</sup>, Marina Kaiser<sup>1</sup>, Tamrat M Mamo<sup>1</sup>, Rui Costa<sup>1,2</sup>, Thomas von Hahn<sup>1,2</sup>, Mark-Oliver Trowe<sup>1</sup> and Andreas Kispert<sup>1\*</sup> 

<sup>1</sup> Institut für Molekularbiologie, Medizinische Hochschule Hannover, Hannover, Germany

<sup>2</sup> Klinik für Gastroenterologie, Hepatologie und Endokrinologie, Medizinische Hochschule Hannover, Hannover, Germany

\*Correspondence to: A Kispert, Medizinische Hochschule Hannover, Institut für Molekularbiologie, OE5250, Carl-Neuberg-Strasse 1, 30625 Hannover, Germany. E-mail: kispert.andreas@mh-hannover.de

### Abstract

The establishment of the peristaltic machinery of the ureter is precisely controlled to cope with the onset of urine production in the fetal kidney. Retinoic acid (RA) has been identified as a signal that maintains the mesenchymal progenitors of the contractile smooth muscle cells (SMCs), while WNTs, SHH, and BMP4 induce their differentiation. How the activity of the underlying signalling pathways is controlled in time, space, and quantity to activate coordinately the SMC programme is poorly understood. Here, we provide evidence that the Zn-finger transcription factor GATA2 is involved in this crosstalk. In mice, *Gata2* is expressed in the undifferentiated ureteric mesenchyme under control of RA signalling. Conditional deletion of *Gata2* by a *Tbx18<sup>cre</sup>* driver results in hydroureter formation at birth, associated with a loss of differentiated SMCs. Analysis at earlier stages and in explant cultures revealed that SMC differentiation is not abrogated but delayed and that dilated ureters can partially regain peristaltic activity when relieved of urine pressure. Molecular analysis identified increased RA signalling as one factor contributing to the delay in SMC differentiation, possibly caused by reduced direct transcriptional activation of *Cyp26a1*, which encodes an RA-degrading enzyme. Our study identified GATA2 as a feedback inhibitor of RA signalling important for precise onset of ureteric SMC differentiation, and suggests that in a subset of cases of human congenital ureter dilatations, temporary relief of urine pressure may ameliorate the differentiation status of the SMC coat.

© 2019 Pathological Society of Great Britain and Ireland. Published by John Wiley & Sons, Ltd.

**Keywords:** ureter; *Gata2*; smooth muscle; hydroureter; CAKUT; differentiation; development

Received 8 January 2019; Revised 3 March 2019; Accepted 21 March 2019

No conflicts of interest were declared.

### Introduction

The ureter is a critical component of the mammalian urinary system since it mediates, by peristaltic contractions of its outer smooth muscle cell (SMC) coat, the efficient removal of urine from the renal pelvis to the bladder. Since urine production starts in the fetal period of life, establishment of the ureteric peristaltic machinery has to be largely achieved in the embryo prior to this event.

In the mouse, a homogeneous precursor pool for all differentiated cell types of the ureter wall surrounds the distal aspect of the epithelium of the ureteric bud at embryonic day (E) 11.5. At E12.5, the ureteric mesenchyme (UM) is histologically subdivided into an inner and an outer region. Cells of the outer region give rise to adventitial fibroblasts; cells of the inner region initiate the SMC programme at E14.5 but further diversify at E15.5 into fibroblastic lamina propria cells adjacent to the ureteric epithelium (UE) and fully contractile SMCs

medially, slightly preceding the onset of urine production in the kidney at E16.5 [1].

The onset of SMC differentiation is controlled by a complex interplay of signalling modules and transcription factor activities. Sonic hedgehog (SHH) from the UE acts in the UM via the transcription factor FOXF1, which, in turn, induces the secreted signalling molecule BMP4 with which it cooperates in SMC activation [2,3]. Epithelial WNT signals restrict via mesenchymal TBX2 and TBX3 adventitial fates to the outer layer and induce SMC differentiation in the inner layer [4,5]. Mesenchymal retinoic acid (RA) delays SMC differentiation, possibly by counteracting WNT signalling. Interestingly, RA signalling is switched off at E14.5, i.e. slightly before the onset of the SMC differentiation programme, arguing for factors that tightly control the temporal limit of its activity [6].

Mutations in genes that control SMC differentiation are likely to contribute to the genetic complexity that



underlies human congenital anomalies of the kidney and the urinary tract (CAKUT) [7]. Identifying such genes and defining their function is important as hydronephrosis formation is a frequent abnormality in preterm babies [8] which can progress to dilatation of the renal pelvis (hydronephrosis), destruction of the renal parenchyma, and culminate in end-stage renal disease in children [9–11].

GATA2 is a member of a small family of zinc finger transcription factors, initially identified as regulators of lineage specification during early haematopoiesis [12]. Conditional gene targeting approaches that circumvented the lethal haematopoietic defects at E10.5 of *Gata2*-null mutants uncovered additional roles for the gene in neuronal differentiation [13–15]. A first requirement in urogenital development was found by analysis of *Gata2*-null mutants carrying a large genomic region of the *Gata2* locus as a transgene. These mice survived until birth and exhibited megaureter [16], a defect that was later correlated with an anterior shift of the ureter budding site [17,18]. Here, we describe a novel and independent requirement for GATA2 in the urogenital system. We show that *Gata2* regulates ureteric SMC differentiation at least partly as a feedback inhibitor of RA signalling.

## Materials and methods

### Animals

*Gata2*<sup>tm1Sac</sup> (synonym *Gata2*<sup>fl</sup>) [19] and *Tbx18*<sup>tm4(cre)Akis</sup> (synonym *Tbx18*<sup>cre</sup>) [20] mouse lines were maintained on an NMRI outbred background. Embryos were obtained from the mating of NMRI wild-type mice, and from the mating of *Tbx18*<sup>cre/+</sup>; *Gata2*<sup>fl/+</sup> males with *Gata2*<sup>fl/fl</sup> females. Littermates without the *Tbx18*<sup>cre</sup> allele were used as controls. For timed pregnancies, vaginal plugs were checked on the morning after mating and noon was taken as E0.5. Embryos and urogenital systems were dissected in PBS. Specimens were fixed in 4% PFA/PBS, transferred to methanol and stored at –20 °C prior to further processing. PCR genotyping was performed on genomic DNA prepared from liver biopsies. All animal work conducted for this study was approved by the local authorities (Niedersächsisches Landesamt für Verbraucherschutz und Lebensmittelsicherheit; permit number AZ33.12-42502-04-13/1356) and was performed at the central animal laboratory of the Medizinische Hochschule Hannover.

### Organ culture

Ureters were explanted on 0.4 µm polyester membrane Transwell supports (#3450; Corning Inc, Lowell, MA, USA) and cultured at the air–liquid interface as previously described [3]. BMS493 (#3509; Tocris Bio-Science, Minneapolis, MN, USA) and RA (#0695; Tocris) were dissolved in DMSO and added to the medium at a final concentration of 1 µM. SOSTDC1

(#9008-SD; R&D Systems, Minneapolis, MN, USA) was dissolved in 4 mM HCl and added at a final concentration of 1 µg/ml. For videos, cultures were equilibrated to room conditions and imaged with a bright-field channel for 1 min with a frame rate of 5 per second. Contractions per minute and peristaltic intensity were measured either manually or via computational Fiji Multi-Kymograph analysis (<http://www.imagej.net>) [21]. For this, the length of the ureter was subdivided into 25 (≙ proximal level), 50 (≙ medial level) or 75 (≙ distal level) percentiles. One contraction was set to 100 frames representing 20 s in real time. Kymograph grey values were divided by the maximum grey value and ratios were plotted using Microsoft Excel (Microsoft Corp, Redmond, WA, USA).

### Histological analysis

Embryos, urogenital systems or explant cultures were paraffin-embedded and sections were cut at 5 µm thickness. Haematoxylin and eosin staining was performed according to standard procedures. Ink injection experiments were performed as described previously [22].

### Cell proliferation and apoptosis assays

*In vivo* cell proliferation rates were investigated by the detection of incorporated BrdU on 5-µm paraffin sections. Apoptosis in tissues was assessed by the TUNEL assay using the ApopTag Plus Fluorescein *In Situ* Apoptosis Detection Kit (S7111; Merck, Darmstadt, Germany) on 5-µm paraffin sections.

### Immunofluorescent detection of antigens

Immunofluorescent analysis on 5-µm paraffin sections was carried out as described previously [1].

### RNA *in situ* hybridisation analysis

Whole-mount *in situ* hybridisation followed a standard procedure with digoxigenin-labelled antisense riboprobes [23]. Stained specimens were transferred in 80% glycerol prior to documentation. *In situ* hybridisation on 10 µm paraffin sections was performed as described previously [24]. For each marker, at least three independent specimens were analysed.

### RT-qPCR analysis

RT-qPCR analysis for *Cyp26a1* and *Rarb* was performed on mRNA reverse-transcribed using total RNA from pooled ureters.

### Microarrays

For microarray analysis, pools of ureters were dissected from male and female E14.5 control and *Tbx18*<sup>cre/+</sup>; *Gata2*<sup>fl/fl</sup> embryos. Total RNA was extracted, labelled, and hybridised to Agilent Whole Mouse Genome Oligo v2 (4x44K) microarrays

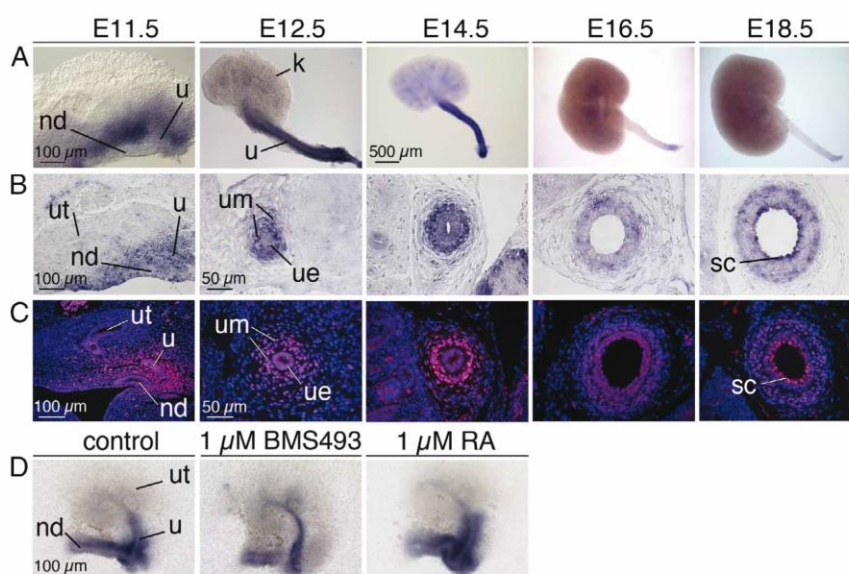


Figure 1. *Gata2* is strongly expressed in the undifferentiated mesenchyme during ureter development. (A, B) RNA *in situ* hybridisation analysis of *Gata2* expression in whole kidneys and ureters (A), and on sections of the metanephros (E11.5) and the proximal ureter region (E12.5 to E18.5) (B) of wild-type embryos. (C) Immunofluorescence analysis of the GATA2 protein on sections of the metanephros (E11.5) and of the proximal ureter region (E12.5 to E18.5) of wild-type embryos. The patterns of *Gata2* mRNA and GATA2 protein overlap throughout ureter development, with expression being most prominent in the undifferentiated UM from E11.5 to E14.5. (D) RNA *in situ* hybridisation of *Gata2* expression in E11.5 ureter/kidney explants grown for 18 h with DMSO (control), 1  $\mu$ M of the pan-RAR inhibitor BMS493 or 1  $\mu$ M RA. Expression of *Gata2* in the UM depends on RA signalling. Stages are as indicated. k, kidney; nd, nephric duct; sc, superficial cells; u, ureter; ue, ureteric epithelium; um, ureteric mesenchyme; ut, ureteric tip.

(G4846A; Agilent Technologies Inc, Santa Clara, CA, USA).

Microarray data have been submitted to GEO (GSE127702; <https://www.ncbi.nlm.nih.gov/geo/query/acc.cgi?acc=GSE127702>).

#### Chromatin immunoprecipitation and DNA-sequencing (ChIP-seq) assays

ChIP-seq analysis was performed on chromatin of ureters using a ChIP-grade rabbit anti-GATA2 antibody (ab22849; Abcam plc, Cambridge, UK). ChIP-seq data were analysed and visualised with the Integrative Genomics Viewer (IGV v.2.3.49; Broad Institute, University of California) [25].

#### Image documentation

Sections and organ cultures were photographed using a DM5000 microscope (Leica Camera, Wetzlar, Germany) with a Leica DFC300FX digital camera, or a Leica DM6000 microscope with a Leica DFC350FX digital camera. Urogenital systems were documented using a Leica M420 microscope with a Fujix HC-300Z digital camera (Fujifilm Holdings, Minato/Tokyo, Japan).

Additional details may be found in supplementary material, Supplementary materials and methods.

## Results

### *Gata2* expression in the UM is regulated by RA signalling

Recently, we profiled by microarray analysis the transcriptional changes caused by manipulation of RA signalling in explant cultures of E12.5 mouse ureters. Amongst the 228 genes that were positively regulated by RA signalling was the transcription factor gene *Gata2* [6]. Here, RNA *in situ* hybridisation revealed a dynamic pattern of *Gata2* expression in ureter development (Figure 1A,B). Strong expression was found in the mesenchymal compartment from E11.5 to E14.5: first in the entire UM (E11.5 to E12.5), then in the inner region (E14.5). At E16.5 and E18.5, expression continued in this domain at reduced levels. From E11.5 to E16.5, low *Gata2* expression was detected in the UE; it increased in superficial cells at E18.5. GATA2 protein expression recapitulated the pattern of *Gata2* mRNA. The protein was confined to the nucleus at all analysed stages (Figure 1C). In the developing bladder, *Gata2*/GATA2 expression was absent from the mesenchymal compartment but occurred in superficial cells at E16.5 and E18.5 (supplementary material, Figure S1).

To determine which expression domain of *Gata2* in the early metanephric field depends on RA signalling, we explanted E11.5 kidney rudiments and treated them



for 18 h with 1  $\mu$ M RA or 1  $\mu$ M of the pan-RA receptor (RAR) antagonist BMS493 [26]. Control explants showed *Gata2* expression in both the epithelium of the nephric duct and the ureter as well as in the surrounding mesenchyme. Manipulation of RA signalling positively affected expression in the mesenchymal domains but left epithelial expression unaltered (Figure 1D).

Loss of *Gata2* in the UM leads to prenatal hydroureteronephrosis

To determine the function of *Gata2* in the UM, we inactivated its expression in the progenitors of the UM by crossing *Tbx18<sup>cre</sup>* [27] with *Gata2<sup>fl/fl</sup>* mice [19]. Tissue-specific inactivation of *Gata2* was confirmed by severe down-regulation of GATA2 expression in the UM of *Tbx18<sup>cre/+</sup>;Gata2<sup>fl/fl</sup>* (*Gata2cKO*) embryos (supplementary material, Figure S2). Morphological and histological inspection of the urogenital system of *Gata2cKO* embryos at E18.5 revealed fully penetrant and sex-independent dilatation of the ureter ( $n = 15$ ) ranging in severity from unilateral hydroureter to bilateral megaureter (supplementary material, Figure S3). Ureter dilatation caused further structural lesions in the kidney – dilatation of the pelvis and compromised renal papilla (Figure 2A–H and supplementary material, Figure S4A–H). Analysis of markers indicating cytodifferentiation of the UM uncovered severely reduced expression of the key regulator of the SMC transcriptional programme *Myocd* and of the SMC structural components ACTA2, MYH11, *Tnnt2*, and *Tagln* at this stage. *Aldh1a2*, a marker for the fibrous lamina propria, was not detectable; *Dpt*, a marker for the fibrous adventitial layer, was slightly reduced in the mutant ureter (Figure 2I–V and supplementary material, Figure S4I–V). Components of the excitation/conduction system were unchanged in the mutant as revealed by normal expression of HCN3, a marker for pelvic pacemaker cells [28], and of KIT, a marker for interstitial Cajal-like cells [29] (supplementary material, Figure S5). Expression of *Upk3b* and of KRT5,  $\Delta$ NP63, and UPK1B which combinatorially mark basal cells (KRT5<sup>+</sup> $\Delta$ NP63<sup>+</sup>UPK1B<sup>-</sup>), intermediate cells (KRT5<sup>-</sup> $\Delta$ NP63<sup>-</sup>UPK1B<sup>+</sup>), and superficial cells (KRT5<sup>-</sup> $\Delta$ NP63<sup>-</sup>UPK1B<sup>+</sup>) in the urothelium [1], was not affected either (Figure 2W–B' and supplementary material, Figure S4W–B').

Possible contribution of physical obstruction to ureter dilatation was examined by intrapelvic ink injection experiments. In control embryos, the ink readily drained to the bladder. In *Gata2cKO* embryos with proximal hydroureter, the ink also reached the bladder ( $n = 3$ ), whereas in specimens with megaureter, most of the ink was retained in the ureter ( $n = 2$ ) (Figure 2C', D' and supplementary material, Figure S4C', D'). Histological staining showed that the distal ureter entered the bladder in the dorsal neck region in control embryos ( $n = 4$ ). In mutant embryos, the vesico-ureteric junction (VUJ) was shifted more cranially when hydroureter was present ( $n = 3$ ); the ureter ended blindly or on the urethra in the

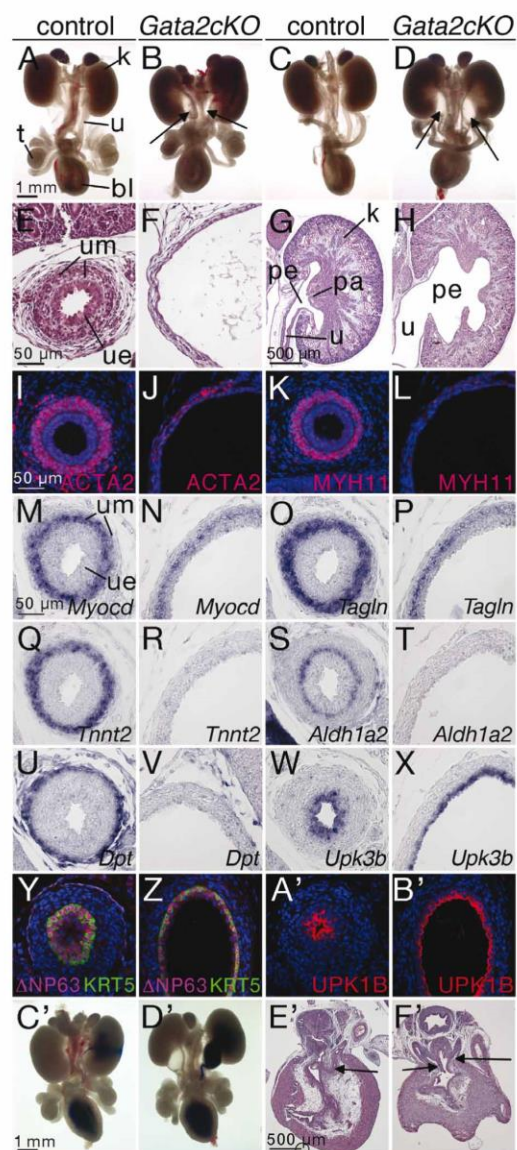


Figure 2. *Gata2cKO* embryos display hydroureteronephrosis at E18.5. (A–D) Morphology of whole urogenital systems of male (A, B) and female embryos (C, D). (B, D) Arrows point to the hydroureter. (E–H) Haematoxylin and eosin staining of transverse sections of the proximal ureter (E, F) and of sagittal kidney sections (G, H). (I–B') Cytodifferentiation of the UM (I–V) and of the urothelium (W–B') as shown by immunofluorescence (I–L and Y–B') and by section RNA *in situ* hybridisation analysis (M–X). Urothelial differentiation is unaffected, but SMC differentiation is severely compromised in the mutant. (C'–F') Analysis of the VUJ by ink injection (C', D') and by haematoxylin and eosin staining of sagittal bladder sections (E', F') excludes physical obstruction at the VUJ in the mutant. Arrows point to the orifice of the ureter into the bladder (E', F'). Genotypes, probes, and antibodies are as indicated. a, adrenal; bl, bladder; k, kidney; pa, papilla; pe, pelvis; u, ureter; ue, ureteric epithelium; um, ureteric mesenchyme; t, testis.



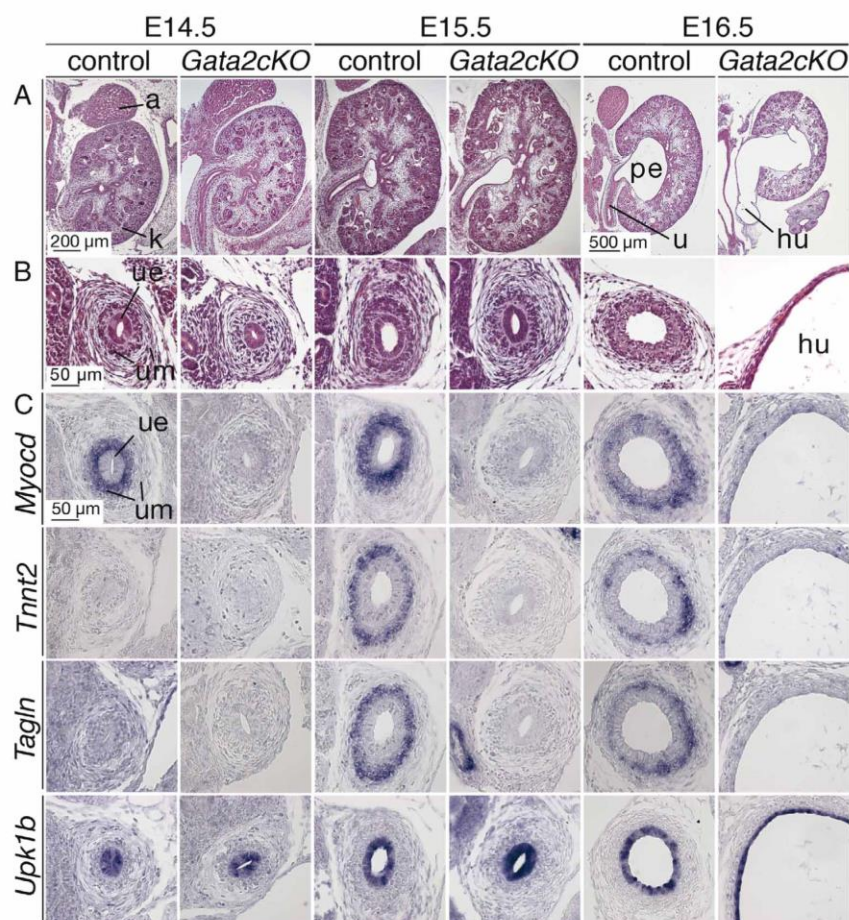


Figure 3. SMC differentiation is not initiated in *Gata2cKO* ureters. (A, B) Haematoxylin and eosin staining of sagittal sections of the kidney (A) and of transverse sections of the proximal ureter (B) shows hydroureter formation in *Gata2cKO* embryos at E16.5. (C) RNA *in situ* hybridisation analysis on proximal ureter sections for expression of markers of SMCs (*Myocd*, *Tnnt2*, *Tagln*) shows their absence in the mutant. Expression of the urothelial marker *Upk1b* is unchanged. a, adrenal; k, kidney; hu, hydroureter; pe, pelvis; u, ureter; ue, ureteric epithelium; um, ureteric mesenchyme.

megaureter condition ( $n = 3$ ) (Figure 2E',F' and supplementary material, Figure S4E',F'). In either condition, the bladder showed a normal presence of SMCs (supplementary material, Figure S6). Taken together, our data demonstrate that hydroureter formation in *Gata2cKO* embryos is caused by lack of ureteric SMCs, i.e. functional insufficiency, whereas megaureters arise from additional physical obstruction at the VUJ as previously reported [17].

#### *Gata2* is required for SMC differentiation in the ureter

To define the onset of urogenital malformations in *Gata2cKO* embryos, we performed histological and molecular analyses at E14.5 to E16.5, i.e. before, at, and after the onset of urine production. Dilatation of the renal pelvis and the ureter manifested in the mutant at E16.5; precursor cells of the inner region of the mutant

UM appeared smaller and less condensed at E14.5 (Figure 3A,B). Expression of *Myocd*, *Tnnt2*, and *Tagln* was not activated in the mutant ureter, whereas urothelial marker expression (*Upk1b*) occurred normally (Figure 3C).

We next asked whether these changes are preceded and/or accompanied by alterations in apoptosis or proliferation. However, we observed no changes in these cellular programmes in *Gata2cKO* ureters at E12.5 and E14.5 (supplementary material, Figure S7 and Table S1). These data show that GATA2 does not act as a survival or pro-proliferative factor but is critically required for SMC differentiation in the UM.

SMC differentiation is delayed in *Gata2cKO* ureters  
SMC differentiation was absent in *Gata2cKO* ureters at E14.5 and E15.5, but a subsequent activation of the programme may be compromised by increased hydrostatic



pressure. We tested this hypothesis by culturing E14.5 ureter explants, i.e. prior to urine formation. Indeed, mutant ureters ( $n = 4$ ) exhibited peristaltic contractions in culture, even though they occurred later and with reduced frequency and intensity compared with the controls ( $n = 5$ ) (Figure 4A,B and supplementary material, Figure S8, Tables S2 and S3, and Videos S1 and S2).

Expression of *Myocd*, *Tnnt2*, *Tagln*, and *Mylh11* was fully activated in wild-type ureters after 2 days of culture and was maintained at the same level for the next 4 days. In *Gata2cKO* ureters, these markers were weakly expressed after 2 days, but were up-regulated on day 4 (*Myocd*, *Mylh11*) or day 6 (*Tnnt2*, *Tagln*) (Figure 4C).

Dilated ureters explanted from E18.5 *Gata2cKO* embryos ( $n = 5$ ) exhibited significantly reduced contractions compared with the control ( $n = 7$ ) from day 2 to day 6 in culture (Figure 4D,E and supplementary material, Table S4). Strikingly, the contraction intensity of the medial and distal part of mutant (hydro-)ureters increased over time close to control levels; the proximal region gained some contractile intensity back but was lower than the control at all time points (Figure 4F and supplementary material, Table S5 and Videos S3–S6). These data show that loss of *Gata2* in the UM does not abrogate but delays SMC differentiation. Contraction intensity can be partially recovered in *ex vivo* culture conditions even when a dilatation has occurred.

#### Molecular analysis indicates enhanced RA signalling in *Gata2cKO* ureters

To identify molecular changes that may cause defective SMC differentiation in *Gata2cKO* ureters, we screened (using *in situ* hybridisation) for activity of pathways and expression of genes that have been implicated in this programme: *Ptch1*, target of SHH signalling [2,30]; *Bmp4* [31]; *Id2*, target of BMP signalling [31,32]; *Axin2*, target of WNT signalling [4,33]; *Rarb*, target of RA signalling [6,34]; and the transcription factor genes *Foxf1* [3], *Tbx18* [22], *Tshz3* [35], and *Sox9* [20]. At E14.5, all of these genes were expressed in the inner UM of mutant ureters as in the control except for *Tbx18*, *Tshz3*, and *Rarb*, which were up-regulated (supplementary material, Figure S9).

#### Transcriptional profiling of *Gata2cKO* ureters by RNA microarray analysis

We next performed transcriptional profiling by microarray analysis to detect differential gene expression between *Gata2cKO* and control ureters at E14.5. Since the *Gata2* expression domain in the UM represents only a fraction of the entire ureter, we employed a relatively low fold-change filter of 1.2. Using an intensity threshold of 100 as an additional filter, we detected 193 genes with reduced expression and 219 with increased expression in mutant ureters (supplementary material, Tables S6 and S7; GEO submission GSE127702). GO term analysis revealed enrichment of genes associated with collagen, the SMC phenotype, and development

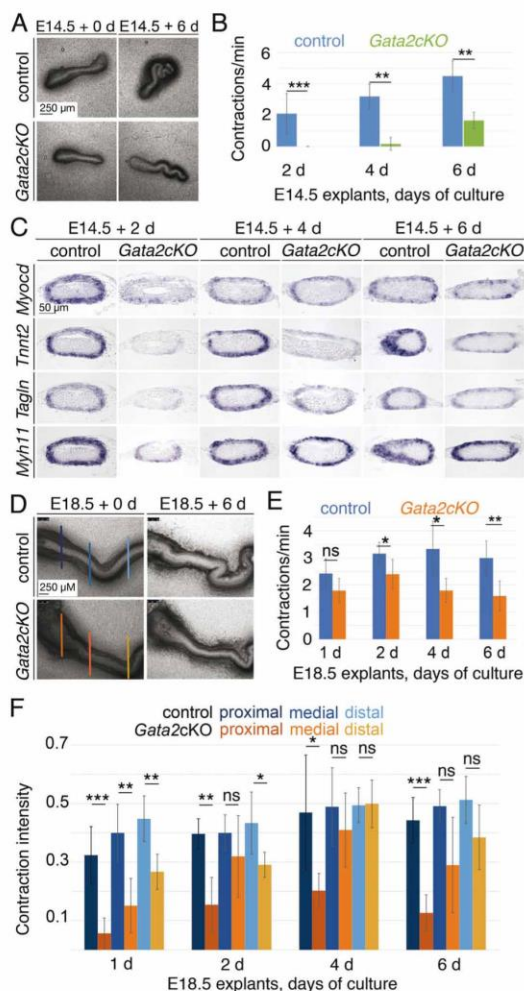


Figure 4. SMC differentiation and peristalsis occur in a delayed fashion in explant cultures of *Gata2cKO* ureters. (A) Morphology of E14.5 ureters grown for 0 and 6 days in culture. (B) Analysis of peristaltic contractions shows that mutant ureters ( $n = 4$ ) initiate peristaltic activity with a delay of 2 days and exhibit a third of the control ( $n = 5$ ) activity after 6 days in culture. (C) Analysis of SMC differentiation of the UM by RNA *in situ* hybridisation analysis of markers on sections of explants of E14.5 ureters grown for 2, 4, and 6 days in culture. SMC differentiation is delayed by 2–4 days in *Gata2cKO* ureters. (D) Morphology of E18.5 ureter explants grown in culture. Vertical lines indicate proximal, medial, and distal ureter levels. (E) Analysis of the contraction frequency in E18.5 ureters cultured for 6 days (mutant  $n = 5$ , control  $n = 7$ ). (F) Analysis of the contraction intensity at proximal, medial, and distal levels of ureters explanted at E18.5 and cultured for 6 days (mutant  $n = 5$ , control  $n = 7$ ). Differences were considered significant with a  $P$  value below 0.05 ( $*p \leq 0.05$ ), highly significant ( $**p \leq 0.01$ ), and extremely significant ( $***p \leq 0.001$ ); two-tailed Student's  $t$ -test. For statistical values see supplementary material, Tables S2, S4, and S5. Stages, time points, genotypes, and probes are as indicated.

Table 1. List of genes with altered expression in microarrays of E14.5 *Gata2cKO* ureters. (A) Genes with decreased expression in the E14.5 *Gata2cKO* microarray. (B) Genes with increased expression in the E14.5 *Gata2cKO* microarray. Shown are the top 15 deregulated genes and selected candidates with their rank, average fold-change (FC), and the presence of an associated ChIP peak

Rank	Gene symbol	Average FC	ChIP peak	Rank	Gene symbol	Average FC	ChIP peak
(A) Genes with decreased expression in the E14.5 <i>Gata2cKO</i> microarray							
1	<i>Cyp26a1</i>	-6.3	Yes	25	<i>Pitx1</i>	-2.6	
2	<i>Higd1c</i>	-5.6		30	<i>Myh11</i>	-2.5	
3	<i>A930009L07Rik</i>	-5.2		33	<i>Actg2</i>	-2.3	
4	<i>Chgb</i>	-4.4		44	<i>Cnn1</i>	-2.2	
5	<i>AB099516</i>	-4.2		52	<i>Ddc</i>	-2.1	
6	<i>Chga</i>	-4.0		54	<i>Myh3</i>	-2.0	
7	<i>C1ql3</i>	-3.7		61	<i>Col9a1</i>	-1.9	
8	<i>Dbh</i>	-4.3		62	<i>Tnnt2</i>	-1.9	
9	<i>Insm1</i>	-3.2		68	<i>Acta1</i>	-1.8	
10	<i>Npy</i>	-3.2		69	<i>Acta2</i>	-1.8	
11	<i>Ctnna2</i>	-3.2		70	<i>Myl1</i>	-1.8	
12	<i>Nefm</i>	-3.0		85	<i>Car3</i>	-1.7	Yes
13	<i>Slc18a2</i>	-3.0		92	<i>Tgfb2</i>	-1.7	
14	<i>Hand2</i>	-2.8		140	<i>Sulf1</i>	-1.5	
15	<i>Colq</i>	-2.8		149	<i>Crym</i>	-1.5	
(B) Genes with increased expression in the E14.5 <i>Gata2cKO</i> microarray							
1	<i>Sostdc1</i>	+4.7		38	<i>Ahr</i>	+1.9	
2	<i>Ddx6</i>	+4.4		43	<i>Nell1</i>	+1.9	
3	<i>2310065F04Rik</i>	+3.7		47	<i>Aldh1a3</i>	+1.9	
4	<i>Htr2b</i>	+3.4		52	<i>Wif1</i>	+1.8	Yes
5	<i>Cntfr</i>	+3.1		56	<i>Enpep</i>	+1.8	Yes
6	<i>Avpr1a</i>	+3.0	Yes	74	<i>Hoxd11</i>	+1.7	
7	<i>Alx1</i>	+2.5		97	<i>Pou3f1</i>	+1.7	
8	<i>EphA8</i>	+2.4		104	<i>Foxl1</i>	+1.6	
9	<i>Dach2</i>	+2.2		106	<i>Sema3c</i>	+1.6	
10	<i>Fzd10</i>	+2.3		140	<i>Ndp</i>	+1.5	
11	<i>Mapk8</i>	+2.3		168	<i>Tnfrsf19</i>	+1.4	
12	<i>D430041D05Rik</i>	+2.2		186	<i>Tshz3</i>	+1.4	
13	<i>Dus4l</i>	+2.2		204	<i>Ecm1</i>	+1.4	
14	<i>Lsm14b</i>	+2.2		201	<i>Plxna2</i>	+1.4	Yes
15	<i>A830039N20Rik</i>	+2.1		209	<i>Rbp4</i>	+1.4	

of the nervous system in the pool of down-regulated genes; the pool of up-regulated genes contained neuron differentiation and WNT signalling, amongst others (supplementary material, Tables S8 and S9).

*Cyp26a1*, encoding an RA-degrading enzyme [36,37], was the top down-regulated gene (-6.3). Strongly up-regulated genes included the anti-differentiation gene *Ddx6* (+4.7) [38], the WNT/BMP regulatory gene *Sostdc1* (+4.4) [39], the receptor gene *Avpr1a* (+3.0), and the transcription factor genes *Dach2* (+2.2) and *Alx1* (+2.5). The RA-synthesizing gene *Aldh1a3* (+1.9) and the well-known target of RA signalling *Ecm1* (+1.4) were also up-regulated (Table 1). Expression of *Axin2*, *Bmp4*, and *Id2* was unchanged, whereas expression of *Tbx18* (+1.3), *Tshz3* (+1.4), and *Rarb* (+1.2) was increased in mutant ureters, corroborating the *in situ* hybridisation data (supplementary material, Tables S6 and S7 and Figure S9).

To identify direct targets of GATA2 transcriptional activity, we performed an *in vivo* chromatin immunoprecipitation (ChIP-seq) analysis on E14.5 ureters, and compared the list of genes associated with peaks of chromatin enrichment with the list of genes with differential expression in the mutant

ureter. In the intersection with down-regulated genes, we identified *Cyp26a1* (-6.3), *Nefl* (-2.2), *Grem2* (-2.1), *Car3* (-1.7), and *Fgf7* (-1.5). Up-regulated genes with binding peaks were *Avpr1a* (+3.0), *Cd83* (+2.1), *Enpep* (+1.8), *Wif1* (+1.8), and *Plxna2* (+1.4). Subsequent *in silico* analysis uncovered the GATA binding motif within the peak regions (Table 1, Figure 5A, and supplementary material, Figures S10 and S11).

We validated expression of direct targets, top regulated genes, and further selected candidates in E14.5 ureters by RNA *in situ* hybridisation analysis. From the group of down-regulated genes, we confirmed reduced mesenchymal expression in mutants for *Higd1c*, *Myh11*, *Cnn1*, *Col9a1*, *Zcchc12*, *Car3*, and *Sulf1* (supplementary material, Figure S12). From the list of up-regulated genes, mesenchymal expression of all putative direct targets appeared enhanced: moderately for *Enpep*, *Cd83*, and *Wif1*; robustly for *Avpr1a* and *Plxna2*. Increased expression was also detected for *Sostdc1*, *Alx1*, *Dach2*, *Fzd10*, *Ahr*, *Pou3f1*, *Sema3c*, *Hey2*, and *Ecm1* (supplementary material, Figure S13). We conclude that loss of *Gata2* in the UM impinges on the expression of genes that modulate the SMC differentiation programme.

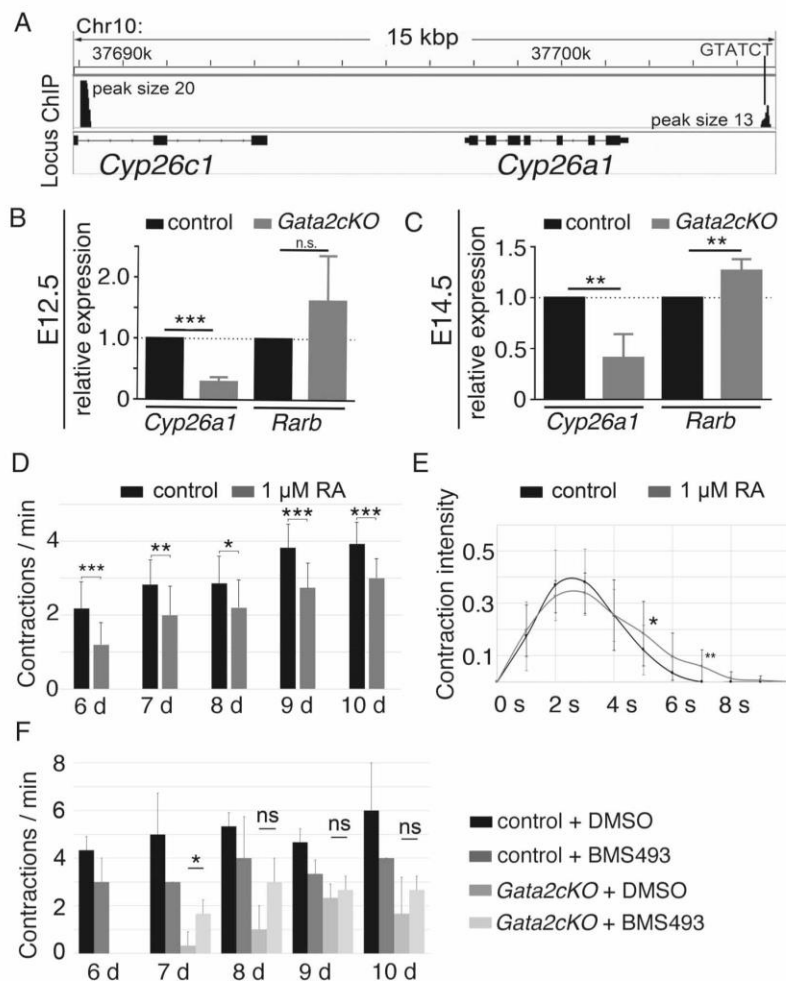


Figure 5. Enhanced RA signalling may contribute to defects in SMC differentiation in *Gata2cKO* ureters. (A) Scheme of the genomic organisation of the *Cyp26a1* locus on chromosome 10 with GATA2 binding peaks as found in ChIP-seq experiments of E14.5 ureters. Exon coding sequences are shown as large black boxes; 3'- and 5'-UTRs are indicated as smaller black boxes. Binding peaks as detected by ChIP-seq analysis are plotted as black vertical lines with relative peak height. A GATA binding site is indicated. (B, C) RT-PCR analysis of expression of *Cyp26a1* and *Rarb* in *Gata2cKO* embryos at E12.5 (B) and E14.5 (C) confirms the microarray data. The relative quantification of the expression of *Rarb* and *Cyp26a1* in E12.5 and E14.5 control versus mutant pools ( $n = 3$ ) is shown. Values are displayed as mean  $\pm$  SD; ns:  $p > 0.05$ , \* $p \leq 0.05$ , \*\* $p \leq 0.01$ , \*\*\* $p \leq 0.001$  by two-tailed Student's  $t$ -test. For statistical values see supplementary material, Table S10. (D, E) Explants of E12.5 wild-type ureters treated with 1  $\mu$ M RA ( $n = 15$ ) have a normal onset of peristalsis but display significantly fewer contractions per minute over the course of the 10-day culture period compared with the DMSO-treated control ( $n = 14$ ) (D). Moreover, the contraction intensity is decreased and the relaxation time increased (E). For values and statistical evaluation see supplementary material, Tables S11 and S12. (F) Explants of E12.5 control ureters treated with 1  $\mu$ M BMS493 have a normal onset of peristalsis but display significantly fewer contractions per minute over the course of the 10-day culture period compared with the DMSO-treated control ( $n = 3$  each) (E). In contrast, in *Gata2cKO* ureters ( $n = 3$ ), BMS493 treatment leads to increased contraction frequencies starting from day 7 of culture. For values and statistical evaluation see supplementary material, Table S13.

Enhanced RA signalling may contribute to the reduced peristaltic activity of *Gata2cKO* ureters

Our analyses identified *Cyp26a1* as a putative direct target of GATA2 transcriptional activation (Figure 5A). Since *in situ* hybridisation analysis was not sufficiently sensitive to detect *Cyp26a1* expression in the UM, we performed an RT-qPCR experiment. We observed a significant down-regulation of *Cyp26a1* expression in E12.5 (3.4-fold) and E14.5 (2.4-fold) mutant ureters.

These changes correlated with an increase of the RA target gene *Rarb* at E12.5 (1.6-fold) and E14.5 (1.2-fold) (Figure 5B,C and supplementary material, Table S10). Comparing the list of genes up-regulated in the *Gata2cKO* microarray ( $n = 219$ ) with the list of genes up-regulated in ureters treated with RA ( $n = 548$ ) that we established recently [6], we found that a highly significant ( $p < 8.91 \times 10^{-18}$ ) number of genes ( $n = 30$ ) were common to the two lists (Table 2), including *Cd83*, *Ecm1*, *Hey2*, and *Pou3f1*, whose increased expression



Table 2. List of genes with increased expression in E14.5 *Gata2cKO* ureters and in E12.5 ureters treated with RA. Shown are all 30 up-regulated genes found with their average fold-change (FC) in the two conditions

Gene symbol	RA-induced		Gene symbol	RA-induced	
	<i>Gata2cKO</i> average FC	average FC		<i>Gata2cKO</i> average FC	average FC
<i>Acs1</i>	+2.1	+1.5	<i>ligp</i>	+1.7	+1.7
<i>AK046833</i>	+2.0	+1.9	<i>Kcnk2</i>	+1.7	+2.7
<i>AK139043</i>	+1.7	+1.4	<i>Kif26b</i>	+1.6	+1.3
<i>Cd83</i>	+2.1	+1.9	<i>Lrfn5</i>	+1.7	+1.4
<i>Cntn1</i>	+2.1	+1.9	<i>Map3k5</i>	+1.4	+1.3
<i>Ecm1</i>	+1.4	+5.8	<i>Mgll</i>	+1.4	+1.3
<i>Elf5</i>	+1.4	+1.5	<i>Myo18b</i>	+2.0	+3.2
<i>Enpep</i>	+1.8	+1.4	<i>Nell1</i>	+1.9	+1.3
<i>Fam155a</i>	+1.7	+1.8	<i>Neto2</i>	+2.1	+1.6
<i>Flrt2</i>	+1.4	+1.4	<i>Palm2</i>	+1.5	+1.4
<i>Foxl1</i>	+1.6	+1.7	<i>Pou3f1</i>	+1.6	+1.6
<i>Fut9</i>	+1.9	+1.9	<i>Syndig1</i>	+1.7	+1.6
<i>Gm4951</i>	+1.6	+1.6	<i>TC1703733</i>	+1.4	+1.4
<i>Hey2</i>	+1.5	+1.7	<i>Tec</i>	+1.6	+1.7
<i>Htr2b</i>	+3.4	+5.5	<i>Trim9</i>	+1.4	+1.5

in *Gata2*-deficient UM we had already confirmed by *in situ* hybridisation. This suggests that increased RA signalling contributes to transcriptional changes in *Gata2cKO* ureters and that reduced degradation of RA at least partly underlies this phenomenon.

To investigate whether enhanced and extended RA signalling suffices to delay the onset of SMC differentiation, we explanted E12.5 ureters and treated them with 1  $\mu$ M RA throughout a culture period of 10 days. Peristaltic activity commenced in ureters treated with 1  $\mu$ M RA ( $n = 15$ ) after 6 days as in the control ( $n = 14$ ), but the contraction rate was significantly reduced over the next 4 days (Figure 5D and supplementary material, Table S11). Moreover, the contraction intensity was diminished and the relaxation time extended (Figure 5E and supplementary material, Table S12 and Videos S7 and S8).

We next tested whether reduction of RA signalling ameliorated the peristaltic changes of *Gata2cKO* ureters. Treatment of control ureters ( $n = 3$ ) with the pan-RAR antagonist BMS493 at 1  $\mu$ M did not affect the onset of contractions but lowered the contraction frequency during the further course of culture. In *Gata2cKO* ureters ( $n = 3$ ), BMS493 treatment did not affect the delayed peristaltic onset but increased the contraction frequency, reaching significance level at day 7 (Figure 5F).

We conclude that increased RA signalling partly contributes to the peristaltic defects observed in *Gata2*-deficient ureters.

## Discussion

Here, we identified GATA2 as a novel regulator of ureteric SMC differentiation in mice. Our findings indicate that GATA2 acts in an RA feedback loop but also regulates additional pathways important for SMC

differentiation. Our work suggests that not only a complete abrogation of SMC differentiation but also a delay by 2–3 days results in ureter dilatation at birth. Temporary relief from the resulting hydrostatic pressure may aid in regaining the SMC performance.

Hydroureter formation relates to a novel and independent function of GATA2 in the UM

Our analysis revealed that the conditional deletion of *Gata2* from the TBX18-positive mesenchymal lineage in the early metanephric field leads to megaureter formation due to physical obstruction at the VUJ in approximately 40% of prenatal embryos. This phenotype resembles the one in mice in which a large *Gata2* transgene rescued the early haematopoietic requirement of the gene, and the one in mice carrying a hypomorphic allele of *Gata2* [16,17]. Analysis of the latter uncovered a role for GATA2 in positioning the ureter bud by maintaining the expression of *Bmp4* in the mesenchyme surrounding the nephric duct [17,18]. The incomplete penetrance of megaureter formation in our setting may relate to incomplete recombination mediated by *Tbx18<sup>cre</sup>* within this domain. In fact, *Tbx18* is expressed in cells surrounding the distal ureter bud and the peri-nephric duct mesenchyme at E10.5 but is excluded from the latter domain within 12–24 h [27]. Of course, we cannot exclude a differential contribution of the genetic background to the severity of the defects in the different mouse models.

Sixty per cent of prenatal *Gata2cKO* embryos exhibited hydroureter with a pronounced proximal dilatation. The argument may arise that this phenotype is simply a weaker manifestation of a megaureter reflecting *Gata2* requirement in one and the same process, namely the positioning of the ureteric bud. However, our analysis showed that hydroureter formation is not associated with physical obstruction of urinary drainage but is due to SMC deficiency. This is best seen in our explant cultures in which E14.5 *Gata2cKO* ureters exhibited delayed SMC differentiation and compromised peristaltic performance in the absence of any urinary pressure. Together with expression of *Gata2* in the undifferentiated UM, this argues for an independent requirement of *Gata2* for ureteric SMC differentiation. We did not find changes in *Bmp4* expression at the critical period in the UM. Hence, GATA2 acts in this tissue via a molecular programme that is different from that in the peri-nephric duct mesenchyme. We would like to note that we did not detect expression or a functional requirement of *Gata2* in SMC differentiation of the bladder mesenchyme. This indicates that the similar organisation of the contractile coat of the ureter and bladder relies, at least partly, on different regulatory modules in development.

GATA2 is a feedback inhibitor of RA signalling but it also regulates other signalling pathways in the UM

*Gata2* expression in the UM coincides with the temporal profile of RA signalling [6]. Pharmacological inhibition



of RA signalling largely abrogated *Gata2* expression, whereas addition of RA increased *Gata2* levels in the UM, identifying RA signalling as the major regulatory input for *Gata2* expression in this tissue.

We have recently shown that reduced RA signalling leads to premature ureteric SMC differentiation [6]. Given our finding that SMC differentiation is delayed in *Gata2cKO* ureters, GATA2 is unlikely to act as a (positive) mediator of RA signalling, but may serve as an essential inhibitor for this pathway in a feedback loop. This is corroborated by increased expression of a set of RA signalling targets in *Gata2*-deficient ureters. Moreover, increased and prolonged RA signalling led to decreased and less intense contractions of wild-type ureters, while reduction of RA signalling in *Gata2cKO* ureters increased the contraction frequency, supporting the notion that the failure to timely dampen the activity of this pathway contributes to the peristaltic changes in the *Gata2cKO* ureter. The gene encoding the RA-degrading enzyme CYP26A1 was strongly reduced in *Gata2cKO* ureters and featured GATA2 binding peaks in a Chip-seq experiment, presenting a possible direct target of GATA2 transcriptional activation and RA signalling regulation in the UM.

However, additional factors and/or pathways need to be deregulated to account for the severe delay of SMC differentiation and peristaltic activity in the mutant. Our work identified *Fam227b/Fgf7*, *Nefl*, *Grem2*, and *Car3* as additional direct targets of GATA2 transcriptional activation. To our knowledge, there are no functional data available for a role of these genes in ureter SMC differentiation. *Grem2* encodes a member of the DAN family of BMP antagonists, indicating enhanced BMP signalling in the mutant UM. *Avpr1a*, *Enpep*, *Plxna2*, *Cd83*, and *Wif1* had GATA2 binding peaks and showed increased expression, indicating that GATA2 acts bimodally, i.e. as an activator as well as a repressor of transcription in this tissue context. *Wif1* encodes a WNT inhibitory factor, arguing for reduced WNT signalling in the UM. Besides these direct targets of transcriptional repression, our analyses characterised increased expression of factors that may additionally impinge on BMP and WNT signalling. *Sostdc1* encodes a secreted protein that prevents the binding of BMPs to their receptors. SOSTDC1 also interacts with LRPs, WNT co-receptors, abrogating this signalling pathway as well [40–42]. Administration of SOSTDC1 to ureter explant cultures lowered the contraction frequency (supplementary material, Figure S14), implicating increased *Sostdc1* in the peristaltic defects of *Gata2*-deficient ureters. Of note, increased *Sostdc1* expression is commonly identified in ureter tissues of human CAKUT patients [43]. POU3F1 is an upstream activator of neural lineage genes, but also represses BMP and WNT signalling [44].

Hence, altered BMP4 and/or WNT signalling may additionally contribute to the failure to activate *Myocd* expression: hence, SMC differentiation in the *Gata2*-deficient UM. Our finding that SMC differentiation is not abrogated but delayed is compatible

with the notion that GATA2 predominantly inhibits anti-differentiation pathways.

A therapeutic option to ameliorate ureter dilatations and its adverse effects

CAKUT belong to the most frequent human birth defects [45,46]. They affect all components of the urinary system as well as their interfaces. Ureter dilatations present a frequent subgroup of these defects, relating to physical obstruction of the ureter and its junctions or to functional insufficiency of the peristaltic machinery. In either case, the condition is worsened by the fact that the increased hydrostatic pressure of the urine prevents differentiation of mesenchymal progenitors and/or induces dedifferentiation of SMCs into myofibroblasts that produce more extracellular matrix and exert reduced contractile activity [47,48]. Physical obstruction can be resolved by surgical bypass; however, organ replacement is the only mechanism currently available to avoid nephropathy caused by the functional insufficiency of the SMC coat.

Our finding that *Gata2*-deficient ureters regain considerable peristaltic performance when relieved from urinary pressure by *ex vivo* culture argues that a temporary artificial bypass *in vivo* may provide an opportunity for the mesenchymal coat to (re-)differentiate contractile SMCs. Of course, such a therapeutic option is irrelevant for genetic insults in positive regulators of SMC differentiation but would apply to a (small) subgroup of genes that coordinate the temporal onset of SMC differentiation such as *Gata2*.

## Acknowledgements

We thank Rolf Kemler for the anti-CDH1 antiserum and Robert Adelstein for the MHY11 antiserum. We are grateful to Sally Camper for providing the floxed *Gata2* mouse line and for critical reading of the manuscript. This work was funded by a grant from the Deutsche Forschungsgemeinschaft (DFG KI728/9 to AK).

## Author contributions statement

ACW, TB, and AK conceived and designed the study. ACW, TC, JK, PB, RA, THL, MJK, LD, MK, and TMM performed experiments. ACW, TB, THL, TMM, RC, TVH, and MOT performed *in silico* and statistical analyses. All the authors contributed to data interpretation. ACW and AK drafted the paper. All the authors approved the final version of the paper.

## References

1. Bohnenpoll T, Feraric S, Nattkemper M, *et al.* Diversification of cell lineages in ureter development. *J Am Soc Nephrol* 2017; **28**: 1792–1801.
2. Yu J, Carroll TJ, McMahon AP. Sonic hedgehog regulates proliferation and differentiation of mesenchymal cells in the mouse metanephric kidney. *Development* 2002; **129**: 5301–5312.

3. Bohnenpoll T, Wittern AB, Mamo TM, et al. A SHH–FOXF1–BMP4 signaling axis regulating growth and differentiation of epithelial and mesenchymal tissues in ureter development. *PLoS Genet* 2017; **13**: e1006951.
4. Trowe MO, Airik R, Weiss AC, et al. Canonical Wnt signaling regulates smooth muscle precursor development in the mouse ureter. *Development* 2012; **139**: 3099–3108.
5. Aydogdu N, Rudat C, Trowe MO, et al. TBX2 and TBX3 act downstream of canonical WNT signaling in patterning and differentiation of the mouse ureteric mesenchyme. *Development* 2018; **145**: pii: dev171827.
6. Bohnenpoll T, Weiss AC, Labuhn M, et al. Retinoic acid signaling maintains epithelial and mesenchymal progenitors in the developing mouse ureter. *Sci Rep* 2017; **7**: 14803.
7. Capone VP, Morello W, Taroni F, et al. Genetics of congenital anomalies of the kidney and urinary tract: the current state of play. *Int J Mol Sci* 2017; **18**: E796.
8. Dudley JA, Haworth JM, McGraw ME, et al. Clinical relevance and implications of antenatal hydronephrosis. *Arch Dis Child Fetal Neonatal Ed* 1997; **76**: F31–F34.
9. Johnson CE, Elder JS, Judge NE, et al. The accuracy of antenatal ultrasonography in identifying renal abnormalities. *Am J Dis Child* 1992; **146**: 1181–1184.
10. Chevalier RL. Pathophysiology of obstructive nephropathy in the newborn. *Semin Nephrol* 1998; **18**: 585–593.
11. Chevalier RL. Perinatal obstructive nephropathy. *Semin Perinatol* 2004; **28**: 124–131.
12. Tsai FY, Keller G, Kuo FC, et al. An early haematopoietic defect in mice lacking the transcription factor GATA-2. *Nature* 1994; **371**: 221–226.
13. Nardelli J, Thiesson D, Fujiwara Y, et al. Expression and genetic interaction of transcription factors GATA-2 and GATA-3 during development of the mouse central nervous system. *Dev Biol* 1999; **210**: 305–321.
14. Craven SE, Lim KC, Ye W, et al. Gata2 specifies serotonergic neurons downstream of sonic hedgehog. *Development* 2004; **131**: 1165–1173.
15. Tsarovina K, Pattyn A, Stubbusch J, et al. Essential role of Gata transcription factors in sympathetic neuron development. *Development* 2004; **131**: 4775–4786.
16. Zhou Y, Lim KC, Onodera K, et al. Rescue of the embryonic lethal hematopoietic defect reveals a critical role for GATA-2 in urogenital development. *EMBO J* 1998; **17**: 6689–6700.
17. Hoshino T, Shimizu R, Ohmori S, et al. Reduced BMP4 abundance in Gata2 hypomorphic mutant mice result in uropathies resembling human CAKUT. *Genes Cells* 2008; **13**: 159–170.
18. Ainoya K, Moriguchi T, Ohmori S, et al. UG4 enhancer-driven GATA-2 and bone morphogenetic protein 4 complementation remedies the CAKUT phenotype in Gata2 hypomorphic mutant mice. *Mol Cell Biol* 2012; **32**: 2312–2322.
19. Charles MA, Saunders TL, Wood WM, et al. Pituitary-specific Gata2 knockout: effects on gonadotrope and thyrotrope function. *Mol Endocrinol* 2006; **20**: 1366–1377.
20. Airik R, Trowe MO, Foik A, et al. Hydrourteronephrosis due to loss of Sox9-regulated smooth muscle cell differentiation of the ureteric mesenchyme. *Hum Mol Genet* 2010; **19**: 4918–4929.
21. Schindelin J, Arganda-Carreras I, Frise E, et al. Fiji: an open-source platform for biological-image analysis. *Nat Methods* 2012; **9**: 676–682.
22. Airik R, Bussen M, Singh MK, et al. Tbx18 regulates the development of the ureteral mesenchyme. *J Clin Invest* 2006; **116**: 663–674.
23. Wilkinson DG, Nieto MA. Detection of messenger RNA by *in situ* hybridization to tissue sections and whole mounts. *Methods Enzymol* 1993; **225**: 361–373.
24. Moorman AF, Houweling AC, de Boer PA, et al. Sensitive non-radioactive detection of mRNA in tissue sections: novel application of the whole-mount *in situ* hybridization protocol. *J Histochem Cytochem* 2001; **49**: 1–8.
25. Robinson JT, Thorvaldsdottir H, Winckler W, et al. Integrative genomics viewer. *Nat Biotechnol* 2011; **29**: 24–26.
26. Chazaud C, Dolle P, Rossant J, et al. Retinoic acid signaling regulates murine bronchial tubule formation. *Mech Dev* 2003; **120**: 691–700.
27. Bohnenpoll T, Bettenhausen E, Weiss AC, et al. Tbx18 expression demarcates multipotent precursor populations in the developing urogenital system but is exclusively required within the ureteric mesenchymal lineage to suppress a renal stromal fate. *Dev Biol* 2013; **380**: 25–36.
28. Hurtado R, Bub G, Herzlinger D. The pelvis–kidney junction contains HCN3, a hyperpolarization-activated cation channel that triggers ureter peristalsis. *Kidney Int* 2010; **77**: 500–508.
29. David SG, Cebrian C, Vaughan ED Jr, et al. c-kit and ureteral peristalsis. *J Urol* 2005; **173**: 292–295.
30. Ingham PW, McMahon AP. Hedgehog signaling in animal development: paradigms and principles. *Genes Dev* 2001; **15**: 3059–3087.
31. Mamo TM, Wittern AB, Kleppa MJ, et al. BMP4 uses several different effector pathways to regulate proliferation and differentiation in the epithelial and mesenchymal tissue compartments of the developing mouse ureter. *Hum Mol Genet* 2017; **26**: 3553–3563.
32. Hollnagel A, Oehlmann V, Heymer J, et al. *Id* genes are direct targets of bone morphogenetic protein induction in embryonic stem cells. *J Biol Chem* 1999; **274**: 19838–19845.
33. Jho EH, Zhang T, Dornon C, et al. Wnt/beta-catenin/Tcf signaling induces the transcription of Axin2, a negative regulator of the signaling pathway. *Mol Cell Biol* 2002; **22**: 1172–1183.
34. Mendelsohn C, Ruberte E, LeMour M, et al. Developmental analysis of the retinoic acid-inducible RAR-beta 2 promoter in transgenic animals. *Development* 1991; **113**: 723–734.
35. Caubit X, Lye CM, Martin E, et al. Teashirt 3 is necessary for ureteral smooth muscle differentiation downstream of SHH and BMP4. *Development* 2008; **135**: 3301–3310.
36. Fujii H, Sato T, Kaneko S, et al. Metabolic inactivation of retinoic acid by a novel P450 differentially expressed in developing mouse embryos. *EMBO J* 1997; **16**: 4163–4173.
37. Pennimpede T, Cameron DA, MacLean GA, et al. The role of CYP26 enzymes in defining appropriate retinoic acid exposure during embryogenesis. *Birth Defects Res A Clin Mol Teratol* 2010; **88**: 883–894.
38. Wang Y, Arribas-Layton M, Chen Y, et al. DDX6 orchestrates mammalian progenitor function through the mRNA degradation and translation pathways. *Mol Cell* 2015; **60**: 118–130.
39. Ahn Y, Sanderson BW, Klein OD, et al. Inhibition of Wnt signaling by Wise (Sostdc1) and negative feedback from Shh controls tooth number and patterning. *Development* 2010; **137**: 3221–3231.
40. Laurikkala J, Kassai Y, Pakkasjarvi L, et al. Identification of a secreted BMP antagonist, ectodin, integrating BMP, FGF, and SHH signals from the tooth enamel knot. *Dev Biol* 2003; **264**: 91–105.
41. Yanagita M, Okuda T, Endo S, et al. Uterine sensitization-associated gene-1 (USAG-1), a novel BMP antagonist expressed in the kidney, accelerates tubular injury. *J Clin Invest* 2006; **116**: 70–79.
42. Lintern KB, Guidato S, Rowe A, et al. Characterization of Wise protein and its molecular mechanism to interact with both Wnt and BMP signals. *J Biol Chem* 2009; **284**: 23159–23168.
43. Jovanovic I, Zivkovic M, Kostic M, et al. Transcriptome-driven integrative exploration of functional state of ureter tissue affected by CAKUT. *Life Sci* 2018; **212**: 1–8.
44. Zhu Q, Song L, Peng G, et al. The transcription factor Pou3f1 promotes neural fate commitment via activation of neural lineage genes and inhibition of external signaling pathways. *Elife* 2014; **3**: e02224.



45. Rodriguez MM. Congenital anomalies of the kidney and the urinary tract (CAKUT). *Fetal Pediatr Pathol* 2014; **33**: 293–320.
46. Nicolaou N, Renkema KY, Bongers EM, *et al*. Genetic, environmental, and epigenetic factors involved in CAKUT. *Nat Rev Nephrol* 2015; **11**: 720–731.
47. Chevalier RL, Thornhill BA, Forbes MS, *et al*. Mechanisms of renal injury and progression of renal disease in congenital obstructive nephropathy. *Pediatr Nephrol* 2010; **25**: 687–697.
48. Chevalier RL. Congenital urinary tract obstruction: the long view. *Adv Chronic Kidney Dis* 2015; **22**: 312–319.

## SUPPLEMENTARY MATERIAL ONLINE

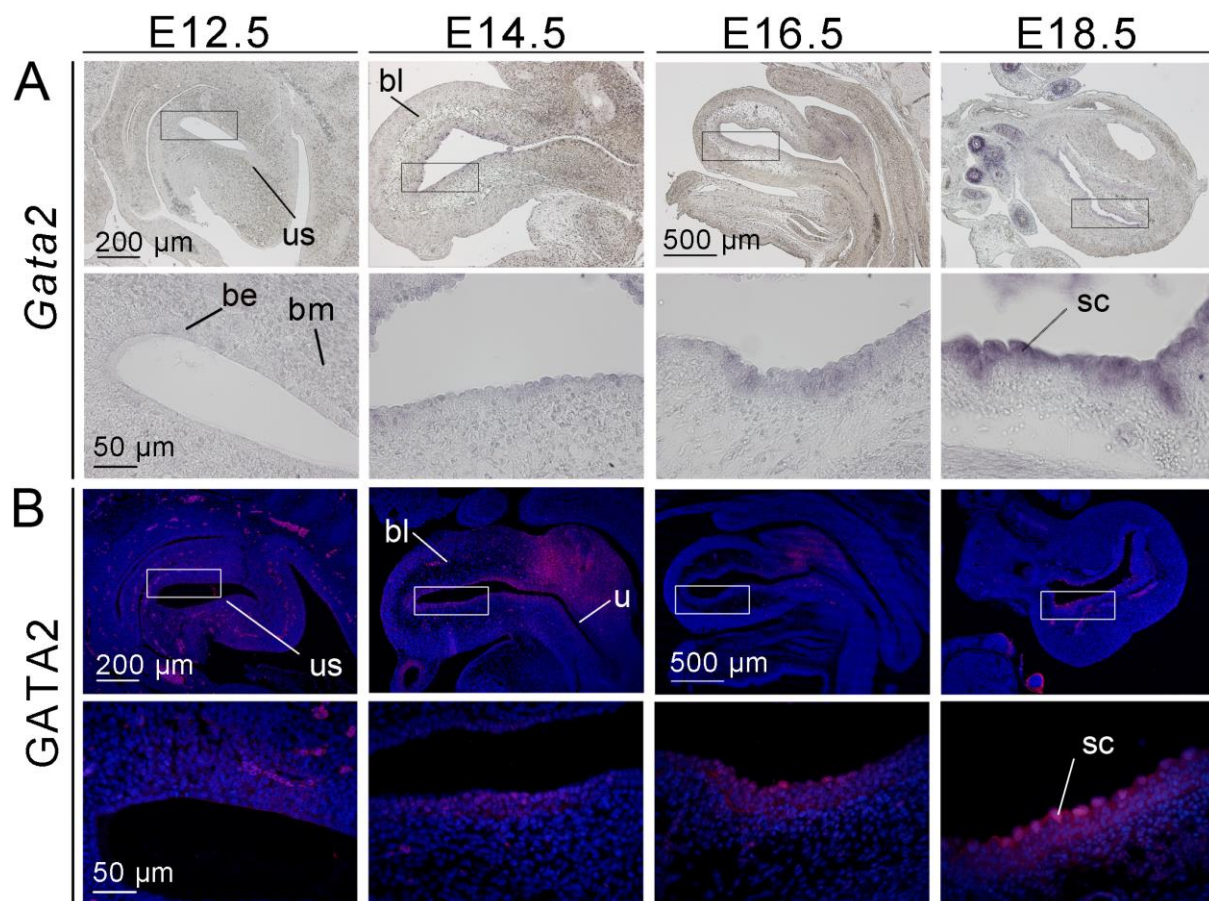
### Supplementary materials and methods

- Figure S1.** *Gata2* expression in the developing bladder is confined to superficial cells
- Figure S2.** Expression of GATA2 is dramatically reduced in the UM of *Gata2cKO* embryos
- Figure S3.** *Gata2cKO* embryos display a range of ureter dilatations at E18.5
- Figure S4.** *Gata2cKO* embryos display megaureter at E18.5
- Figure S5.** Loss of *Gata2* in the UM does not affect the excitation/conduction system of the upper urinary tract
- Figure S6.** *Gata2cKO* embryos do not exhibit SMC defects in the bladder at E18.5
- Figure S7.** Proliferation and apoptosis are not affected in *Gata2cKO* ureters at E12.5 and E14.5
- Figure S8.** E14.5 *Gata2cKO* ureters display reduced contraction intensity after 6 days of culture
- Figure S9.** Expression of signalling pathways and transcription factors relevant for SMC differentiation of the UM in *Gata2cKO* embryos at E14.5
- Figure S10.** GATA2 binding peaks in ChIP-seq experiments of E14.5 ureters; group of genes with reduced expression in *Gata2cKO* ureters
- Figure S11.** GATA2 binding peaks in ChIP-seq experiments of E14.5 ureters; group of genes with increased expression in *Gata2cKO* ureters
- Figure S12.** Expression of genes down-regulated in microarrays of *Gata2cKO* ureters at E14.5
- Figure S13.** Expression of genes up-regulated in microarrays of *Gata2cKO* ureters at E14.5
- Figure S14.** SOSTDC1 affects ureter peristalsis
- Table S1.** Statistical evaluation of the BrdU incorporation assay in E14.5 control and *Gata2cKO* ureters (relates to Figure S7)
- Table S2.** Statistical analysis of the peristaltic frequency of E14.5 control and *Gata2cKO* ureters cultured for 6 days (relates to Figure 4B)
- Table S3.** Statistical analysis of the contraction intensities of E14.5 ureters from control and *Gata2cKO* embryos after 6 days of culture (relates to Figure S8)
- Table S4.** Statistical analysis of the peristaltic frequency of E18.5 control and *Gata2cKO* ureters over 6 days of culture (relates to Figure 4E)
- Table S5.** Statistical analysis of E18.5 control and *Gata2cKO* ureter contraction intensities over 6 days of culture (relates to Figure 4F)
- Table S6.** Transcripts identified by microarray analysis that were down-regulated in E14.5 ureters of *Gata2cKO* embryos (relates to Table 1)
- Table S7.** Transcripts identified by microarray analysis that were up-regulated in E14.5 ureters of *Gata2cKO* embryos (relates to Table 1)
- Table S8.** Functional annotation clustering analysis for transcripts that were down-regulated in E14.5 ureters of *Gata2cKO* embryos
- Table S9.** Functional annotation clustering analysis for transcripts that were up-regulated in E14.5 ureters of *Gata2cKO* embryos
- Table S10.** RT-PCR calculations and statistics (relates to Figure 5B,C)
- Table S11.** Statistical analysis of the ureter contraction frequency in explants of E12.5 wild-type upper urogenital systems treated with either DMSO or 1  $\mu$ M RA over 10 days of culture (relates to Figure 5D)
- Table S12.** Intensity of one ureter contraction in explants of E12.5 upper urinary systems at day 10 of culture in the presence of DMSO or 1  $\mu$ M RA (relates to Figure 5E)
- Table S13.** Statistical analysis of ureter contraction frequency in explants of E12.5 control and *Gata2cKO* ureters treated with either DMSO or 1  $\mu$ M BMS over 10 days of culture (relates to Figure 5F)
- Video S1.** Peristalsis of an E14.5 ureter explant grown for 6 days in culture, control
- Video S2.** Peristalsis of an E14.5 ureter explant grown for 6 days in culture, *Gata2cKO*
- Video S3.** Peristalsis of an E18.5 ureter explant grown for 1 day in culture, control
- Video S4.** Peristalsis of an E18.5 ureter explant grown for 6 days in culture, control
- Video S5.** Peristalsis of an E18.5 ureter explant grown for 1 day in culture, *Gata2cKO*
- Video S6.** Peristalsis of an E18.5 ureter explant grown for 6 days in culture, *Gata2cKO*
- Video S7.** Peristalsis of an E12.5 ureter explant grown for 10 days in culture, DMSO control
- Video S8.** Peristalsis of an E12.5 ureter explant grown for 10 days in culture, RA-treated

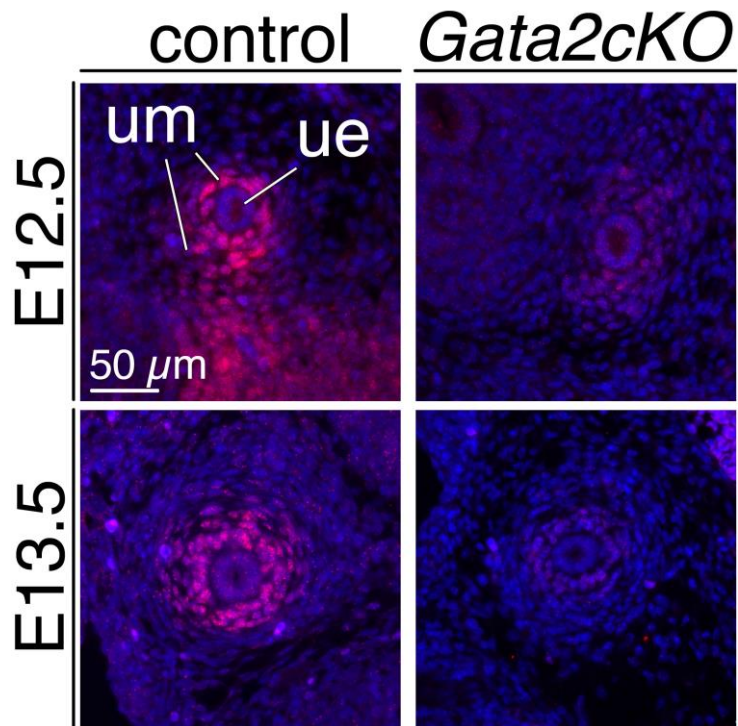
**Delayed onset of smooth muscle cell differentiation leads to hydroureter formation in mice with conditional loss of the zinc finger transcription factor gene *Gata2* in the ureteric mesenchyme**

Weiss A-C *et al. J Pathol* DOI: 10.1002/path.5270

**Supplementary Figures**

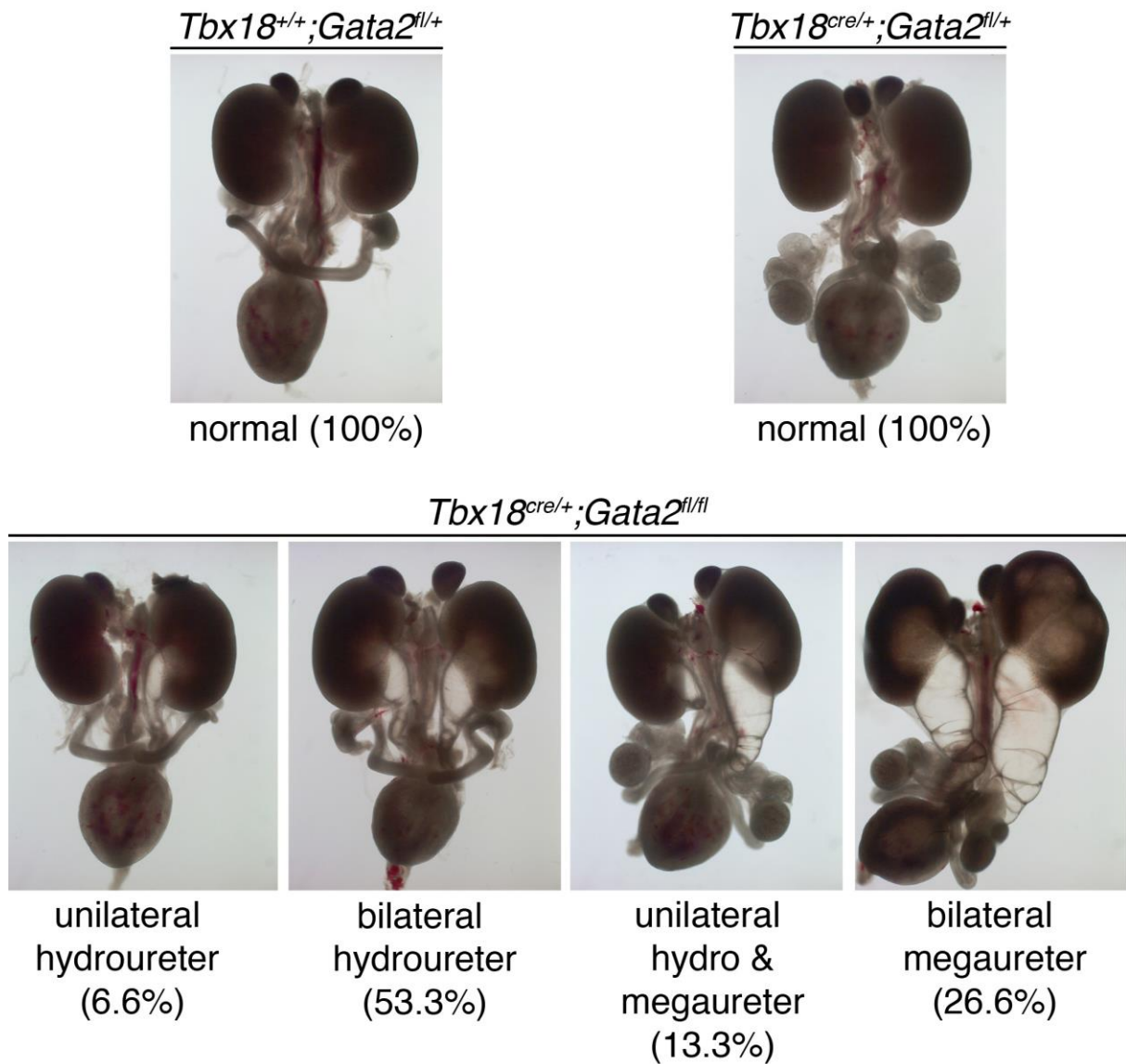


**Figure S1.** *Gata2* expression in the developing bladder is confined to superficial cells. (A, B) *In situ* hybridisation analysis of *Gata2* mRNA (A) and immunofluorescence analysis of GATA2 protein expression (B) on sagittal bladder sections of wild-type embryos from E12.5 to E18.5. The expression patterns of *Gata2* mRNA and GATA2 protein overlap throughout bladder development. Expression is absent in the mesenchymal compartment but found in superficial cells of the urothelium at E16.5 and E18.5. bl, bladder; be, bladder epithelium; bm, bladder mesenchyme; sc, superficial cells; us, urogenital sinus.

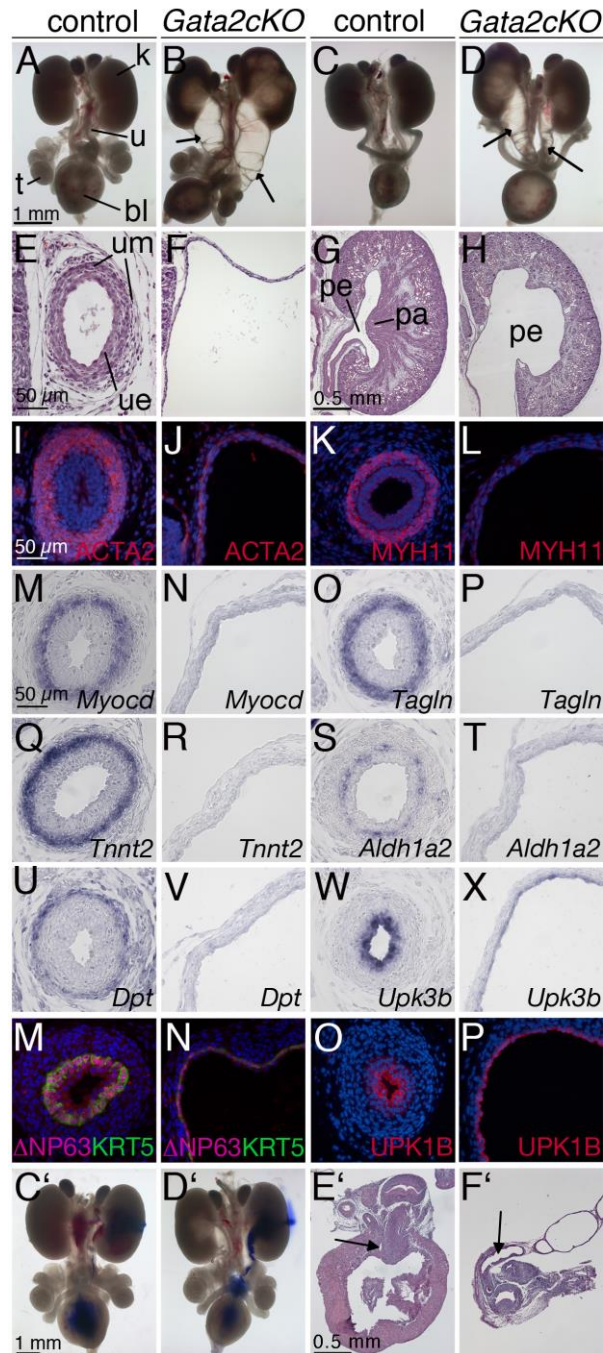


**Figure S2.** Expression of GATA2 is dramatically reduced in the UM of *Gata2cKO* embryos. Immunofluorescence analysis of GATA2 expression on sections of the proximal ureter region of control and *Gata2cKO* (*Tbx18<sup>cre/+</sup>;Gata2<sup>fl/fl</sup>*) embryos at E12.5 and E13.5. ue, ureteric epithelium; um, ureteric mesenchyme.

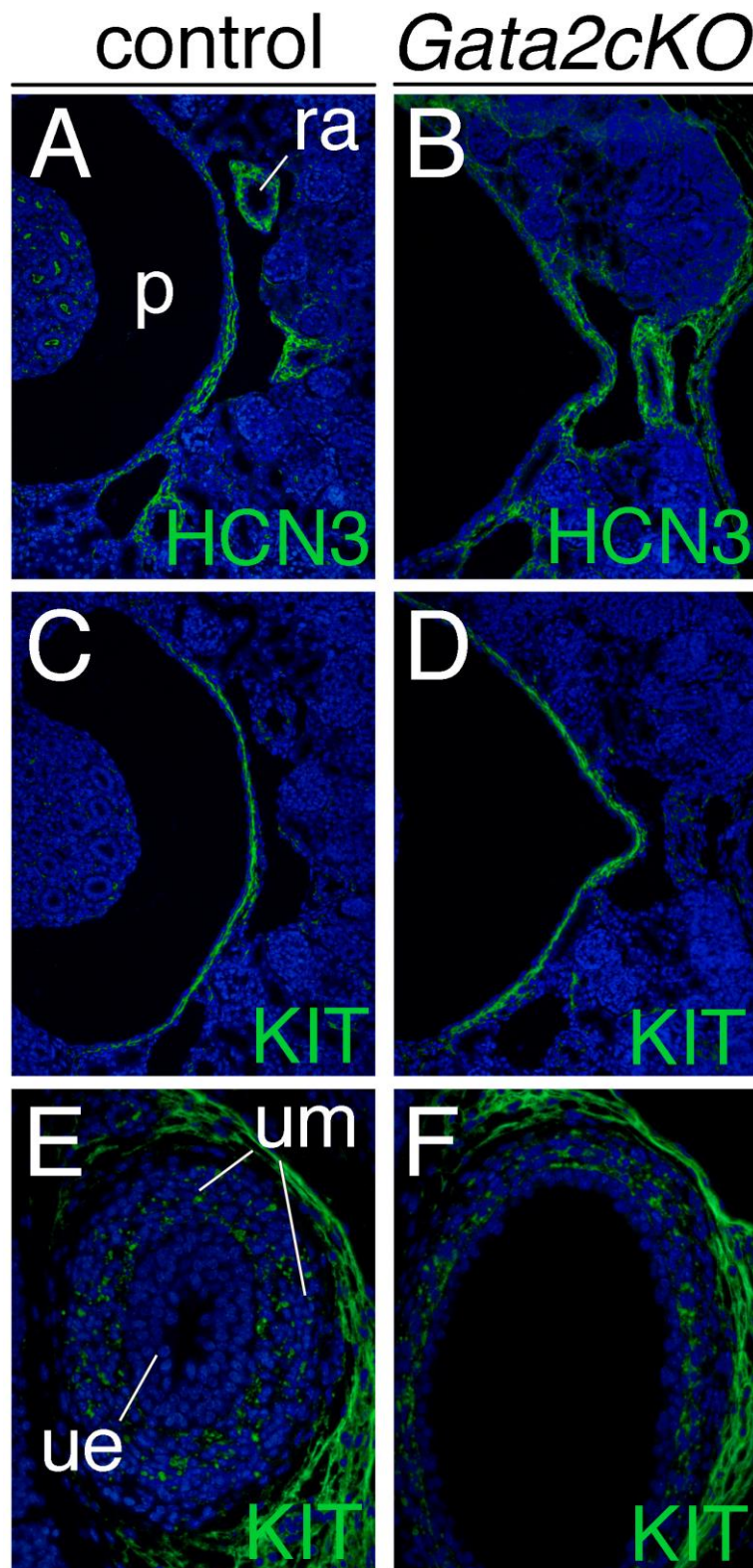




**Figure S3.** *Gata2*cKO embryos display a range of ureter dilatations at E18.5. Morphology of whole urogenital systems of *Tbx18<sup>+/+</sup>;Gata2<sup>fl/+</sup>*, *Tbx18<sup>cre/+</sup>;Gata2<sup>fl/+</sup>*, and *Tbx18<sup>cre/+</sup>;Gata2<sup>fl/fl</sup>* embryos at E18.5. Heterozygous loss of *Gata2* in the UM does not result in morphological defects, whereas homozygous loss leads to ureter dilatations of different severities, ranging from unilateral hydroureter to bilateral megaureter. Numbers indicate the frequency of the observed phenotype ( $n = 15$ ).

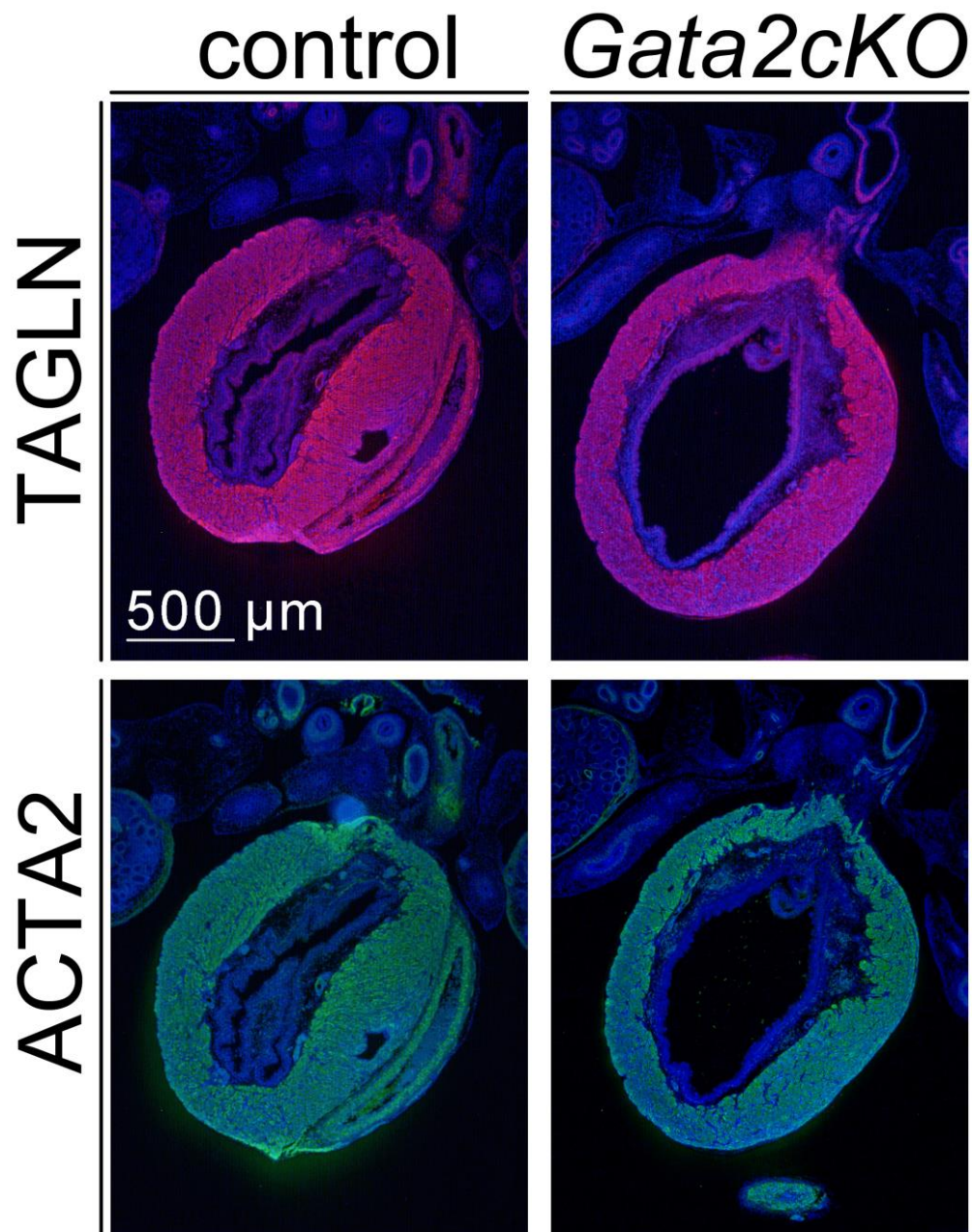


**Figure S4.** *Gata2cKO* embryos display megaureter at E18.5. (A–D) Morphology of whole urogenital systems of male (A, B) and female embryos (C, D). (B, D) Arrows point to the megaureter. (E–H) Haematoxylin and eosin staining of transverse ureter sections (E, F) and of sagittal kidney sections (G, H). (I–L) Cytodifferentiation of the UM (I–V) and of the urothelium (W–X) as shown by immunofluorescence (I–L and Y–X) and by section RNA *in situ* hybridisation analysis (M–X). Urothelial differentiation appears unaffected, but SMC differentiation is severely compromised in the mutant. (C'–F') Analysis of the VUJ by ink injection (C', D') and by haematoxylin and eosin staining of sagittal bladder sections (E', F') shows physical obstruction caused by blind-ending ureters in the mutant. Arrows point to the orifice of the ureter (E', F'). Genotypes, probes, and antigens are as indicated. bl, bladder; k, kidney; pa, papilla; pe, pelvis; u, ureter; ue, ureteric epithelium; um, ureteric mesenchyme; t, testis.

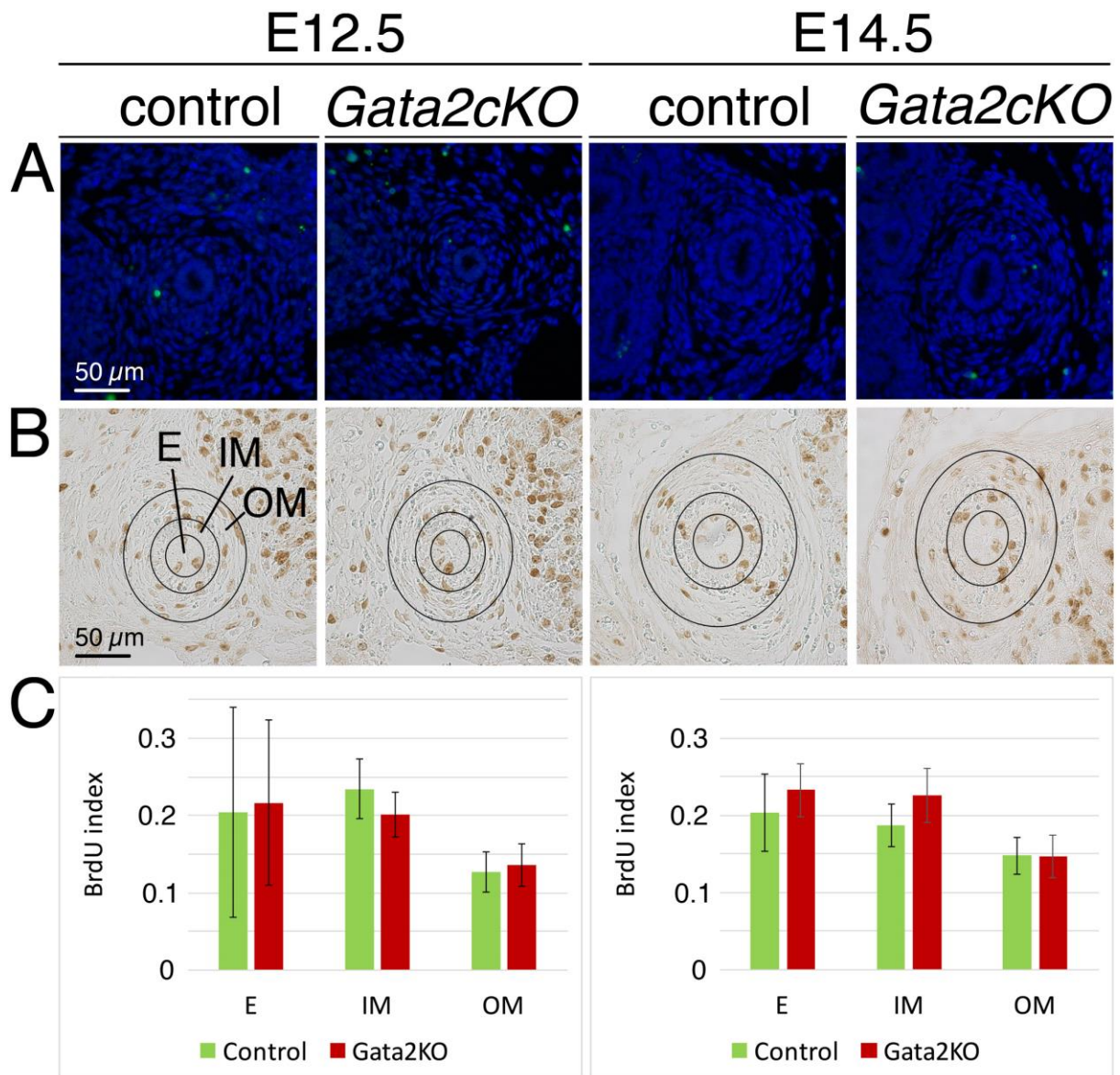


**Figure S5.** Loss of *Gata2* in the UM does not affect the excitation/conduction system of the upper urinary tract. Immunofluorescence analysis of sagittal kidney (A–D) and proximal ureter sections (E, F) of E18.5 control and *Gata2cKO* (*Tbx18<sup>cre/+</sup>;Gata2<sup>fl/fl</sup>*) embryos. Expression of HCN3, a marker for the pacemaker cells in the renal pelvis, and of KIT, a marker for interstitial Cajal-like cells in the renal pelvis and outer mesenchymal region of the ureter, is unchanged. ra, renal artery; ue, ureteric epithelium; um, ureteric mesenchyme.

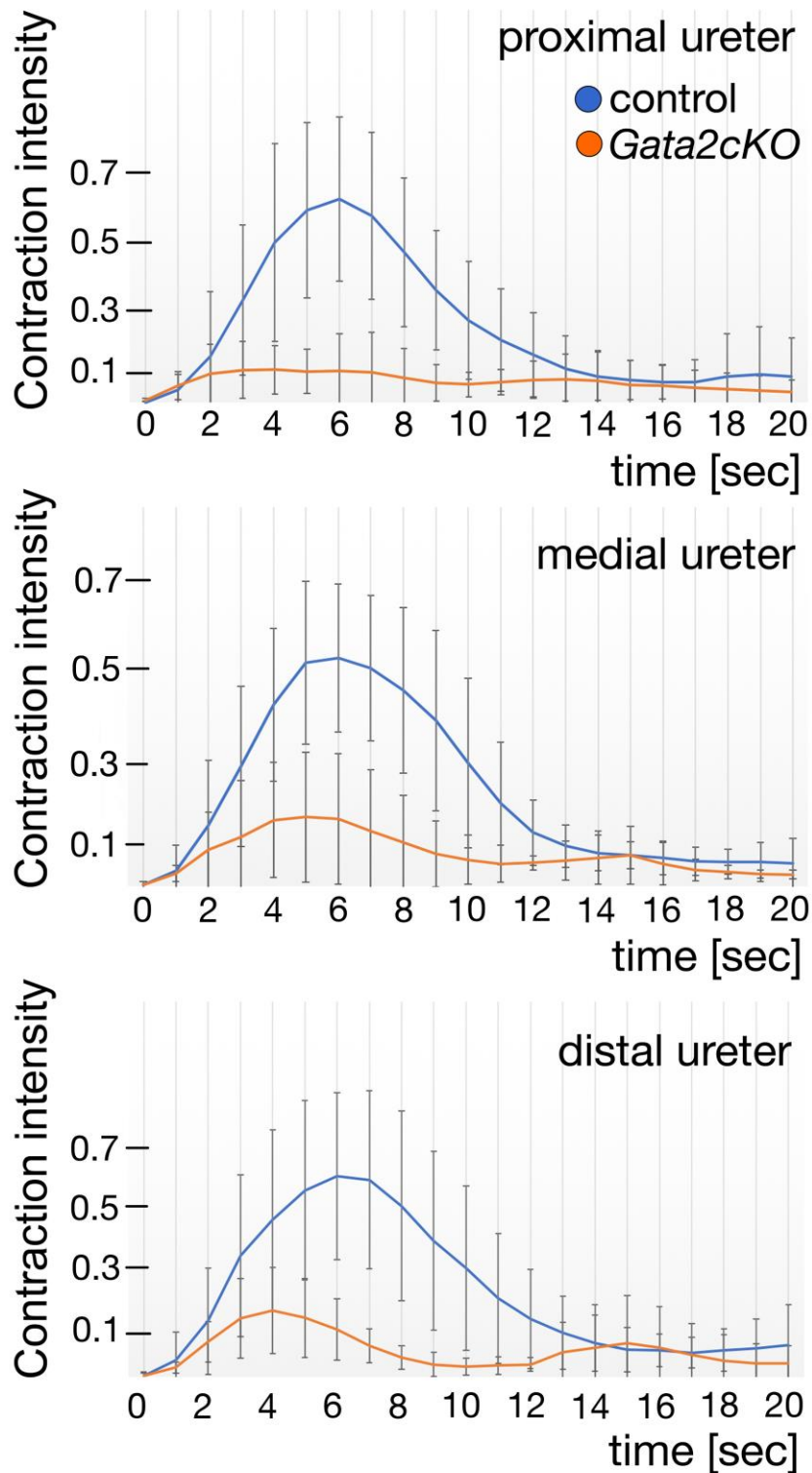




**Figure S6.** *Gata2cKO* embryos do not exhibit SMC defects in the bladder at E18.5. Immunofluorescence analysis of expression of the two SMC structural proteins TAGLN and ACTA2 on sagittal sections of the bladder of control and *Gata2cKO* (*Tbx18<sup>cre/+</sup>;Gata2<sup>fl/fl</sup>*) embryos. Note that the *Tbx18<sup>cre</sup>* line mediates recombination in the bladder mesenchyme. Hence, even weak expression of *Gata2* in the bladder mesenchyme would be interrogated for functional relevance.

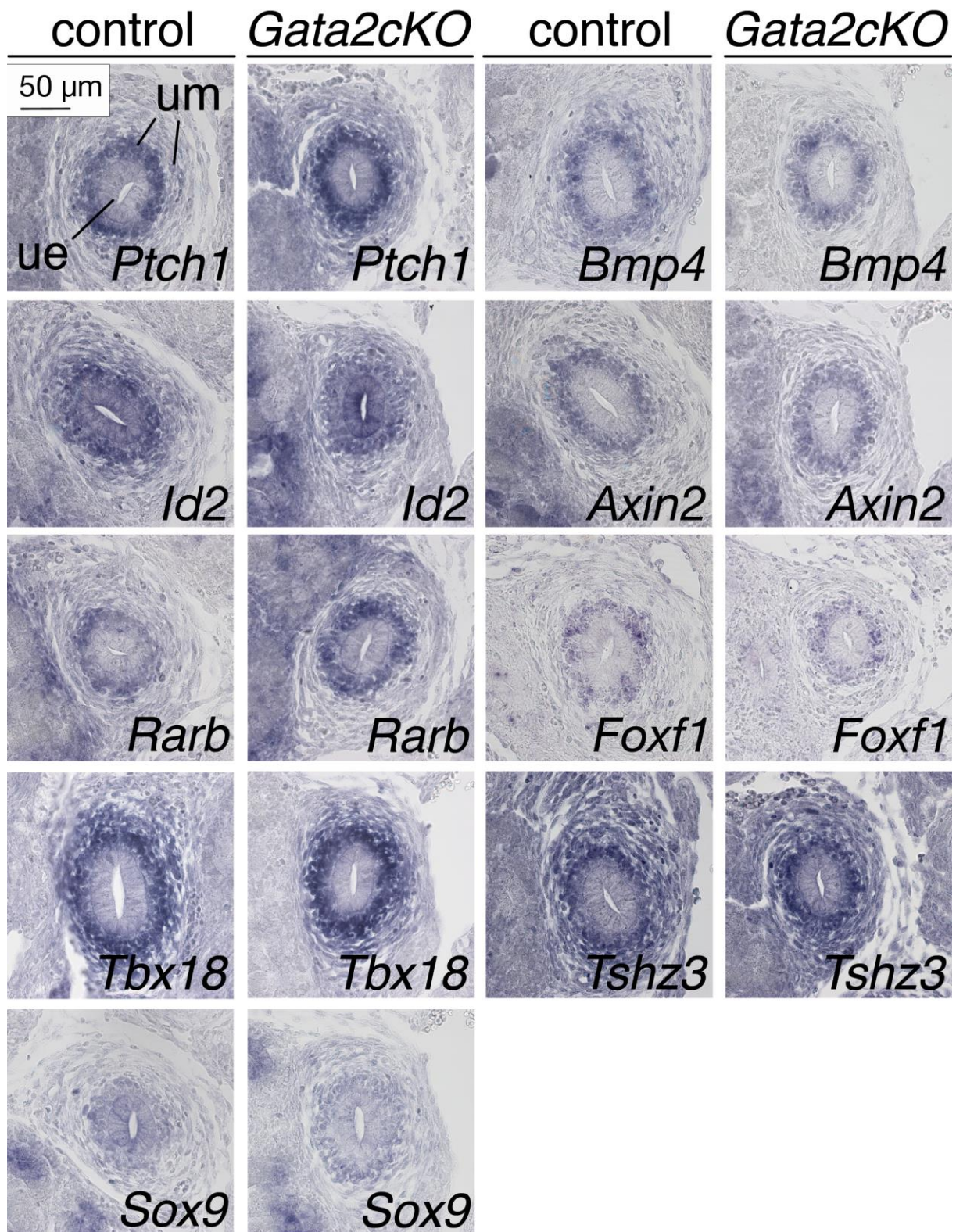


**Figure S7.** Proliferation and apoptosis are not affected in *Gata2cKO* ureters at E12.5 and E14.5. (A) Immunofluorescent analysis (green) of apoptosis by the TUNEL assay on proximal ureter sections. Nuclei are counter-stained with DAPI (blue). Loss of *Gata2* in the UM does not lead to an increase in apoptosis. (B) Immunohistochemical detection of BrdU on proximal ureter sections. Black circles demarcate the ureteric epithelium (E) and the inner and outer mesenchymal cell populations (IM and OM). (C) Cell proliferation is unaffected in the epithelial and mesenchymal tissue compartments of *Gata2cKO* (*Tbx18<sup>cre/+</sup>;Gata2<sup>fl/fl</sup>*) ureters as quantified by the BrdU index in the areas indicated in B. Values are displayed as mean  $\pm$  SD. \* $p \leq 0.05$ ; \*\* $p \leq 0.01$ ; \*\*\* $p \leq 0.001$  two-tailed Student's *t*-test. For statistical values see the supplementary material, Table S1.

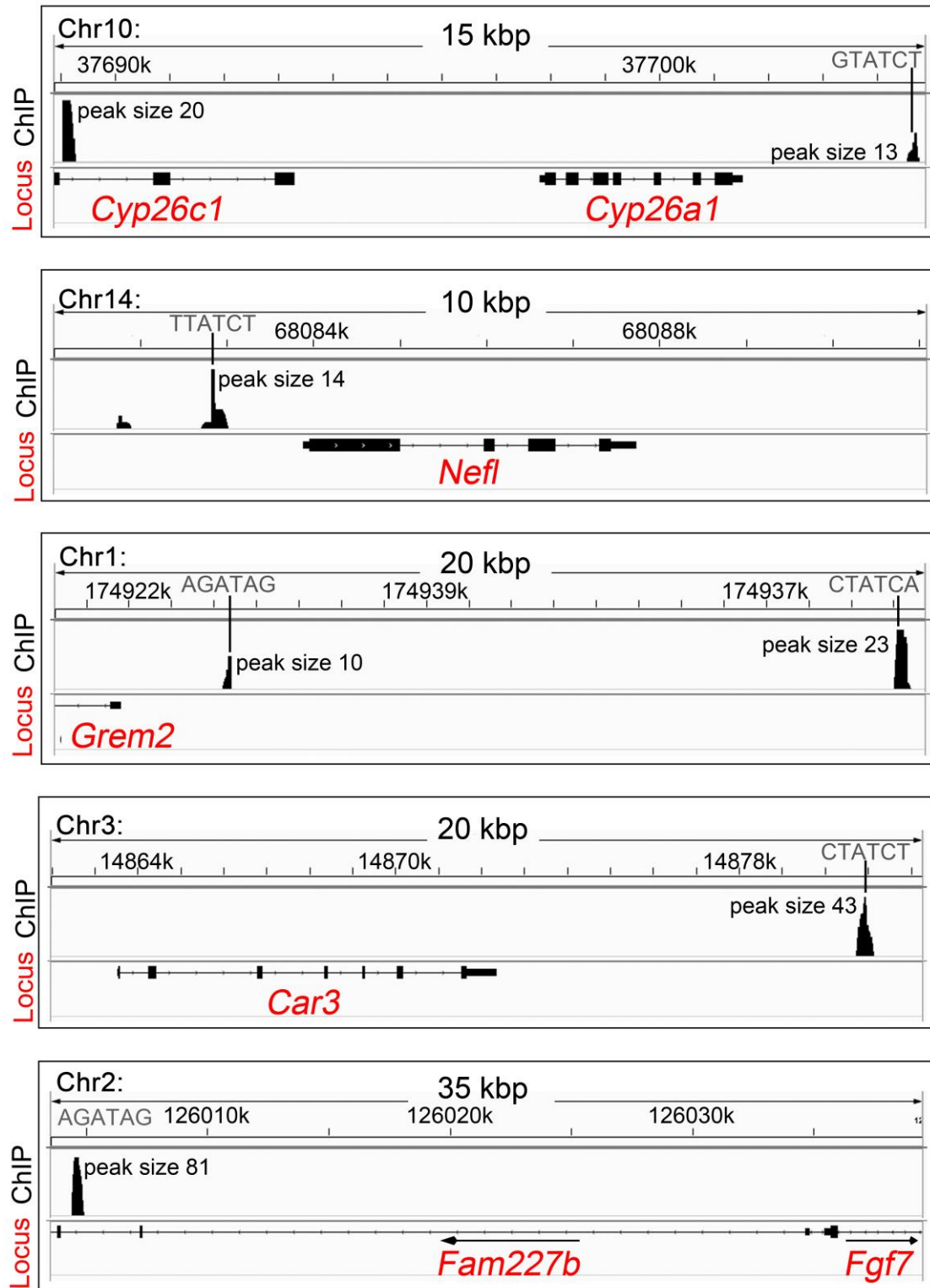


**Figure S8.** E14.5 *Gata2cKO* ureters display reduced contraction intensity after 6 days of culture. Plot of multi-kymograph ratios representing the intensity of one contraction of E14.5 control and *Gata2cKO* (*Tbx18<sup>cre/+</sup>;Gata2<sup>fl/fl</sup>*) ureters after 6 days in culture. Video-monitored were 100 frames per second and displayed as 20 s real time. Wild-type ureters reach their intensity peak of approximately 70% after 8 s and relax afterwards, whereas the mutant ureters reach only 10% contraction intensity in the proximal region and up to 30% at medial and distal levels. For values and statistical significances at each time-point see the supplementary material, Table S3.

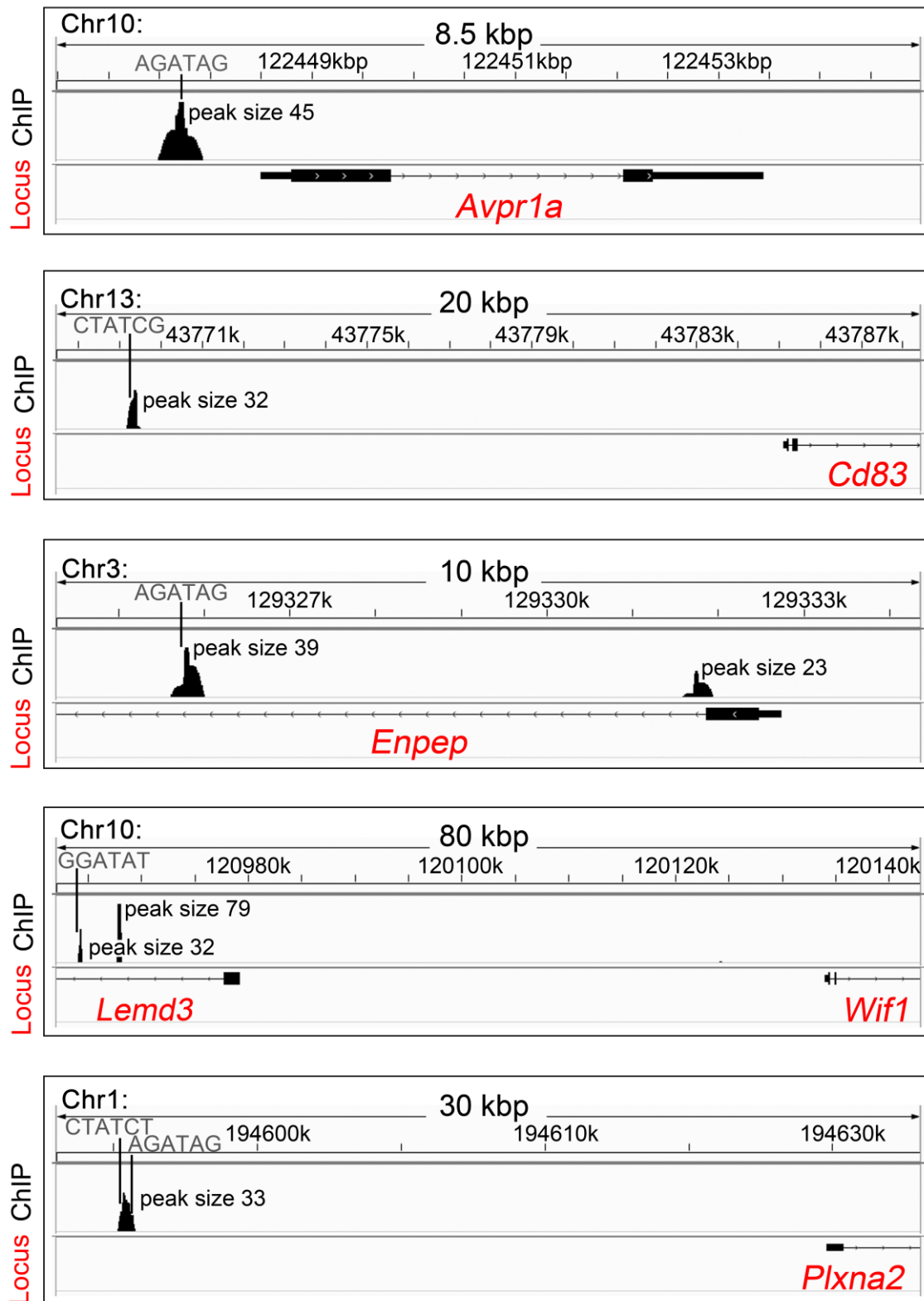




**Figure S9.** Expression of signalling pathways and transcription factors relevant for SMC differentiation of the UM in *Gata2cKO* embryos at E14.5. Shown are RNA *in situ* hybridisation analyses of proximal ureter sections of control and *Gata2cKO* (*Tbx18<sup>cre/+</sup>;Gata2<sup>fl/fl</sup>*) embryos. Probes and genotypes are indicated. ue, ureteric epithelium; um, ureteric mesenchyme.

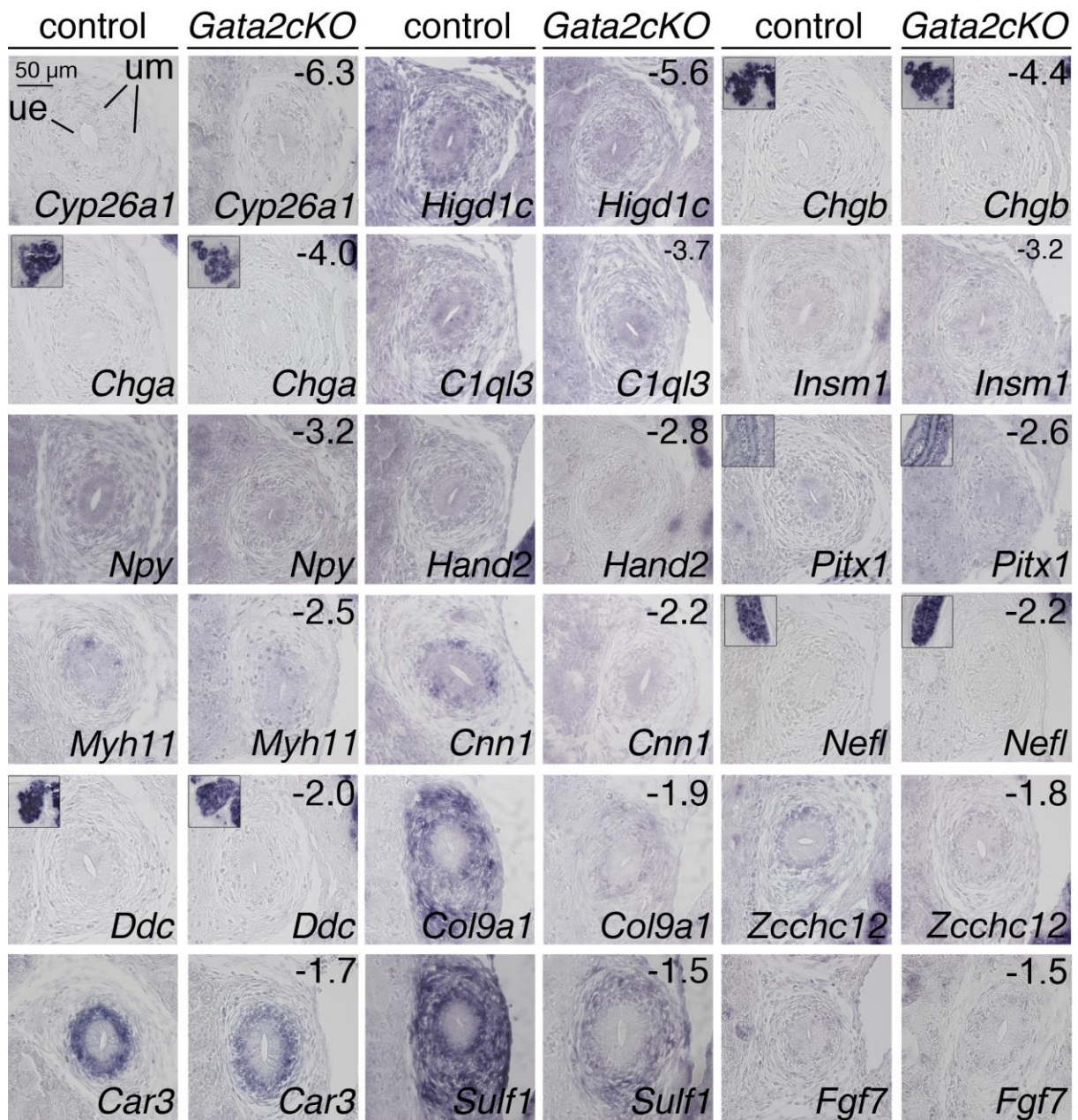


**Figure S10.** GATA2 binding peaks in ChIP-seq experiments of E14.5 ureters; group of genes with reduced expression in *Gata2cKO* ureters. Schemes depict the genomic organisation of loci which harbour GATA2 binding peaks from the group of down-regulated transcripts. Exon coding sequences are shown as large black boxes, 3'- and 5'-UTRs are indicated as smaller black boxes. Binding peaks as detected by ChIP-seq analysis are plotted as black vertical lines with relative peak height. GATA sites are indicated.



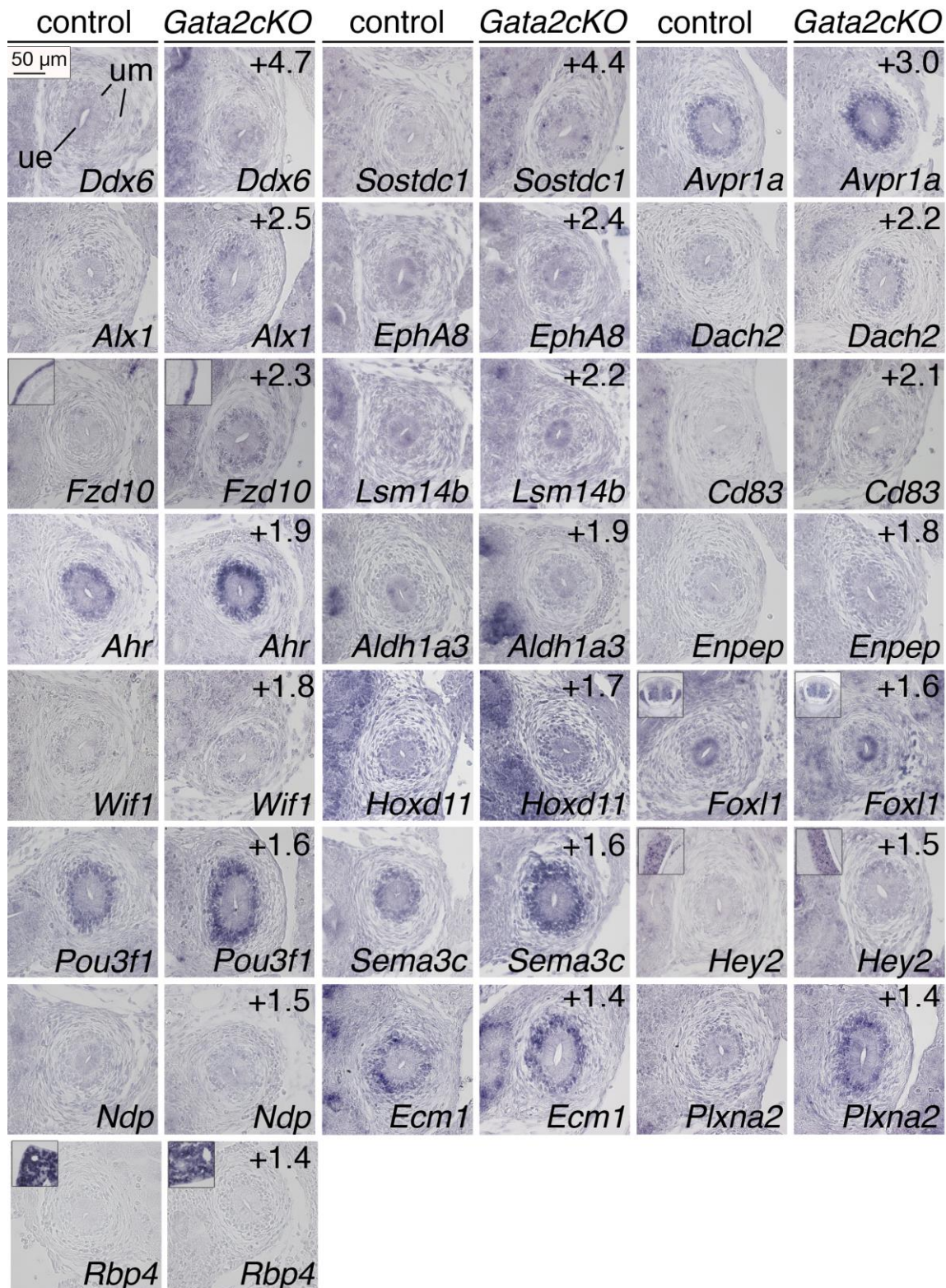
**Figure S11.** GATA2 binding peaks in ChIP-seq experiments of E14.5 ureters; group of genes with increased expression in *Gata2cKO* ureters. Schemes depict the genomic organisation of loci which harbour GATA2 binding peaks from the group of up-regulated transcripts. Exon coding sequences are shown as large black boxes, 3'- and 5'-UTRs are indicated as smaller black boxes. Binding peaks as detected by ChIP-seq analysis are plotted as black vertical lines with relative peak height. GATA sites are indicated.



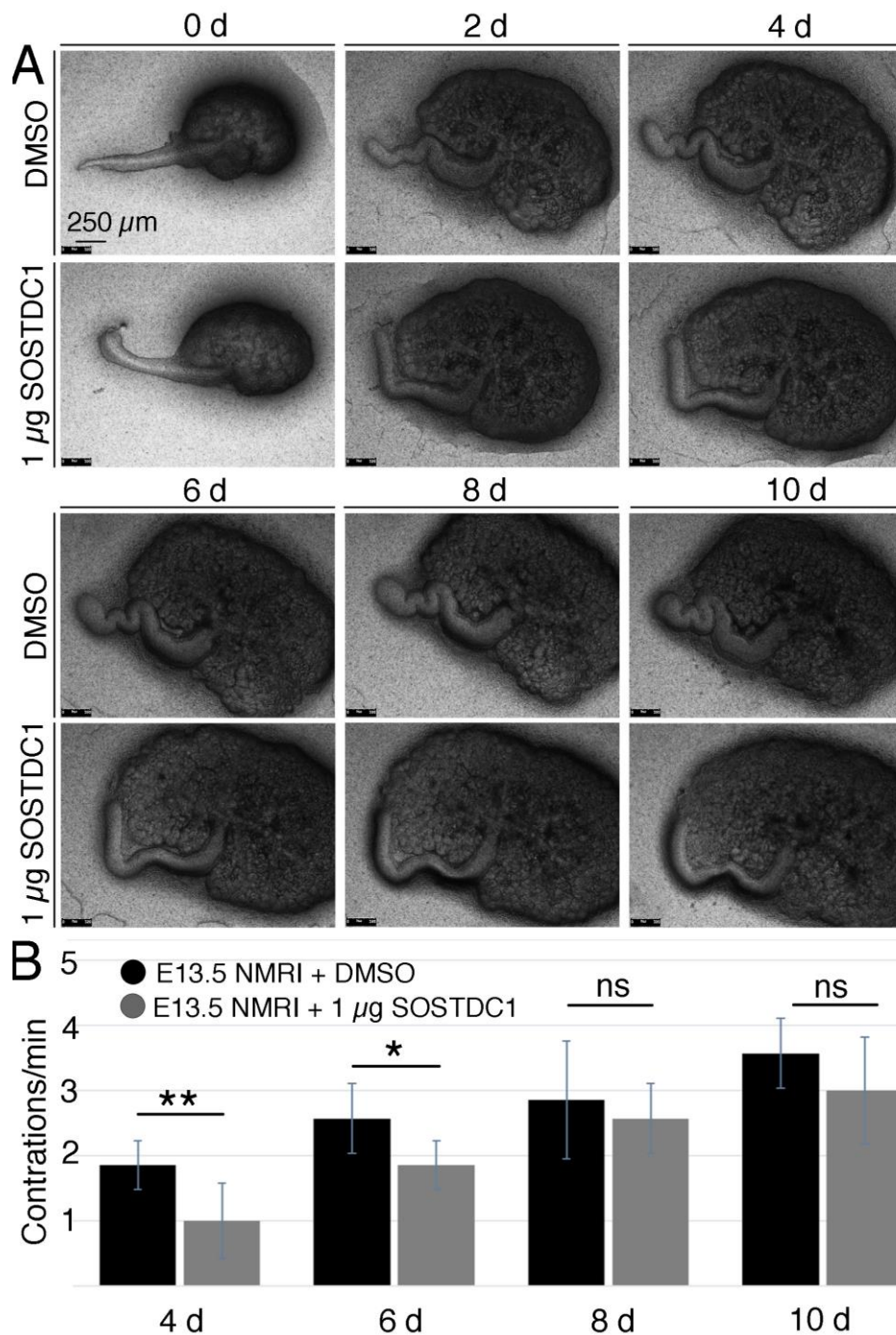


**Figure S12.** Expression of genes down-regulated in microarrays of *Gata2cKO* ureters at E14.5. Shown are RNA *in situ* hybridisation analyses of proximal ureter sections of control and *Gata2cKO* (*Tbx18<sup>cre/+</sup>;Gata2<sup>fl/fl</sup>*) embryos. Insets display positive control regions. Probes, genotypes, and fold changes in the microarray are as indicated. ue, ureteric epithelium; um, ureteric mesenchyme.





**Figure S13.** Expression of genes up-regulated in microarrays of *Gata2cKO* ureters at E14.5. Shown are RNA *in situ* hybridisation analyses of proximal ureter sections of control and *Gata2cKO* (*Tbx18<sup>cre/+</sup>;Gata2<sup>fl/fl</sup>*) embryos. Insets display positive control regions. Probes, genotypes, and fold changes in the microarray are as indicated. ue, ureteric epithelium; um, ureteric mesenchyme.



**Figure S14.** SOSTDC1 affects ureter peristalsis. Administration of 1  $\mu$ g SOSTDC1 protein or DMSO as a control to explants of E13.5 wild-type ureters. (A) Bright-field images of the morphology of E13.5 ureters grown for 10 days in culture. (B) Analysis of peristaltic contractions from day 4 to day 10 of culture shows that SOSTDC1-treated ureters exhibit a significantly reduced contraction frequency at days 4 and 6 of the culture compared with the control. Contraction frequency at 4 days: DMSO  $1.86 \pm 0.37$ ; 1  $\mu$ g SOSTDC1  $1 \pm 0.58$ ,  $p = 0.007846381$ . Contraction frequency at 6 days: DMSO  $2.58 \pm 0.54$ ; 1  $\mu$ g SOSTDC1  $1.85 \pm 0.37$ ,  $p = 0.01504815$ . Contraction frequency at 8 days: DMSO  $2.85 \pm 0.89$ ; 1  $\mu$ g SOSTDC1  $2.57 \pm 0.53$ ,  $p = 0.48703625$ . Contraction frequency at 10 days: DMSO  $3.57 \pm 0.53$ ; 1  $\mu$ g SOSTDC1  $3 \pm 0.81$ ,  $p = 0.15136401$ . Differences were considered significant with a  $P$  value below 0.05 ( $*p < 0.05$ ), highly significant ( $**p \leq 0.01$ ), and extremely significant ( $***p \leq 0.001$ ); two-tailed Student's  $t$ -test. Stages, time points, and genotypes are indicated.



## Supplementary Tables

**Table S1.** Statistical evaluation of the BrdU incorporation assay in E14.5 control and *Gata2cKO* ureters (relates to Figure S7). The BrdU incorporation assay was quantified on 5- $\mu$ m proximal ureter sections (12 per stage and genotype). BrdU positive nuclei were counted per ureter compartment (E, epithelium; IM, inner mesenchyme; OM, outer mesenchyme) and the ratio with the total cell number (as determined by DAPI counterstaining) was determined. Shown are averages and corresponding standard deviations in control and *Gata2cKO* (*Tbx18<sup>cre/+</sup>;Gata2<sup>fl/fl</sup>*) ureters. Significance was calculated by the two-tailed Student's t-test. \*:  $p \leq 0.05$ ; \*\*:  $p \leq 0.01$ ; \*\*\*:  $p \leq 0.001$ .

<b>E12.5</b>	<b>E</b>	<b>IM</b>	<b>OM</b>
<b>control</b>	0.20 $\pm$ 0.13	0.23 $\pm$ 0.03	0.12 $\pm$ 0.02
<b><i>Gata2cKO</i></b>	0.21 $\pm$ 0.10	0.20 $\pm$ 0.02	0.13 $\pm$ 0.03
<b>t-Test</b>	0.91065726	0.29937511	0.72227853

<b>E14.5</b>	<b>E</b>	<b>IM</b>	<b>OM</b>
<b>control</b>	0.20 $\pm$ 0.05	0.18 $\pm$ 0.03	0.14 $\pm$ 0.02
<b><i>Gata2cKO</i></b>	0.23 $\pm$ 0.03	0.22 $\pm$ 0.03	0.15 $\pm$ 0.03
<b>t-Test</b>	0.45844349	0.20211307	0.94839743

**Table S2.** Statistical analysis of the peristaltic frequency of E14.5 control and *Gata2cKO* ureters cultured for 6 days (relates to Figure 4B). Average frequency and corresponding standard deviations of peristaltic contractions per min after 2, 4, 6 days after ureter explantation at E14.5. Video-monitored was a duration of one minute. The statistical significance was calculated by a two-tailed Student's t-test. \*:  $p \leq 0.05$ ; \*\*:  $p \leq 0.01$ ; \*\*\*:  $p \leq 0.001$ .

		<b>2 days</b>	<b>4 days</b>	<b>6 days</b>
<b>control (n=5)</b>	<b>average</b>	0.78 $\pm$ 0.4	1.71 $\pm$ 0.6	2.64 $\pm$ 0.5
<b><i>Gata2cKO</i> (n=4)</b>	<b>average</b>	0	0	0.63 $\pm$ 0.5
	<b>t-Test</b>	1.07855E-05	1.0258E-07	1.74402E-09

**Table S3.** Statistical analysis of contraction intensities of E14.5 ureters from control and *Gata2cKO* embryos after 6 days of culture (relates to Figure S8). Average intensity and corresponding standard deviations (STDV) in one sec intervals of one peristaltic contraction at day 6 of culture after ureter explantation at E14.5. n=5 (control), n=4 (*Gata2cKO*). Video-monitored was a duration of one minute. Contraction intensity equals to Multi-Kymograph grey value ratios (grey value at “t” / maximum grey value). The proximal level equals to 25%, medial to 50% and distal to 75% of the entire ureter length. The statistical significance was calculated by a two-tailed Student’s t-test. \*:  $p \leq 0.05$ ; \*\*:  $p \leq 0.01$ ; \*\*\*:  $p \leq 0.001$ .

Timepoint (in sec)	control proximal	STDV	<i>Gata2cKO</i> proximal	STDV	t-Test
0	0.00	0.00	0.01	0.01	0.00157561
1	0.03	0.04	0.04	0.04	0.0012542
2	0.12	0.16	0.07	0.08	0.00104161
3	0.26	0.19	0.08	0.07	0.00106694
4	0.41	0.25	0.08	0.06	0.00187384
5	0.49	0.22	0.08	0.06	0.00589432
6	0.52	0.21	0.08	0.09	0.01479269
7	0.47	0.21	0.08	0.10	0.02396151
8	0.38	0.19	0.06	0.08	0.02886091
9	0.29	0.15	0.05	0.05	0.04992738
10	0.21	0.15	0.05	0.03	0.06795031
11	0.16	0.13	0.05	0.03	0.05840695
12	0.12	0.11	0.06	0.05	0.03854484
13	0.09	0.08	0.06	0.06	0.02180735
14	0.07	0.06	0.05	0.08	0.01096675
15	0.06	0.05	0.04	0.06	0.00566344
16	0.05	0.04	0.04	0.05	0.00347323
17	0.05	0.06	0.04	0.04	0.00259946
18	0.06	0.11	0.03	0.04	0.0022656
19	0.07	0.12	0.03	0.04	0.00218852
20	0.07	0.10	0.03	0.03	0.002183

Timepoint (in sec)	control medial	STDV	<i>Gata2cKO</i> medial	STDV	t-Test
0	0.00	0.01	0.00	0.01	0.00336054
1	0.04	0.06	0.03	0.02	0.00270399
2	0.15	0.16	0.09	0.09	0.00233837
3	0.29	0.19	0.12	0.14	0.00231253
4	0.44	0.19	0.16	0.14	0.00344189
5	0.54	0.20	0.17	0.16	0.0090724
6	0.55	0.18	0.16	0.16	0.02037417
7	0.53	0.18	0.13	0.15	0.03221451
8	0.48	0.20	0.11	0.12	0.03355946

Part 2 – GATA2 in SMC differentiation

9	0.40	0.22	0.08	0.08	0.03287271
10	0.30	0.21	0.06	0.06	0.03511169
11	0.20	0.15	0.06	0.04	0.03307849
12	0.13	0.08	0.06	0.02	0.02321655
13	0.10	0.05	0.06	0.05	0.01266561
14	0.08	0.04	0.07	0.06	0.00629986
15	0.08	0.03	0.08	0.07	0.00307111
16	0.07	0.04	0.06	0.05	0.00178719
17	0.06	0.03	0.04	0.03	0.00128548
18	0.06	0.03	0.03	0.02	0.00109533
19	0.06	0.05	0.03	0.01	0.00103776
20	0.06	0.06	0.03	0.01	0.00104157

<b>Timepoint (in sec)</b>	<b>control distal</b>	<b>STDV</b>	<b><i>Gata2cKO</i> distal</b>	<b>STDV</b>	<b>t-Test</b>
0	0.01	0.01	0.01	0.01	0.0012391
1	0.04	0.07	0.03	0.01	0.00092983
2	0.14	0.13	0.09	0.05	0.00081026
3	0.31	0.20	0.15	0.10	0.00098022
4	0.40	0.23	0.17	0.11	0.00164506
5	0.47	0.23	0.15	0.10	0.00274485
6	0.51	0.21	0.12	0.08	0.00447283
7	0.50	0.22	0.08	0.04	0.00661784
8	0.43	0.24	0.05	0.03	0.00869617
9	0.34	0.22	0.03	0.03	0.01060501
10	0.27	0.21	0.03	0.02	0.01350981
11	0.20	0.16	0.03	0.02	0.01440688
12	0.15	0.12	0.03	0.02	0.01933683
13	0.11	0.09	0.06	0.08	0.04789275
14	0.09	0.07	0.08	0.11	0.11718208
15	0.07	0.06	0.09	0.12	0.13910195
16	0.07	0.04	0.07	0.10	0.0386886
17	0.06	0.04	0.06	0.08	0.00430585
18	0.07	0.05	0.04	0.06	0.00337879
19	0.07	0.07	0.04	0.05	0.06599274
20	0.08	0.10	0.04	0.04	



**Table S4.** Statistical analysis of the peristaltic frequency of E18.5 control and *Gata2cKO* ureters over 6 days of culture (relates to Figure 4E). Average and corresponding standard deviations of peristaltic contractions per minute after 1, 2, 4 and 6 days after ureter explantation at E18.5. Video-monitored was a duration of one minute. The statistical significance was calculated by a two-tailed Student's t-test. \*:  $p \leq 0.05$ ; \*\*:  $p \leq 0.01$ ; \*\*\*:  $p \leq 0.001$ .

		1 day	2 days	4 days	6 days
<b>control (n=7)</b>	<b>average</b>	2.42±0.5	3.16±0.41	3.33±1.03	3±0.6
<b><i>Gata2cKO</i> (n=5)</b>	<b>average</b>	1.00±1.2	1.2±1.7	1.45±1.7	1.21±1.6
	<b>t-Test</b>	0.052438237	0.03475948	0.013229092	0.003462174

**Table S5.** Statistical analysis of E18.5 control and *Gata2cKO* ureter contraction intensities over 6 days of culture (relates to Figure 4F). Average contraction intensity and corresponding standard deviations of peristaltic contractions per minute after 1, 2, 4 and 6 days after ureter explantation at E18.5. Video-monitored was a duration of one minute. Contraction intensity equals to the ratio of the diameter of the contracted ureter divided by the diameter of the relaxed ureter. The proximal level equals to 25%, medial to 50% and distal to 75% of the entire ureter length. The statistical significance was calculated by a two-tailed Student's t-test. \*:  $p \leq 0.05$ ; \*\*:  $p \leq 0.01$ ; \*\*\*:  $p \leq 0.001$ .

	1 day	2 days	4 days	6 days
<b>control proximal</b>	0.32±0.09	0.39±0.05	0.46±0.19	0.44±0.07
<b><i>Gata2cKO</i> proximal</b>	0.06±0.05	0.15±0.09	0.20±0.05	0.12±0.06
<b>t-Test</b>	0.00057491	0.00775937	0.01950715	0.00012569
<b>control medial</b>	0.39±0.09	0.39±0.06	0.48±1.33	0.49±0.05
<b><i>Gata2cKO</i> medial</b>	0.15±0.09	0.31±0.13	0.40±0.12	0.28±0.16
<b>t-Test</b>	0.00521827	0.34278877	0.37353749	0.08621248
<b>control distal</b>	0.44±0.07	0.43±0.1	0.49±0.06	0.51±0.08
<b><i>Gata2cKO</i> distal</b>	0.26±0.06	0.29±0.04	0.49±0.08	0.38±0.11
<b>t-Test</b>	0.00352458	0.02158559	0.93060563	0.10343251

**Table S6.** Transcripts identified by microarray analysis that were downregulated in E14.5 ureters of *Gata2cKO* embryos (relates to Table 1). Two pools of mutant ureters were compared to controls and the resulting fold changes (FC) in expression are displayed. Intensity thresholds were  $\geq 100$ ; Fold changes were  $> 1.3$ .

Gene Symbol	FC 1	FC 2	avg FC
<i>Cyp26a1</i>	-8.1	-4.4	-6.3
<i>Higd1c</i>	-5.5	-5.7	-5.6
<i>A930009L07Rik</i>	-7.9	-2.5	-5.2
<i>Chgb</i>	-5.2	-3.6	-4.4
<i>Mettl7a2Higd1c</i>	-4.7	-3.7	-4.2
<i>Chga</i>	-4.9	-3.1	-4.0
<i>C1ql3</i>	-3.3	-4.2	-3.7
<i>Dbh</i>	-4.2	-2.6	-3.4
<i>C2cd4b</i>	-3.6	-2.9	-3.2
<i>Insm1</i>	-3.8	-2.5	-3.2
<i>Npy</i>	-4.0	-2.3	-3.2
<i>Ctnna2</i>	-3.2	-2.8	-3.0
<i>Nefm</i>	-4.4	-1.4	-2.9
<i>Slc18a2</i>	-3.0	-2.8	-2.9
<i>Hand2</i>	-3.8	-1.9	-2.8
<i>Colq</i>	-3.1	-2.5	-2.8
<i>Epyc</i>	-2.4	-3.0	-2.7
<i>Prph</i>	-2.6	-2.8	-2.7
<i>Slc18a1</i>	-3.2	-2.1	-2.7
<i>Phox2a</i>	-3.2	-2.1	-2.6
<i>Tlx2</i>	-3.4	-1.8	-2.6
<i>Cartpt</i>	-3.5	-1.7	-2.6
<i>Gnas</i>	-3.3	-1.9	-2.6
<i>Dgkk</i>	-2.9	-2.3	-2.6
<i>Pitx1</i>	-2.8	-2.4	-2.6
<i>4632427E13Rik</i>	-2.6	-2.4	-2.5
<i>LOC102636514</i>	-3.3	-1.7	-2.5
<i>Rgs4</i>	-2.8	-2.2	-2.5
<i>Th</i>	-2.7	-2.2	-2.5
<i>Myh11</i>	-2.3	-2.6	-2.5
<i>Tmem130</i>	-2.3	-2.4	-2.3
<i>Actg2</i>	-2.0	-2.5	-2.3
<i>Ina</i>	-2.5	-2.1	-2.3
<i>D930019F10Rik</i>	-2.1	-2.4	-2.3
<i>Stmn3</i>	-2.1	-2.4	-2.2
<i>Calca</i>	-2.0	-2.5	-2.2
<i>Dusp26</i>	-2.7	-1.7	-2.2
<i>Phox2b</i>	-2.4	-2.0	-2.2
<i>Stmn4</i>	-2.4	-2.0	-2.2
<i>Nefl</i>	-2.3	-2.0	-2.2
<i>Slc18a3</i>	-2.5	-1.9	-2.2
<i>Myog</i>	-1.4	-2.9	-2.2
<i>Cnn1</i>	-1.8	-2.5	-2.2
<i>Celsr3</i>	-2.4	-1.9	-2.1
<i>Scg5</i>	-2.3	-2.0	-2.1
<i>Smpd3</i>	-2.2	-2.1	-2.1
<i>Celf3</i>	-2.6	-1.6	-2.1
<i>Grem2</i>	-1.5	-2.6	-2.1
<i>Slc35d3</i>	-2.4	-1.7	-2.1
<i>Ddc</i>	-2.2	-1.9	-2.0
<i>Myh3</i>	-1.4	-2.6	-2.0
<i>Ednrb</i>	-2.3	-1.7	-2.0
<i>Srrm4</i>	-2.3	-1.6	-2.0
<i>A_55_P1968618</i>	-1.5	-2.4	-1.9
<i>Fbxl22</i>	-1.4	-2.4	-1.9
<i>Col9a1</i>	-1.9	-1.9	-1.9
<i>Tnnt2</i>	-1.4	-2.4	-1.9
<i>Lhfpl3</i>	-2.0	-1.7	-1.9
<i>Gpr17</i>	-2.1	-1.6	-1.9
<i>Fmo1</i>	-1.9	-1.8	-1.9
<i>Rtn1</i>	-1.9	-1.8	-1.8
<i>Insc</i>	-2.0	-1.7	-1.8
<i>Acta1</i>	-1.5	-2.2	-1.8
<i>Acta2</i>	-1.5	-2.1	-1.8
<i>Myl1</i>	-1.4	-2.2	-1.8
<i>Ccdc109b</i>	-1.8	-1.8	-1.8
<i>Zcchc12</i>	-1.9	-1.7	-1.8
<i>Pcsk1n</i>	-1.9	-1.7	-1.8
<i>Prdm6</i>	-1.8	-1.8	-1.8
<i>Colec11</i>	-1.8	-1.8	-1.8
<i>Ret</i>	-2.1	-1.4	-1.8
<i>Tubb3</i>	-1.9	-1.6	-1.8

Gene Symbol	FC 1	FC 2	avg FC
<i>Kif5a</i>	-2.0	-1.5	-1.8
<i>Pcp4</i>	-1.8	-1.7	-1.8
<i>Tmem179</i>	-2.1	-1.4	-1.7
<i>Stmn2</i>	-1.6	-1.9	-1.7
<i>Mia</i>	-2.0	-1.5	-1.7
<i>Etv1</i>	-1.9	-1.5	-1.7
<i>Fam46a</i>	-1.8	-1.6	-1.7
<i>Car3</i>	-2.1	-1.4	-1.7
<i>Cthrc1</i>	-1.5	-1.9	-1.7
<i>Asic4</i>	-1.6	-1.8	-1.7
<i>Aspn</i>	-1.5	-1.9	-1.7
<i>Tnnc1</i>	-1.4	-2.0	-1.7
<i>Mapk10</i>	-2.0	-1.4	-1.7
<i>Batf</i>	-1.8	-1.6	-1.7
<i>Tgfb2</i>	-1.9	-1.5	-1.7
<i>Lsamp</i>	-1.6	-1.6	-1.6
<i>Asic1</i>	-1.5	-1.8	-1.6
<i>Hpgd</i>	-1.9	-1.4	-1.6
<i>Rpp25</i>	-1.5	-1.7	-1.6
<i>Gdap111</i>	-1.6	-1.6	-1.6
<i>Kcnk3</i>	-1.3	-1.9	-1.6
<i>E130308A19Rik</i>	-1.4	-1.9	-1.6
<i>Ndufa4l2</i>	-1.6	-1.6	-1.6
<i>Ascl1</i>	-1.7	-1.5	-1.6
<i>Sox10</i>	-1.7	-1.5	-1.6
<i>Morf4l2</i>	-1.6	-1.6	-1.6
<i>Ecel1</i>	-1.7	-1.5	-1.6
<i>Ap3b2</i>	-1.5	-1.7	-1.6
<i>Gch1</i>	-1.6	-1.5	-1.6
<i>Tmeff2</i>	-1.5	-1.6	-1.6
<i>Foxd2os</i>	-1.6	-1.6	-1.6
<i>9430076C15Rik</i>	-1.6	-1.5	-1.6
<i>Angptl7</i>	-1.6	-1.5	-1.6
<i>Col12a1</i>	-1.4	-1.7	-1.6
<i>Prss12</i>	-1.5	-1.6	-1.6
<i>Scm1</i>	-1.7	-1.4	-1.6
<i>Nacad</i>	-1.4	-1.7	-1.6
<i>BC049730</i>	-1.4	-1.6	-1.5
<i>Fgf7</i>	-1.7	-1.4	-1.5
<i>Zfhx4</i>	-1.4	-1.7	-1.5
<i>Tmem74b</i>	-1.5	-1.5	-1.5
<i>Rundc3a</i>	-1.5	-1.6	-1.5
<i>Efhf1</i>	-1.6	-1.5	-1.5
<i>Tagln3</i>	-1.7	-1.3	-1.5
<i>Wnt11</i>	-1.4	-1.6	-1.5
<i>Cpxm2</i>	-1.4	-1.6	-1.5
<i>Fam189a1</i>	-1.4	-1.6	-1.5
<i>C1qa</i>	-1.6	-1.4	-1.5
<i>Tmem37</i>	-1.7	-1.3	-1.5
<i>Cgref1</i>	-1.6	-1.4	-1.5
<i>Camp</i>	-1.6	-1.4	-1.5
<i>Rnd2</i>	-1.6	-1.4	-1.5
<i>Sntg1</i>	-1.5	-1.5	-1.5
<i>Tnni1</i>	-1.4	-1.6	-1.5
<i>Sulf1</i>	-1.5	-1.5	-1.5
<i>Cxcl14</i>	-1.3	-1.6	-1.5
<i>Mapk8ip2</i>	-1.5	-1.5	-1.5
<i>Fndc1</i>	-1.5	-1.5	-1.5
<i>BC100530</i>	-1.5	-1.4	-1.5
<i>Smoc1</i>	-1.4	-1.5	-1.5
<i>Inhba</i>	-1.4	-1.5	-1.5
<i>Snap91</i>	-1.6	-1.3	-1.5
<i>Crym</i>	-1.5	-1.4	-1.5
<i>Hhip</i>	-1.5	-1.5	-1.5
<i>Ppm1e</i>	-1.6	-1.3	-1.5
<i>Socs2</i>	-1.6	-1.3	-1.5
<i>Apoe</i>	-1.5	-1.4	-1.5
<i>Uchl1</i>	-1.4	-1.5	-1.5
<i>TC1589582</i>	-1.5	-1.4	-1.5
<i>Aspa</i>	-1.5	-1.4	-1.4
<i>Dlk1</i>	-1.5	-1.4	-1.4
<i>Ptprz1</i>	-1.6	-1.3	-1.4

Gene Symbol	FC 1	FC 2	avg FC
<i>Dok7</i>	-1.3	-1.6	-1.4
<i>Arl13b</i>	-1.6	-1.3	-1.4
<i>Wnk2</i>	-1.4	-1.4	-1.4
<i>Col2a1</i>	-1.5	-1.4	-1.4
<i>Plod2</i>	-1.5	-1.4	-1.4
<i>Plxna4</i>	-1.3	-1.5	-1.4
<i>Foxp2</i>	-1.4	-1.5	-1.4
<i>Gng3</i>	-1.5	-1.3	-1.4
<i>Gap43</i>	-1.5	-1.3	-1.4
<i>Sult4a1</i>	-1.4	-1.4	-1.4
<i>Gas1</i>	-1.4	-1.5	-1.4
<i>Has2os</i>	-1.5	-1.3	-1.4
<i>Nrn1</i>	-1.4	-1.4	-1.4
<i>Tox</i>	-1.4	-1.4	-1.4
<i>Nnat</i>	-1.5	-1.3	-1.4
<i>Vcam1</i>	-1.4	-1.4	-1.4
<i>Camk2b</i>	-1.4	-1.4	-1.4
<i>Loxl1</i>	-1.3	-1.5	-1.4
<i>Lrrc24</i>	-1.4	-1.4	-1.4
<i>Apbb1ip</i>	-1.4	-1.4	-1.4
<i>LOC102642487</i>	-1.5	-1.3	-1.4
<i>A_55_P2091328</i>	-1.4	-1.4	-1.4
<i>Myl4</i>	-1.4	-1.4	-1.4
<i>Gkn3</i>	-1.3	-1.5	-1.4
<i>Ramp1</i>	-1.3	-1.4	-1.4
<i>ENSMUST00000103426</i>	-1.4	-1.4	-1.4
<i>Myo1f</i>	-1.4	-1.4	-1.4
<i>Prss23</i>	-1.4	-1.4	-1.4
<i>Ngfr</i>	-1.4	-1.4	-1.4
<i>A_55_P2083725</i>	-1.4	-1.4	-1.4
<i>S100b</i>	-1.4	-1.3	-1.4
<i>Lin7a</i>	-1.4	-1.4	-1.4
<i>Ak5</i>	-1.3	-1.4	-1.4
<i>Scx</i>	-1.3	-1.4	-1.4
<i>Fcrls</i>	-1.3	-1.4	-1.4
<i>S1pr2</i>	-1.4	-1.3	-1.4
<i>Irak3</i>	-1.4	-1.4	-1.4
<i>Csf1r</i>	-1.4	-1.4	-1.4
<i>Rbm24</i>	-1.3	-1.4	-1.4
<i>Aph1b</i>	-1.4	-1.3	-1.4
<i>Rgs9</i>	-1.3	-1.4	-1.4
<i>Khk</i>	-1.3	-1.4	-1.3
<i>Eva1c</i>	-1.4	-1.3	-1.3
<i>Ctsf</i>	-1.3	-1.4	-1.3
<i>A_55_P2023176</i>	-1.3	-1.3	-1.3
<i>Fkbp1b</i>	-1.4	-1.3	-1.3
<i>Ablim1</i>	-1.3	-1.3	-1.3
<i>Efcab4a</i>	-1.3	-1.3	-1.3
<i>Pdgfrl</i>	-1.3	-1.3	-1.3

**Table S7.** Transcripts identified by microarray analysis that were upregulated in E14.5 ureters of *Gata2cKO* embryos (relates to Table 1). Two pools of mutant ureters were compared to controls and the resulting fold changes (FC) in expression are displayed. Intensity thresholds were  $\geq 100$ ; Fold changes were  $> 1.3$ .

Gene Symbol	FC 1	FC 2	avg FC
<i>Sostdc1</i>	5.0	4.5	4.7
<i>Ddx6</i>	4.7	4.7	4.7
<i>Mapk8</i>	3.2	5.5	4.4
<i>Z310065F04Rik</i>	5.7	1.7	3.7
<i>C920006O11Rik</i>	4.3	3.0	3.7
<i>Htr2b</i>	3.1	3.7	3.4
<i>ENSMUST00000181359</i>	4.3	2.5	3.4
<i>Lrriq1</i>	3.3	3.4	3.4
<i>Kcnip1</i>	3.4	2.7	3.1
<i>Cntfr</i>	2.9	3.2	3.1
<i>Avpr1a</i>	2.7	3.3	3.0
<i>ENSMUST00000099683</i>	1.3	4.7	3.0
<i>Notumos</i>	2.8	2.8	2.8
<i>Dach2</i>	2.3	2.9	2.6
<i>Alx1</i>	2.7	2.4	2.5
<i>Epha8</i>	2.7	2.0	2.4
<i>Kcnma1</i>	2.7	2.0	2.3
<i>Fzd10</i>	2.5	2.0	2.3
<i>Lsm14b</i>	2.4	2.0	2.2
<i>Cldn1</i>	2.4	2.0	2.2
<i>D430041D05Rik</i>	2.4	2.0	2.2
<i>Dus4l</i>	1.7	2.7	2.2
<i>Cd83</i>	1.9	2.3	2.1
<i>Acsl1</i>	2.2	2.0	2.1
<i>Neto2</i>	2.1	2.1	2.1
<i>Cntn1</i>	2.5	1.7	2.1
<i>Myo18b</i>	2.5	1.5	2.0
<i>Kcnd3</i>	1.9	2.1	2.0
<i>Thoc2</i>	1.7	2.3	2.0
<i>Megf10</i>	1.8	2.2	2.0
<i>AK046833</i>	1.8	2.1	2.0
<i>Ahr</i>	1.8	2.1	1.9
<i>Lix1</i>	1.9	2.0	1.9
<i>Npr3</i>	1.8	2.0	1.9
<i>Rps6ka3</i>	1.4	2.4	1.9
<i>Nell1</i>	2.0	1.9	1.9
<i>AK167004</i>	1.7	2.1	1.9
<i>Fut9</i>	1.9	1.9	1.9
<i>Aldh1a3</i>	2.2	1.5	1.9
<i>Cldn4</i>	2.2	1.5	1.9
<i>Lamc3</i>	2.0	1.7	1.8
<i>Leo1</i>	2.2	1.5	1.8
<i>A_55_P2087963</i>	1.7	1.9	1.8
<i>Wif1</i>	2.2	1.5	1.8
<i>AK156275</i>	1.5	2.2	1.8
<i>A_55_P2041693</i>	1.9	1.7	1.8
<i>Mid1</i>	1.9	1.7	1.8
<i>Enpep</i>	1.8	1.7	1.8
<i>Cftr2</i>	1.8	1.7	1.8
<i>Plcb1</i>	1.5	2.0	1.8
<i>Arhgap15</i>	1.9	1.6	1.8
<i>Cfh</i>	1.5	2.0	1.8
<i>Vvwc2</i>	1.7	1.8	1.8
<i>9030425P06Rik</i>	1.7	1.8	1.8
<i>Ackr1</i>	2.1	1.4	1.8
<i>AI314604</i>	1.6	1.9	1.8
<i>Prkg2</i>	1.7	1.8	1.8
<i>4833424O15Rik</i>	1.5	2.0	1.8
<i>AK149769</i>	1.5	2.0	1.7
<i>Fam155a</i>	1.8	1.7	1.7
<i>Tmem132c</i>	1.5	1.9	1.7
<i>Nipal1</i>	2.0	1.5	1.7
<i>AK139043</i>	1.6	1.9	1.7
<i>Hoxd11</i>	1.7	1.8	1.7
<i>Slc22a3</i>	1.9	1.5	1.7
<i>Lrnf5</i>	1.4	2.0	1.7
<i>Gabra3</i>	1.7	1.7	1.7
<i>AK137931</i>	2.1	1.3	1.7
<i>Kcnv2</i>	1.5	1.9	1.7
<i>Asgr1</i>	1.7	1.7	1.7
<i>Fam19a5</i>	1.7	1.7	1.7
<i>Nrxn1</i>	1.4	2.0	1.7

Gene Symbol	FC 1	FC 2	avg FC
<i>Emd</i>	1.7	1.7	1.7
<i>A_55_P2161390</i>	1.4	2.0	1.7
<i>Kcnk2</i>	1.9	1.5	1.7
<i>Laptm4a</i>	1.9	1.5	1.7
<i>D230018H15Rik</i>	1.7	1.7	1.7
<i>Sprr2a2</i>	2.0	1.4	1.7
<i>Fgd4</i>	1.4	1.9	1.7
<i>ligp1</i>	1.5	1.9	1.7
<i>Syndig1</i>	2.0	1.3	1.7
<i>Rnu2-10</i>	1.4	1.9	1.6
<i>BC057651</i>	1.6	1.7	1.6
<i>Nav2</i>	1.9	1.4	1.6
<i>Kif26b</i>	1.8	1.5	1.6
<i>Pou3f1</i>	1.9	1.4	1.6
<i>Mfap4</i>	1.8	1.4	1.6
<i>Baalc</i>	1.3	1.9	1.6
<i>8030498J20Rik</i>	1.8	1.4	1.6
<i>Luc7l2</i>	1.9	1.3	1.6
<i>D9Wsu90e</i>	1.8	1.4	1.6
<i>Foxl1</i>	1.5	1.7	1.6
<i>Sfrp5</i>	1.9	1.3	1.6
<i>Sema3c</i>	1.5	1.7	1.6
<i>Rhoa</i>	1.7	1.5	1.6
<i>Eddm3b</i>	1.7	1.5	1.6
<i>Gm4951</i>	1.5	1.7	1.6
<i>Syt16</i>	1.6	1.6	1.6
<i>Wnk1</i>	1.5	1.7	1.6
<i>Icosl</i>	1.6	1.5	1.6
<i>Dach1</i>	1.5	1.7	1.6
<i>Raly</i>	1.6	1.6	1.6
<i>Tec</i>	1.6	1.5	1.6
<i>Ell2</i>	1.7	1.5	1.6
<i>Rnf182</i>	1.8	1.3	1.6
<i>Stxbp6</i>	1.5	1.6	1.6
<i>ENSMUST00000166899</i>	1.4	1.7	1.6
<i>Tbc1d4</i>	1.5	1.7	1.6
<i>Ube4a</i>	1.5	1.6	1.6
<i>Akap13</i>	1.5	1.6	1.6
<i>Gm4788</i>	1.6	1.5	1.6
<i>Slitrk4</i>	1.6	1.5	1.6
<i>Nhlrc2</i>	1.7	1.4	1.6
<i>Ggps1</i>	1.4	1.7	1.6
<i>Gm6403</i>	1.5	1.6	1.6
<i>Cutal</i>	1.6	1.5	1.5
<i>Gabra1</i>	1.3	1.8	1.5
<i>Hsd3b2</i>	1.4	1.7	1.5
<i>Rif1</i>	1.4	1.7	1.5
<i>Sall1</i>	1.5	1.6	1.5
<i>F830014O18Rik</i>	1.3	1.7	1.5
<i>Tmod2</i>	1.5	1.5	1.5
<i>9630055L06Rik</i>	1.7	1.4	1.5
<i>Ndp</i>	1.4	1.6	1.5
<i>Gm3364</i>	1.4	1.6	1.5
<i>TC1611451</i>	1.5	1.6	1.5
<i>D630033O11Rik</i>	1.5	1.5	1.5
<i>Nr2c2</i>	1.5	1.5	1.5
<i>Mal</i>	1.5	1.5	1.5
<i>ENSMUST00000072014</i>	1.3	1.7	1.5
<i>Nrg1</i>	1.5	1.5	1.5
<i>Palms2</i>	1.5	1.5	1.5
<i>Bre</i>	1.5	1.5	1.5
<i>Ergic1</i>	1.5	1.5	1.5
<i>AW549542</i>	1.4	1.6	1.5
<i>ENSMUST000000051253</i>	1.3	1.7	1.5
<i>A130077B15Rik</i>	1.5	1.5	1.5
<i>Ank</i>	1.6	1.4	1.5
<i>Fbxl12os</i>	1.5	1.5	1.5
<i>6720482D04</i>	1.5	1.4	1.5
<i>C030005K06Rik</i>	1.3	1.6	1.5
<i>Hey2</i>	1.5	1.5	1.5
<i>Taf15</i>	1.6	1.4	1.5
<i>A_55_P2108486</i>	1.4	1.6	1.5

Gene Symbol	FC 1	FC 2	avg FC
<i>Kcnq1ot1</i>	1.4	1.5	1.5
<i>Pla2g7</i>	1.4	1.5	1.5
<i>A830054O07Rik</i>	1.5	1.5	1.5
<i>Zfp951</i>	1.3	1.6	1.5
<i>Tnfrsf19</i>	1.4	1.6	1.5
<i>Gdgd3</i>	1.6	1.3	1.5
<i>Cpd</i>	1.4	1.5	1.5
<i>Cntn6</i>	1.3	1.6	1.5
<i>Tbpl1</i>	1.4	1.6	1.5
<i>Copg2</i>	1.4	1.5	1.5
<i>Bpnt1</i>	1.5	1.4	1.5
<i>Galnt3</i>	1.4	1.5	1.5
<i>Fat3</i>	1.5	1.4	1.5
<i>Pipox</i>	1.4	1.5	1.4
<i>Chst2</i>	1.4	1.5	1.4
<i>Mgll</i>	1.5	1.4	1.4
<i>Slc35g2</i>	1.3	1.6	1.4
<i>C230096K16Rik</i>	1.4	1.5	1.4
<i>Arl6ip5</i>	1.4	1.5	1.4
<i>G6pc2</i>	1.5	1.4	1.4
<i>A_55_P2050988</i>	1.4	1.5	1.4
<i>Tshz3</i>	1.6	1.3	1.4
<i>Ntf3</i>	1.4	1.4	1.4
<i>Col22a1</i>	1.4	1.4	1.4
<i>Fam208a</i>	1.5	1.4	1.4
<i>Greb1l</i>	1.4	1.4	1.4
<i>Gcm1</i>	1.3	1.5	1.4
<i>Otop2</i>	1.3	1.6	1.4
<i>Map3k5</i>	1.5	1.3	1.4
<i>Cask</i>	1.4	1.5	1.4
<i>Rnu3b1</i>	1.3	1.5	1.4
<i>A_55_P1993371</i>	1.3	1.5	1.4
<i>TC1703733</i>	1.4	1.4	1.4
<i>Elf5</i>	1.4	1.5	1.4
<i>Plxna2</i>	1.4	1.4	1.4
<i>Foxi1</i>	1.5	1.4	1.4
<i>Vstm4</i>	1.4	1.4	1.4
<i>Ecm1</i>	1.5	1.4	1.4
<i>Tmx3</i>	1.4	1.4	1.4
<i>A630089N07Rik</i>	1.3	1.5	1.4
<i>Galnt12</i>	1.5	1.3	1.4
<i>D930030O05Rik</i>	1.4	1.4	1.4
<i>A_55_P2150737</i>	1.3	1.5	1.4
<i>Mbd4</i>	1.4	1.4	1.4
<i>D230040A04Rik</i>	1.4	1.4	1.4
<i>Fcho2</i>	1.5	1.3	1.4
<i>Pspc1</i>	1.3	1.5	1.4
<i>Flrt2</i>	1.3	1.5	1.4
<i>Man1a</i>	1.4	1.3	1.4
<i>Sh3gl2</i>	1.3	1.5	1.4
<i>Trim9</i>	1.5	1.3	1.4
<i>D930016D06Rik</i>	1.4	1.3	1.4
<i>A_55_P1968600</i>	1.5	1.3	1.4
<i>4633401B06Rik</i>	1.4	1.4	1.4
<i>Nkd1</i>	1.4	1.4	1.4
<i>Egr1</i>	1.3	1.4	1.4
<i>Pura</i>	1.4	1.4	1.4
<i>Gm14858</i>	1.4	1.3	1.4
<i>4930429F24Rik</i>	1.4	1.4	1.4
<i>Adcy7</i>	1.4	1.3	1.4
<i>Ccbe1</i>	1.4	1.3	1.4
<i>Elovl6</i>	1.3	1.4	1.4
<i>Dcaf17</i>	1.4	1.3	1.4
<i>LOC102642336</i>	1.3	1.4	1.4
<i>Rbp4</i>	1.4	1.3	1.4
<i>Zfp536</i>	1.4	1.3	1.4
<i>Nckap5</i>	1.4	1.4	1.4
<i>AK013651</i>	1.3	1.4	1.4
<i>Etl4</i>	1.4	1.3	1.4
<i>Zbtb4</i>	1.3	1.4	1.3
<i>D8Ert158e</i>	1.3	1.3	1.3
<i>Fgf14</i>	1.3	1.3	1.3

Gene Symbol	FC 1	FC 2	avg FC
<i>A_55_P2040490</i>	1.3	1.3	1.3
<i>Pigt</i>	1.3	1.3	1.3
<i>Pid1</i>	1.3	1.3	1.3

**Table S8.** Functional annotation clustering analysis for transcripts that were downregulated in E14.5 ureters of *Gata2cKO* embryos. Functional enrichment analysis for 193 downregulated genes was performed with DAVID 6.8 websoftware (<https://david.ncicfcrf.gov>) using default settings. Shown are the TOP10 Annotation clusters.

Annotation Cluster 1	Enrichment Score: 5.60																		
Category	Term	Count	%	PValue	Genes	List Total	Pop Hits	Pop Total	Fold Enrichment	Bonferroni	Benjamini	FDR							
UP_KEYWORDS	Secreted	37	20.2	2.19E-08	ASPN, MIA, CTHRC1, FGF7, COL2A1, GREM2, TGFB2, CALCA, ANGPTL7, COL9A1, CGREF1, APOE, SMOG1, COL12A1, SCG5, HHIP, LOXL1, PRSS12, PTPRZ1, CAMP, CPXM2, COLEC11, C1QA, INHBA, CHGA, GKN3, CXCL14, NPY, PDGFRL, CARTPT, GNAS, C1QL3, WNT11, EPYC, PRSS23, PCSK1N, CHGB	177	1685	22680	2.8	4.4E-06	2.2E-06	2.7E-05							
UP_KEYWORDS	Glycoprotein	59	32.2	1.20E-07	ASPN, CTHRC1, FGF7, PLXNA4, UCHL1, DLK1, TMEM179, TGFB2, S1PR2, EDNRB, PLOD2, APOE, COL12A1, HHIP, INA, TMEFF2, RET, EVA1C, CPXM2, LRRC24, TMEM130, C1QA, INHBA, CHGA, LSAMP, PDGFRL, GNAS, WNT11, GPR17, NGFR, EPYC, CHGB, CTSF, SNAP91, ECEL1, COL2A1, NRN1, GREM2, CALCA, VCAM1, ANGPTL7, SMOG1, NEFL, PRSS12, NEFM, CSF1R, PTPRZ1, ASIC4, CELSR3, GAS1, ASIC1, DBH, KCNK3, GKN3, SULF1, SLC18A2, SLC18A3, SLC18A1, PRSS23	177	3815	22680	2.0	2.4E-05	8.0E-06	1.5E-04							
UP_SEQ_FEATURE	signal peptide	57	31.1	3.52E-07	ASPN, CTHRC1, FGF7, PLXNA4, DLK1, TGFB2, EDNRB, CGREF1, PLOD2, APOE, PCP4, COL12A1, HHIP, LOXL1, RAMP1, TMEFF2, RET, EVA1C, CAMP, CPXM2, COLEC11, LRRC24, TMEM130, FCRLS, C1QA, INHBA, CHGA, COLQ, LSAMP, PDGFRL, CARTPT, C1QL3, WNT11, NGFR, EPYC, CHGB, CTSF, MIA, COL2A1, NRN1, GREM2, CALCA, VCAM1, ANGPTL7, COL9A1, SMOG1, SCG5, PRSS12, CSF1R, PTPRZ1, CELSR3, GAS1, CXCL14, NPY, SULF1, PRSS23, PCSK1N	169	3124	18012	1.9	2.0E-04	2.0E-04	5.2E-04							
GOTERM_CC_DIRECT	GO:0005576-extracellular region	38	20.8	4.91E-07	ASPN, MIA, CTHRC1, FGF7, COL2A1, GREM2, TGFB2, CALCA, ANGPTL7, COL9A1, CGREF1, APOE, SMOG1, COL12A1, SCG5, HHIP, LOXL1, PRSS12, PTPRZ1, CAMP, CPXM2, COLEC11, C1QA, INHBA, CHGA, GKN3, CXCL14, NPY, S100B, PDGFRL, CARTPT, GNAS, C1QL3, WNT11, EPYC, PRSS23, PCSK1N, CHGB	175	1753	19662	2.4	1.0E-04	5.1E-05	6.2E-04							
UP_KEYWORDS	Signal	64	35.0	7.75E-07	ASPN, CTHRC1, FGF7, PLXNA4, UCHL1, DLK1, TGFB2, EDNRB, CGREF1, PLOD2, APOE, COL12A1, HHIP, LOXL1, RAMP1, TMEFF2, RET, EVA1C, CAMP, CPXM2, COLEC11, LRRC24, TMEM130, FCRLS, C1QA, INHBA, CHGA, COLQ, LSAMP, PDGFRL, CARTPT, GNAS, C1QL3, WNT11, NGFR, EPYC, CHGB, CTSF, MIA, COL2A1, FAM46A, NRN1, GREM2, CALCA, ANGPTL7, VCAM1, COL9A1, IRAK3, FAM189A1, SMOG1, FNDC1, SCG5, PRSS12, CSF1R, PTPRZ1, CELSR3, GAS1, GKN3, BC049730, CXCL14, NPY, SULF1, PRSS23, PCSK1N	177	4543	22680	1.8	1.5E-04	3.9E-05	9.7E-04							
UP_KEYWORDS	Disulfide bond	49	26.8	1.72E-06	MIA, ASPN, PLXNA4, COL2A1, DLK1, GREM2, TGFB2, CALCA, ANGPTL7, VCAM1, COL9A1, EDNRB, SMOG1, COL12A1, SCG5, HHIP, RAMP1, LOXL1, PRSS12, CSF1R, TMEFF2, RET, PTPRZ1, ASIC4, CAMP, CPXM2, CELSR3, ASIC1, COLEC11, LRRC24, DBH, FCRLS, C1QA, INHBA, CHGA, GKN3, CXCL14, COLQ, LSAMP, PDGFRL, SLC18A2, CARTPT, WNT11, GPR17, NGFR, EPYC, PRSS23, CHGB, CTSF	177	3124	22680	2.0	3.4E-04	6.9E-05	2.2E-03							
GOTERM_CC_DIRECT	GO:0005615-extracellular space	33	18.0	2.87E-06	CTHRC1, FGF7, COL2A1, DLK1, NRN1, GREM2, TGFB2, CALCA, VCAM1, ACTG2, APOE, COL12A1, LOXL1, RAMP1, INA, ACTA1, PTPRZ1, ACTA2, CAMP, CPXM2, DBH, INHBA, CHGA, GKN3, CXCL14, NPY, S100B, SULF1, CARTPT, WNT11, PCSK1N, EPYC, CTSF	175	1504	19662	2.5	5.9E-04	1.5E-04	3.6E-03							

**Table S8.** Functional annotation clustering analysis for transcripts that were downregulated in E14.5 ureters of *Gata2cKO* embryos. Functional enrichment analysis for 193 downregulated genes was performed with DAVID 6.8 websoftware (<https://david.ncicfcrf.gov>) using default settings. Shown are the TOP10 Annotation clusters.

Annotation Cluster 1	Enrichment Score: 5.60																		
Category	Term	Count	%	PValue	Genes	List Total	Pop Hits	Pop Total	Fold Enrichment	Bonferroni	Benjamini	FDR							
UP_KEYWORDS	Secreted	37	20.2	2.19E-08	ASPN, MIA, CTHRC1, FGF7, COL2A1, GREM2, TGFB2, CALCA, ANGPTL7, COL9A1, CGREF1, APOE, SMOG1, COL12A1, SCG5, HHIP, LOXL1, PRSS12, PTPRZ1, CAMP, CPXM2, COLEC11, C1QA, INHBA, CHGA, GKN3, CXCL14, NPY, PDGFRL, CARTPT, GNAS, C1QL3, WNT11, EPYC, PRSS23, PCSK1N, CHGB	177	1685	22680	2.8	4.4E-06	2.2E-06	2.7E-05							
UP_KEYWORDS	Glycoprotein	59	32.2	1.20E-07	ASPN, CTHRC1, FGF7, PLXNA4, UCHL1, DLK1, TMEM179, TGFB2, S1PR2, EDNRB, PLOD2, APOE, COL12A1, HHIP, INA, TMEFF2, RET, EVA1C, CPXM2, LRRC24, TMEM130, C1QA, INHBA, CHGA, LSAMP, PDGFRL, GNAS, WNT11, GPR17, NGFR, EPYC, CHGB, CTSF, SNAP91, ECEL1, COL2A1, NRN1, GREM2, CALCA, VCAM1, ANGPTL7, SMOG1, NEFL, PRSS12, NEFM, CSF1R, PTPRZ1, ASIC4, CELSR3, GAS1, ASIC1, DBH, KCNK3, GKN3, SULF1, SLC18A2, SLC18A3, SLC18A1, PRSS23	177	3815	22680	2.0	2.4E-05	8.0E-06	1.5E-04							
UP_SEQ_FEATURE	signal peptide	57	31.1	3.52E-07	ASPN, CTHRC1, FGF7, PLXNA4, DLK1, TGFB2, EDNRB, CGREF1, PLOD2, APOE, PCP4, COL12A1, HHIP, LOXL1, RAMP1, TMEFF2, RET, EVA1C, CAMP, CPXM2, COLEC11, LRRC24, TMEM130, FCRLS, C1QA, INHBA, CHGA, COLQ, LSAMP, PDGFRL, CARTPT, C1QL3, WNT11, NGFR, EPYC, CHGB, CTSF, MIA, COL2A1, NRN1, GREM2, CALCA, VCAM1, ANGPTL7, COL9A1, SMOG1, SCG5, PRSS12, CSF1R, PTPRZ1, CELSR3, GAS1, CXCL14, NPY, SULF1, PRSS23, PCSK1N	169	3124	18012	1.9	2.0E-04	2.0E-04	5.2E-04							
GOTERM_CC_DIRECT	GO:0005576-extracellular region	38	20.8	4.91E-07	ASPN, MIA, CTHRC1, FGF7, COL2A1, GREM2, TGFB2, CALCA, ANGPTL7, COL9A1, CGREF1, APOE, SMOG1, COL12A1, SCG5, HHIP, LOXL1, PRSS12, PTPRZ1, CAMP, CPXM2, COLEC11, C1QA, INHBA, CHGA, GKN3, CXCL14, NPY, S100B, PDGFRL, CARTPT, GNAS, C1QL3, WNT11, EPYC, PRSS23, PCSK1N, CHGB	175	1753	19662	2.4	1.0E-04	5.1E-05	6.2E-04							
UP_KEYWORDS	Signal	64	35.0	7.75E-07	ASPN, CTHRC1, FGF7, PLXNA4, UCHL1, DLK1, TGFB2, EDNRB, CGREF1, PLOD2, APOE, COL12A1, HHIP, LOXL1, RAMP1, TMEFF2, RET, EVA1C, CAMP, CPXM2, COLEC11, LRRC24, TMEM130, FCRLS, C1QA, INHBA, CHGA, COLQ, LSAMP, PDGFRL, CARTPT, GNAS, C1QL3, WNT11, NGFR, EPYC, CHGB, CTSF, MIA, COL2A1, FAM46A, NRN1, GREM2, CALCA, ANGPTL7, VCAM1, COL9A1, IRAK3, FAM189A1, SMOG1, FNDC1, SCG5, PRSS12, CSF1R, PTPRZ1, CELSR3, GAS1, GKN3, BC049730, CXCL14, NPY, SULF1, PRSS23, PCSK1N	177	4543	22680	1.8	1.5E-04	3.9E-05	9.7E-04							
UP_KEYWORDS	Disulfide bond	49	26.8	1.72E-06	MIA, ASPN, PLXNA4, COL2A1, DLK1, GREM2, TGFB2, CALCA, ANGPTL7, VCAM1, COL9A1, EDNRB, SMOG1, COL12A1, SCG5, HHIP, RAMP1, LOXL1, PRSS12, CSF1R, TMEFF2, RET, PTPRZ1, ASIC4, CAMP, CPXM2, CELSR3, ASIC1, COLEC11, LRRC24, DBH, FCRLS, C1QA, INHBA, CHGA, GKN3, CXCL14, COLQ, LSAMP, PDGFRL, SLC18A2, CARTPT, WNT11, GPR17, NGFR, EPYC, PRSS23, CHGB, CTSF	177	3124	22680	2.0	3.4E-04	6.9E-05	2.2E-03							
GOTERM_CC_DIRECT	GO:0005615-extracellular space	33	18.0	2.87E-06	CTHRC1, FGF7, COL2A1, DLK1, NRN1, GREM2, TGFB2, CALCA, VCAM1, ACTG2, APOE, COL12A1, LOXL1, RAMP1, INA, ACTA1, PTPRZ1, ACTA2, CAMP, CPXM2, DBH, INHBA, CHGA, GKN3, CXCL14, NPY, S100B, SULF1, CARTPT, WNT11, PCSK1N, EPYC, CTSF	175	1504	19662	2.5	5.9E-04	1.5E-04	3.6E-03							



Part 2 – GATA2 in SMC differentiation

UP_SEQ_FEATURE	disulfide bond	42	23.0	1.91E-04	ASPN, MIA, PLXNA4, DLK1, GREM2, TGFB2, CALCA, ANGPTL7, VCAM1, EDNRB, COL9A1, PCP4, SMOC1, SCG5, HHIP, RAMP1, PRSS12, CSF1R, TMEFF2, CAMP, ASIC4, CELSR3, CPXM2, COLEC11, ASIC1, DBH, LRRC24, C1QA, INHBA, CHGA, CXCL14, COLQ, LSAMP, PDGFRL, SLC18A2, CARTPT, GPR17, NGFR, EPYC, PRSS23, CHGB, CTSF	169	2510	18012	1.8	1.0E-01	3.5E-02	2.8E-01
UP_SEQ_FEATURE	glycosylation site:N-linked (GlcNAc...)	47	25.7	1.04E-02	ASPN, CTHRC1, FGF7, PLXNA4, ECEL1, DLK1, GREM2, TMEM179, TGFB2, S1PR2, CALCA, ANGPTL7, VCAM1, EDNRB, PLOD2, PCP4, SMOC1, COL12A1, HHIP, PRSS12, CSF1R, TMEFF2, RET, EVA1C, ASIC4, CELSR3, CPXM2, ASIC1, GAS1, DBH, TMEM130, LRRC24, KCNK3, C1QA, INHBA, LSAMP, PDGFRL, SULF1, SLC18A2, SLC18A3, WNT11, GPR17, SLC18A1, NGFR, EPYC, PRSS23, CTSF	169	3563	18012	1.4	1.0E+00	4.2E-01	1.4E+01
<b>Annotation Cluster 2</b>	<b>Enrichment Score: 3.40</b>											
<b>Category</b>	<b>Term</b>	<b>Count</b>	<b>%</b>	<b>PValue</b>	<b>Genes</b>	<b>List Total</b>	<b>Pop Hits</b>	<b>Pop Total</b>	<b>Fold Enrichment</b>	<b>Bonferroni</b>	<b>Benjamini</b>	<b>FDR</b>
GOTERM_BP_DIRECT	GO:0048265~response to pain	5	2.7	3.07E-05	CALCA, EDNRB, RET, DBH, GCH1	160	21	18082	26.9	3.8E-02	7.6E-03	5.0E-02
GOTERM_BP_DIRECT	GO:0042311~vasodilation	4	2.2	9.09E-04	CALCA, EDNRB, APOE, GCH1	160	22	18082	20.5	6.8E-01	7.3E-02	1.5E+00
GOTERM_BP_DIRECT	GO:0008217~regulation of blood pressure	5	2.7	2.16E-03	CALCA, EDNRB, NPY, ACTA2, GCH1	160	62	18082	9.1	9.3E-01	1.2E-01	3.5E+00
Annotation Cluster 3	Enrichment Score: 3.3831317880271587											
<b>Category</b>	<b>Term</b>	<b>Count</b>	<b>%</b>	<b>PValue</b>	<b>Genes</b>	<b>List Total</b>	<b>Pop Hits</b>	<b>Pop Total</b>	<b>Fold Enrichment</b>	<b>Bonferroni</b>	<b>Benjamini</b>	<b>FDR</b>
UP_KEYWORDS	Collagen	8	4.4	4.46E-06	C1QA, CTHRC1, COL9A1, COLQ, COL12A1, COL2A1, C1QL3, COLEC11	177	85	22680	12.1	8.9E-04	1.5E-04	5.6E-03
GOTERM_CC_DIRECT	GO:0005581~collagen trimer	8	4.4	8.88E-06	C1QA, CTHRC1, COL9A1, COLQ, COL12A1, COL2A1, C1QL3, COLEC11	175	83	19662	10.8	1.8E-03	2.6E-04	1.1E-02
INTERPRO	IPR008160:Collagen triple helix repeat	7	3.8	3.67E-05	C1QA, COL9A1, COLQ, COL12A1, COL2A1, C1QL3, COLEC11	169	76	20594	11.2	1.4E-02	6.8E-03	5.1E-02
UP_SEQ_FEATURE	domain:Collagen-like	4	2.2	3.54E-03	C1QA, CTHRC1, C1QL3, COLEC11	169	33	18012	12.9	8.6E-01	2.8E-01	5.1E+00
UP_KEYWORDS	Hydroxylation	5	2.7	4.93E-03	C1QA, COL9A1, CELSR3, COL12A1, COL2A1	177	88	22680	7.3	6.3E-01	4.8E-02	6.0E+00
KEGG_PATHWAY	mmu04974:Protein digestion and absorption	3	1.6	1.98E-01	COL9A1, COL12A1, COL2A1	73	88	7720	3.6	1.0E+00	7.5E-01	9.3E+01
Annotation Cluster 4	Enrichment Score: 3.3200427459828528											
<b>Category</b>	<b>Term</b>	<b>Count</b>	<b>%</b>	<b>PValue</b>	<b>Genes</b>	<b>List Total</b>	<b>Pop Hits</b>	<b>Pop Total</b>	<b>Fold Enrichment</b>	<b>Bonferroni</b>	<b>Benjamini</b>	<b>FDR</b>
UP_KEYWORDS	Cleavage on pair of basic residues	11	6.0	2.53E-05	CALCA, INHBA, CHGA, NPY, CARTPT, GNAS, SCG5, PCSK1N, CHGB, LOXL1, TGFB2	177	248	22680	5.7	5.0E-03	5.1E-04	3.2E-02
GOTERM_BP_DIRECT	GO:007218~neuropeptide signaling pathway	6	3.3	5.52E-04	CALCA, ECEL1, NPY, CARTPT, SCG5, PCSK1N	160	76	18082	8.9	5.0E-01	6.6E-02	8.9E-01
UP_KEYWORDS	Neuropeptide	4	2.2	1.17E-03	NPY, CARTPT, SCG5, PCSK1N	177	27	22680	19.0	2.1E-01	1.6E-02	1.5E+00
GOTERM_CC_DIRECT	GO:0030141~secretory granule	6	3.3	3.21E-03	CHGA, CARTPT, SCG5, PCSK1N, CHGB, TGFB2	175	112	19662	6.0	4.8E-01	4.6E-02	4.0E+00
<b>Annotation Cluster 5</b>	<b>Enrichment Score: 3.16</b>											
<b>Category</b>	<b>Term</b>	<b>Count</b>	<b>%</b>	<b>PValue</b>	<b>Genes</b>	<b>List Total</b>	<b>Pop Hits</b>	<b>Pop Total</b>	<b>Fold Enrichment</b>	<b>Bonferroni</b>	<b>Benjamini</b>	<b>FDR</b>
UP_KEYWORDS	Developmental protein	22	12.0	2.38E-05	INSM1, PHOX2A, INA, PHOX2B, NNAT, CELSR3, COLEC11, INSC, GREM2, CTNNA2, ASCL1, HAND2, SMOC1, WNT11, MYOG, NGFR, TLX2, SCX, SMPD3, GAP43, PITX1, ARL13B	177	976	22680	2.9	4.8E-03	5.3E-04	3.0E-02
GOTERM_BP_DIRECT	GO:0007275~multicellular organism development	22	12.0	2.73E-04	INSM1, PHOX2A, INA, PHOX2B, NNAT, CELSR3, COLEC11, INSC, GREM2, CTNNA2, ASCL1, HAND2, SMOC1, WNT11, MYOG, NGFR, TLX2, SCX, SMPD3, GAP43, PITX1, ARL13B	160	1029	18082	2.4	2.9E-01	4.2E-02	4.4E-01
GOTERM_BP_DIRECT	GO:0007399~nervous system development	12	6.6	5.16E-04	INA, INSM1, ASCL1, RET, PLXNA4, SRRM4, CAMK2B, RGS9, NGFR, INSC, NRN1, GAP43	160	377	18082	3.6	4.7E-01	6.9E-02	8.3E-01
GOTERM_BP_DIRECT	GO:0030154~cell differentiation	17	9.3	1.44E-03	INSM1, INA, SOX10, RBM24, INSC, DLK1, CTNNA2, BATF, ASCL1, SRRM4, HAND2, SMOC1, MYOG, CAMK2B, NGFR, SCX, GAP43	160	780	18082	2.5	8.3E-01	9.0E-02	2.3E+00
UP_KEYWORDS	Differentiation	14	7.7	1.65E-03	INA, BATF, INSM1, ASCL1, RBM24, SRRM4, HAND2, SMOC1, CAMK2B, MYOG, INSC, NGFR, GAP43, CTNNA2	177	646	22680	2.8	2.8E-01	2.0E-02	2.0E+00
UP_KEYWORDS	Neurogenesis	7	3.8	1.28E-02	INA, INSM1, ASCL1, CAMK2B, NGFR, INSC, GAP43	177	247	22680	3.6	9.2E-01	1.2E-01	1.5E+01
<b>Annotation Cluster 6</b>	<b>Enrichment Score: 2.64</b>											

Part 2 – GATA2 in SMC differentiation

Category	Term	Count	%	PValue	Genes	List Total	Pop Hits	Pop Total	Fold Enrichment	Bonferroni	Benjamini	FDR
GOTERM_BP_DIRECT	GO:0003358~noradrenergic neuron development	3	1.6	2.29E-04	INSM1, PHOX2B, ASCL1	160	3	18082	113.0	2.5E-01	4.0E-02	3.7E-01
GOTERM_BP_DIRECT	GO:0061549~sympathetic ganglion development	3	1.6	2.66E-03	INSM1, PHOX2B, ASCL1	160	9	18082	37.7	9.6E-01	1.3E-01	4.2E+00
GOTERM_BP_DIRECT	GO:0010468~regulation of gene expression	8	4.4	1.93E-02	INSM1, PHOX2B, ASCL1, APOE, COL2A1, DLK1, NGFR, FAM46A	160	308	18082	2.9	1.0E+00	4.7E-01	2.7E+01
Annotation Cluster 7	Enrichment Score: 2.633839147587959											
Category	Term	Count	%	PValue	Genes	List Total	Pop Hits	Pop Total	Fold Enrichment	Bonferroni	Benjamini	FDR
GOTERM_CC_DIRECT	GO:0043195~terminal bouton	9	4.9	7.44E-06	CALCA, SNAP91, NPY, TH, SLC18A2, SLC18A3, SLC18A1, DBH, PRSS12	175	113	19662	8.9	1.5E-03	2.6E-04	9.4E-03
GOTERM_CC_DIRECT	GO:0008021~synaptic vesicle	5	2.7	2.58E-02	DDC, SNAP91, TH, SLC18A2, SLC18A3	175	126	19662	4.5	1.0E+00	2.1E-01	2.8E+01
GOTERM_BP_DIRECT	GO:0007268~chemical synaptic transmission	5	2.7	6.54E-02	SNAP91, SLC18A2, SLC18A3, CARTPT, SLC18A1	160	172	18082	3.3	1.0E+00	7.3E-01	6.7E+01
Annotation Cluster 8	Enrichment Score: 2.54											
Category	Term	Count	%	PValue	Genes	List Total	Pop Hits	Pop Total	Fold Enrichment	Bonferroni	Benjamini	FDR
UP_KEYWORDS	Oxidation	5	2.7	7.71E-06	ACTG2, CHGA, ACTA1, ACTA2, APOE	177	17	22680	37.7	1.5E-03	2.2E-04	9.7E-03
GOTERM_CC_DIRECT	GO:0030027~lamellipodium	8	4.4	6.54E-04	ABLIM1, ACTG2, ACTA1, STMN2, ACTA2, PTPRZ1, APBB1IP, CTNNA2	175	164	19662	5.5	1.3E-01	1.3E-02	8.2E-01
GOTERM_BP_DIRECT	GO:0090131~mesenchyme migration	3	1.6	7.55E-04	ACTG2, ACTA1, ACTA2	160	5	18082	67.8	6.1E-01	7.5E-02	1.2E+00
GOTERM_CC_DIRECT	GO:0030175~filopodium	5	2.7	4.85E-03	VCAM1, ACTG2, ACTA1, ACTA2, PTPRZ1	175	77	19662	7.3	6.3E-01	6.5E-02	5.9E+00
INTERPRO	IPR004001:Actin conserved site	3	1.6	4.86E-03	ACTG2, ACTA1, ACTA2	169	13	20594	28.1	8.4E-01	3.6E-01	6.5E+00
INTERPRO	IPR020902:Actin/actin-like conserved site	3	1.6	5.64E-03	ACTG2, ACTA1, ACTA2	169	14	20594	26.1	8.8E-01	3.4E-01	7.5E+00
UP_SEQ_FEATURE	propeptide:Removed in mature form	8	4.4	7.06E-03	RND2, ACTG2, ACTA1, ACTA2, LSAMP, GAS1, GNG3, NRN1	169	238	18012	3.6	9.8E-01	3.6E-01	9.9E+00
GOTERM_CC_DIRECT	GO:0044297~cell body	5	2.7	1.29E-02	ACTG2, ACTA1, ACTA2, SLC18A2, GNG3	175	102	19662	5.5	9.3E-01	1.2E-01	1.5E+01
INTERPRO	IPR004000:Actin-related protein	3	1.6	2.33E-02	ACTG2, ACTA1, ACTA2	169	29	20594	12.6	1.0E+00	7.1E-01	2.8E+01
SMART	SM00268:ACTIN	3	1.6	3.30E-02	ACTG2, ACTA1, ACTA2	104	29	10425	10.4	9.6E-01	9.6E-01	3.1E+01
Annotation Cluster 9	Enrichment Score: 2.52											
Category	Term	Count	%	PValue	Genes	List Total	Pop Hits	Pop Total	Fold Enrichment	Bonferroni	Benjamini	FDR
GOTERM_BP_DIRECT	GO:0051216~cartilage development	6	3.3	7.81E-04	COL9A1, SULF1, GNAS, COL2A1, SCX, PITX1	160	82	18082	8.3	6.2E-01	7.2E-02	1.3E+00
GOTERM_BP_DIRECT	GO:0001894~tissue homeostasis	4	2.2	1.18E-03	COL9A1, GNAS, COL2A1, SCX	160	24	18082	18.8	7.7E-01	7.8E-02	1.9E+00
GOTERM_BP_DIRECT	GO:0001958~endochondral ossification	3	1.6	2.85E-02	GNAS, COL2A1, SCX	160	30	18082	11.3	1.0E+00	5.3E-01	3.7E+01
Annotation Cluster 10	Enrichment Score: 2.51											
Category	Term	Count	%	PValue	Genes	List Total	Pop Hits	Pop Total	Fold Enrichment	Bonferroni	Benjamini	FDR
UP_KEYWORDS	Muscle protein	10	5.5	2.30E-10	TNNT2, ACTG2, MYL4, ACTA1, ACTA2, TNNC1, MYH3, MYL1, MYH11, TNNI1	177	52	22680	24.6	4.6E-08	4.6E-08	2.9E-07
UP_KEYWORDS	Myosin	5	2.7	5.22E-04	MYL4, MYH3, MYL1, MYH11, MYO1F	177	48	22680	13.3	9.9E-02	8.7E-03	6.5E-01
UP_KEYWORDS	Calmodulin-binding	7	3.8	7.68E-04	PCP4, MYH3, MYH11, MYO1F, CAMK2B, CNN1, GAP43	177	139	22680	6.5	1.4E-01	1.1E-02	9.6E-01
GOTERM_CC_DIRECT	GO:0016459~myosin complex	5	2.7	1.15E-03	MYL4, MYH3, MYL1, MYH11, MYO1F	175	52	19662	10.8	2.1E-01	2.1E-02	1.4E+00
UP_SEQ_FEATURE	domain:IQ	5	2.7	1.84E-03	PCP4, MYH3, MYH11, MYO1F, GAP43	169	56	18012	9.5	6.5E-01	1.9E-01	2.7E+00
UP_KEYWORDS	Motor protein	6	3.3	3.26E-03	MYL4, KIF5A, MYH3, MYL1, MYH11, MYO1F	177	128	22680	6.0	4.8E-01	3.4E-02	4.0E+00
GOTERM_MF_DIRECT	GO:0005516~calmodulin binding	7	3.8	5.11E-03	PCP4, MYH3, MYH11, MYO1F, CAMK2B, CNN1, GAP43	152	182	17446	4.4	8.1E-01	3.4E-01	6.7E+00
GOTERM_CC_DIRECT	GO:0030016~myofibril	4	2.2	5.29E-03	TNNT2, MYH3, MYL1, MYH11	175	40	19662	11.2	6.6E-01	6.6E-02	6.5E+00
UP_KEYWORDS	Actin-binding	7	3.8	1.41E-02	ABLIM1, MYH3, MYH11, SNTG1, MYO1F, CNN1, TNNI1	177	252	22680	3.6	9.4E-01	1.2E-01	1.6E+01
UP_SEQ_FEATURE	region of interest:Actin-binding	3	1.6	2.09E-02	MYH3, MYH11, MYO1F	169	24	18012	13.3	1.0E+00	6.0E-01	2.7E+01
GOTERM_MF_DIRECT	GO:0003779~actin binding	8	4.4	2.79E-02	TNNT2, ABLIM1, MYH3, MYH11, SNTG1, MYO1F, CNN1, TNNI1	152	338	17446	2.7	1.0E+00	6.0E-01	3.2E+01
UP_SEQ_FEATURE	domain:Myosin head-like	3	1.6	2.98E-02	MYH3, MYH11, MYO1F	169	29	18012	11.0	1.0E+00	6.1E-01	3.6E+01
INTERPRO	IPR000048:IQ motif, EF-hand binding site	4	2.2	3.53E-02	MYH3, MYH11, MYO1F, GAP43	169	88	20594	5.5	1.0E+00	7.0E-01	3.9E+01
INTERPRO	IPR001609:Myosin head, motor domain	3	1.6	4.03E-02	MYH3, MYH11, MYO1F	169	39	20594	9.4	1.0E+00	6.9E-01	4.3E+01
SMART	SM00242:MYSc	3	1.6	5.65E-02	MYH3, MYH11, MYO1F	104	39	10425	7.7	1.0E+00	8.5E-01	4.8E+01
GOTERM_MF_DIRECT	GO:0003774~motor activity	3	1.6	1.49E-01	MYH3, MYH11, MYO1F	152	79	17446	4.4	1.0E+00	9.0E-01	8.9E+01

**Table S9.** Functional annotation clustering analysis for transcripts that were upregulated in E14.5 ureters of *Gata2cKO* embryos. Functional enrichment analysis for 219 upregulated genes was performed with DAVID 6.8 websoftware (<https://david.ncifcrf.gov>) using default settings. Shown are the TOP10 Annotation clusters.

Annotation Cluster 1	Enrichment Score: 3.48												
Category	Term	Count	%	PValue	Genes	List Total	Pop Hits	Pop Total	Fold Enrichment	Bonferroni	Benjamini	FDR	
UP_KEYWORDS	Glycoprotein	55	28.5	2.13E-07	ADCY7, PLXNA2, NELL1, ENPEP, MEGF10, ASGR1, SOSTDC1, CCBE1, CFH, SLC22A3, SEMA3C, NIPAL1, ETL4, ELOVL6, ICOSL, CNTN6, CHST2, ACKR1, PIGT, NRXN1, ERGIC1, TMEM132C, CD83, SLITRK4, LAMC3, PLA2G7, CNTN1, CPD, MFAP4, NETO2, GALNT3, FUT9, TMX3, CNTFR, G6PC2, ACSL1, FAT3, MAN1A, TNFRSF19, LRFN5, FLRT2, VSTM4, GABRA1, NTF3, GABRA3, NPR3, ECM1, KCNV2, KCNK2, FZD10, EPHA8, AVPR1A, FAM155A, WIF1, HTR2B	163	3815	22680	2.0	4.0E-05	4.0E-05	2.6E-04	
UP_KEYWORDS	Disulfide bond	45	23.3	5.13E-06	NETO2, GALNT3, RBP4, PLXNA2, NELL1, NDP, TMX3, CNTFR, ENPEP, MEGF10, GM4788, ASGR1, CFHR2, FAT3, SOSTDC1, CCBE1, MAN1A, CFH, SEMA3C, TNFRSF19, LRFN5, FCHO2, GALNT12, FLRT2, VSTM4, ICOSL, GABRA1, NTF3, CNTN6, GABRA3, CHST2, ACKR1, PIGT, NRXN1, NPR3, KCNK2, SFRP5, CD83, FZD10, LAMC3, CLDN1, AVPR1A, CNTN1, WIF1, HTR2B	163	3124	22680	2.0	9.5E-04	4.8E-04	6.4E-03	
UP_SEQ_FEATURE	topological domain:Cytoplasmic	44	22.8	9.58E-06	NETO2, GALNT3, FUT9, CLDN4, ADCY7, PLXNA2, TMX3, ENPEP, MEGF10, G6PC2, ASGR1, ANK, ACSL1, FAT3, MAN1A, TNFRSF19, NIPAL1, LRFN5, ARL6IP5, GALNT12, KCNMA1, KCND3, ICOSL, GABRA1, GABRA3, CHST2, ACKR1, PIGT, MAL, NRXN1, NPR3, GPPD3, ERGIC1, KCNK2, KCNV2, TMEM132C, CD83, FZD10, SLITRK4, EPHA8, CLDN1, AVPR1A, CPD, HTR2B	141	2880	18012	2.0	5.1E-03	5.1E-03	1.4E-02	
UP_SEQ_FEATURE	glycosylation site:N-linked (GlcNAc...)	50	25.9	1.72E-05	NETO2, GALNT3, FUT9, ADCY7, PLXNA2, NELL1, TMX3, CNTFR, ENPEP, MEGF10, G6PC2, ASGR1, FAT3, SOSTDC1, CCBE1, CFH, MAN1A, TNFRSF19, SEMA3C, SLC22A3, NIPAL1, LRFN5, ICOSL, GABRA1, NTF3, CNTN6, GABRA3, ACKR1, CHST2, PIGT, NRXN1, NPR3, ERGIC1, KCNK2, KCNV2, ECM1, TMEM132C, CD83, SLITRK4, FZD10, LAMC3, EPHA8, AVPR1A, PLA2G7, FAM155A, CNTN1, WIF1, CPD, HTR2B, MFAP4	141	3563	18012	1.8	9.2E-03	4.6E-03	2.5E-02	
UP_SEQ_FEATURE	transmembrane region	54	28.0	1.58E-04	CLDN4, ADCY7, PLXNA2, ENPEP, MEGF10, RNF182, ASGR1, ANK, SLC22A3, NIPAL1, ELOVL6, DCAF17, KCNMA1, KCND3, ICOSL, CHST2, ACKR1, PIGT, NRXN1, ERGIC1, TMEM132C, CD83, SLITRK4, CLDN1, CPD, NETO2, HSD3B2, GALNT3, FUT9, TMX3, G6PC2, FAM19A5, ACSL1, FAT3, MAN1A, OTOP2, TNFRSF19, LRFN5, EMD, GALNT12, ARL6IP5, LAPTM4A, GABRA1, GABRA3, MAL, NPR3, GPPD3, KCNV2, KCNK2, FZD10, EPHA8, AVPR1A, FAM155A, HTR2B	141	4312	18012	1.6	8.1E-02	2.8E-02	2.3E-01	
UP_KEYWORDS	Membrane	86	44.6	1.63E-04	ADCY7, CLDN4, PLXNA2, CASK, ENPEP, PRKG2, ARHGAP15, RNF182, KCNIP1, MEGF10, ASGR1, ANK, FBXL12OS, CUTAL, CCBE1, RHOA, MGLL, SLC22A3, NIPAL1, ELOVL6, PLCB1, NRG1, DCAF17, KCNMA1, KCND3, ICOSL, CNTN6, CHST2, ACKR1, PIGT, D430041D05RIK, NRXN1, ERGIC1, TMEM132C, CD83, SLITRK4, COPG2, STXBP6, CLDN1, CNTN1, CPD, SH3GL2, NETO2, GALNT3, HSD3B2, NKD1, FUT9, SYNDIG1, TMX3, AKAP13, CNTFR, FAM19A5, G6PC2, ACSL1, FAT3, PALM2, OTOP2, MAN1A, TNFRSF19, IIGP1, LRFN5, ARL6IP5, GALNT12, EMD, FCHO2, TEC, FLRT2, VSTM4, GABRA1, LAPTM4A, NTF3, GABRA3, MAL, BAALC, NPR3, GPPD3, KCNV2, KCNK2, FZD10, NCKAP5, EPHA8, SLC35G2, AVPR1A, FAM155A, HTR2B, GREB1L	163	8683	22680	1.4	3.0E-02	1.0E-02	2.0E-01	

Part 2 – GATA2 in SMC differentiation

GOTERM_CC_DIRECT	GO:0016020~membrane	80	41.5	1.76E-04	ADCY7, CLDN4, PLXNA2, CASK, ENPEP, PRKG2, ARHGAP15, RNF182, KCNIP1, MEGF10, ASGR1, ANK, RHOA, MGLL, SLC22A3, NIPAL1, ELOVL6, PLCB1, DCAF17, KCNMA1, KCND3, ICOSL, CNTN6, CHST2, WNK1, ACKR1, PIGT, NRXN1, ERGIC1, TMEM132C, CD83, SLITRK4, COPG2, STXBP6, CLDN1, CNTN1, CPD, SH3GL2, NETO2, GALNT3, HSD3B2, NKD1, FUT9, SYNDIG1, TMX3, AKAP13, CNTFR, FAM19A5, G6PC2, ACSL1, FAT3, MAN1A, OTOP2, TNFRSF19, IIGP1, LRFN5, GALNT12, EMD, FCHO2, ARL6IP5, TEC, FLRT2, VSTM4, GABRA1, LAPTM4A, GABRA3, MAL, BAALC, NPR3, GDPD3, KCNV2, KCNK2, DDX6, FZD10, EPHA8, SLC35G2, AVPR1A, FAM155A, HTR2B, GREB1L	160	6998	19662	1.4	3.4E-02	3.4E-02	2.2E-01
UP_SEQ_FEATURE	disulfide bond	35	18.1	7.08E-04	NETO2, GALNT3, RBP4, NELL1, NDP, TMX3, CNTFR, MEGF10, ASGR1, FAT3, SOSTDC1, CCBE1, MAN1A, CFH, SEMA3C, TNFRSF19, GALNT12, FCHO2, ICOSL, GABRA1, NTF3, GABRA3, CNTN6, ACKR1, PIGT, NRXN1, NPR3, SFRP5, CD83, FZD10, LAMC3, AVPR1A, CNTN1, WIF1, HTR2B	141	2510	18012	1.8	3.2E-01	9.1E-02	1.0E+00
UP_KEYWORDS	Signal	50	25.9	1.26E-03	PLXNA2, NELL1, MEGF10, CFHR2, SOSTDC1, CCBE1, CFH, SEMA3C, NRG1, KCND3, ICOSL, EDDM3B, CNTN6, COL22A1, WNK1, PIGT, D430041D05RIK, NRXN1, TMEM132C, CD83, SLITRK4, LAMC3, PLA2G7, CNTN1, CPD, MFAP4, NETO2, RBP4, NDP, TMX3, AKAP13, CNTFR, GM4788, FAT3, VWC2, TNFRSF19, LRFN5, FLRT2, VSTM4, LAPTM4A, GABRA1, NTF3, GABRA3, NPR3, MID1, ECM1, SFRP5, FZD10, EPHA8, WIF1	163	4543	22680	1.5	2.1E-01	3.8E-02	1.5E+00
UP_KEYWORDS	Transmembrane helix	68	35.2	2.30E-03	ADCY7, CLDN4, PLXNA2, CASK, ENPEP, RNF182, MEGF10, ASGR1, ANK, FBXL12OS, CUTAL, CCBE1, SLC22A3, NIPAL1, ELOVL6, NRG1, DCAF17, KCNMA1, KCND3, ICOSL, CHST2, ACKR1, PIGT, D430041D05RIK, NRXN1, ERGIC1, TMEM132C, CD83, SLITRK4, CLDN1, CNTN1, CPD, NETO2, GALNT3, HSD3B2, FUT9, SYNDIG1, TMX3, FAM19A5, G6PC2, ACSL1, FAT3, MAN1A, OTOP2, TNFRSF19, LRFN5, GALNT12, EMD, ARL6IP5, FLRT2, VSTM4, LAPTM4A, GABRA1, NTF3, GABRA3, MAL, NPR3, GDPD3, KCNV2, KCNK2, FZD10, NCKAP5, EPHA8, SLC35G2, AVPR1A, FAM155A, HTR2B, GREB1L	163	6938	22680	1.4	3.5E-01	4.2E-02	2.8E+00
UP_SEQ_FEATURE	signal peptide	39	20.2	2.45E-03	NETO2, RBP4, PLXNA2, NELL1, NDP, TMX3, CNTFR, MEGF10, GM4788, CFHR2, FAT3, SOSTDC1, CCBE1, CFH, SEMA3C, TNFRSF19, VWC2, LRFN5, ICOSL, GABRA1, NTF3, GABRA3, CNTN6, PIGT, NRXN1, NPR3, ECM1, TMEM132C, SFRP5, CD83, FZD10, SLITRK4, LAMC3, EPHA8, PLA2G7, CNTN1, WIF1, CPD, MFAP4	141	3124	18012	1.6	7.3E-01	2.0E-01	3.5E+00
UP_KEYWORDS	Transmembrane	68	35.2	2.46E-03	ADCY7, CLDN4, PLXNA2, CASK, ENPEP, RNF182, MEGF10, ASGR1, ANK, FBXL12OS, CUTAL, CCBE1, SLC22A3, NIPAL1, ELOVL6, NRG1, DCAF17, KCNMA1, KCND3, ICOSL, CHST2, ACKR1, PIGT, D430041D05RIK, NRXN1, ERGIC1, TMEM132C, CD83, SLITRK4, CLDN1, CNTN1, CPD, NETO2, GALNT3, HSD3B2, FUT9, SYNDIG1, TMX3, FAM19A5, G6PC2, ACSL1, FAT3, MAN1A, OTOP2, TNFRSF19, LRFN5, GALNT12, EMD, ARL6IP5, FLRT2, VSTM4, LAPTM4A, GABRA1, NTF3, GABRA3, MAL, NPR3, GDPD3, KCNV2, KCNK2, FZD10, NCKAP5, EPHA8, SLC35G2, AVPR1A, FAM155A, HTR2B, GREB1L	163	6955	22680	1.4	3.7E-01	4.1E-02	3.0E+00
UP_SEQ_FEATURE	topological domain:Extracellular	29	15.0	7.83E-03	NETO2, CLDN4, PLXNA2, ENPEP, MEGF10, ASGR1, ANK, FAT3, TNFRSF19, NIPAL1, LRFN5, KCNMA1, ICOSL, GABRA1, GABRA3, ACKR1, MAL, NRXN1, NPR3, GDPD3, TMEM132C, CD83, FZD10, SLITRK4, EPHA8, CLDN1, AVPR1A, CPD, HTR2B	141	2256	18012	1.6	9.9E-01	4.5E-01	1.1E+01

Part 2 – GATA2 in SMC differentiation

GOTERM_CC_DIRECT	GO:0016021~integral component of membrane	71	36.8	1.11E-02	ADCY7, CLDN4, PLXNA2, CASK, ENPEP, RNF182, MEGF10, ASGR1, ANK, FBXL120S, CUTAL, CCBE1, SLC22A3, NIPAL1, ELOVL6, NRG1, DCAF17, KCNMA1, KCND3, ICOSL, CHST2, ACKR1, PIGT, D430041D05RIK, NRXN1, ERGIC1, TMEM132C, CD83, SLITRK4, STXBP6, CLDN1, CNTN1, CPD, NETO2, GALNT3, HSD3B2, FUT9, SYNDIG1, TMX3, FAM19A5, G6PC2, ACSL1, FAT3, MAN1A, OTOP2, TNFRSF19, LRFN5, GALNT12, EMD, ARL6IP5, FLRT2, VSTM4, LAPTM4A, GABRA1, NTF3, GABRA3, MAL, NPR3, GDPD3, KCNV2, KCNK2, SFRP5, FZD10, NCKAP5, EPHA8, SLC35G2, AVPR1A, FAM155A, SYT16, HTR2B, GREB1L	160	6878	19662	1.3	8.9E-01	4.2E-01	1.3E+01
GOTERM_CC_DIRECT	GO:0005886~plasma membrane	49	25.4	7.01E-02	CLDN4, ADCY7, PLXNA2, CASK, PRKG2, ENPEP, MEGF10, KCNIP1, ANK, CFH, RHOA, NRG1, PLCB1, KCNMA1, KCND3, CNTN6, ACKR1, NRXN1, STXBP6, CLDN1, CNTN1, CPD, NETO2, NKD1, SYNDIG1, CNTFR, ACSL1, FAT3, PALM2, TNFRSF19, FCHO2, ARL6IP5, TEC, FLRT2, VSTM4, LAPTM4A, GABRA1, GABRA3, MAL, NPR3, KCNV2, KCNK2, FZD10, SLC35G2, EPHA8, AVPR1A, FAM155A, SYT16, HTR2B	160	4874	19662	1.2	1.0E+00	7.0E-01	6.0E+01
<b>Annotation Cluster 2</b>	<b>Enrichment Score: 2.12</b>											
<b>Category</b>	<b>Term</b>	<b>Count</b>	<b>%</b>	<b>PValue</b>	<b>Genes</b>	<b>List Total</b>	<b>Pop Hits</b>	<b>Pop Total</b>	<b>Fold Enrichment</b>	<b>Bonferroni</b>	<b>Benjamini</b>	<b>FDR</b>
UP_KEYWORDS	Lipoprotein	15	7.8	1.46E-03	KCNMA1, NKD1, CNTN6, CNTFR, MAL, BAALC, PRKG2, ASGR1, PALM2, AVPR1A, RHOA, CNTN1, IIGP1, CPD, HTR2B	163	780	22680	2.7	2.4E-01	3.3E-02	1.8E+00
UP_SEQ_FEATURE	lipid moiety-binding region:S-palmitoyl cysteine	6	3.1	1.30E-02	ASGR1, PALM2, AVPR1A, BAALC, CPD, HTR2B	141	179	18012	4.3	1.0E+00	5.4E-01	1.7E+01
UP_KEYWORDS	Palmitate	7	3.6	2.25E-02	KCNMA1, ASGR1, PALM2, AVPR1A, BAALC, CPD, HTR2B	163	304	22680	3.2	9.9E-01	1.8E-01	2.5E+01
<b>Annotation Cluster 3</b>	<b>Enrichment Score: 2.09</b>											
<b>Category</b>	<b>Term</b>	<b>Count</b>	<b>%</b>	<b>PValue</b>	<b>Genes</b>	<b>List Total</b>	<b>Pop Hits</b>	<b>Pop Total</b>	<b>Fold Enrichment</b>	<b>Bonferroni</b>	<b>Benjamini</b>	<b>FDR</b>
UP_KEYWORDS	Wnt signaling pathway	8	4.1	2.79E-04	SFRP5, FZD10, NKD1, NDP, SOSTDC1, RTF1, LEO1, WIF1	163	176	22680	6.3	5.1E-02	1.0E-02	3.5E-01
KEGG_PATHWAY	mmu04310:Wnt signaling pathway	7	3.6	1.33E-03	SFRP5, FZD10, NKD1, RHOA, WIF1, MAPK8, PLCB1	68	141	7720	5.6	1.9E-01	1.9E-01	1.6E+00
GOTERM_BP_DIRECT	GO:0016055~Wnt signaling pathway	8	4.1	1.95E-03	SFRP5, FZD10, NKD1, NDP, SOSTDC1, RTF1, LEO1, WIF1	150	213	18082	4.5	8.8E-01	8.8E-01	3.1E+00
GOTERM_BP_DIRECT	GO:0090090~negative regulation of canonical Wnt signaling pathway	5	2.6	1.01E-02	EGR1, SFRP5, NKD1, SOSTDC1, WIF1	150	102	18082	5.9	1.0E+00	7.9E-01	1.5E+01
GOTERM_MF_DIRECT	GO:0017147~Wnt-protein binding	3	1.6	2.31E-02	SFRP5, FZD10, WIF1	138	30	17446	12.6	1.0E+00	6.4E-01	2.7E+01
GOTERM_BP_DIRECT	GO:0030178~negative regulation of Wnt signaling pathway	3	1.6	7.78E-02	SFRP5, NKD1, WIF1	150	56	18082	6.5	1.0E+00	9.5E-01	7.3E+01
GOTERM_BP_DIRECT	GO:0060070~canonical Wnt signaling pathway	3	1.6	1.67E-01	SFRP5, FZD10, NDP	150	89	18082	4.1	1.0E+00	9.9E-01	9.5E+01
<b>Annotation Cluster 4</b>	<b>Enrichment Score: 1.77</b>											
<b>Category</b>	<b>Term</b>	<b>Count</b>	<b>%</b>	<b>PValue</b>	<b>Genes</b>	<b>List Total</b>	<b>Pop Hits</b>	<b>Pop Total</b>	<b>Fold Enrichment</b>	<b>Bonferroni</b>	<b>Benjamini</b>	<b>FDR</b>
GOTERM_CC_DIRECT	GO:0045202~synapse	13	6.7	8.49E-04	NETO2, FLRT2, GABRA1, SYNDIG1, GABRA3, CASK, NRXN1, TRIM9, MGLL, VWC2, HTR2B, NRG1, SH3GL2	160	505	19662	3.2	1.5E-01	8.1E-02	1.1E+00
UP_KEYWORDS	Synapse	8	4.1	1.45E-02	FLRT2, GABRA1, SYNDIG1, GABRA3, TRIM9, VWC2, NRXN1, HTR2B	163	357	22680	3.1	9.3E-01	1.3E-01	1.7E+01
UP_KEYWORDS	Cell junction	10	5.2	4.82E-02	FLRT2, GABRA1, SYNDIG1, CLDN4, GABRA3, TRIM9, CLDN1, VWC2, NRXN1, HTR2B	163	661	22680	2.1	1.0E+00	2.6E-01	4.6E+01
GOTERM_CC_DIRECT	GO:0030054~cell junction	10	5.2	1.29E-01	FLRT2, GABRA1, SYNDIG1, CLDN4, GABRA3, TRIM9, CLDN1, VWC2, NRXN1, HTR2B	160	718	19662	1.7	1.0E+00	7.4E-01	8.2E+01
<b>Annotation Cluster 5</b>	<b>Enrichment Score: 1.63</b>											
<b>Category</b>	<b>Term</b>	<b>Count</b>	<b>%</b>	<b>PValue</b>	<b>Genes</b>	<b>List Total</b>	<b>Pop Hits</b>	<b>Pop Total</b>	<b>Fold Enrichment</b>	<b>Bonferroni</b>	<b>Benjamini</b>	<b>FDR</b>
SMART	SM00181:EGF	8	4.1	1.07E-03	FAT3, LAMC3, NELL1, CCBE1, WIF1, NRXN1, NRG1, MEGF10	93	181	10425	5.0	1.0E-01	1.0E-01	1.2E+00
UP_SEQ_FEATURE	domain:EGF-like 3	5	2.6	1.74E-03	FAT3, NELL1, WIF1, NRXN1, MEGF10	141	66	18012	9.7	6.1E-01	1.7E-01	2.5E+00
INTERPRO	IPR000742:Epidermal growth factor-like domain	8	4.1	2.58E-03	FAT3, LAMC3, NELL1, CCBE1, WIF1, NRXN1, NRG1, MEGF10	161	237	20594	4.3	6.3E-01	3.9E-01	3.5E+00



Part 2 – GATA2 in SMC differentiation

INTERPRO	IPR001791:Laminin G domain	4	2.1	1.04E-02	FAT3, NELL1, COL22A1, NRXN1	161	58	20594	8.8	9.8E-01	7.4E-01	1.3E+01
UP_SEQ_FEATURE	domain:EGF-like 1	5	2.6	1.10E-02	FAT3, NELL1, WIF1, NRXN1, MEGF10	141	111	18012	5.8	1.0E+00	5.3E-01	1.5E+01
INTERPRO	IPR013032:EGF-like, conserved site	6	3.1	1.90E-02	FAT3, NELL1, CCBE1, WIF1, NRG1, MEGF10	161	197	20594	3.9	1.0E+00	8.4E-01	2.3E+01
UP_KEYWORDS	EGF-like domain	6	3.1	2.26E-02	FAT3, NELL1, CCBE1, WIF1, NRXN1, MEGF10	163	224	22680	3.7	9.9E-01	1.8E-01	2.5E+01
INTERPRO	IPR013320:Concavalin A-like lectin/glucanase subgroup	6	3.1	2.46E-02	FAT3, TRIM9, NELL1, COL22A1, NRXN1, MID1	161	211	20594	3.6	1.0E+00	8.5E-01	2.9E+01
UP_SEQ_FEATURE	domain:EGF-like 2	4	2.1	2.77E-02	FAT3, WIF1, NRXN1, MEGF10	141	84	18012	6.1	1.0E+00	7.5E-01	3.4E+01
INTERPRO	IPR000152:EGF-type aspartate/asparagine hydroxylation site	4	2.1	4.10E-02	FAT3, NELL1, CCBE1, NRXN1	161	98	20594	5.2	1.0E+00	9.0E-01	4.4E+01
SMART	SM00282:LamG	3	1.6	5.06E-02	FAT3, NELL1, NRXN1	93	41	10425	8.2	9.9E-01	8.3E-01	4.4E+01
UP_SEQ_FEATURE	domain:EGF-like 4	3	1.6	6.82E-02	NELL1, WIF1, MEGF10	141	55	18012	7.0	1.0E+00	9.3E-01	6.4E+01
INTERPRO	IPR018097:EGF-like calcium-binding, conserved site	3	1.6	1.74E-01	FAT3, NELL1, CCBE1	161	97	20594	4.0	1.0E+00	9.9E-01	9.3E+01
INTERPRO	IPR001881:EGF-like calcium-binding	3	1.6	2.56E-01	FAT3, NELL1, CCBE1	161	126	20594	3.0	1.0E+00	1.0E+00	9.8E+01
SMART	SM00179:EGF_CA	3	1.6	3.06E-01	FAT3, NELL1, CCBE1	93	126	10425	2.7	1.0E+00	9.8E-01	9.8E+01
<b>Annotation Cluster 6</b>												
<b>Enrichment Score:</b>	<b>1.59</b>											
<b>Category</b>	<b>Term</b>	<b>Count</b>	<b>%</b>	<b>PValue</b>	<b>Genes</b>	<b>List Total</b>	<b>Pop Hits</b>	<b>Pop Total</b>	<b>Fold Enrichment</b>	<b>Bonferroni</b>	<b>Benjamini</b>	<b>FDR</b>
KEGG_PATHWAY	mmu04310:Wnt signaling pathway	7	3.6	1.33E-03	SFRP5, FZD10, NKD1, RHOA, WIF1, MAPK8, PLCB1	68	141	7720	5.6	1.9E-01	1.9E-01	1.6E+00
KEGG_PATHWAY	mmu04071:Sphingolipid signaling pathway	4	2.1	9.25E-02	MAP3K5, RHOA, MAPK8, PLCB1	68	124	7720	3.7	1.0E+00	7.3E-01	6.9E+01
KEGG_PATHWAY	mmu05200:Pathways in cancer	7	3.6	1.29E-01	FZD10, ADCY7, FGF14, LAMC3, RHOA, MAPK8, PLCB1	68	397	7720	2.0	1.0E+00	6.9E-01	8.1E+01
<b>Annotation Cluster 7</b>												
<b>Enrichment Score:</b>	<b>1.536630639086191</b>											
<b>Category</b>	<b>Term</b>	<b>Count</b>	<b>%</b>	<b>PValue</b>	<b>Genes</b>	<b>List Total</b>	<b>Pop Hits</b>	<b>Pop Total</b>	<b>Fold Enrichment</b>	<b>Bonferroni</b>	<b>Benjamini</b>	<b>FDR</b>
UP_KEYWORDS	Transcription regulation	25	13.0	2.19E-03	RALY, EGR1, TSHZ3, FOXL1, ELF5, DACH1, NR2C2, AHR, PURA, HOXD11, FAM208A, ELL2, GCM1, DACH2, SALL1, RTF1, HEY2, ZBTB4, PSPC1, LEO1, POU3F1, ZFP536, FOXI1, TBPL1, ALX1	163	1799	22680	1.9	3.3E-01	4.4E-02	2.7E+00
UP_KEYWORDS	Transcription	25	13.0	3.34E-03	RALY, EGR1, TSHZ3, FOXL1, ELF5, DACH1, NR2C2, AHR, PURA, HOXD11, FAM208A, ELL2, GCM1, DACH2, SALL1, RTF1, HEY2, ZBTB4, PSPC1, LEO1, POU3F1, ZFP536, FOXI1, TBPL1, ALX1	163	1859	22680	1.9	4.6E-01	5.1E-02	4.1E+00
UP_KEYWORDS	Repressor	11	5.7	5.15E-03	TSHZ3, DACH2, SALL1, HEY2, PSPC1, ZBTB4, DACH1, AHR, NR2C2, ALX1, FAM208A	163	534	22680	2.9	6.2E-01	7.1E-02	6.2E+00
UP_KEYWORDS	DNA-binding	21	10.9	1.06E-02	EGR1, TSHZ3, FOXL1, ELF5, MBD4, DACH1, NR2C2, AHR, PURA, HOXD11, GCM1, DACH2, SALL1, RTF1, HEY2, ZBTB4, POU3F1, ZFP536, FOXI1, TBPL1, ALX1	163	1604	22680	1.8	8.6E-01	1.2E-01	1.2E+01
GOTERM_MF_DIRECT	GO:0043565~sequence-specific DNA binding	12	6.2	1.13E-02	EGR1, FOXL1, ELF5, HEY2, ZBTB4, POU3F1, FOXI1, ZFP536, AHR, NR2C2, ALX1, HOXD11	138	633	17446	2.4	9.7E-01	5.8E-01	1.4E+01
UP_KEYWORDS	Activator	11	5.7	1.44E-02	EGR1, ELF5, RTF1, PSPC1, LEO1, DACH1, FOXI1, AHR, NR2C2, ALX1, PURA	163	624	22680	2.5	9.3E-01	1.4E-01	1.6E+01
GOTERM_BP_DIRECT	GO:0006351~transcription. DNA-templated	25	13.0	2.05E-02	RALY, EGR1, TSHZ3, FOXL1, ELF5, DACH1, NR2C2, AHR, PURA, HOXD11, FAM208A, ELL2, GCM1, DACH2, SALL1, RTF1, HEY2, ZBTB4, PSPC1, LEO1, POU3F1, ZFP536, FOXI1, TBPL1, ALX1	150	1885	18082	1.6	1.0E+00	8.0E-01	2.8E+01
GOTERM_BP_DIRECT	GO:0006355~regulation of transcription. DNA-templated	28	14.5	3.24E-02	RALY, TSHZ3, ELF5, A630089N07RIK, NR2C2, HOXD11, ZFP951, RTF1, HEY2, LEO1, POU3F1, TBPL1, ALX1, EGR1, FOXL1, DACH1, AHR, PURA, FAM208A, ELL2, GCM1, DACH2, SALL1, ZBTB4, PSPC1, MAPK8, FOXI1, ZFP536	150	2279	18082	1.5	1.0E+00	8.6E-01	4.1E+01
GOTERM_BP_DIRECT	GO:0045892~negative regulation of transcription. DNA-templated	10	5.2	5.05E-02	TSHZ3, SALL1, HEY2, PSPC1, ZBTB4, DACH1, NRG1, PLCB1, AHR, PURA	150	579	18082	2.1	1.0E+00	9.3E-01	5.6E+01
GOTERM_MF_DIRECT	GO:0003677~DNA binding	21	10.9	8.60E-02	EGR1, TSHZ3, FOXL1, ELF5, MBD4, DACH1, NR2C2, AHR, PURA, HOXD11, GCM1, DACH2, SALL1, RTF1, HEY2, ZBTB4, POU3F1, ZFP536, FOXI1, TBPL1, ALX1	138	1847	17446	1.4	1.0E+00	9.2E-01	7.0E+01
GOTERM_MF_DIRECT	GO:0003700~transcription factor activity. sequence-specific DNA binding	12	6.2	8.76E-02	EGR1, GCM1, FOXL1, ELF5, HEY2, DACH1, POU3F1, FOXI1, AHR, NR2C2, ALX1, PURA	138	883	17446	1.7	1.0E+00	9.0E-01	7.1E+01

Part 2 – GATA2 in SMC differentiation

UP_KEYWORDS	Nucleus	40	20.7	1.15E-01	RALY, TSHZ3, FGF14, ELF5, NELL1, AKAP13, CASK, NR2C2, HOXD11, HEY2, RTF1, IIGP1, LEO1, LUC7L2, POU3F1, PLCB1, EMD, DCAF17, TBPL1, ALX1, EGR1, FOXL1, MBD4, DACH1, AHR, PURA, DDX6, ELL2, FAM208A, RPS6KA3, GCM1, DACH2, SALL1, PSPC1, BRE, ZBTB4, MAPK8, THOC2, FOXI1, ZFP536	163	4534	22680	1.2	1.0E+00	4.7E-01	7.8E+01
GOTERM_BP_DIRECT	GO:000122~negative regulation of transcription from RNA polymerase II promoter	9	4.7	2.54E-01	EGR1, SALL1, HEY2, RTF1, ZBTB4, DACH1, ZFP536, AHR, ALX1	150	729	18082	1.5	1.0E+00	1.0E+00	9.9E+01
GOTERM_CC_DIRECT	GO:0005634~nucleus	48	24.9	6.43E-01	RALY, TSHZ3, FGF14, ELF5, NELL1, AKAP13, CASK, NR2C2, HOXD11, HEY2, RTF1, RHOA, CFH, LEO1, IIGP1, LUC7L2, POU3F1, NRG1, PLCB1, EMD, DCAF17, TBPL1, ALX1, EGR1, FOXL1, UBE4A, MBD4, DACH1, KCNK2, AHR, PURA, DDX6, ELL2, FAM208A, RPS6KA3, GCM1, TAF15, DACH2, SALL1, SPRR2A2, PSPC1, BRE, ZBTB4, MAPK8, CPD, THOC2, ZFP536, FOXI1	160	6019	19662	1.0	1.0E+00	1.0E+00	1.0E+02
<b>Annotation Cluster 8</b>												
<b>Enrichment Score:</b>	<b>1.39</b>											
<b>Category</b>	<b>Term</b>	<b>Count</b>	<b>%</b>	<b>PValue</b>	<b>Genes</b>	<b>List Total</b>	<b>Pop Hits</b>	<b>Pop Total</b>	<b>Fold Enrichment</b>	<b>Bonferroni</b>	<b>Benjamini</b>	<b>FDR</b>
KEGG_PATHWAY	mmu04723:Retrograde endocannabinoid signaling	6	3.1	1.92E-03	GABRA1, ADCY7, GABRA3, MGLL, MAPK8, PLCB1	68	103	7720	6.6	2.7E-01	1.4E-01	2.3E+00
KEGG_PATHWAY	mmu04727:GABAergic synapse	3	1.6	1.74E-01	GABRA1, ADCY7, GABRA3	68	87	7720	3.9	1.0E+00	7.6E-01	9.0E+01
KEGG_PATHWAY	mmu05032:Morphine addiction	3	1.6	1.93E-01	GABRA1, ADCY7, GABRA3	68	93	7720	3.7	1.0E+00	7.5E-01	9.3E+01
<b>Annotation Cluster 9</b>												
<b>Enrichment Score:</b>	<b>1.34</b>											
<b>Category</b>	<b>Term</b>	<b>Count</b>	<b>%</b>	<b>PValue</b>	<b>Genes</b>	<b>List Total</b>	<b>Pop Hits</b>	<b>Pop Total</b>	<b>Fold Enrichment</b>	<b>Bonferroni</b>	<b>Benjamini</b>	<b>FDR</b>
KEGG_PATHWAY	mmu04723:Retrograde endocannabinoid signaling	6	3.1	1.92E-03	GABRA1, ADCY7, GABRA3, MGLL, MAPK8, PLCB1	68	103	7720	6.6	2.7E-01	1.4E-01	2.3E+00
KEGG_PATHWAY	mmu04750:Inflammatory mediator regulation of TRP channels	4	2.1	9.60E-02	ADCY7, MAPK8, PLCB1, HTR2B	68	126	7720	3.6	1.0E+00	7.2E-01	7.1E+01
KEGG_PATHWAY	mmu05200:Pathways in cancer	7	3.6	1.29E-01	FZD10, ADCY7, FGF14, LAMC3, RHOA, MAPK8, PLCB1	68	397	7720	2.0	1.0E+00	6.9E-01	8.1E+01
KEGG_PATHWAY	mmu04912:GnRH signaling pathway	3	1.6	1.77E-01	ADCY7, MAPK8, PLCB1	68	88	7720	3.9	1.0E+00	7.3E-01	9.1E+01
<b>Annotation Cluster 10</b>												
<b>Enrichment Score:</b>	<b>1.32</b>											
<b>Category</b>	<b>Term</b>	<b>Count</b>	<b>%</b>	<b>PValue</b>	<b>Genes</b>	<b>List Total</b>	<b>Pop Hits</b>	<b>Pop Total</b>	<b>Fold Enrichment</b>	<b>Bonferroni</b>	<b>Benjamini</b>	<b>FDR</b>
UP_KEYWORDS	Potassium channel	5	2.6	1.35E-03	KCNMA1, KCND3, KCNIP1, KCNK2, KCNV2	163	67	22680	10.4	2.2E-01	3.5E-02	1.7E+00
GOTERM_MF_DIRECT	GO:0005267~potassium channel activity	5	2.6	3.63E-03	KCNMA1, KCND3, KCNIP1, KCNK2, KCNV2	138	80	17446	7.9	6.7E-01	3.1E-01	4.8E+00
GOTERM_CC_DIRECT	GO:0008076~voltage-gated potassium channel complex	5	2.6	3.87E-03	KCNMA1, KCND3, KCNIP1, KCNK2, KCNV2	160	79	19662	7.8	5.4E-01	2.3E-01	4.7E+00
GOTERM_BP_DIRECT	GO:0071805~potassium ion transmembrane transport	5	2.6	6.54E-03	KCNMA1, KCND3, KCNIP1, KCNK2, KCNV2	150	90	18082	6.7	1.0E+00	7.0E-01	1.0E+01
UP_KEYWORDS	Potassium transport	5	2.6	7.32E-03	KCNMA1, KCND3, KCNIP1, KCNK2, KCNV2	163	107	22680	6.5	7.5E-01	9.3E-02	8.7E+00
UP_KEYWORDS	Potassium	5	2.6	1.09E-02	KCNMA1, KCND3, KCNIP1, KCNK2, KCNV2	163	120	22680	5.8	8.7E-01	1.2E-01	1.3E+01
GOTERM_MF_DIRECT	GO:0005249~voltage-gated potassium channel activity	4	2.1	1.77E-02	KCNMA1, KCND3, KCNK2, KCNV2	138	70	17446	7.2	1.0E+00	6.6E-01	2.1E+01
GOTERM_BP_DIRECT	GO:0006813~potassium ion transport	5	2.6	2.10E-02	KCNMA1, KCND3, KCNIP1, KCNK2, KCNV2	150	127	18082	4.7	1.0E+00	7.9E-01	2.9E+01
UP_KEYWORDS	Ion channel	7	3.6	3.40E-02	KCNMA1, KCND3, GABRA1, GABRA3, KCNIP1, KCNK2, KCNV2	163	336	22680	2.9	1.0E+00	2.1E-01	3.5E+01
GOTERM_MF_DIRECT	GO:0005216~ion channel activity	5	2.6	4.51E-02	KCNMA1, KCND3, GABRA1, GABRA3, KCNV2	138	170	17446	3.7	1.0E+00	8.3E-01	4.6E+01
GOTERM_BP_DIRECT	GO:0006811~ion transport	10	5.2	5.28E-02	KCNMA1, KCND3, GABRA1, GABRA3, WNK1, SLC22A3, NIPAL1, KCNIP1, KCNK2, KCNV2	150	584	18082	2.1	1.0E+00	9.2E-01	5.8E+01
UP_KEYWORDS	Voltage-gated channel	4	2.1	7.39E-02	KCNMA1, KCND3, KCNIP1, KCNV2	163	136	22680	4.1	1.0E+00	3.6E-01	6.1E+01
UP_KEYWORDS	Ion transport	9	4.7	7.67E-02	KCNMA1, KCND3, GABRA1, GABRA3, SLC22A3, NIPAL1, KCNIP1, KCNK2, KCNV2	163	619	22680	2.0	1.0E+00	3.6E-01	6.3E+01
GOTERM_MF_DIRECT	GO:0005244~voltage-gated ion channel activity	4	2.1	8.87E-02	KCNMA1, KCND3, KCNIP1, KCNV2	138	134	17446	3.8	1.0E+00	8.9E-01	7.1E+01
GOTERM_BP_DIRECT	GO:0034765~regulation of ion transmembrane transport	4	2.1	1.01E-01	KCNMA1, KCND3, KCNIP1, KCNV2	150	135	18082	3.6	1.0E+00	9.7E-01	8.2E+01

## Part 2 – GATA2 in SMC differentiation

INTERPRO	IPR005821:Ion transport domain	3	1.6	2.02E-01	KCNMA1, KCND3, KCNV2	161	107	20594	3.6	1.0E+00	9.9E-01	9.6E+01
GOTERM_BP_DIRECT	GO:0051260~protein homooligomerization	4	2.1	2.20E-01	KCNMA1, KCND3, CLDN1, KCNV2	150	197	18082	2.4	1.0E+00	1.0E+00	9.8E+01
GOTERM_CC_DIRECT	GO:0043025~neuronal cell body	7	3.6	2.64E-01	KCNMA1, KCND3, NRXN1, HTR2B, KCNIP1, KCNK2, PURA	160	534	19662	1.6	1.0E+00	9.0E-01	9.8E+01
GOTERM_CC_DIRECT	GO:0045211~postsynaptic membrane	4	2.1	2.67E-01	KCNMA1, GABRA1, SYNDIG1, GABRA3	160	222	19662	2.2	1.0E+00	9.0E-01	9.8E+01
UP_KEYWORDS	Transport	15	7.8	4.93E-01	KCNMA1, RBP4, KCND3, LAPTM4A, GABRA1, GABRA3, KCNIP1, KCNV2, KCNK2, ERGIC1, ANK, COG2, SLC22A3, NIPAL1, THOC2	163	1901	22680	1.1	1.0E+00	8.4E-01	1.0E+02
GOTERM_BP_DIRECT	GO:0055085~transmembrane transport	4	2.1	5.80E-01	KCNMA1, KCND3, SLC22A3, KCNV2	150	364	18082	1.3	1.0E+00	1.0E+00	1.0E+02
GOTERM_BP_DIRECT	GO:0006810~transport	15	7.8	6.49E-01	KCNMA1, RBP4, KCND3, LAPTM4A, GABRA1, GABRA3, KCNIP1, KCNV2, KCNK2, ERGIC1, ANK, COG2, SLC22A3, NIPAL1, THOC2	150	1822	18082	1.0	1.0E+00	1.0E+00	1.0E+02

**Table S10.** RT-PCR calculations and statistics (relates to Figure 5, B and C). Gel band quantification with image J (now Fiji). RT-PCR reactions were done in technical triplicates. Ratios were calculated by division of the mutant values to the control values after normalization to the housekeeping gene *Gapdh*. Fold-deregulation was determined by setting the wildtype values to 1.

E12.5	Normalized to <i>Gapdh</i>	<i>Rarb</i> wt	<i>Rarb</i> mut	<i>Cyp26a1</i> wt	<i>Cyp26a1</i> mut	mut/wt			
		0.13	0.32	0.52	0.11	4.89			
		0.60	0.64	1.32	0.42	3.15			
		0.77	1.03	1.92	0.68	2.82			
	Average	0.51	0.66	1.25	0.40				
	STDV	0.27	0.29	0.57	0.23				
E14.5	Normalized to <i>Gapdh</i>	<i>Rarb</i> wt	<i>Rarb</i> mut	<i>Cyp26a1</i> wt	<i>Cyp26a1</i> mut	<i>Rarb</i> wt/wt	<i>Rarb</i> mut/wt	<i>Cyp26a1</i> wt/wt	<i>Cyp26a1</i> mut/wt
		0.28	0.39	1.46	0.3	1	1.39	1	0.2
		0.56	0.64	0.58	0.48	1	1.14	1	0.84
		1.35	1.56	0.93	0.23	1	1.16	1	0.24
		0.94	1.25	0.49	0.2	1	1.33	1	0.41
		1.39	1.67	1.02	0.3	1	1.2	1	0.29
		0.98	1.35	0.56	0.27	1	1.38	1	0.47
	Average	0.84	0.3	0.92	1.14	1	1.27	1	0.41
	STDV	0.37	0.1	0.44	0.52	N.A	0.23	N.A	0.11

**Table S11.** Statistical analysis of ureter contraction frequency in explants of E12.5 wildtype upper urogenital systems treated with either DMSO or 1  $\mu$ M RA over 10 days of culture (relates to Figure 5D). Average frequency and corresponding standard deviations of peristaltic contractions per minute after 6 days until 10 days after upper urinary system explantation at E12.5. Monitored was a duration of one minute. The statistical significance was calculated by a two-tailed Student's t-test. \*:  $p \leq 0.05$ ; \*\*:  $p \leq 0.01$ ; \*\*\*  $p: \leq 0.001$ .

		6 days	7 days	8 days	9 days	10 days
<b>DMSO control (n=14)</b>	<b>Average</b>	2.17 $\pm$ 0.72	2.82 $\pm$ 0.67	2.85 $\pm$ 0.74	3.82 $\pm$ 0.63	3.92 $\pm$ 0.58
	<b>t-Test</b>	0.00044294	0.005246874	0.025557023	0.00013667	0.000131816

**Table S12.** Intensity of one ureter contraction in explants of E12.5 upper urinary systems at day 10 of culture in presence of DMSO or 1  $\mu$ M RA (relates to Figure 5E). Video-monitored was a duration of one minute. Contraction intensity equals to the ratio of the diameter of the contracted proximal ureter divided by the diameter of the relaxed proximal ureter. The statistical significance was calculated by a two-tailed Student's t-test. \*:  $p \leq 0.05$ ; \*\*:  $p \leq 0.01$ ; \*\*\*  $p: \leq 0.001$

	1s	2s	3s	4s	5s	6s	7s	8s	9s	10s
<b>DMSO control</b>	17.43	36.90	38.09	25.29	12.17	3.39	0	0	0	0
<b>1 <math>\mu</math>MRA</b>	19.51	32.57	33.88	25.48	18.38	9.58	5.79	1.22	0.51	0
<b>t-Test</b>	0.6343	0.2739	0.2872	0.9663	0.1554	0.0532	0.0035	0.1104	0.3086	0
						*	**			

**Table S13.** Statistical analysis of ureter contraction frequency in explants of E12.5 control and *Gata2cKO* ureters treated with either DMSO or 1  $\mu$ M BMS over 10 days of culture (relates to Figure 5F). Average frequency and corresponding standard deviations of peristaltic contractions per minute after 6 days until 10 days after upper urinary system explantation. Monitored was a duration of one minute. The statistical significance was calculated by a two-tailed Student's t-test. \*  $p \leq 0.05$ ; \*\*  $p \leq 0.01$ ; \*\*\*  $p \leq 0.001$ .

		6 days	7 days	8 days	9 days	10 days
control + DMSO (n=3)	average	4.33 $\pm$ 0.57	5 $\pm$ 1.73	5.33 $\pm$ 0.58	4.66 $\pm$ 0.58	6 $\pm$ 2
control + 1 $\mu$ M BMS493 (n=3)	average	3 $\pm$ 1.0	3 $\pm$ 0	4 $\pm$ 1.73	3.33 $\pm$ 0.58	4 $\pm$ 0
<i>Gata2cKO</i> + DMSO (n=3)	average	0	0.33 $\pm$ 0.58	1 $\pm$ 0.58	2.33 $\pm$ 0.58	1.66 $\pm$ 1.53
<i>Gata2cKO</i> + 1 $\mu$ M BMS493 (n=3)	average	0	1.66 $\pm$ 0.58	3 $\pm$ 1	2.66 $\pm$ 0.58	2.66 $\pm$ 0.58
	t-Test ( <i>Gata2cKO</i> + DMSO versus <i>Gata2cKO</i> + 1 $\mu$ M BMS493)	/	0.047421 (*)	0.0704839	0.51851851	0.3785307
	t-Test (control + DMSO versus control + 1 $\mu$ M BMS493)	0.13358	0.1835	0.3132725	0.0474207 (*)	0.2254033
	t-Test (control + DMSO versus <i>Gata2cKO</i> + DMSO)	0.00587 (**)	0.0326 (*)	0.0060506 (**)	0.0077626 (**)	0.0442361 (*)
	t-Test (control + BMS493 versus <i>Gata2cKO</i> + 1 $\mu$ M BMS493)	0.0351 (*)	0.0572	0.446539	0.2301996	0.057191



## Part – 3 Notch signaling in SMC differentiation

### Notch signaling is a novel regulator of visceral smooth muscle cell differentiation in the murine ureter

Anna-Carina Weiss<sup>1,\*</sup>, Jennifer Kurz<sup>1,\*</sup>, Hauke Thiesler<sup>2</sup>, Jaskiran Kaur<sup>1</sup>, Lena Deuper<sup>1</sup>, Irina Wojahn<sup>1</sup>, Fairouz Qasrawi<sup>1</sup>, Herbert Hildebrandt<sup>2</sup>, Mark-Oliver Trowe<sup>1</sup> and Andreas Kispert<sup>1,3</sup>

<sup>1</sup> Institut für Molekularbiologie, Medizinische Hochschule Hannover, 30625 Hannover, Germany

<sup>2</sup> Institut für Klinische Biochemie, Medizinische Hochschule Hannover, 30625 Hannover, Germany

\* These authors contributed equally to this work

<sup>3</sup> Address correspondence to: Andreas Kispert, Institut für Molekularbiologie, OE5250, Medizinische Hochschule Hannover, Carl-Neuberg-Str. 1, D-30625 Hannover, Germany. Phone: +49 511 5324017, Fax: +49 511 5324283, E-Mail: kispert.andreas@mh-hannover.de

Short title: Notch regulates visceral SMC differentiation

KEY WORDS: ureter, smooth muscle, visceral, Notch, Myocd, Tnnt2,

**Type of authorship:** Co-First author

**Type of article:** Research article

**Share of the work:** 40%

**Contribution to the publication:** performed experiments, analyzed data, prepared figures, assisted in writing the paper

**Journal:** Development

**Impact factor:** 6.192

**Number of citations:** 0

**Date of publication:** submitted

**DOI:** -

## Abstract

The contractile phenotype of smooth muscle cells (SMCs) is transcriptionally controlled by a complex of the DNA-binding protein SRF and the transcriptional co-activator MYOCD. The pathways that activate expression of *Myocd* and of SMC structural genes in mesenchymal progenitors are diverse reflecting different signaling inputs from adjacent epithelial or endothelial primordia. Taking the ureter as a model, we analyzed whether Notch signaling, a pathway previously implicated in vascular SMC development, also affects visceral SMC differentiation. We show that mice with a conditional deletion of the unique Notch mediator RBPJ in the undifferentiated ureteric mesenchyme exhibit altered ureter peristalsis with a delayed onset and decreased contraction frequency and intensity at fetal stages, culminating in hydroureter formation after birth. Notch signaling is required for precise temporal activation of *Myocd* expression, and independently, for expression of a group of late SMC structural genes. Hence, Notch signaling regulates visceral SMC differentiation but its molecular function differs from that in the vascular system.

## Introduction

Smooth muscle cells (SMCs) are found in the mesenchymal wall of many visceral tubular organs but also as an ensheathment of endothelial cells in the vascular system. Due to their contractile activity, they play a decisive role in maintaining the flexibility and rigidity of these tubes and in mediating the unidirectional transport of their luminal content. SMCs arise from a diverse range of progenitors and show a high phenotypic plasticity, yet their specialized contractile phenotype seems universally transcriptionally controlled by a complex of the DNA-binding protein serum response factor (SRF) and the coactivator Myocardin (MYOCD) (Norman et al., 1988; Yoshida et al., 2003; Wang and Olson, 2004). Expression of *Myocd* and of SMC structural genes occurs in SMC progenitors as a response to a multitude of extrinsic and intrinsic signals. The nature of these signals seems fundamentally different in vascular and visceral SMC progenitors, probably due to their specific association with endothelial and epithelial primordia, respectively (Creemers et al., 2006; Mack, 2011; Shi and Chen, 2016; Donadon and Santoro, 2021).

Due to its simple design, its pharmacological and genetic accessibility and its relevance for congenital anomalies in humans, the murine ureter is an attractive model to unravel the regulatory network that drives visceral SMC differentiation during organogenesis (Woolf and Davies, 2013; Bohnenpoll and Kispert, 2014; Woolf et al., 2019). Previous work has shown that visceral SMCs of the mouse ureter arise from a *Tbx18*<sup>+</sup> mesenchymal progenitor pool that surrounds the distal aspect of the ureteric bud, an epithelial diverticulum of the nephric duct, at embryonic day (E)11.0 (Bohnenpoll et al., 2013). Until E14.5, two signals from the ureteric epithelium (UE), SHH and WNTs, act on the undifferentiated ureteric mesenchyme (UM) to maintain its proliferative expansion and trigger SMC differentiation. SHH activates the expression of the transcription factor gene *Foxf1* in the UM which, in turn, induces and synergizes with the signaling molecule BMP4 in activation of *Myocd* and SMC structural genes (Yu et al., 2002; Bohnenpoll et al., 2017c; Mamo et al., 2017). WNTs, at least partly, act through the transcription factors TBX2 and TBX3 to maintain BMP4 signaling and suppress an outer adventitial fate (Trowe et al., 2012; Aydogdu et al., 2018). Retinoic acid (RA) synthesized in both the UM and UE inhibits SMC differentiation possibly by counteracting WNT signaling (Bohnenpoll et al., 2017b). As a consequence of a poorly understood interplay of these and most likely additional signals *Myocd* is precisely activated

in the inner layer of the proximal UM at E14.5, expression of SMC structural genes starts at E15.5, and a peristaltically active SMC layer is established concomitantly with onset of urine production in the kidney around E16.5 (Bohnenpoll et al., 2017a).

Notch is an evolutionary conserved signaling pathway that mediates contact-dependent cell-to-cell communication in a variety of developmental contexts. In mammals, four Notch receptors (NOTCH1-4) and five ligands (Jagged1 and 2 (JAG1,2), Delta-like 1, 3, and 4 (DLL1,3,4)) are described which are all type I transmembrane proteins. Ligand-receptor interaction triggers proteolytic cleavages that release the intracellular domain of the receptor (NICD) from the membrane. NICD translocates to the nucleus where it forms an active transcriptional complex with the transcription factor RBPJ and several co-activators (Kopan, 2012; Kovall et al., 2017; Henrique and Schweisguth, 2019). Notch signaling has been characterized as a crucial pathway for vascular SMC differentiation (Baeten and Lilly, 2017; Fouillade et al., 2012) whereas its potential role in visceral SMC development has remained unexplored.

Here, we set out to analyze a possible role of Notch signaling in visceral SMC differentiation in the murine ureter. We show that the pathway is essential to timely activate and maintain expression of *Myocd* and of late SMC structural genes, and hence, to achieve and maintain proper peristaltic activity in this organ.

## Materials and Methods

### Mouse strains and husbandry

All alleles used in this study were maintained on an NMRI outbred background: *Rbpj*<sup>tm1.1Hon</sup> (synonym: *Rbpj*<sup>fl</sup>) (Tanigaki et al., 2002), *Gt(ROSA)26Sor*<sup>tm1(Notch1)Dam</sup> (synonym: *Rosa26*<sup>NICD</sup>) (Murtaugh et al., 2003), *Tbx18*<sup>tm4(cre)Akis</sup> (synonym: *Tbx18*<sup>cre</sup>) (Trowe et al., 2010), *Gt(ROSA)26Sor*<sup>tm4(ACTB-tdTomato,-EGFP)Luo</sup> (synonym: *Rosa26*<sup>mTmG</sup>) (Muzumdar et al., 2007). Embryos for expression analysis of genes encoding Notch components were obtained from matings of NMRI wild-type mice. *Tbx18*<sup>cre/+</sup>;*Rbpj*<sup>fl/+</sup> males were mated with *Rbpj*<sup>fl/fl</sup> females, *Tbx18*<sup>cre/+</sup> males with *Rosa26*<sup>NICD/NICD</sup> females, to obtain embryos for phenotypic characterization. Littermates without the *Tbx18*<sup>cre</sup> allele were used as controls. Pregnancies were timed as embryonic day (E) 0.5 by vaginal plugs in the morning after mating. Embryos and urogenital systems were dissected in PBS. Specimens were fixed in 4% PFA/PBS, transferred to methanol and stored at -20°C prior to further processing. PCR genotyping was performed on genomic DNA prepared from liver biopsies or yolk sacs.

All animal work conducted for this study was approved by the local authorities (Niedersächsisches Landesamt für Verbraucherschutz und Lebensmittelsicherheit; permit number AZ33.12-42502-04-13/1356) and was performed at the central animal laboratory of the Medizinische Hochschule Hannover.

### Organ cultures

Ureters were explanted on 0.4 µm polyester membrane Transwell supports (#3450, Corning Inc., Lowell, MA, USA) and cultured in DMEM/F12 supplemented with 1% of concentrated stocks of penicillin/streptomycin, sodium pyruvate, glutamax, non-essential amino acids and IST-G (insulin-transferrin-selenium) (Thermo Fisher Scientific, Waltham, MA, USA) at the air-liquid interface as previously described (Bohnenpoll et al., 2013). DAPT (GSI-IX) (#S2215, Selleckchem, Houston, TX, USA) was used at final concentrations of 1 or 2.5 µM. Culture medium was replaced every 48 hours. Analysis of frequencies and intensities of ureter contractions in explant cultures was performed by videomicroscopy as recently described (Weiss et al., 2019).



### **Histological and immunofluorescence analysis**

Embryos, urogenital systems or explant cultures were paraffin-embedded and sections were cut at 5- $\mu$ m thickness. Hematoxylin and eosin staining was performed according to standard procedures. For immunofluorescent stainings labeling with primary antibodies was performed at 4°C overnight after antigen retrieval (15 min at 100°C, #H-3300, Vector Laboratories, Burlingame, CA, USA), blocking of endogenous peroxidases with 3% H<sub>2</sub>O<sub>2</sub>/PBS for 15 min (for TSA amplification only) and incubation in blocking buffer provided from the TSA kit (TNB) for 45 min. The following primary antibodies were used: polyclonal rabbit-anti-KRT5 (1:250; #PRB-160P, Covance, Princeton, NJ, USA), polyclonal rabbit-anti- $\Delta$ NP63 (1:250; #619001, BioLegend, San Diego, CA, USA), monoclonal mouse-anti-UPK1B (1:250; #WH0007348M2, Sigma-Aldrich, St. Louis, MO, USA), polyclonal rabbit-anti-TAGLN (1:200; #ab14106, Abcam, Cambridge, UK), monoclonal mouse-anti-ACTA2 (1:200; #A5228, Sigma-Aldrich), monoclonal rat-anti-EMCN (1:5, a kind gift of D. Vestweber, MPI Münster; Germany), polyclonal rabbit-anti-CD31 (1:400, #50408-T16, Sino Biological, Beijing, China), monoclonal mouse-anti-GFP (1:200, #11814460001 Roche, Sigma-Aldrich) and polyclonal rabbit-anti-GFP (1:250, #ab290, Abcam).

Primary antibodies were detected using the following secondary antibodies: biotinylated goat-anti-mouse IgG (1:400; #115-065-003, Dianova, Hamburg, Germany), biotinylated goat-anti-rabbit IgG (1:400; #111-065-033, Dianova), biotinylated goat anti-rat IgG (1:400; #112-065-003, Dianova), biotinylated donkey anti-goat IgG (1:400; #705-065-003, Dianova), Alexa 488-conjugated goat anti-rabbit IgG (1:500; #A11034, Thermo Fisher Scientific), Alexa 488-conjugated donkey anti-mouse IgG (1:500; A21202, Thermo Fisher Scientific), Alexa 555-conjugated goat anti-mouse IgG (1:500; A21422, Thermo Fisher Scientific) and Alexa 555-conjugated goat anti-mouse IgG (1:500; A21428, Thermo Fisher Scientific). The signals of  $\Delta$ NP63 and EMCN were amplified using the Tyramide Signal Amplification system (#NEL702001KT, Perkin Elmer, Waltham, MA, USA).

### ***In situ* hybridization analysis**

*In situ* hybridization was done on 10  $\mu$ m paraffin sections essentially as described (Moorman et al., 2001).

### Microarray

Ureters were dissected from male and female control and *Tbx18<sup>cre/+</sup>;Rbpj<sup>fl/fl</sup>* embryos. 40 specimens for each sex and genotype were pooled for analysis at E14.5, and 12 specimens each for analysis at E18.5. Total RNA was extracted using peqGOLD RNA-pure (#732-3312, #30-1010; PeqLab Biotechnologie GmbH, Erlangen, Germany) and subsequently sent to the Research Core Unit Transcriptomics of Hannover Medical School, where RNA was Cy3-labelled and hybridised to Agilent Whole Mouse Genome Oligo v2 (4x44K) microarrays (#G4846A; Agilent Technologies Inc, Santa Clara, CA, USA). To identify differentially expressed genes, normalised expression data were filtered using Excel (Microsoft Corp., Redmond, WA, USA) based on an intensity threshold of 100 and a more than 1.4-fold change in all pools. Microarray data have been submitted to Gene Expression Omnibus (GEO, <http://www.ncbi.nlm.nih.gov/geo/>) (GSE169661, GSE169662).

### Reverse transcription-polymerase chain reaction (RT-PCR)

RNA extraction and RT-PCR analysis for *Myocd* and *Foxf1* expression was performed on pools of 10 ureters each of E14.5 control and *Tbx18<sup>cre/+</sup>;Rbpj<sup>fl/fl</sup>* embryos as previously described (Weiss et al., 2019). For all other analyses, we isolated total RNA using TRIzol (#15596-018, Thermo Fisher Scientific) and synthesized cDNA from 2.5 µg total RNA applying RevertAid H Minus reverse transcriptase (#EP0452, Thermo Fisher Scientific) as described (Thiesler et al., 2021). The NCBI tool Primer3 version4.1 (Untergasser et al., 2012; Ye et al., 2012) was used to design specific primers (Table S1). RT-quantitative (q)PCR of mouse genes was performed in 10 µl 1:2 diluted BIO SyGreen Lo-ROX mix (PCR Biosystems, London, UK) with 400 nM primers and 1 ng/µl cDNA applying a QuantStudio3 PCR system fluorometric thermal cycler (Thermo Fisher Scientific). Each of the three biological replicates represents the average of four technical replicates. Data were processed by QuantStudio data analysis software (version1.5.1, Thermo Fisher Scientific) using the comparative threshold cycle ( $\Delta\Delta C_T$ ) method with *Gapdh* and *Ppia* as reference genes (Werneburg et al., 2015).

### Statistics

Statistical analysis was performed using the unpaired, two-tailed Student's *t*-test (GraphPad Prism version 7.03, GraphPad Software, San Diego, CA, USA). Values are indicated as mean  $\pm$  s.d.  $P < 0.05$  was considered significant.

**Image documentation**

Sections and organ cultures were photographed using a DM5000 microscope (Leica Camera, Wetzlar, Germany) with Leica DFC300FX digital camera or a Leica DM6000 microscope with Leica DFC350FX digital camera. Urogenital systems were documented using a Leica M420 microscope with a Fujix HC-300Z digital camera (Fujifilm Holdings, Minato/Tokyo, Japan). All images were processed in Adobe Photoshop CS4.

## Results

### Notch signaling components are expressed in ureter development

To determine the abundance of Notch signalling components in ureter development, we analyzed expression of genes encoding Notch ligands and receptors by RNA *in situ* hybridization on transverse sections of the proximal ureter region of E12.5 to E18.5 wild-type embryos (Fig. 1). *Jag1* was expressed in the UE and the UM at E12.5; from E14.5 onwards, expression occurred at low levels in both compartments. *Jag2* was robustly expressed in the UE at E14.5. At E16.5 and E18.5, expression in this tissue was predominantly found in the basal cell layer. Expression was also found in endothelial cells of vessels in the outer UM from E12.5 to E18.5. *Dll1* and *Dll3* expression was not detected in ureter development. *Dll4* expression was found in endothelial cells in the UM at all stages (Fig. 1A). *Notch1* was weakly expressed in the UE from E12.5 to E16.5, and in some basal cells at E18.5. Expression also occurred in endothelial linings in the outer UM from E12.5 to E18.5. *Notch2* was strongly expressed in the UM at E12.5 and E14.5, and more weakly at E16.5 and E18.5. *Notch3* expression was found in the UM at E12.5, and in perivascular cells in the outer UM at E12.5 to E18.5. Weak expression of both *Notch 2* and *Notch3* was found in the UE at all stages. *Notch4* expression was associated with endothelia in the outer UM throughout ureter development (Fig. 1B). The distribution of Notch components is compatible with the occurrence of Notch pathway activity both in the epithelial and mesenchymal compartment of the ureter as well as in the associated vessels.

### Conditional inactivation of *Rbpj* in the UM leads to changes in SMC differentiation at E18.5

To investigate the role of canonical Notch signaling in the UM, we employed a tissue-specific gene inactivation approach using a *Tbx18<sup>cre</sup>* line generated in our laboratory (Airik et al., 2010), and a floxed allele of *Rbpj* (synonym: *Rbpj<sup>fl</sup>*) (Tanigaki et al., 2002), the unique intracellular mediator of this signaling pathway (Jarriault et al., 1995). *Tbx18<sup>cre</sup>* mediates recombination in precursors of all differentiated cell types of the UM: fibroblasts of the inner *lamina propria* and the outer *tunica adventitia*, SMCs of the medial *tunica muscularis* (Bohnenpoll et al., 2013) and vascular SMCs but not endothelial cells (Fig. S1). Absence of *Rbpj* expression in the UM of *Tbx18<sup>cre/+</sup>;Rbpj<sup>fl/fl</sup>* (*Rbpj-cKO*) embryos confirmed the suitability of our approach (Fig. S2).

We started our phenotypic analysis at the end of embryogenesis, at E18.5, when all differentiated cell types of the ureter are established. At this stage, the urogenital system of *Rbpj-cKO* embryos was morphologically unaffected with the exception of the ureter that appeared more translucent than in the control (Fig. 2A). The kidney was histologically normal but the *tunica muscularis* of the ureter appeared less condensed (Fig. 2B). Expression of the SMC proteins ACTA2 and TAGLN was unchanged in the *tunica muscularis* of the mutant ureter but was reduced in large adventitial vessels (Fig. 2C). Expression of the SMC structural genes *Cnn1* and *Myh11* appeared unaffected, whereas *Tagln* was weakly and *Tnnt2* was strongly reduced in the ureteric muscle layer. The *lamina propria* marker *Aldh1a2* and the adventitial marker *Dpt* were unchanged (Fig. 2D). The distribution of endomucin (EMCN) (Morgan et al., 1999) and of KRT5,  $\Delta$ NP63, UPK1B (Bohnenpoll et al., 2017a) reflected normal vascular endowment and urothelial differentiation, respectively (Fig. 2E).

To profile transcriptional changes in E18.5 *Rbpj-cKO* ureters in a global and unbiased fashion, we used microarray analysis. Using a threshold of at least 1.5-fold change and an expression intensity robustly above background ( $>100$ ), we detected 93 genes with reduced expression and 45 with increased expression in *Rbpj-cKO* ureters (Table S2A,B; GEO submission GSE169662). Functional annotation using the DAVID software tool (Huang da et al., 2009) revealed a highly significant enrichment of gene ontology (GO) terms and clusters related to “muscle contraction” for the pool of downregulated genes whereas variable terms and clusters with low significance were found for the pool of upregulated genes (Fig. 2F, Table S3,4). Manual inspection of the list of down-regulated genes detected *Rbpj* (-2.4) and the Notch effector gene *Hey1* (-2.9) confirming the loss of Notch signaling activity. *Tnnt2* expression was strongly reduced (-2.1), *Tagln* (-1.2), *Cnn1* (-1.3) and *Myh11* (-1.3) weakly, *Acta2* was unchanged largely confirming our *in situ* hybridization analysis (Fig. 2G).

We validated expression of a subset of the down-regulated genes by *in situ* hybridization analysis. We found strongly reduced expression of *Pcp4*, *Ckm*, *Myl4*, *Pcp4l1*, *Mfap4*, *Rhoa* and *Synpo2* in the muscle layer of the mutant ureter. *Tpm2* appeared weakly affected; other candidates were not detected by this method (Fig. 2H, Fig. S3). RT-qPCR confirmed slightly (*Tagln*, *Tpm2*) and strongly (*Ckm*, *Pcp4*, *Pcp4l1*, *Tnnt2*) reduced expression of SMC genes at this stage (Fig. 2I, Table S5A). We conclude that *Rbpj-cKO* ureters exhibit defects in visceral SMC differentiation shortly before birth.



### **Loss of *Rbpj* in the UM compromises ureter peristalsis and leads to hydroureter in adolescent mice**

To investigate whether the observed changes in visceral SMC differentiation translate into functional deficits in ureter peristalsis after birth, we isolated ureters at E18.5 and cultured them for 6 days in a transwell setting (Fig. 3A-C). Mutant ureters exhibited a significantly reduced contraction frequency at day 1 and 2 of culture but reached the level of the control from day 3 onwards (Fig. 3B, Table S6A). At day 1, the contraction occurred less rapidly and reached lower intensities; the relaxation wave was, however, unaffected. At day 3, the mutant ureters reached the contraction intensity of the control albeit with a slight but significant delay. At day 6, the mutant ureters reached higher contraction intensities and maintained them for longer. This was most prominent at the medial position (Fig. 3C, Table S6B).

After 6 days in culture, SMC differentiation was still partly compromised: *Cnn1* and *Myh11* appeared unaffected, *Tagln* and *Tpm2* were weakly reduced; *Ckm*, *Pcp4*, *Pcp4l1* and *Tnnt2* were strongly reduced (Fig. 3D,E; Table S5B).

We investigated the long-term *in vivo* consequences of loss of *Rbpj*-dependent Notch signaling in the UM, by analyzing a small number of mutant mice that survived until postnatal day (P)14. At this stage, the mutant ureter was invariably dilated at the proximal level. Some SMC genes seemed unchanged (*Cnn1*, *Myh11*, *Tpm2*), others were strongly reduced (*Ckm*, *Pcp4*, *Pcp4l1*, *Tagln*, *Tnnt2*) in their expression (Fig. 3F). These findings show that loss of *Rbpj* in the UM leads to cytodifferentiation defects in visceral SMCs that translate into peristaltic changes and hydroureter formation after birth.

### **SMC differentiation is delayed in *Rbpj-cKO* ureters**

To define the onset of SMC defects in *Rbpj-cKO* ureters, we performed histological and molecular analyses at stages (E14.5 to E16.5) when the SMC phenotype is progressively established. Histological analysis showed that the UM of the mutant was subdivided into an inner layer with rhomboid-shaped condensed cells and an outer layer with loosely organized fibroblast-like cells at all analyzed stages as in the control but the inner layer appeared less condensed at E15.5 and E16.5 (Fig. 4A). In the control, *Cnn1*, *Myh11*, *Tagln*, *Tpm2* expression commenced at E15.5, *Tnnt2* at E16.5 in the inner layer of the UM. In *Rbpj-cKO* ureters, expression of *Cnn1*, *Myh11* and *Tpm2* occurred normally from E15.5 onwards. *Tagln* was reduced at E15.5 and at E16.5;

*Tnnt2* expression was not observed in the mutants. *Ckm*, *Myl4*, *Pcp4* and *Pcp4l1* mRNA was neither detected in the control nor in the mutant ureter in the analyzed time window (Fig. 4B).

SMC differentiation defects were associated with functional insufficiency of fetal (E14.5) *Rbpj-cKO* ureters in explant cultures (Fig. 4C-E). Mutant ureters exhibited a 1.5-day delay in onset of peristaltic activity (Fig. 4D, Table S7A). The contraction frequency was significantly decreased until day 6 and reached control levels only at day 7 and 8 of the culture (Fig. 4E, Table S7B). The contraction intensity was strongly reduced at all analyzed levels throughout the entire contraction wave at day 4 of the culture. At the endpoint, at day 8, the initial contraction velocity in the proximal and the medial part was normal but the contraction intensities remained lower throughout the contraction wave (Fig. 4F, Table S7C). Hence, loss of *Rbpj* in the UM affects the structure and function of visceral SMCs in the fetal ureter.

#### **Loss of *Rbpj* affects onset of *Myocd* expression in the UM**

To identify molecular changes that may cause delayed and reduced SMC differentiation in *Rbpj-cKO* ureters in an unbiased fashion, we performed microarray-based gene expression profiling of E14.5 ureters. Using an intensity threshold of 100 and fold changes of at least 1.5 in the two individual arrays, we detected 30 genes with increased and 16 with decreased expression in mutant ureters (Fig. 5A; Table S8A,B; GEO submission GSE169661).

Functional annotation using the DAVID software tool (Huang da et al., 2009) revealed an enrichment of GO terms related to the differentiation of secretory cells, dopaminergic neurons and/or chromaffine cells in the pool of upregulated genes but *in situ* hybridization did not detect expression of any of the selected candidates in control and mutant ureters (Table S9A, Fig. S4). In the pool of downregulated genes GO terms related to protein binding and negative regulation of WNT signaling (*Mdf1*, *Shisa2*, *Wif1*) were found (Table S9B). Manual inspection of the list identified *Rbpj* (-1.9) confirming the functionality of our genetic approach, and *Myocd* (-2.0), the key regulator of SMC differentiation (Fig. 5A). *In situ* hybridization of candidate downregulated genes detected reduced expression of *Mdf1*, *Car3*, *Shisa2* and *Myocd* in the inner UM of mutant embryos (Fig. 5B). Other candidates showed unspecific or no expression in control and mutant ureters (Fig. S5).

In agreement with our microarray data, we did not detect expression changes of genes encoding cellular signals, signaling targets and transcription factors that have previously been implicated in *Myocd* activation and SMC differentiation in the ureter by *in situ* hybridization analysis (Figure S6A,B). These findings validate that reduced expression of the WNT antagonist *Shisa2* does not translate into changes of WNT signaling, and that known regulators of *Myocd* expression are unchanged in E14.5 *Rbpj-cKO* ureters.

To characterize whether *Myocd* expression is delayed in *Rbpj-cKO* ureters, we analyzed its expression at subsequent stages. *In situ* hybridization detected normal expression at E15.5, E16.5 and at E18.5. Expression in E18.5 explants cultured for 6 days was weak but appeared reduced (Fig. 5C). RT-qPCR analysis confirmed strongly reduced expression of *Myocd* at E14.5 whereas expression of *Foxf1*, activator of *Myocd* expression, was unchanged (Fig. 5D, Table S5C). Expression of *Myocd* was unchanged at E18.5, but showed a trend for reduction in 6-day explants of E18.5 ureters supporting the *in situ* hybridization results (Fig. 5E, Table S5D). We conclude that *Rbpj*-dependent Notch signaling is required for precise activation of *Myocd* at E14.5 but not for its further maintenance at fetal stages.

### **Notch signaling is required for onset and maintenance of SMC differentiation in the ureter**

To exclude the possibility that RBPJ acts independently of Notch receptors in the context of the UM, and to distinguish early from late requirements of this pathway, we performed time-controlled pharmacological Notch pathway interference experiments with the gamma-secretase inhibitor DAPT (Cheng et al., 2003) in ureter explant cultures. Administration of 1  $\mu$ M and 2.5  $\mu$ M DAPT (Cheng et al., 2003) to E12.5 ureter explants led to a dose-dependent delay in the onset of the peristaltic activity and a reduction of contraction frequency similar to the situation observed in explants of E14.5 *Rbpj-cKO* ureters (Fig. 6A, Table S10).

We next explanted wild-type ureters at E18.5 and treated them with 1  $\mu$ M of DAPT. These ureters showed a normal peristaltic onset but a reduced contraction frequency until day 3 of culture, again similar to *Rbpj-cKO* ureters (Fig. 6B; Table S11). After 18 h in culture, expression of *Ckm* and *Tnnt2* was significantly reduced, expression of *Myocd*, *Pcp4*, *Pcp4I1*, *Tagln* and *Tpm2* appeared unaffected (Fig. 6C, Table S5E). After 6 days in culture, expression of *Ckm*, *Myocd*, *Pcp4*, *Pcp4I1*, *Tagln* and *Tnnt2* was

strongly reduced; expression of *Cnn1*, *Myh11* and *Tpm2* was unaffected (Fig. 6D,E; Table S5F). Hence, Notch signaling is required both for onset and/or maintenance of expression of *Myocd* and late SMC genes.

### **Notch signaling is not sufficient to induce SMC development**

We finally asked whether Notch signaling is sufficient to induce SMC relevant genes in ureter development. For this, we combined our *Tbx18<sup>cre</sup>* driver line with a *Rosa26* knock-in allele (*Rosa26<sup>NICD</sup>*) (Murtaugh et al., 2003) allowing conditional expression of the Notch1 intracellular domain (NICD) in the undifferentiated UM. Since *Tbx18<sup>cre/+</sup>;Rosa26<sup>NICD/+</sup>* embryos died around E13.5 (Grieskamp et al., 2011), we used E12.5 ureters for section *in situ* hybridization analysis. We did not find ectopic and/or precocious expression of the SMC regulators *Foxf1* and *Myocd*, of SMC structural genes, and of *Car3* and *Shisa2* indicating that Notch signaling is required but not sufficient to activate SMC regulatory and structural genes in the developing ureter (Fig. S7).

## Discussion

### Notch signaling is a novel regulator of SMC differentiation in the ureter

Previous genetic work provided compelling evidence that Notch signaling is a critical regulator of vascular SMC differentiation (for reviews see (Fouillade et al., 2012; Baeten and Lilly, 2017)). This applies both to neural crest cells from which SMCs of the great vessels including the aorta derive (High et al., 2007; Feng et al., 2010; Manderfield et al., 2012) as well as to mesothelial cells and other progenitors of arterial SMCs in different organ systems (Etchevers et al., 2001; Grieskamp et al., 2011; Volz et al., 2015). In either case loss of Notch signaling (components) was associated with severely reduced expression of SMC structural genes including early differentiation markers ACTA2 and TAGLN and subsequent vessel dilatation.

To unravel the function of Notch signaling in the development of the UM, we used a combination of genetic and pharmacological pathway inhibition experiments. Loss of the Notch signaling mediator *Rbpj* did neither affect ureter shape and length nor the subdivision of its mesenchymal wall at fetal and postnatal stages, excluding a role of the pathway in survival, proliferation and patterning of the UM. We found largely unchanged levels of early SMC proteins/genes (ACTA2, TAGLN, *Myh11*, *Cnn1*) indicating that visceral SMC specification and early differentiation has occurred. However, we observed a delayed onset of *Myocd* expression and reduced expression of late SMC genes at fetal and postnatal stages combined with delayed onset of peristaltic activity, reduced contraction frequency and intensity in fetal life compatible with a role of Notch signaling in modifying, enhancing and/or fine-tuning visceral SMC differentiation. We detected hydroureter formation in mutant mice at P14, indicating that the mutant SMC layer has reduced capacity to withstand the hydrostatic pressure of the urine with time. The phenotypic burden of *Rbpj-cKO* mice prevented analysis at later stages in adults. However, it is likely that under the permanent pressure exerted by the urine even weak reduction of SMC structural proteins will cause further deficits of SMC contractility and rigidity that will translate in progressive ureter dilatation, hydronephrosis and end-stage renal disease. Mutations that affect expression of Notch components may therefore underlie human congenital anomalies of the kidney and ureteric tract (CAKUT), a group of diseases for which the genetic cause has only partly been resolved (Kohl et al., 2021).



Our time-controlled pharmacological pathway inhibition experiments validated a Notch-dependent function of RBPJ in the UM, and proved that Notch signaling is required both for precise temporal activation of the SMC differentiation program and for its full execution and maintenance in homeostasis.

We identified expression of *Jag2* in the UE from E14.5 onwards, juxtaposed to expression of *Notch2* in the UM. Although this finding points to a continuous epithelial-mesenchymal cross-talk similar to the ones detected for SHH and WNT signaling (Yu et al., 2002; Trowe et al., 2012; Bohnenpoll et al., 2017c), we cannot exclude that low level expression of *Jag1* and *Notch3* in the undifferentiated UM indicates the presence of an alternative ligand-receptor pair involved in the initial activation of Notch signaling. The individual involvement of Notch signaling components can only be dissected by conditional gene targeting strategies.

Although not analyzed in any detail, we would like to mention that we noted reduced ACTA2 and TAGLN expression in cells surrounding endothelial linings in the advential layer of *Rbpj-cKO* ureters indicating that Notch signaling is essential for vascular SMC differentiation in the ureter as in many if not all other organs.

### **Notch signaling impacts expression of *Myocd* and late SMC genes**

We found that the regulator of the SMC differentiation *Myocd*, is activated with a delay of one day in *Rbpj-cKO* ureters. Importantly, we did not detect changes in the activity of signaling pathways (SHH, BMP4, WNT, RA) and transcription factors (*Foxf1*, *Tshz3*, *Sox9*) that have been implicated in the regulation of *Myocd* at E14.5 (Caubit et al., 2008; Airik et al., 2010; Trowe et al., 2012; Bohnenpoll et al., 2017b; Bohnenpoll et al., 2017c; Mamo et al., 2017). Hence, *Myocd* may be a direct target of RBPJ or of HES/HEY bHLH proteins that mediate the activity of this pathway in many contexts (Fischer et al., 2004; Bray and Bernard, 2010). Irrespective of the precise mode of action, we posit that Notch signaling provides an important independent positive input for precise temporal activation of *Myocd* transcription in the ureter.

Our expression analyses uncovered that SMC structural genes are differentially affected in *Rbpj-cKO* ureters. Some genes (*Acta2*, *Cnn1*, *Myh11*, *Tpm2*, *Tagln*) were not or marginally changed in their expression whereas others (*Ckm*, *Pcp4*, *Pcp4l1*, *Tnnt2*) were strongly reduced. Pharmacological Notch signaling inhibition of E18.5 ureters resulted in similar changes. Interestingly, we found that in wildtype ureters “Notch-independent” genes are activated early after *Myocd* expression at E14.5 to E15.5 whereas

“Notch-dependent” genes are activated later at E16.5 to E18.5. Given unchanged *Myocd* expression in mutant ureters at E16.5 to E18.5, we suggest that Notch signaling provides a critical direct input on the expression of these “late” SMC genes. Importantly, misexpression of NICD did not activate any of the SMC genes tested, reinforcing that Notch is a modulator and not a driver of the visceral SMC program.

„Late“ SMC genes affected in *Rbpj-cKO* ureters have been implicated in constriction (*Tnnt2*), relaxation (*Pcp4*) and energy conservation (*Ckm*) of cardiomyocytes, and in cardiomyopathies when deficient (Rentschler et al., 2012; Kim et al., 2014; Wei and Jin, 2016; Walker et al., 2021). Therefore, reduced expression of these genes/proteins may affect constriction and/or relaxation of ureteric SMCs, and contribute to hydronephrosis formation in *Rbpj-cKO* mice.

In the vascular system, Notch signaling regulates and synergizes with PDGFRB and TGF $\beta$  signaling in activation of early SMC genes (for reviews see Fouillade et al., 2012; Baeten and Lilly, 2017). Notch function is mediated through *Hey* genes and direct target of its activity comprise *Acta2*, *Pdgfrb*, *Notch3* and *Jag1* (Nosedá et al., 2006; Jin et al., 2008; Liu et al., 2009; Bray and Bernard, 2010; Manderfield et al., 2012). We did not find changes of any of these genes in our transcriptional profiling experiments suggesting that the molecular circuits regulated by Notch signaling in the control of SMC differentiation are different in the vascular and visceral context.

We conclude that Notch signaling regulates visceral SMC differentiation in the ureter in a bimodal and biphasic manner. First, it enhances *Myocd* expression to a critical level at E14.5; second, it enhances from E16.5 onwards expression of a set of “late” SMC genes critical for long-term maintenance of ureter peristaltic activity.

### **Acknowledgments**

We thank Doug Melton and Tasuku Honjo for mice, Dietmar Vestweber, Anja-Münster Kühnel and Henry Wedekind for antibodies, the Research Core Unit Transcriptomics of Hannover Medical School for microarray analyses, and Patricia Zarnovican for excellent technical support.

### **Competing interests**

No competing interests declared.

### **Author Contributions**

A.-C.W. and A.K. designed and supervised the study; A.-C.W., J.K., H.T., J.K., L.D. collected or provided the data; A.-C.W., J.K., H.T., J.K., L.D., M.-O.T. and A.K. analyzed the data; I.W. and F.Q. performed mouse work; A.-C.W. and A.K. drafted the manuscript; H.H. and A.K. provided funding; all authors edited the manuscript and approved it.

### **Funding**

This work was supported by the Deutsche Forschungsgemeinschaft (DFG, German Research Foundation), project numbers 207786640 (Ki728/9-2), 84948123 (Ki 728/7-2), 171943101 (Ki728/8-2) to A.K., project number 432236295 (Hi 678/10-1) to H.H., and by the Horizon 2020 Marie Skłodowska-Curie Actions Initial Training Network (942937) [RENALTRACT to J.K. and A.K.];

### **Data availability**

Microarray data have been submitted to Gene Expression Omnibus (GEO, <http://www.ncbi.nlm.nih.gov/geo/>) (GSE169661 and GSE169662).

## References

- Airik, R., Trowe, M. O., Foik, A., Farin, H. F., Petry, M., Schuster-Gossler, K., Schweizer, M., Scherer, G., Kist, R. and Kispert, A. (2010). Hydrourteronephrosis due to loss of Sox9-regulated smooth muscle cell differentiation of the ureteric mesenchyme. *Hum Mol Genet* **19**, 4918-4929.
- Aydogdu, N., Rudat, C., Trowe, M. O., Kaiser, M., Ludtke, T. H., Taketo, M. M., Christoffels, V. M., Moon, A. and Kispert, A. (2018). TBX2 and TBX3 act downstream of canonical WNT signaling in patterning and differentiation of the mouse ureteric mesenchyme. *Development* **145**, dev:171827.
- Baeten, J. T. and Lilly, B. (2017). Notch Signaling in Vascular Smooth Muscle Cells. *Adv Pharmacol* **78**, 351-382.
- Bohnenpoll, T., Bettenhausen, E., Weiss, A. C., Foik, A. B., Trowe, M. O., Blank, P., Airik, R. and Kispert, A. (2013). Tbx18 expression demarcates multipotent precursor populations in the developing urogenital system but is exclusively required within the ureteric mesenchymal lineage to suppress a renal stromal fate. *Dev Biol* **380**, 25-36.
- Bohnenpoll, T., Feraric, S., Nattkemper, M., Weiss, A. C., Rudat, C., Meuser, M., Trowe, M. O. and Kispert, A. (2017a). Diversification of Cell Lineages in Ureter Development. *J Am Soc Nephrol* **28**, 1792-1801.
- Bohnenpoll, T. and Kispert, A. (2014). Ureter growth and differentiation. *Semin Cell Dev Biol* **36**, 21-30.
- Bohnenpoll, T., Weiss, A. C., Labuhn, M., Ludtke, T. H., Trowe, M. O. and Kispert, A. (2017b). Retinoic acid signaling maintains epithelial and mesenchymal progenitors in the developing mouse ureter. *Sci Rep* **7**, 14803.
- Bohnenpoll, T., Wittern, A. B., Mamo, T. M., Weiss, A. C., Rudat, C., Kleppa, M. J., Schuster-Gossler, K., Wojahn, I., Ludtke, T. H., Trowe, M. O., et al. (2017c). A SHH-FOXF1-BMP4 signaling axis regulating growth and differentiation of epithelial and mesenchymal tissues in ureter development. *PLoS Genet* **13**, e1006951.
- Bray, S. and Bernard, F. (2010). Notch targets and their regulation. *Curr Top Dev Biol* **92**, 253-275.
- Caubit, X., Lye, C. M., Martin, E., Core, N., Long, D. A., Vola, C., Jenkins, D., Garratt, A. N., Skaer, H., Woolf, A. S., et al. (2008). Teashirt 3 is necessary for ureteral smooth muscle differentiation downstream of SHH and BMP4. *Development* **135**, 3301-3310.
- Cheng, H. T., Miner, J. H., Lin, M., Tansey, M. G., Roth, K. and Kopan, R. (2003). Gamma-secretase activity is dispensable for mesenchyme-to-epithelium transition but required for podocyte and proximal tubule formation in developing mouse kidney. *Development* **130**, 5031-5042.
- Creemers, E. E., Sutherland, L. B., McAnally, J., Richardson, J. A. and Olson, E. N. (2006). Myocardin is a direct transcriptional target of Mef2, Tead and Foxo proteins during cardiovascular development. *Development* **133**, 4245-4256.
- Donadon, M. and Santoro, M. M. (2021). The origin and mechanisms of smooth muscle cell development in vertebrates. *Development* **148**, dev197384.
- Etchevers, H. C., Vincent, C., Le Douarin, N. M. and Couly, G. F. (2001). The cephalic neural crest provides pericytes and smooth muscle cells to all blood vessels of the face and forebrain. *Development* **128**, 1059-1068.
- Feng, X., Krebs, L. T. and Gridley, T. (2010). Patent ductus arteriosus in mice with smooth muscle-specific Jag1 deletion. *Development* **137**, 4191-4199.

- Fischer, A., Schumacher, N., Maier, M., Sendtner, M. and Gessler, M.** (2004). The Notch target genes *Hey1* and *Hey2* are required for embryonic vascular development. *Genes Dev* **18**, 901-911.
- Fouillade, C., Monet-Leprêtre, M., Baron-Menguy, C. and Joutel, A.** (2012). Notch signalling in smooth muscle cells during development and disease. *Cardiovasc Res* **95**, 138-146
- Grieskamp, T., Rudat, C., Ludtke, T. H., Norden, J. and Kispert, A.** (2011). Notch signaling regulates smooth muscle differentiation of epicardium-derived cells. *Circ Res* **108**, 813-823.
- Henrique, D. and Schweisguth, F.** (2019). Mechanisms of Notch signaling: a simple logic deployed in time and space. *Development* **146**, dev172148.
- High, F. A., Zhang, M., Proweller, A., Tu, L., Parmacek, M. S., Pear, W. S. and Epstein, J. A.** (2007). An essential role for Notch in neural crest during cardiovascular development and smooth muscle differentiation. *J Clin Invest* **117**, 353-363.
- Huang da, W., Sherman, B. T. and Lempicki, R. A.** (2009). Systematic and integrative analysis of large gene lists using DAVID bioinformatics resources. *Nat Protoc* **4**, 44-57.
- Jarriault, S., Brou, C., Logeat, F., Schroeter, E. H., Kopan, R. and Israel, A.** (1995). Signalling downstream of activated mammalian Notch. *Nature* **377**, 355-358.
- Jin, S., Hansson, E. M., Tikka, S., Lanner, F., Farnebo, F., Baumann, M., Kalimo, H. and Lendahl, U.** (2008). Notch signaling regulates platelet-derived growth factor receptor-beta expression in vascular smooth muscle cells. *Circ Res* **102**, 1483-1491.
- Kim, E. E., Shekhar, A., Lu, J., Lin, X., Liu, F. Y., Zhang, J., Delmar, M. and Fishman, G. I.** (2014). PCP4 regulates Purkinje cell excitability and cardiac rhythmicity. *J Clin Invest* **124**, 5027-5036.
- Kohl, S., Habbig, S., Weber, L. T. and Liebau, M. C.** (2021). Molecular causes of congenital anomalies of the kidney and urinary tract (CAKUT). *Mol Cell Pediatr* **8**, 2.
- Kopan, R.** (2012). Notch signaling. *Cold Spring Harb Perspect Biol.* **4**, a011213.
- Kovall, R. A., Gebelein, B., Sprinzak, D. and Kopan, R.** (2017). The Canonical Notch Signaling Pathway: Structural and Biochemical Insights into Shape, Sugar, and Force. *Dev Cell* **41**, 228-241.
- Liu, H., Kennard, S. and Lilly, B.** (2009). NOTCH3 expression is induced in mural cells through an autoregulatory loop that requires endothelial-expressed JAGGED1. *Circ Res* **104**, 466-475.
- Mack, C. P.** (2011). Signaling mechanisms that regulate smooth muscle cell differentiation. *Arterioscler Thromb Vasc Biol* **31**, 1495-1505.
- Mamo, T. M., Wittern, A. B., Kleppa, M. J., Bohnenpoll, T., Weiss, A. C. and Kispert, A.** (2017). BMP4 uses several different effector pathways to regulate proliferation and differentiation in the epithelial and mesenchymal tissue compartments of the developing mouse ureter. *Hum Mol Genet* **26**, 3553-3563.
- Manderfield, L. J., High, F. A., Engleka, K. A., Liu, F., Li, L., Rentschler, S. and Epstein, J. A.** (2012). Notch activation of Jagged1 contributes to the assembly of the arterial wall. *Circulation* **125**, 314-323.
- Moorman, A. F., Houweling, A. C., de Boer, P. A. and Christoffels, V. M.** (2001). Sensitive nonradioactive detection of mRNA in tissue sections: novel application of the whole-mount in situ hybridization protocol. *J Histochem Cytochem* **49**, 1-8.

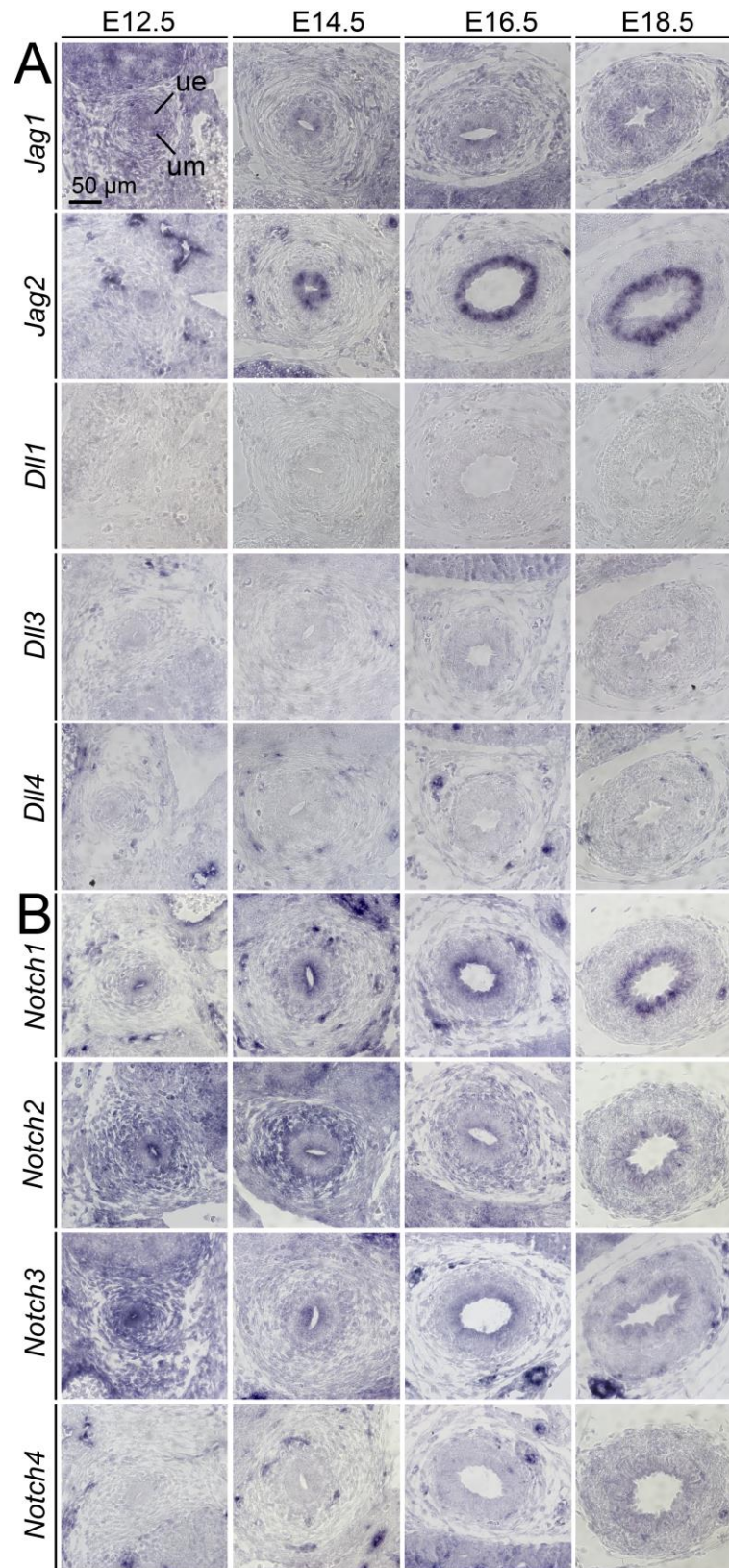


- Morgan, S. M., Samulowitz, U., Darley, L., Simmons, D. L. and Vestweber, D.** (1999). Biochemical characterization and molecular cloning of a novel endothelial-specific sialomucin. *Blood* **93**, 165-175.
- Murtaugh, L. C., Stanger, B. Z., Kwan, K. M. and Melton, D. A.** (2003). Notch signaling controls multiple steps of pancreatic differentiation. *Proc Natl Acad Sci U S A* **100**, 14920-14925.
- Muzumdar, M. D., Tasic, B., Miyamichi, K., Li, L. and Luo, L.** (2007). A global double-fluorescent Cre reporter mouse. *Genesis* **45**, 593-605.
- Norman, C., Runswick, M., Pollock, R. and Treisman, R.** (1988). Isolation and properties of cDNA clones encoding SRF, a transcription factor that binds to the c-fos serum response element. *Cell* **55**, 989-1003.
- Nosedá, M., Fu, Y., Niessen, K., Wong, F., Chang, L., McLean, G. and Karsan, A.** (2006). Smooth Muscle alpha-actin is a direct target of Notch/CSL. *Circ Res* **98**, 1468-1470.
- Rentschler, S., Yen, A., Lu, J., Petrenko, N., Lu, M., Manderfield, L., Patel, V., Fishman, G. and Epstein, J.** (2012). Myocardial Notch signaling reprograms cardiomyocytes to a conduction-like phenotype. *Circulation* **126**, 1058-1066.
- Shi, N. and Chen, S. Y.** (2016). Smooth Muscle Cell Differentiation: Model Systems, Regulatory Mechanisms, and Vascular Diseases. *J Cell Physiol* **231**, 777-787.
- Tanigaki, K., Han, H., Yamamoto, N., Tashiro, K., Ikegawa, M., Kuroda, K., Suzuki, A., Nakano, T. and Honjo, T.** (2002). Notch-RBP-J signaling is involved in cell fate determination of marginal zone B cells. *Nat Immunol* **3**, 443-450.
- Thiesler, H., Beimdiek, J. and Hildebrandt, H.** (2021). Polysialic acid and Siglec-E orchestrate negative feedback regulation of microglia activation. *Cell Mol Life Sci* **78**, 1637-1653.
- Trowe, M. O., Airik, R., Weiss, A. C., Farin, H. F., Foik, A. B., Bettenhausen, E., Schuster-Gossler, K., Taketo, M. M. and Kispert, A.** (2012). Canonical Wnt signaling regulates smooth muscle precursor development in the mouse ureter. *Development* **139**, 3099-3108.
- Trowe, M. O., Shah, S., Petry, M., Airik, R., Schuster-Gossler, K., Kist, R. and Kispert, A.** (2010). Loss of Sox9 in the periotic mesenchyme affects mesenchymal expansion and differentiation, and epithelial morphogenesis during cochlea development in the mouse. *Dev Biol* **342**, 51-62.
- Untergasser, A., Cutcutache, I., Koressaar, T., Ye, J., Faircloth, B. C., Remm, M. and Rozen, S. G.** (2012). Primer3-new capabilities and interfaces. *Untergasser A, Cutcutache I, Koressaar T, Ye J, Faircloth BC, Remm M, Rozen SG (2012) Primer3-new capabilities and interfaces. Nucleic Acids Res 40 (15):e115. 40, e115.*
- Volz, K. S., Jacobs, A. H., Chen, H. I., Poduri, A., McKay, A. S., Riordan, D. P., Kofler, N., Kitajewski, J., Weissman, I. and Red-Horse, K.** (2015). Pericytes are progenitors for coronary artery smooth muscle. *Elife* **4**, e10036.
- Walker, M. A., Chavez, J., Villet, O., Tang, X., Keller, A., Bruce, J. E. and Tian, R.** (2021). Acetylation of muscle creatine kinase negatively impacts high-energy phosphotransfer in heart failure. *JCI Insight* **6**, e144301.
- Wang, D. Z. and Olson, E. N.** (2004). Control of smooth muscle development by the myocardin family of transcriptional coactivators. *Curr Opin Genet Dev* **14**, 558-566.
- Wei, B. and Jin, J. P.** (2016). TNNT1, TNNT2, and TNNT3: Isoform genes, regulation, and structure-function relationships. *Gene* **582**, 1-13.
- Weiss, A. C., Bohnenpoll, T., Kurz, J., Blank, P., Airik, R., Ludtke, T. H., Kleppa, M. J., Deuper, L., Kaiser, M., Mamo, T. M., et al.** (2019). Delayed onset of

smooth muscle cell differentiation leads to hydroureter formation in mice with conditional loss of the zinc finger transcription factor gene *Gata2* in the ureteric mesenchyme. *J Pathol* **248**, 452-463.

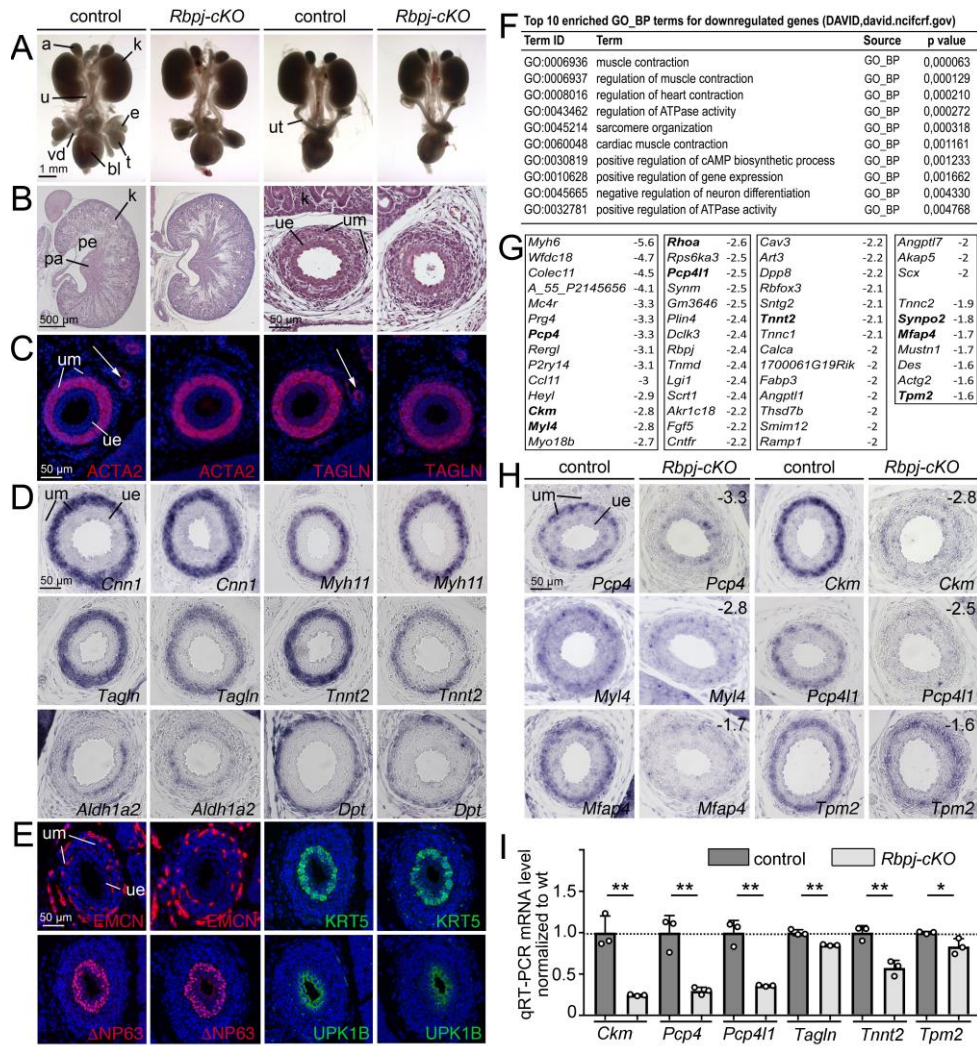
- Werneburg, S., Buettner, F. F., Mühlenhoff, M. and Hildebrandt, H.** (2015). Polysialic acid modification of the synaptic cell adhesion molecule SynCAM 1 in human embryonic stem cell-derived oligodendrocyte precursor cells. *Stem Cell Res* **14**, 339-346.
- Woolf, A. S. and Davies, J. A.** (2013). Cell biology of ureter development. *J Am Soc Nephrol* **24**, 19-25.
- Woolf, A. S., Lopes, F. M., Ranjzad, P. and Roberts, N. A.** (2019). Congenital Disorders of the Human Urinary Tract: Recent Insights From Genetic and Molecular Studies. *Front Pediatr* **7**, 136.
- Ye, J., Coulouris, G., Zaretskaya, I., Cutcutache, I., Rozen, S. and Madden, T. L.** (2012). Primer-BLAST: a tool to design target-specific primers for polymerase chain reaction. *BMC Bioinformatics* **13**, 134.
- Yoshida, T., Sinha, S., Dandre, F., Wamhoff, B. R., Hoofnagle, M. H., Kremer, B. E., Wang, D. Z., Olson, E. N. and Owens, G. K.** (2003). Myocardin is a key regulator of CArG-dependent transcription of multiple smooth muscle marker genes. *Circ Res* **92**, 856-864.
- Yu, J., Carroll, T. J. and McMahon, A. P.** (2002). Sonic hedgehog regulates proliferation and differentiation of mesenchymal cells in the mouse metanephric kidney. *Development* **129**, 5301-5312.

## Figures and figure legends

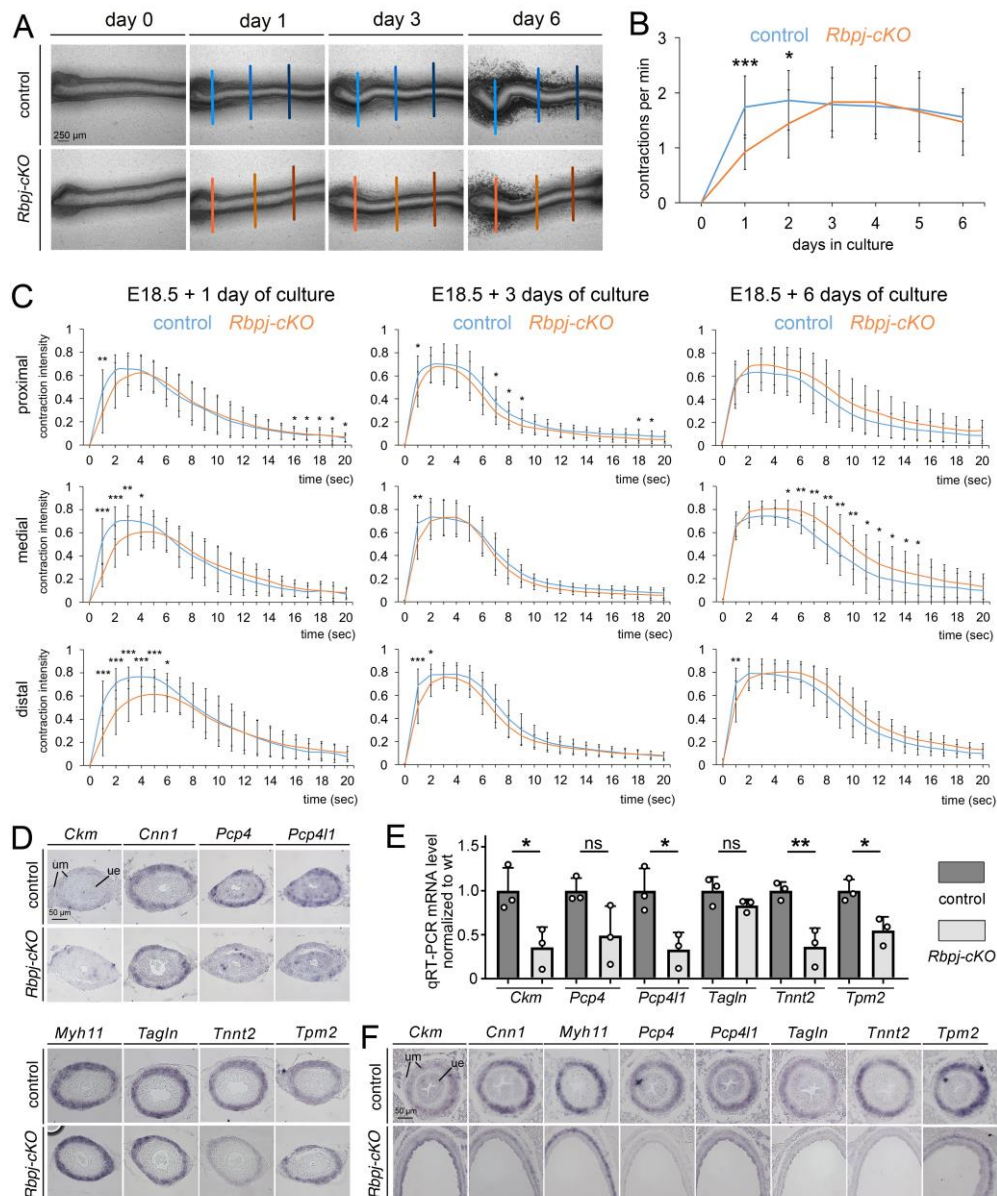


**Fig. 1. Notch signaling components are expressed during murine ureter development.** (A,B) *In situ* hybridization analysis on transverse sections of the proximal ureter for expression of genes encoding Notch ligands (A) and Notch receptors (B).  $n \geq 3$  for all probes. ue, ureteric epithelium; um, ureteric mesenchyme.





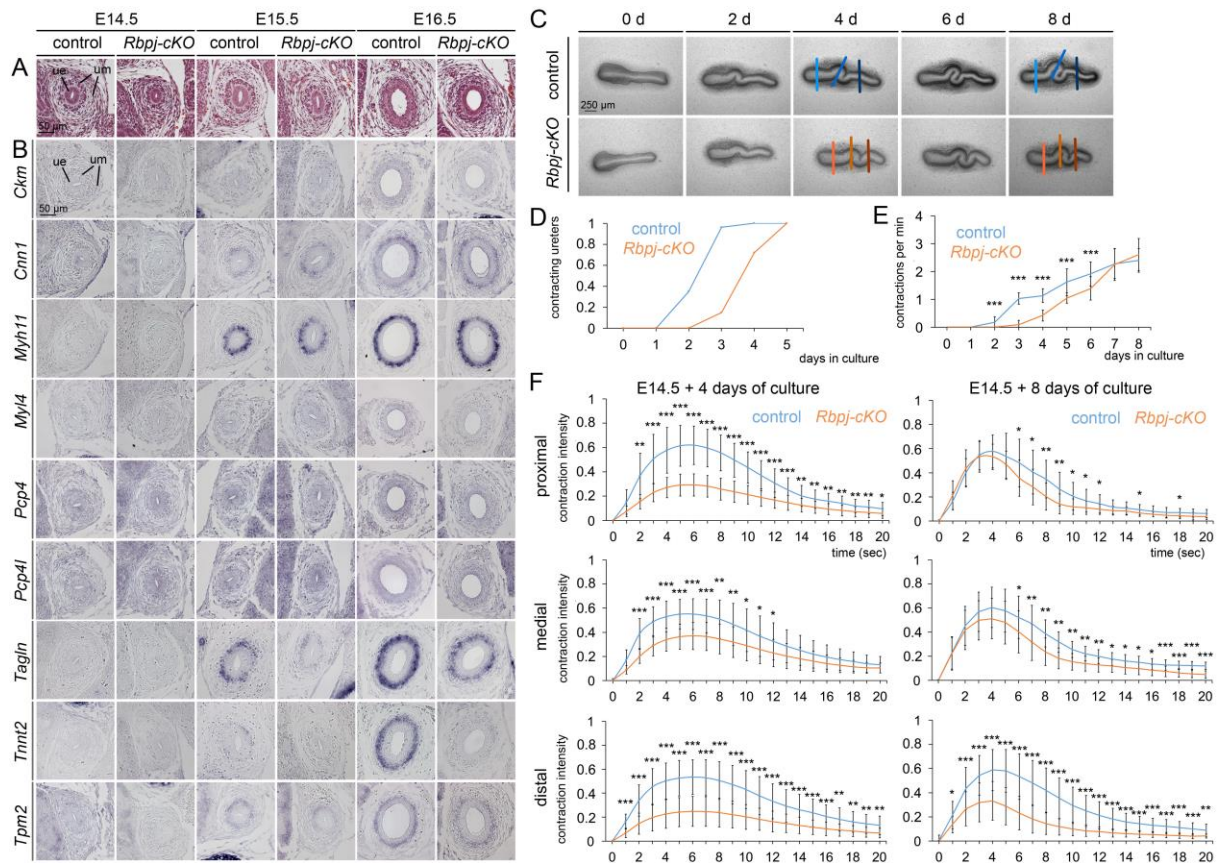
**Fig. 2. *Rbpj-cKO* ureters exhibit SMC defects at E18.5.** (A) Morphology of whole urogenital systems of male (column 1 and 2) and female (column 3 and 4) embryos; n>10 for each sex and genotype. (B) Hematoxylin and eosin staining of sagittal sections of kidneys (column 1 and 2) and of transverse sections of the proximal ureter (column 3 and 4). (C) Immunofluorescence analysis of the SMC marker proteins ACTA2 and TAGLN on transverse sections of the proximal ureter. Nuclei (blue) are counterstained with DAPI. White arrows point to vascular SMCs. (D) RNA *in situ* hybridization analysis on transverse sections of the proximal ureter for the SMC marker genes *Cnn1*, *Myh11*, *Tagln*, *Tnnt2*, the lamina propria marker *Aldh1a2*, and the adventitial marker *Dpt*. (E) Immunofluorescence analysis on proximal ureter sections for endothelial (EMCN) and urothelial (KRT5, ΔNP63, UPK1B) differentiation; nuclei (blue) are counterstained with DAPI. KRT5, ΔNP63 and UPK1B combinatorially mark basal cells (KRT5<sup>+</sup>ΔNP63<sup>-</sup>UPK1B<sup>-</sup>), intermediate cells (KRT5<sup>+</sup>ΔNP63<sup>+</sup>UPK1B<sup>+</sup>) and superficial cells (KRT5<sup>-</sup>ΔNP63<sup>-</sup>UPK1B<sup>+</sup>). (F) List of top 10 gene ontology annotations over-represented in the set of genes with reduced expression using DAVID web software. (G) List of genes with reduced expression (at least <-1.9) and selected candidates in the microarray analysis of E18.5 *Rbpj-cKO* ureters. In bold are genes with validated expression in the tunica muscularis of control embryos. (H) RNA *in situ* hybridization analysis on transverse sections of the proximal ureter at E18.5 for microarray candidate genes. The numbers indicate the fold down-regulation. n>=3 for all assays and probes (B-E,H). (I) qRT-PCR results for expression of selected SMC structural genes in three independent RNAs pools of control and *Rbpj-cKO* ureters. Differences were considered significant (\*p) with a p-value ≤0.05, highly significant (\*\*) p≤0.01; two-tailed Student's t-test. For values and statistics see Table S5A. a, adrenal; bl, bladder; e, epididymides; k, kidney; pa, papilla; pe, pelvis; te, testis; u, ureter; ue, ureteric epithelium; um, ureteric mesenchyme; ut, uterus; vd, vas deferens.



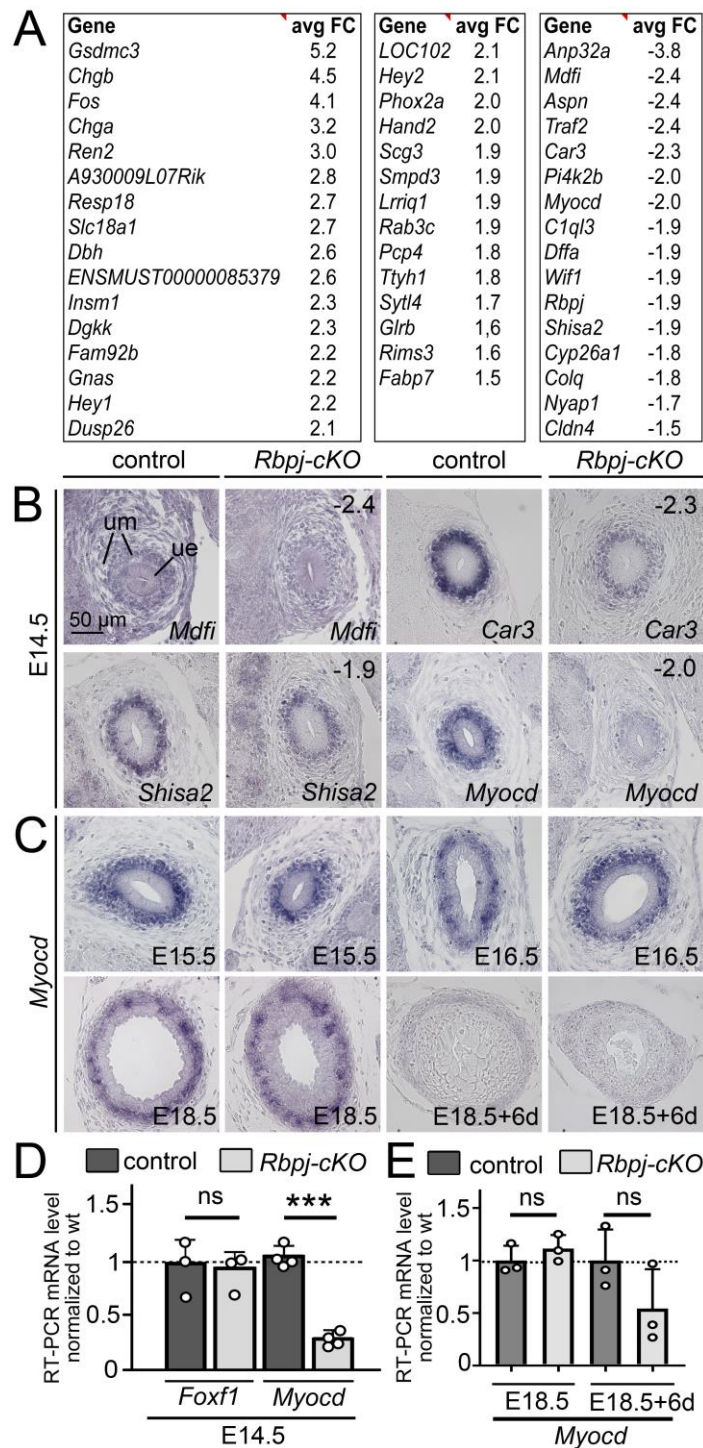
**Fig. 3. SMC differentiation and peristalsis are affected in *Rbpj-cKO* ureters at postnatal stages.** (A-C) Analysis of peristaltic contractions of E18.5 ureter explants in culture; control: n=26, *Rbpj-cKO*: n=16. (A) Morphological analysis by brightfield microscopy. Vertical lines indicate the positions along the ureter at which contraction intensities were measured during one contraction wave. Positions relate to 25% (proximal), 50% (medial) and 75% (distal) of ureter length. (B) Analysis of contraction onset and frequency in a 6-day culture period. For values and statistics see Table S6A. (C) Analysis of the contraction intensity at proximal, medial, and distal levels of ureters explanted at E18.5 and cultured for 1, 3 and 6 days. For statistical values see Table S6B. Differences were considered significant (\*) with p-value  $\leq 0.05$ , highly significant (\*\*)  $p \leq 0.01$ , extremely significant (\*\*\*)  $p \leq 0.001$ ; two-tailed Student's t-test (B,C). (D) RNA *in situ* hybridization analysis of expression of SMC structural genes on transverse sections of the proximal ureter of E18.5 explants cultured for 6 days.  $n \geq 3$  for all probes. (E) qRT-PCR results of expression of selected SMC structural genes in three independent RNAs pools of control and *Rbpj-cKO* ureters cultured for 6 days. For statistical values see Table S5B. Differences were considered non-significant (ns) with  $p > 0.05$ ; significant (\*)  $p \leq 0.05$ , highly significant (\*\*)  $p \leq 0.01$ ; two-tailed Student's t-test. (F) RNA *in situ* hybridization analysis of expression of SMC structural genes on transverse sections of the proximal ureter of P14 mice.  $n \geq 3$  for all probes ue, ureteric epithelium; um, ureteric mesenchyme.



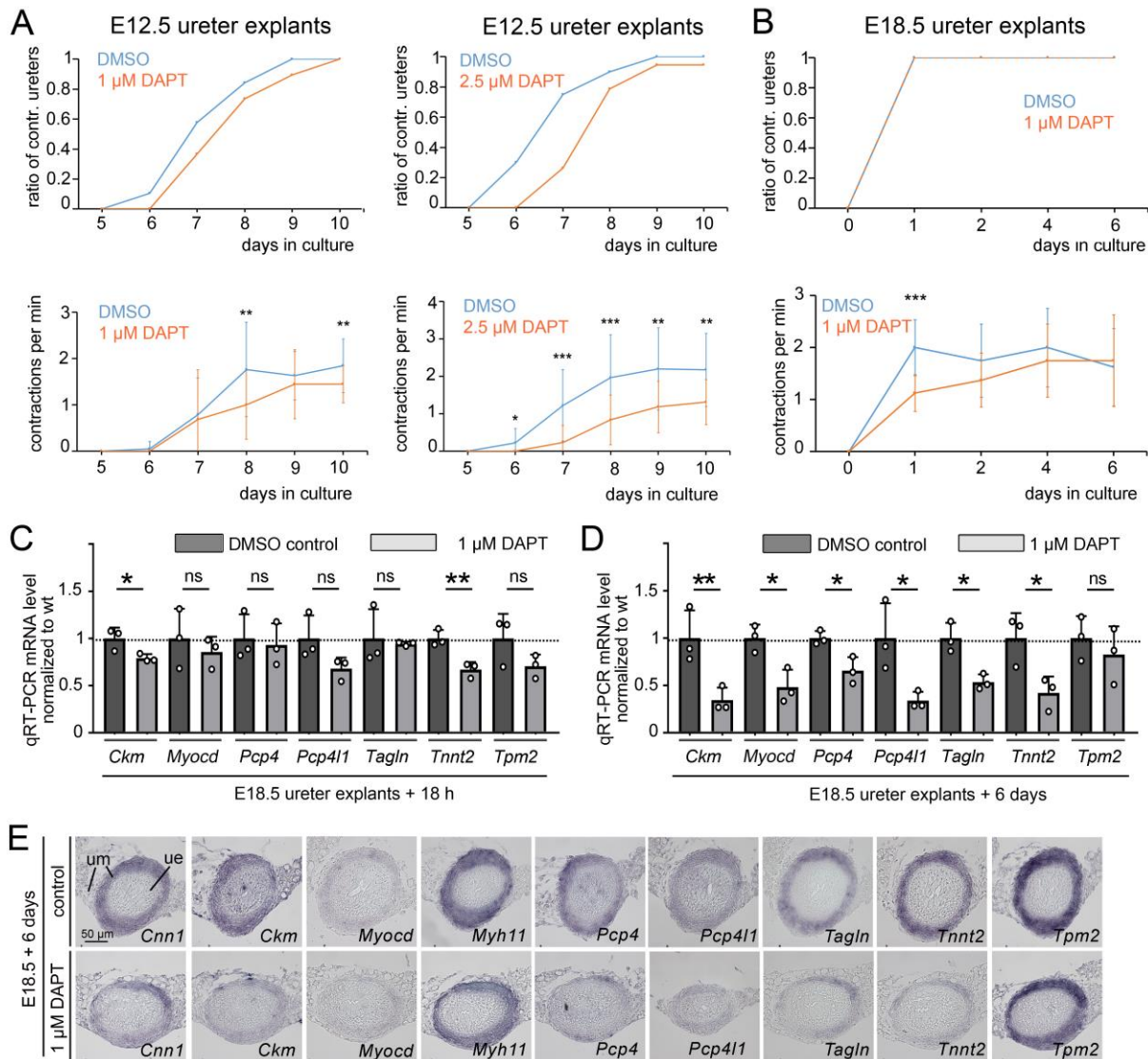
## Part – 3 Notch signaling in SMC differentiation



**Fig. 4. SMC differentiation and peristalsis occur in a delayed fashion in fetal *Rbpj-cKO* ureters.** (A,B) Hematoxylin and eosin stainings (A) and RNA *in situ* hybridization analysis of expression of SMC marker genes (B) on transverse sections of the proximal ureter region at E14.5, E15.5 and E16.5.  $n \geq 3$  for all probes. (C-F) Analysis of peristaltic contractions of E14.5 ureter explants in culture; control:  $n=23$ , *Rbpj-cKO*:  $n=16$ . (C) Morphological analysis by bright-field microscopy. Vertical lines indicate the positions along the ureter at which contraction intensities were measured during one contraction wave at day 4 and day 8 of culture. Positions relate to 25% (proximal), 50% (medial) and 75% (distal) of ureter length. (D) Analysis of contraction onset in a 8-day culture period. For statistical values see Table S7A. (E) Analysis of the contraction frequency in E14.5 ureter explants cultured for 8 days. For statistical values see Table S7B. (F) Analysis of the contraction intensity at proximal, medial and distal levels of E14.5 ureter explants at day 4 and day 8 of culture. For statistical values see Table S7C. Differences were considered significant (\*) with a P-value below 0.05, highly significant (\*\*)  $p \leq 0.01$ , extremely significant (\*\*\*)  $p \leq 0.001$ ; two-tailed Student's t-test (E,F). ue, ureteric epithelium; um, ureteric mesenchyme.



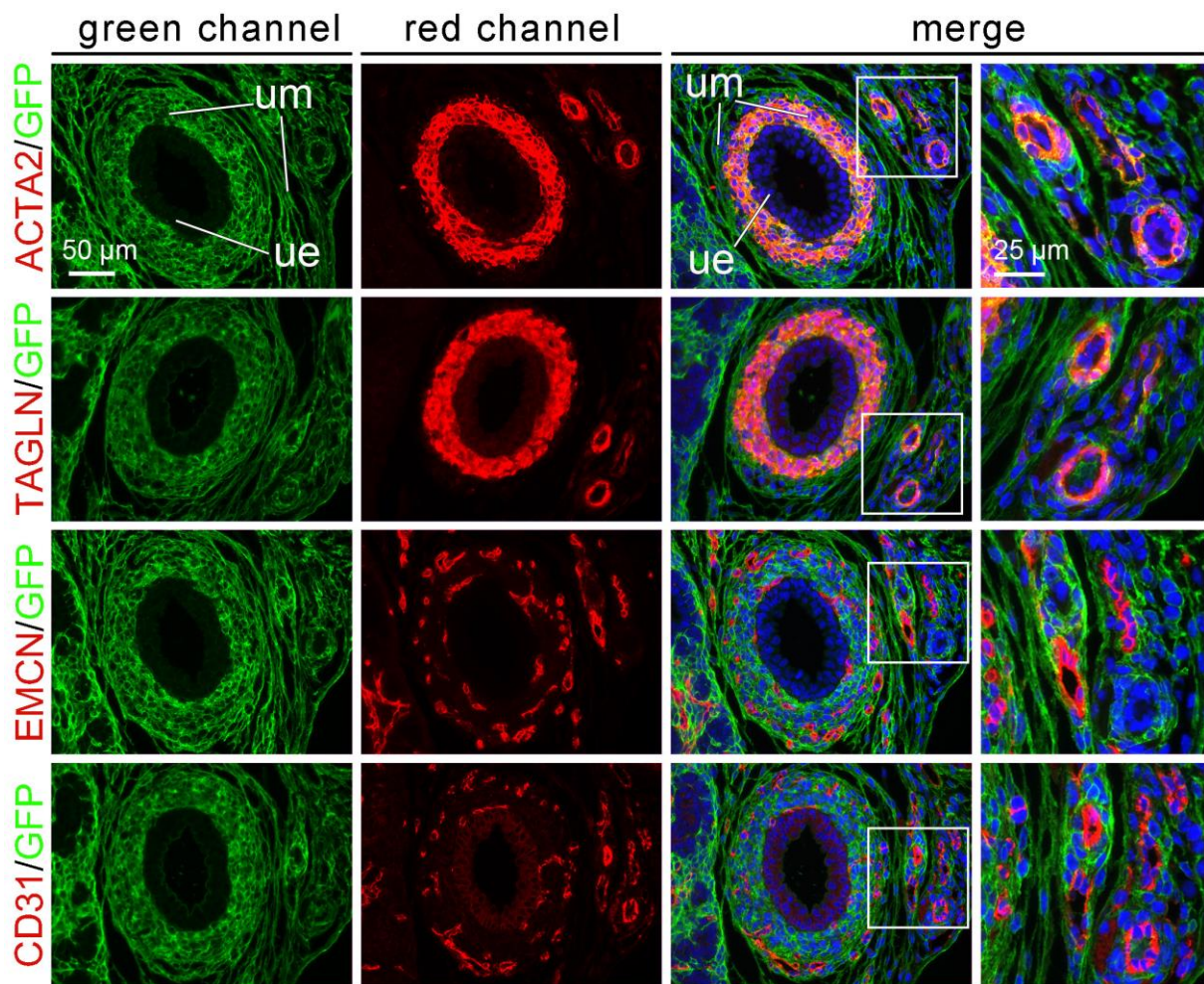
**Fig. 5. Onset of *Myocd* expression is affected in *Rbpj*-cKO ureters.** (A) List of genes with increased (average fold change (avgFC) $\geq$ 1.5) and reduced expression (avgFC $\leq$ -1.5) in the microarray analysis of E14.5 *Rbpj*-cKO ureters. (B,C) RNA *in situ* hybridization analysis on transverse sections of the proximal ureter for microarray candidate genes at E14.5 (B) and for *Myocd* expression at E15.5, E16.5, E18.5 and in 6-day cultures of E18.5 ureter explants (C).  $n \geq 3$  for all probes. (D,E) qRT-PCR results for expression of *Foxf1* and *Myocd* in RNAs pools of control and *Rbpj*-cKO ureters at E14.5 (D), and of *Myocd* expression in E18.5 ureters and in 6-day cultures of E18.5 ureter explants (E). Differences were considered non-significant (ns) with a P-value above 0.05; significant (\*)  $p \leq 0.05$ , highly significant (\*\*)  $p \leq 0.01$ , extremely significant (\*\*\*)  $p \leq 0.001$ ; two-tailed Student's t-test. For values and statistics see Table S5C,D. ue, ureteric epithelium; um, ureteric mesenchyme.



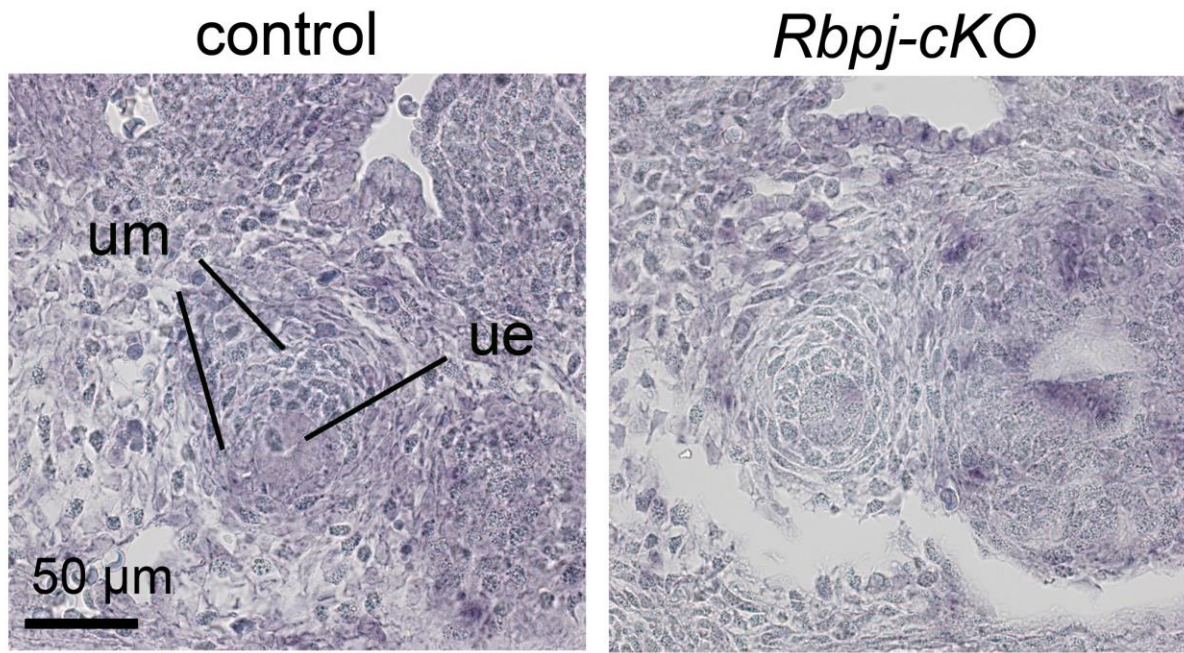
**Fig. 6. Pharmacological inhibition of Notch signaling affects onset and maintenance of SMC differentiation.** (A,B) Analysis of onset (first row) and frequency (second row) of peristaltic contractions in cultures of E12.5 ureter explants treated with DMSO (control) or with 1  $\mu$ M (control: n=19, DAPT-treated: n=19) or 2.5  $\mu$ M (control: n=20, DAPT-treated: n=19) of the Notch signaling inhibitor DAPT (A), and in cultures of E18.5 ureter explants treated with DMSO (control) or with 1  $\mu$ M DAPT (control: n=8, DAPT-treated: n=8) (B). For values and statistics see Table S10,11. Differences were considered significant (\*) with a p-value  $\leq 0.05$ , highly significant (\*\*)  $p \leq 0.01$ , extremely significant (\*\*\*)  $p \leq 0.001$ ; two-tailed Student's t-test. (C,D) qRT-PCR results of expression of selected SMC genes in three independent RNAs pools of control and *Rbpj-cKO* ureters explanted at E18.5 and cultured for 18 h (C) and 6 days (D), respectively, in FCS-free (ITS) medium supplemented with DMSO (control) or with 1  $\mu$ M DAPT. Differences were considered non-significant (ns) with a P-value  $> 0.05$ ; significant (\*)  $p \leq 0.05$ , highly significant (\*\*)  $p \leq 0.01$ ; two-tailed Student's t-test. For values and statistics see Table S5E,F. (E) RNA *in situ* hybridization analysis of SMC genes on transverse sections of the proximal ureter after 6-days in culture.  $n \geq 3$  for all probes. ue, ureteric epithelium; um, ureteric mesenchyme.



## Supplementary Figures

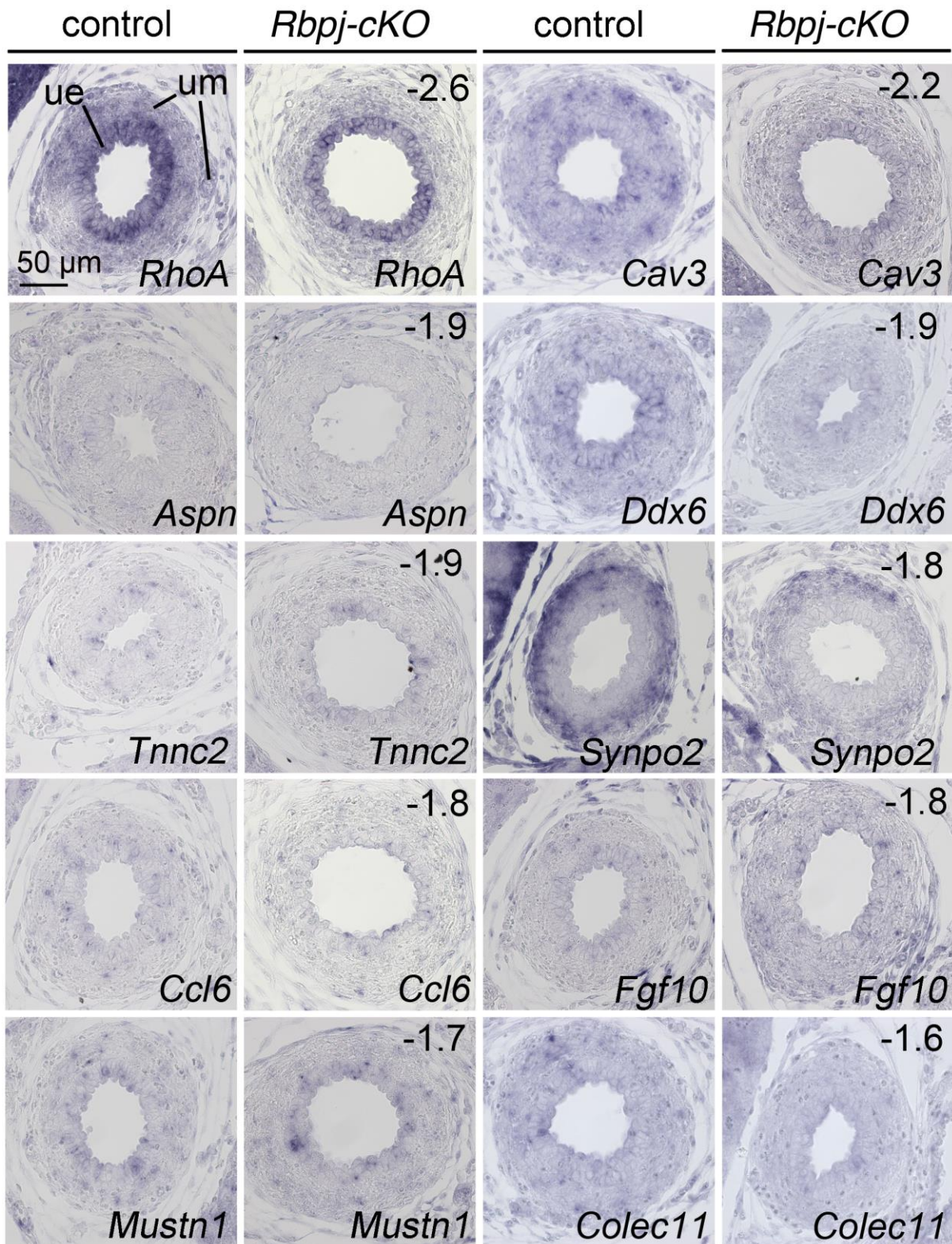


**Fig. S1. Lineage analysis of *Tbx18*<sup>+</sup> descendants in the ureter.** Co-immunofluorescence analysis on transverse sections of the proximal ureter of E18.5 *Tbx18*<sup>cre/+</sup>;*R26*<sup>mTmG/+</sup> embryos for expression of the lineage marker GFP and of differentiation markers for SMCs (ACTA2, TAGLN) and endothelial cells (EMCN, CD31). Shown are the green channel for GFP expression (first row), the red channel for the differentiation marker (second row), and a merge of the two channels (third and fourth row). The fourth row shows higher magnification images of the regions marked by a white square in the third row, which contain vessels with SMC investment. n=5 for all markers. Note that visceral and vascular SMCs arise from *Tbx18*<sup>+</sup> mesenchymal progenitors whereas endothelial cells are of a different origin. ue, ureteric epithelium; um, ureteric mesenchyme.



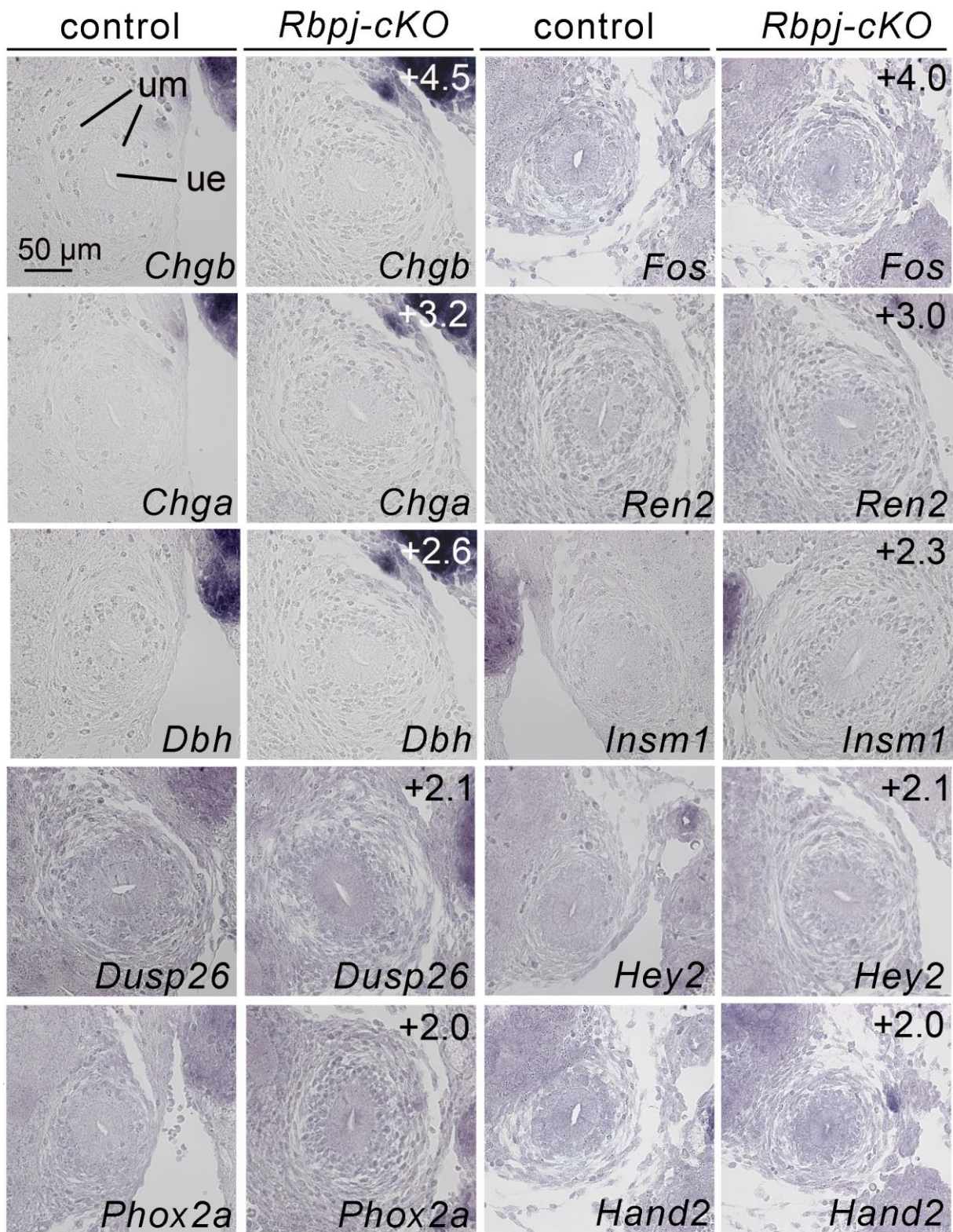
**Fig. S2. Loss of *Rbpj* expression in the UM of *Rbpj-cKO* embryos.** RNA *in situ* hybridization analysis of *Rbpj* expression in control and *Rbpj-cKO* ureters at E12.5; n=3 for both genotypes. ue, ureteric epithelium; um, ureteric mesenchyme.





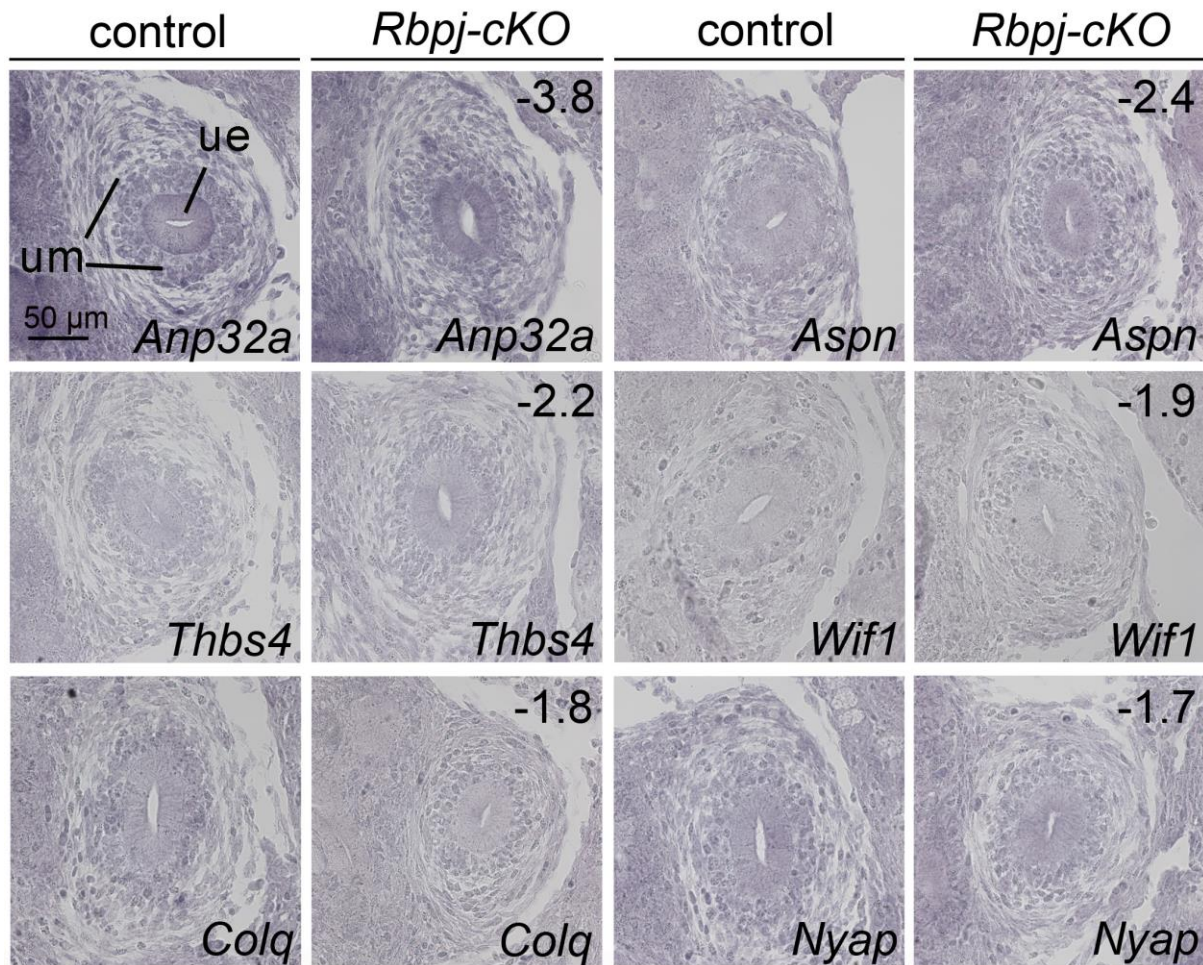
**Fig. S3. RNA *in situ* hybridization analysis of candidate genes with decreased expression in microarrays of E18.5 *Rbpj-cKO* ureters.** RNA *in situ* hybridization of selected candidate genes with decreased expression in microarrays of E18.5 *Rbpj-cKO* ureters were performed on transverse sections of the proximal ureter region. Probes, genotypes and fold changes in the microarray are as indicated.  $n \geq 3$  for all probes. ue, ureteric epithelium; um, ureteric mesenchyme.



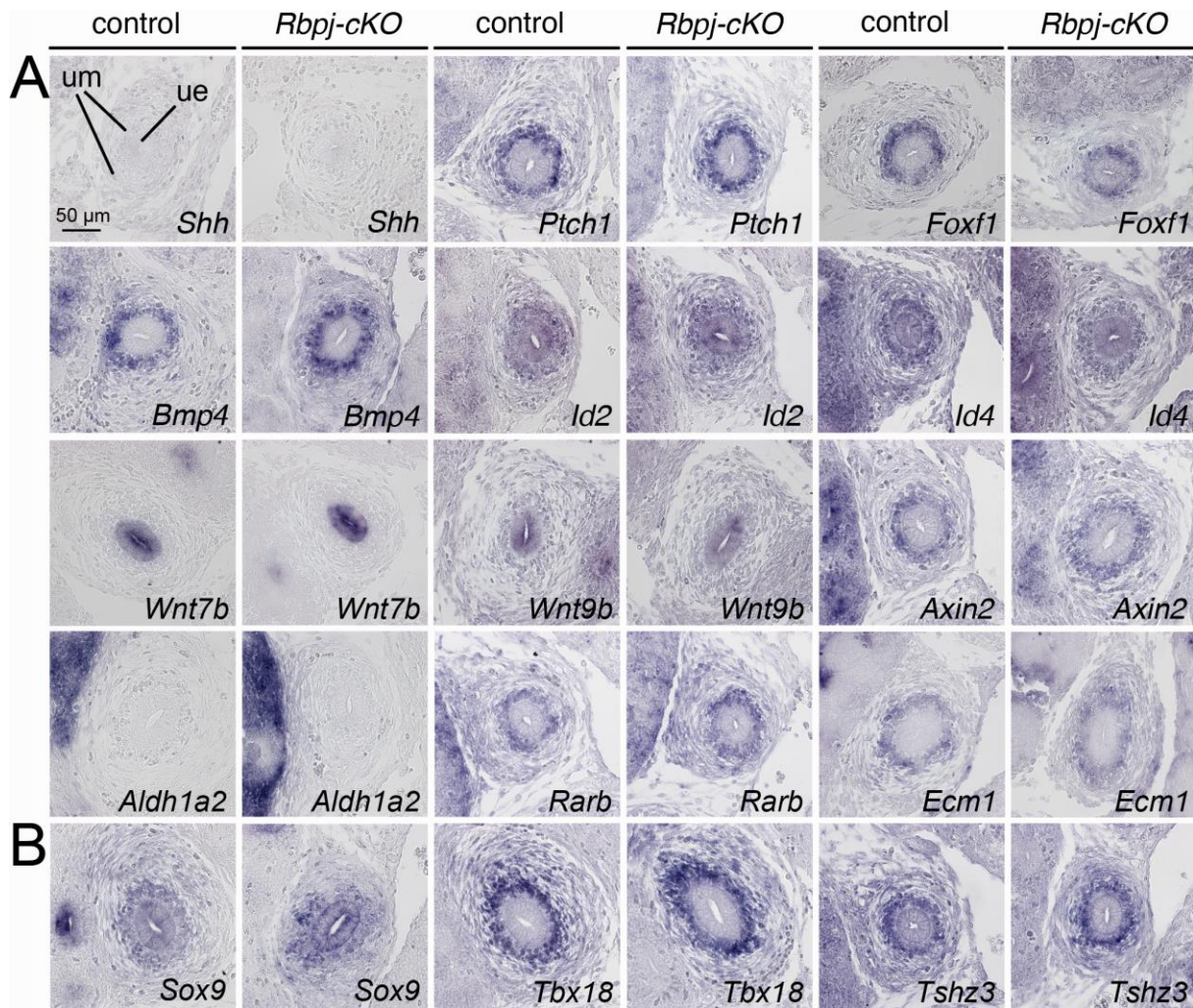


**Fig. S4. RNA *in situ* hybridization analysis of candidate genes with increased expression in microarrays of E14.5 *Rbpj-cKO* ureters.** RNA *in situ* hybridization of selected candidate genes with increased expression in microarrays of E14.5 *Rbpj-cKO* ureters were performed on transverse sections of the proximal ureter region. Numbers refer to fold increase in the microarray.  $n \geq 3$  for all probes. ue, ureteric epithelium; um, ureteric mesenchyme.



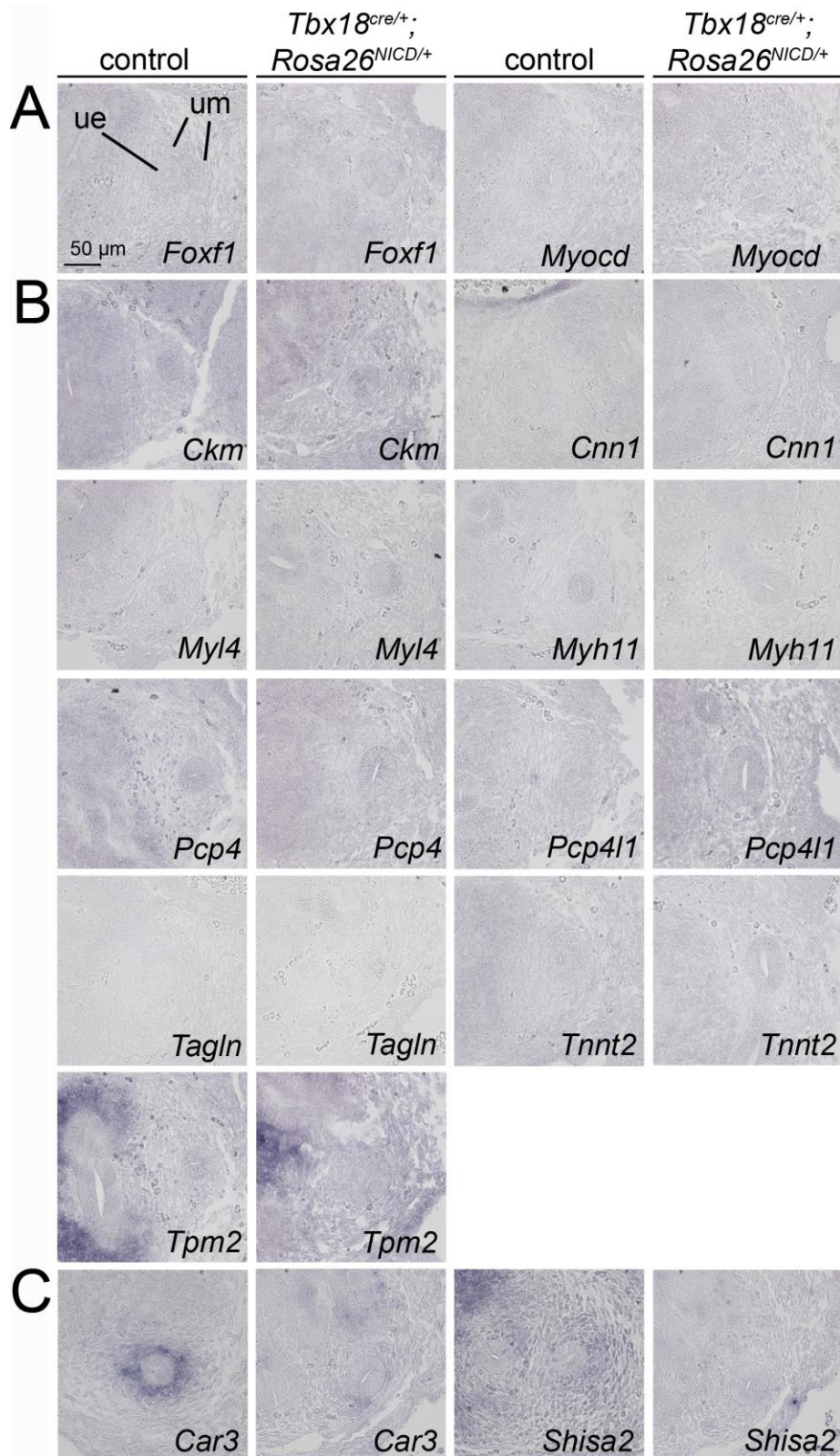


**Fig. S5. RNA *in situ* hybridization analysis of candidate genes with decreased expression in microarrays of E14.5 *Rbpj-cKO* ureters.** RNA *in situ* hybridization of selected candidate genes with decreased expression in microarrays of E14.5 *Rbpj-cKO* ureters were performed on transverse sections of the proximal ureter region. Numbers refer to fold increase in the microarray.  $n \geq 3$  for all probes. ue, ureteric epithelium; um, ureteric mesenchyme.



**Fig. S6. Signaling pathways and transcription factor genes relevant for SMC differentiation are unchanged in their activity/expression in *Rbpj-cKO* ureters at E14.5.** (A,B) RNA *in situ* hybridization analysis of *Shh*, its target gene *Ptch1* and its effector gene *Foxf1*; of *Bmp4*, its target genes *Id2* and *Id4*; of *Wnt7b* and *Wnt9b*, and the WNT target gene *Axin2*; of the gene encoding the RA synthesizing enzyme *Aldh1a2*, and the targets of RA signaling activity in the UM, *Rarb* and *Ecm1* (A) and of the transcription factor genes *Sox9*, *Tbx18* and *Tshz3* (B) on transverse sections of the proximal ureter of control and *Rbpj-cKO* embryos at E14.5. Genotypes, probes and fold change in the microarray are shown.  $n \geq 3$  for all probes. ue, ureteric epithelium; um, ureteric mesenchyme.





**Fig. S7. Ectopic expression of the Notch1 intracellular domain (NICD) does not induce expression of SMC regulatory and structural genes in the UM.** (A) RNA *in situ* hybridization analysis on transverse sections of E12.5 *Tbx18<sup>cre/+</sup>; Rosa26<sup>NICD/+</sup>* ureters for expression of SMC regulatory genes (A), SMC structural genes (B) and genes with reduced expression in E14.5 *Rbpj-cKO* microarray, *Car3* and *Shisa2* (C); n=3 for all probes. ue, ureteric epithelium; um, ureteric mesenchyme.



Gene	Forward primer	Reverse primer
<i>Ckm</i>	5'-CCCAGGTCACCCCTTCATC-3'	5'-CGGTCTTATGCTTGTCTGTGG-3'
<i>Foxf1</i>	5'-CAAGGCATCCCTCGGTATCA-3'	5'-AGATCCTCCGCCTGTTGTATG-3'
<i>Gapdh</i>	5'-ATGACATCAAGAAGGTGGTG-3'	5'-CATAACCAGGAAATGAGCTTG-3'
<i>Myocd</i>	5'-CACACCTCAAAGAACCAAATGAAC	5'-TTTTGACAGGGGATAGAGGGG-3'
<i>Pcp4</i>	5'-TGAGAGACAAAGTGCCGGAG-3'	5'-TGGACTTTCTTCTGCCCATCA-3'
<i>Pcp4l1</i>	5'-GCGAGCTTAACACCAAACAC-3'	5'-CCAGGCTTCCCTTTTTCCTC-3'
<i>Ppia</i>	5'-GATTCATGTGCCAGGGTGGT-3'	5'-GCCATTCAGTCTTGGCAGTG-3'
<i>Tagln</i>	5'-AGATGGAACAGGTGGCTCAA-3'	5'-TGCTGCCATATCCTTACCTTCA-3'
<i>Tnnt2</i>	5'-GAGGCCAACGTAGAAGAGGT-3'	5'-CTCTCCATCGGGGATCTTGG-3'
<i>Tpm2</i>	5'-ATGTGGCCTCTCTGAACCG-3'	5'-TCCTCTCTCGCTCTCATCCG-3'

**Table S1. Primer for qRT-PCR analysis of gene expression.**

Part – 3 Notch signaling in SMC differentiation

GeneName	Intensities				Fold change (FC)		
	control 1	mutant 1	control 2	mutant 2	FC1	FC2	FC_avg
<i>Myh6</i>	949	170	1109	200	-5,6	-5,6	-5,6
<i>Wfdc18</i>	518	96	401	98	-5,4	-4,1	-4,7
<i>Colec11</i>	737	135	527	147	-5,5	-3,6	-4,5
<i>A_55_P2145656</i>	733	200	873	193	-3,7	-4,5	-4,1
<i>Mc4r</i>	334	110	298	81	-3,0	-3,7	-3,3
<i>Prg4</i>	248	75	172	50	-3,3	-3,4	-3,3
<i>Pcp4</i>	37026	10851	36156	11506	-3,4	-3,1	-3,3
<i>Rergl</i>	812	225	730	280	-3,6	-2,6	-3,1
<i>P2ry14</i>	198	70	204	61	-2,8	-3,4	-3,1
<i>Ccl11</i>	1129	381	985	319	-3,0	-3,1	-3,0
<i>Heyl</i>	872	279	777	295	-3,1	-2,6	-2,9
<i>Ckm</i>	1330	492	1212	412	-2,7	-2,9	-2,8
<i>Myl4</i>	6953	2163	6056	2634	-3,2	-2,3	-2,8
<i>Myo18b</i>	197	78	222	78	-2,5	-2,9	-2,7
<i>Rhoa</i>	9392	3376	13259	5642	-2,8	-2,3	-2,6
<i>Rps6ka3</i>	622	350	1545	473	-1,8	-3,3	-2,5
<i>Pcp4l1</i>	2414	1041	2570	950	-2,3	-2,7	-2,5
<i>Sym</i>	177	99	201	64	-1,8	-3,1	-2,5
<i>Gm3646</i>	272	80	206	137	-3,4	-1,5	-2,5
<i>Plin4</i>	228	83	230	107	-2,7	-2,2	-2,4
<i>Dclk3</i>	399	121	222	144	-3,3	-1,5	-2,4
<i>Rbpj</i>	5235	1695	4093	2327	-3,1	-1,8	-2,4
<i>Tnmd</i>	189	82	161	64	-2,3	-2,5	-2,4
<i>Lgi1</i>	429	157	397	198	-2,7	-2,0	-2,4
<i>Scrt1</i>	248	109	271	111	-2,3	-2,4	-2,4
<i>Akr1c18</i>	904	347	644	356	-2,6	-1,8	-2,2
<i>Fgf5</i>	205	107	261	105	-1,9	-2,5	-2,2
<i>Cntfr</i>	353	180	566	233	-2,0	-2,4	-2,2
<i>Cav3</i>	1655	959	1929	728	-1,7	-2,7	-2,2
<i>Art3</i>	192	114	257	97	-1,7	-2,7	-2,2
<i>Dpp8</i>	1894	1037	2352	950	-1,8	-2,5	-2,2
<i>Rbfox3</i>	994	498	981	425	-2,0	-2,3	-2,1
<i>Sntg2</i>	1360	670	1676	745	-2,0	-2,3	-2,1
<i>Tnnt2</i>	18032	9028	16990	7696	-2,0	-2,2	-2,1
<i>Tnnc1</i>	229	97	246	135	-2,4	-1,8	-2,1
<i>Calca</i>	288	117	212	132	-2,5	-1,6	-2,0
<i>1700061G19Rik</i>	322	167	390	183	-1,9	-2,1	-2,0
<i>Fabp3</i>	681	360	759	356	-1,9	-2,1	-2,0
<i>Angpt1</i>	443	224	552	272	-2,0	-2,0	-2,0
<i>Thsd7b</i>	167	75	175	99	-2,2	-1,8	-2,0
<i>Smim12</i>	209	136	308	125	-1,5	-2,5	-2,0
<i>Ramp1</i>	559	353	627	261	-1,6	-2,4	-2,0
<i>Angptl7</i>	1756	891	1642	829	-2,0	-2,0	-2,0
<i>Akap5</i>	195	82	155	99	-2,4	-1,6	-2,0
<i>Scx</i>	301	144	331	179	-2,1	-1,8	-2,0
<i>Myrip</i>	158	75	174	97	-2,1	-1,8	-1,9
<i>Aspn</i>	14889	7352	13827	7598	-2,0	-1,8	-1,9
<i>Tnnc2</i>	752	406	797	401	-1,9	-2,0	-1,9
<i>Ddx6</i>	1380	788	2396	1152	-1,8	-2,1	-1,9
<i>Nrxn1</i>	556	245	501	321	-2,3	-1,6	-1,9
<i>Mup1</i>	159	102	170	77	-1,6	-2,2	-1,9
<i>6430519N07Rik</i>	401	217	428	223	-1,8	-1,9	-1,9
<i>Mamdc2</i>	234	123	249	135	-1,9	-1,8	-1,9
<i>Laptm4a</i>	40229	19736	37074	21835	-2,0	-1,7	-1,9
<i>Gm2115</i>	298	160	308	168	-1,9	-1,8	-1,8
<i>Synpo2</i>	7814	3775	8177	5163	-2,1	-1,6	-1,8
<i>C1qtnf3</i>	2404	1439	3512	1780	-1,7	-2,0	-1,8
<i>Ptger3</i>	264	145	196	110	-1,8	-1,8	-1,8
<i>Fgf10</i>	1072	558	1085	646	-1,9	-1,7	-1,8

Part – 3 Notch signaling in SMC differentiation

<i>Leprel1</i>	238	157	231	112	-1,5	-2,1	-1,8
<i>Egfl6</i>	995	558	939	540	-1,8	-1,7	-1,8
<i>Aoc3</i>	1385	821	1377	759	-1,7	-1,8	-1,8
<i>Rtf1</i>	176	94	188	116	-1,9	-1,6	-1,8
<i>Irx3</i>	317	181	272	156	-1,8	-1,7	-1,7
<i>Foxd1</i>	6048	3329	5662	3371	-1,8	-1,7	-1,7
<i>Htra4</i>	263	140	220	137	-1,9	-1,6	-1,7
<i>Ryr3</i>	863	509	977	550	-1,7	-1,8	-1,7
<i>Stac</i>	1433	796	1353	815	-1,8	-1,7	-1,7
<i>Mfap4</i>	16154	8353	23954	15803	-1,9	-1,5	-1,7
<i>Pilra</i>	216	116	228	145	-1,9	-1,6	-1,7
<i>Ifi202b</i>	1555	989	1848	1003	-1,6	-1,8	-1,7
<i>Rgs2</i>	35389	22839	35236	18947	-1,5	-1,9	-1,7
<i>Casq1</i>	262	161	243	136	-1,6	-1,8	-1,7
<i>Optc</i>	534	322	590	341	-1,7	-1,7	-1,7
<i>Sh3bgr</i>	6320	3931	6645	3736	-1,6	-1,8	-1,7
<i>Sync</i>	443	279	402	225	-1,6	-1,8	-1,7
<i>Col24a1</i>	456	265	446	271	-1,7	-1,6	-1,7
<i>Aard</i>	681	367	652	434	-1,9	-1,5	-1,7
<i>Fam134c</i>	774	480	839	485	-1,6	-1,7	-1,7
<i>Rrad</i>	150	100	160	87	-1,5	-1,8	-1,7
<i>Plac8</i>	2569	1497	2193	1356	-1,7	-1,6	-1,7
<i>Mustn1</i>	1951	1273	2280	1273	-1,5	-1,8	-1,7
<i>Fam212b</i>	190	122	190	108	-1,6	-1,8	-1,7
<i>Olf78</i>	124	79	140	80	-1,6	-1,7	-1,7
<i>Rtn4</i>	4029	2659	5259	3029	-1,5	-1,7	-1,6
<i>Des</i>	603	380	436	269	-1,6	-1,6	-1,6
<i>Mfn2</i>	396	257	401	244	-1,5	-1,6	-1,6
<i>Ldb3</i>	1183	727	1247	812	-1,6	-1,5	-1,6
<i>Actg2</i>	35735	22573	33264	21065	-1,6	-1,6	-1,6
<i>Gm9758</i>	225	148	219	134	-1,5	-1,6	-1,6
<i>Tpm2</i>	30764	19848	26106	16552	-1,5	-1,6	-1,6
<i>Itpkc</i>	174	112	175	111	-1,6	-1,6	-1,6
<i>Cited1</i>	2552	1616	3013	1985	-1,6	-1,5	-1,5

**Table S2A. Genes with decreased expression in microarrays of E18.5*Rbpj*-cKO ureters.** Shown are gene names, individual intensities of the two control and mutant samples and the individual and average fold change.

Part – 3 Notch signaling in SMC differentiation

GeneName_RCU	Intensities				Fold change (FC)		
	control 1	mutant 1	control 2	mutant 2	FC1	FC2	FC_avg
A_55_P2036952	81	694	70	795	8,5	11,3	9,9
Crhbp	82	179	32	418	2,2	13,2	7,7
TC1699341	96	373	74	470	3,9	6,3	5,1
Btb49	576	1493	159	976	2,6	6,2	4,4
Gdnf	64	224	98	267	3,5	2,7	3,1
Cyp2e1	217	650	193	587	3,0	3,0	3,0
Cntn6	238	799	364	874	3,4	2,4	2,9
Six2	86	290	191	406	3,4	2,1	2,8
Tac1	122	371	169	358	3,0	2,1	2,6
Grem2	57	188	98	166	3,3	1,7	2,5
Sostdc1	181	556	131	215	3,1	1,6	2,4
Cadps	318	687	341	810	2,2	2,4	2,3
Cntn4	167	381	174	376	2,3	2,2	2,2
AI314604	64	146	83	167	2,3	2,0	2,1
Otop2	163	275	139	346	1,7	2,5	2,1
A_55_P2097820	4760	10418	3846	7097	2,2	1,8	2,0
Scg3	91	143	76	184	1,6	2,4	2,0
Ahrr	176	391	237	415	2,2	1,8	2,0
Hey1	1417	3017	1617	2972	2,1	1,8	2,0
Retnlg	166	284	178	393	1,7	2,2	2,0
Kif26b	288	604	295	523	2,1	1,8	1,9
Scgb1c1	92	214	137	208	2,3	1,5	1,9
Nap1l2	226	381	225	469	1,7	2,1	1,9
Coch	79	156	98	174	2,0	1,8	1,9
Lrfn5	270	431	294	626	1,6	2,1	1,9
TC1726805	463	845	358	672	1,8	1,9	1,9
Crym	545	1020	586	1067	1,9	1,8	1,8
H2-T9	665	1034	462	982	1,6	2,1	1,8
Rnf39	91	175	84	148	1,9	1,8	1,8
Pisd-ps3	258	448	200	354	1,7	1,8	1,8
Khdrbs2	136	230	142	257	1,7	1,8	1,7
Itga4	1308	2453	1448	2322	1,9	1,6	1,7
Cux2	77	128	80	140	1,7	1,7	1,7
9330159M07Rik	134	226	137	234	1,7	1,7	1,7
Npy1r	352	578	391	678	1,6	1,7	1,7
Ppm1e	512	942	701	1060	1,8	1,5	1,7
Mpo	396	599	569	1045	1,5	1,8	1,7
Mmp8	88	149	114	187	1,7	1,6	1,7
Fbln7	89	161	104	159	1,8	1,5	1,7
Cutal	107	177	135	226	1,7	1,7	1,7
Zbtb43	201	318	156	271	1,6	1,7	1,7
Tanc1	159	248	137	236	1,6	1,7	1,6
Lama1	228	364	229	375	1,6	1,6	1,6
Kcnip4	181	305	180	278	1,7	1,5	1,6
Pitx1	195	293	170	268	1,5	1,6	1,5

**Table S2B. Genes with increased expression in microarrays of E18.5 Rbpj-cKO ureters.** Shown are gene names, individual intensities of the two control and mutant samples and the individual and average fold change.





Part – 3 Notch signaling in SMC differentiation

Annotation Cluster 1 Enrichment Score: 3.5503365006839274												
Category	Term	Count	%	PValue	Genes	List Total	Pop Hits	Pop Total	Fold Enrichment	Bonferroni	Benjamini	FDR
UP_KEYWORDS	Muscle protein	9	9.89010989	2.68E-11	TNNT2, ACTG2, MYL4, DES, TNNC2, TNNC1, MYH6, TPM2, CASQ1	90	52	22680	43.61638462	3.49E-09	3.49E-09	3.11E-08
GOTERM_BP_DIRECT	GO:0043462--regulation of ATPase activity	3	3.298703297	2.72E-04	TNNC1, MYH6, TPM2	79	6	18082	114.443038	0.194569806	0.052657597	0.417029306
KEGG_PATHWAY	mmu04260:Cardiac muscle contraction	5	5.494505495	3.84E-04	TNNT2, MYL4, TNNC1, MYH6, TPM2	36	77	7691	13.87265512	0.029535987	0.029535987	0.405754989
GOTERM_BP_DIRECT	GO:0060048--cardiac muscle contraction	4	4.395604396	0.001161449	TNNT2, MYL4, TNNC1, MYH6	79	48	18082	19.07383986	0.602566036	0.142546002	1.766314896
KEGG_PATHWAY	mmu04261:Adrenergic signalling in cardiomyocytes	5	5.494505495	0.003739656	TNNT2, MYL4, TNNC1, MYH6, TPM2	36	142	7691	7.522496088	0.253410622	0.135945963	3.8856445
GOTERM_MF_DIRECT	GO:0005200--structural constituent of ribosome	4	4.395604396	0.004271165	TNNT2, DES, SYNM, TPM2	74	78	17446	12.09009009	0.59122289	0.200402105	5.260180715
KEGG_PATHWAY	mmu05410:Hypertrophic cardiomyopathy	4	4.395604396	0.005389803	TNNT2, DES, TNNC1, TPM2	36	79	7691	10.81715883	0.343965375	0.131088416	5.556317913
KEGG_PATHWAY	mmu05414:Dilated cardiomyopathy	4	4.395604396	0.008185203	TNNT2, DES, TNNC1, TPM2	36	83	7691	10.29585007	0.383652295	0.11395364	6.352180684
GOTERM_BP_DIRECT	GO:0065010--ventricular cardiac muscle tissue morphogenesis	3	3.298703297	0.0064572	TNNT2, TNNC1, MYH6	79	28	18082	24.52350814	0.994163603	0.373498293	9.456636685
Annotation Cluster 2 Enrichment Score: 2.7965886269487434												
Category	Term	Count	%	PValue	Genes	List Total	Pop Hits	Pop Total	Fold Enrichment	Bonferroni	Benjamini	FDR
UP_KEYWORDS	Calmodulin-binding	6	6.593406593	2.21E-04	PCP4, RYR3, AKAP5, RRAD, ITPKC, MYH6	90	139	22680	10.87769784	0.028533285	0.009603018	0.257360401
GOTERM_MF_DIRECT	GO:0005516--calmodulin binding	6	6.593406593	9.90E-04	PCP4, RYR3, AKAP5, RRAD, ITPKC, MYH6	74	182	17446	7.772200772	0.187002014	0.098334992	1.242707296
UP_SEQ_FEATURE	region of interest/Calmodulin-binding	3	3.298703297	0.018632473	RRAD, ITPKC, MYH6	78	49	18012	14.13814757	0.999508022	0.172785004	22.64746234
Annotation Cluster 3 Enrichment Score: 2.5035663399204235												
Category	Term	Count	%	PValue	Genes	List Total	Pop Hits	Pop Total	Fold Enrichment	Bonferroni	Benjamini	FDR
UP_KEYWORDS	Secreted	19	20.87912088	8.16E-05	COL24A1	90	1685	22680	2.841543027	0.010628919	0.005328657	0.095077864
GOTERM_CC_DIRECT	GO:0005576--extracellular region	19	20.87912088	2.67E-04	COL24A1	83	1753	19662	2.567564038	0.039587449	0.01337388	0.319294494
UP_SEQ_FEATURE	signal peptide	26	28.57142857	9.04E-04	COL24A1, CASQ1	78	3124	18012	1.921895006	0.268605925	0.268605925	1.226756586
UP_KEYWORDS	Glycoprotein	26	28.57142857	0.006312548	AOC3, PILRA	90	3815	22680	1.717431183	0.502320481	0.109791723	6.022685223
UP_KEYWORDS	Signal	28	30.76923077	0.013508928	ASPEN, FGF5, MAMDC2, FGF10, CNTFR, ANGPTL7, CALCA, ART3, C1QTNF3, PCP4, ANGPTL1, LGH1, RAMP1, PILRA, OPTC, MUP1, EGFL6, PRG4, WFDC18, NRXN1, COLEC11, THSD7B, CCL11, MFAP4, CASQ1	90	4543	22680	1.553158706	0.831651309	0.224720082	14.66668256
UP_KEYWORDS	Disulfide bond	21	23.07692308	0.017112278	RAMP1, AOC3	90	3124	22680	1.693982074	0.699765329	0.222160051	18.23164304
UP_SEQ_FEATURE	disulfide bond	19	20.87912088	0.017310106	AOC3	78	2510	18012	1.748023291	0.997622582	0.779186114	21.21216322
UP_SEQ_FEATURE	glycosylation site/N-linked (GlcNAc...)	24	26.37362637	0.022343977	LGH1, MFAP4, COL24A1, CASQ1, PILRA, AOC3	78	3563	18012	1.555473996	0.999597854	0.728316089	26.54752045

Category	Term	Count	%	PValue	Genes	List Total	Pop Hits	Pop Total	Fold Enrichment	Bonferroni	Benjamini	FDR	
<b>Annotation Cluster 4</b> Enrichment Score: 2.279142260634431													
Category	Term	Count	%	PValue	Genes								
INTERPRO	IPR014715:Fibrinogen, alpha/beta/gamma chain, C-terminal globular, subdomain 2	3	3.296703297	0.003353848	ANGPTL7, ANGPTL1, MFAP4		22	20594	34.24722838	0.492881284	0.492881284	4.129921494	
SMART	SM00166:FBG	3	3.296703297	0.004339006	ANGPTL7, ANGPTL1, MFAP4		48	10425	29.61647727	0.212174707	0.212174707	4.1868683939	
INTERPRO	IPR014716:Fibrinogen, alpha/beta/gamma chain, C-terminal globular, subdomain 1	3	3.296703297	0.005790598	ANGPTL7, ANGPTL1, MFAP4		82	20594	25.98056601	0.690593907	0.443757164	7.031429246	
UP_SEQ_FEATURE	domain:Fibrinogen C-terminal	3	3.296703297	0.006796139	ANGPTL7, ANGPTL1, MFAP4		78	18012	23.8859416	0.9055317	0.692643042	8.890423294	
INTERPRO	IPR002181:Fibrinogen, alpha/beta/gamma chain, C-terminal globular domain	3	3.296703297	0.007020522	ANGPTL7, ANGPTL1, MFAP4		82	20594	23.54466951	0.759045429	0.377739079	8.465036894	
<b>Annotation Cluster 5</b> Enrichment Score: 2.210270970699543													
Category	Term	Count	%	PValue	Genes								
UP_KEYWORDS	Extracellular matrix	6	6.593406593	0.002344195	OPTC, ASPN, MAMDC2, EGF6, COL24A1, MFAP4		90	22680	6.434042553	0.26468038	0.059637654	2.699750154	
INTERPRO	IPR013320:Concavalin A-like lectin/glucanase, subgroup	5	5.494505495	0.009641725	MAMDC2, EGF6, RYR3, NRXN1, COL24A1		82	20594	5.951335106	0.858729448	0.386925983	11.45269411	
GOTERM_CC_DIRECT	GO:0005578-proteinaceous extracellular matrix	6	6.593406593	0.010352343	OPTC, ASPN, MAMDC2, EGF6, COL24A1, MFAP4		83	19662	4.497941132	0.792235812	0.269678412	11.6963456	
<b>Annotation Cluster 6</b> Enrichment Score: 1.6910146659217582													
Category	Term	Count	%	PValue	Genes								
GOTERM_CC_DIRECT	GO:0042383-sarcolemma	7	7.692307692	9.93E-06	CAV3, DES, RYR3, SYNC, SYNM, CASO1, SNTG2		83	19662	14.05288952	0.001497837	7.49E-04	0.011867272	
UP_SEQ_FEATURE	region of interest:Linker 1	3	3.296703297	0.032442871	DES, SYNC, SYNM		78	18012	10.4985035	0.99989931	0.759832796	36.25635595	
UP_SEQ_FEATURE	region of interest:Coil 1B	3	3.296703297	0.032442871	DES, SYNC, SYNM		78	18012	10.4985035	0.99989931	0.759832796	36.25635595	
UP_SEQ_FEATURE	region of interest:Coil 1A	3	3.296703297	0.032442871	DES, SYNC, SYNM		78	18012	10.4985035	0.99989931	0.759832796	36.25635595	
UP_SEQ_FEATURE	region of interest:Rod	3	3.296703297	0.033350141	DES, SYNC, SYNM		78	18012	10.33983927	0.99991999	0.72854734	37.06762252	
UP_KEYWORDS	Intermediate filament	3	3.296703297	0.035118632	DES, SYNC, SYNM		90	22680	10.08	0.990751239	0.302499114	34.09102804	
UP_SEQ_FEATURE	region of interest:Head	3	3.296703297	0.035194274	DES, SYNC, SYNM		78	18012	10.04013378	0.99995668	0.710519322	38.68720836	
INTERPRO	IPR001664:Intermediate filament protein	3	3.296703297	0.03707209	DES, SYNC, SYNM		82	76	9.913671374	0.999405293	0.710009425	36.97373178	
UP_SEQ_FEATURE	region of interest:Tail	3	3.296703297	0.04164266	DES, SYNC, SYNM		78	71	18012	9.757313109	0.99997898	0.695296796	40.30094634
SMART	SM01391:SMO1391	3	3.296703297	0.04164266	DES, SYNC, SYNM		48	10425	9.049479167	0.903654591	0.541534082	34.19008946	
GOTERM_MF_DIRECT	GO:0005198-structural molecule activity	4	4.395604396	0.07636989	DES, SYNC, SYNM		74	236	3.95877233	0.99999938	0.641951157	63.31909193	
GOTERM_CC_DIRECT	GO:0005882-intermediate filament	3	3.296703297	0.085785939	DES, SYNC, SYNM		83	117	19662	6.074142725	0.999998687	0.619921118	65.777431
<b>Annotation Cluster 7</b> Enrichment Score: 1.4411822444299607													
Category	Term	Count	%	PValue	Genes								
INTERPRO	IPR001478:PDZ domain	4	4.395604396	0.022887431	LDB3, HTRA4, SYNPO2, SNTG2		82	154	20594	6.523281596	0.990693011	25.22427409	
SMART	SM00228:PDZ domain:PDZ	4	4.395604396	0.029856954	LDB3, HTRA4, SYNPO2, SNTG2		48	150	10425	5.791686667	0.811214938	0.565650597	25.78036357
UP_SEQ_FEATURE	domain:PDZ	3	3.296703297	0.069472148	LDB3, SYNPO2, SNTG2		78	101	18012	6.859101295	1	0.852863531	62.58470762
<b>Annotation Cluster 8</b> Enrichment Score: 1.375282655877302													
Category	Term	Count	%	PValue	Genes								
INTERPRO	IPR008160:Collagen triple helix repeat	3	3.296703297	0.036101722	C1QTNF3, COLEC11, COL24A1		82	76	20594	9.913671374	0.999405293	0.710009425	36.97373178
UP_KEYWORDS	Collagen	3	3.296703297	0.044063229	C1QTNF3, COLEC11, COL24A1		90	85	22680	8.894117647	0.957269634	0.344046698	40.87418352
GOTERM_CC_DIRECT	GO:0005581-collagen trimer	3	3.296703297	0.047048718	C1QTNF3, COLEC11, COL24A1		83	83	19662	8.562345769	0.999308686	0.454694818	43.79406897
<b>Annotation Cluster 9</b> Enrichment Score: 1.366768138115769													
Category	Term	Count	%	PValue	Genes								
GOTERM_BP_DIRECT	GO:0030819-positive regulation of cAMP biosynthetic process	4	4.395604396	0.001233375	PTGER3, AKAP5, MC4R, RAMP1		79	49	18082	18.68457763	0.624653072	0.130629909	1.874734632
UP_KEYWORDS	Lipoprotein	6	6.593406593	0.191873122	ART3, PTGER3, AKAP5, MC4R, RHOA, CNTFR		90	780	22680	1.938461538	1	0.752262893	91.66157139
UP_KEYWORDS	Palmitate	3	3.296703297	0.335417825	PTGER3, AKAP5, MC4R		90	304	22680	2.486842105	1	0.88246827	99.1475411
<b>Annotation Cluster 10</b> Enrichment Score: 1.1555715155703252													
Category	Term	Count	%	PValue	Genes								
KEGG_PATHWAY	mmu04020:Calcium signaling pathway	5	5.494505495	0.008623684	PTGER3, TNNC2, TNNC1, RYR3, ITPKC		36	180	7691	5.93441358	0.491130908	0.126382722	8.754384703
INTERPRO	IPR002048:EF-hand domain	4	4.395604396	0.057803149	MYL4, TNNC2, TNNC1, RYR3		82	223	20594	4.504867111	0.999994021	0.777629784	52.64516833
UP_SEQ_FEATURE	domain:EF-hand 3	3	3.296703297	0.05787452	MYL4, TNNC2, TNNC1		78	91	18012	7.61284669	0.999999999	0.82074596	55.69056984
INTERPRO	IPR011992:EF-hand-like domain	4	4.395604396	0.092767953	MYL4, TNNC2, TNNC1, RYR3		82	273	20594	3.679799875	0.999999997	0.887536243	70.54355725
GOTERM_MF_DIRECT	GO:00051015-actin filament binding	3	3.296703297	0.105620272	MYL4, TNNC2, TNNC1		74	132	17446	5.358108108	1	0.902891745	75.56568344
UP_SEQ_FEATURE	domain:EF-hand 2	3	3.296703297	0.169013203	MYL4, TNNC2, TNNC1		78	173	18012	4.094446241	1	0.981751679	92.01665214
UP_SEQ_FEATURE	domain:EF-hand 1	3	3.296703297	0.170530383	MYL4, TNNC2, TNNC1		78	174	18012	3.981432361	1	0.977748925	92.21337711

**Table S3B. Clustering of functional annotations of genes with decreased expression in the microarray of E18.5 Rbpj-cKO ureters.** Functional clustering was performed on functional annotation terms by DAVID 6.8 web software (<https://david.ncifcrf.gov>) for 93 genes with decreased expression in the microarray of E18.5 Rbpj-cKO ureters. Shown are the top 10 clusters.

Category	Term	Count %	PValue	Genes	List Total	Pop	Hits	Pop	Total	Fold	Enrichmen	Bonferroni	Benjamini	FDR
GOTERM_BP_DIREC	GO:0007155--cell adhesion	5	12,19512195	LAMA1, CNTN6, FBLN7, CNTN4,	33	485	18082	5,648859731	0,96246567	0,96246567	0,96246567	0,96246567	12,86340624	
GOTERM_BP_DIREC	GO:0003337--mesenchymal to epithelial transition	2	4,87804878	SIX2, GDNF	33	7	18082	156,5541126	0,981558214	0,981558214	0,864199464	0,864199464	15,42257772	
GOTERM_BP_DIREC	involved in metanephros morphogenesis	2	4,87804878	SIX2, GDNF	33	9	18082	121,7643098	0,994108924	0,994108924	0,819394261	0,819394261	19,37591083	
GOTERM_BP_DIREC	GO:0030432--peristalsis	3	7,317073171	NPY1R, GDNF	33	139	18082	11,82603009	0,999714984	0,999714984	0,870067688	0,870067688	28,99483544	
GOTERM_BP_DIREC	GO:0031175--neuron projection development	3	7,317073171	LAMA1, CNTN4,	33	149	18082	11,03233679	0,999908465	0,999908465	0,844289673	0,844289673	32,29855841	
GOTERM_BP_DIREC	GO:0009948--axon guidance	2	4,87804878	LAMA1, CNTN4,	33	22	18082	49,81267218	0,999996473	0,999996473	0,8766623159	0,8766623159	40,94235603	
GOTERM_BP_DIREC	GO:0007411--axon guidance	2	4,87804878	HEY1, SIX2	33	24	18082	45,66161616	0,999988874	0,999988874	0,858682039	0,858682039	43,70507939	
GOTERM_BP_DIREC	GO:0006805--xenobiotic metabolic process	2	4,87804878	AHR, CYP2E1	33	27	18082	40,58810325	0,999999797	0,999999797	0,854317968	0,854317968	47,60926075	
GOTERM_BP_DIREC	GO:0035987--endodermal cell differentiation	2	4,87804878	MMP8, ITGA4	33	34	18082	32,23172906	0,999999996	0,999999996	0,884286544	0,884286544	55,70037288	
GOTERM_BP_DIREC	GO:0007616--long-term memory	2	4,87804878	TAC1, BTBD9	33	38	18082	28,83891547	1	1	0,885772707	0,885772707	59,75089253	
GOTERM_BP_DIREC	GO:0001656--metanephros development	2	4,87804878	SIX2, GDNF	33	44	18082	24,90633609	1	1	0,898137624	0,898137624	65,14434869	
GOTERM_BP_DIREC	GO:0051496--positive regulation of stress fiber assembly	2	4,87804878	PPM1E, TAC1	33	46	18082	23,82345191	1	1	0,887980448	0,887980448	66,77684322	
GOTERM_BP_DIREC	GO:0030514--negative regulation of BMP signaling pathway	2	4,87804878	SOSTDC1, GREM2	33	579	18082	3,785418956	1	1	0,87888333	0,87888333	68,37337719	
GOTERM_BP_DIREC	GO:0045892--negative regulation of transcription, DNA-templated	2	9,756097561	AHR, HEY1, PITY1,	33	54	18082	20,29405163	1	1	0,889547255	0,889547255	72,57866832	
GOTERM_BP_DIREC	GO:0003151--outflow tract morphogenesis	2	4,87804878	CUX2, PITY1, NPY1R	33	54	18082	20,29405163	1	1	0,889547255	0,889547255	72,57866832	

**Table S4A. Functional annotation of genes with increased expression in the microarray of E18.5 Rbpj-cKO ureters.** Functional annotation was performed by DAVID 6.8 web software (<https://david.ncifcrf.gov>) for 45 genes with decreased expression in the microarray of E18.5 Rbpj-cKO ureters.

Part – 3 Notch signaling in SMC differentiation

Annotation Cluster 1 Enrichment Score: 3.258991348465056												
Category	Term	Count	%	PValue	Genes	List Total	Pop Hits	Pop Total	Fold Enrichment	Bonferroni	Benjamini	FDR
UP_KEYWORDS	Secreted	12	29.26829288	5.17E-05	COCH, SCGB1C1, LAMA1, CRHBP, SOSTDC1, MMP8, FBLN7, SCG3, TAC1, CNTN4, GREM2, GDNF	38	1685	22680	4.250507575	0.005100773	0.005100773	0.057208569
UP_SEQ_FEATURE	signal peptide	17	41.46341463	6.00E-05	COCH, CNTN6, CRHBP, MMP8, TAC1, RETNLG, ITGA4, GREM2, GDNF, SCGB1C1, LAMA1, SOSTDC1, FBLN7, SCG3, MPO, CNTN4, LRFN5	35	3124	18012	2.800475581	0.011807791	0.011807791	0.075039559
GOTERM_CC_DIRECT	GO:0005576-extracellular region	12	29.26829288	2.02E-04	COCH, SCGB1C1, LAMA1, CRHBP, SOSTDC1, MMP8, FBLN7, SCG3, TAC1, CNTN4, GREM2, GDNF	37	1753	19662	3.637686746	0.012638993	0.012638993	0.204223467
UP_KEYWORDS	Disulfide bond	15	36.58536585	2.31E-04	COCH, CNTN6, CRHBP, MMP8, NPY1R, ITGA4, GREM2, GDNF, LAMA1, H2-T9, SOSTDC1, FBLN7, MPO, CNTN4, LRFN5	38	3124	22680	2.865759148	0.022645312	0.011387494	0.255991551
UP_KEYWORDS	Signal	18	43.90243902	3.31E-04	COCH, CNTN6, CRHBP, MMP8, TAC1, RETNLG, ITGA4, GREM2, GDNF, SCGB1C1, LAMA1, H2-T9, SOSTDC1, FBLN7, SCG3, MPO, CNTN4, LRFN5	38	4543	22680	2.364771714	0.032227918	0.010860155	0.365906311
GOTERM_CC_DIRECT	GO:0005615-extracellular space	10	24.3802439	0.001241024	COCH, LAMA1, CRHBP, SOSTDC1, MMP8, MPO, TAC1, RETNLG, GREM2, GDNF, COCH, CNTN6, CRHBP, MMP8, NPY1R, ITGA4, GREM2, GDNF, LAMA1, SOSTDC1, FBLN7, MPO, CNTN4	37	1504	19662	3.533280621	0.075251118	0.038361356	1.2495128
UP_SEQ_FEATURE	disulfide bond	13	31.70731707	0.001454282	COCH, CNTN6, CRHBP, MMP8, NPY1R, ITGA4, GREM2, GDNF, LAMA1, SOSTDC1, FBLN7, MPO, CNTN4, LRFN5	35	2510	18012	2.665406844	0.250353511	0.13417872	1.804610132
UP_KEYWORDS	Glycoprotein	14	34.14634146	0.005468321	COCH, CNTN6, CRHBP, MMP8, NPY1R, ITGA4, GREM2, GDNF, LAMA1, SOSTDC1, FBLN7, MPO, CNTN4, LRFN5	38	3815	22680	2.190246258	0.4200656	0.127340707	5.914753198
UP_SEQ_FEATURE	glycosylation site:N-linked (GlcNAc...)	14	34.14634146	0.009842038	COCH, CNTN6, CRHBP, MMP8, NPY1R, ITGA4, GREM2, GDNF, LAMA1, SOSTDC1, FBLN7, MPO, CNTN4, LRFN5	35	3563	18012	2.022116194	0.85891274	0.479408866	11.64141232
Annotation Cluster 2 Enrichment Score: 1.0328126159661437												
Category	Term	Count	%	PValue	Genes	List Total	Pop Hits	Pop Total	Fold Enrichment	Bonferroni	Benjamini	FDR
UP_KEYWORDS	Calcium	6	14.63414634	0.010554404	CADPS, MMP8, FBLN7, MPO, ITGA4, KCNIP4	38	827	22680	4.330172469	0.650215891	0.160604418	11.09009732
UP_KEYWORDS	Metal-binding	9	21.95121951	0.179592951	CADPS, PPM1E, RNF39, MMP8, MPO, ITGA4, CYP2E1, KCNIP4, ZBTB43	38	3395	22680	1.58220293	0.999999997	0.753359197	88.84194468
GOTERM_MF_DIRECT	GO:0046872-metal ion binding	8	19.51219512	0.420570847	CADPS, PPM1E, MMP8, MPO, ITGA4, CYP2E1, KCNIP4, ZBTB43	33	3355	17446	1.260606061	1	0.998662237	99.75758797
Annotation Cluster 3 Enrichment Score: 0.8721611608459209												
Category	Term	Count	%	PValue	Genes	List Total	Pop Hits	Pop Total	Fold Enrichment	Bonferroni	Benjamini	FDR
INTERPRO	IPR013098:immunoglobulin I-set	3	7.317073171	0.028631425	CNTN6, CNTN4, LRFN5	38	147	20594	11.06015038	0.971102916	0.971102916	28.42783821
INTERPRO	IPR003961:Fibronectin, type III	3	7.317073171	0.05505221	CNTN6, CNTN4, LRFN5	38	211	20594	7.705412821	0.999000568	0.900018935	47.89807883
INTERPRO	IPR003598:immunoglobulin subtype 2	3	7.317073171	0.070020058	CNTN6, CNTN4, LRFN5	38	242	20594	6.718355807	0.99857512	0.890744266	56.6473856
SMART	SM004081:IG2	3	7.317073171	0.113661152	CNTN6, CNTN4, LRFN5	26	242	10425	4.970597584	0.900955353	0.900955353	66.620847
UP_KEYWORDS	immunoglobulin domain	3	7.317073171	0.18480096	CNTN6, CNTN4, LRFN5	38	481	22680	3.722507933	0.999999998	0.717548494	89.60202208
INTERPRO	IPR007110:immunoglobulin-like domain	4	9.756097561	0.228152812	H2-T9, CNTN6, CNTN4, LRFN5	38	920	20594	2.356292906	1	0.989039467	94.92924002
INTERPRO	IPR003599:immunoglobulin subtype	3	7.317073171	0.238374095	CNTN6, CNTN4, LRFN5	38	518	20594	3.138691323	1	0.984276072	95.65076066
INTERPRO	IPR013783:immunoglobulin-like fold	4	9.756097561	0.31614347	H2-T9, CNTN6, CNTN4, LRFN5	38	1099	20594	1.972510895	1	0.994207596	98.74153303
SMART	SM00409:IG	3	7.317073171	0.354832985	CNTN6, CNTN4, LRFN5	26	518	10425	2.322171072	0.999999962	0.996644649	98.14147423

Annotation Cluster 4	Enrichment Score: 0.8319786054424863	Count %	PValue	Genes	List Total	Pop Hits	Pop Total	Fold Enrichment	Bonferroni	Benjamini	FDR	
Category	Term											
UP_KEYWORDS	GO:0045892--negative regulation of transcription, DNA-templated	3	7.317073171	0.04307166	SDX2, CUJX2, PITX1	38	184	20594	8.930989386	0.996372751	0.931976115	39.7903062
UP_KEYWORDS	GO:0009787-RNA polymerase II core promoter proximal region	3	7.317073171	0.045212579	SDX2, CUJX2, PITX1	35	180	18012	8.771472687	0.998834919	0.938753333	43.95128302
UP_KEYWORDS	GO:0003682-DNA-binding	5	12.195121956	0.073308492	HEY1, SDX2, GREN2, PITX1, KIF26B	38	976	22880	3.057952752	0.998467177	0.967200337	56.97738485
UP_KEYWORDS	GO:0045892--negative regulation of transcription, DNA-templated	3	7.317073171	0.076278325	SDX2, CUJX2, PITX1	38	280	22880	6.394739842	0.998612232	0.944112974	59.4804003
GOTERM_BP_DIRECT	GO:0009787-RNA polymerase II promoter	4	9.756097561	0.0819593	AHRH, HEY1, CUJX2, PITX1	33	579	18082	3.795418996	1	0.989561876	68.37337719
INTERPRO	IPR015658-Homocysteine S-methyltransferase	3	7.317073171	0.085054807	SDX2, CUJX2, PITX1	38	271	20594	5.999417953	0.999380657	0.985794564	64.07820349
GOTERM_BP_DIRECT	GO:0002735-multicellular organism development	5	12.195121956	0.108398393	HEY1, SDX2, GREN2, PITX1, KIF26B	33	1029	18082	2.692384907	1	0.999276566	78.05080561
GOTERM_BP_DIRECT	GO:0045892--negative regulation of transcription, DNA-templated	4	9.756097561	0.108800342	HEY1, SDX2, CUJX2, PITX1	33	653	17446	3.540703635	0.999885759	0.996227545	71.90772506
UP_KEYWORDS	GO:0003682-DNA-binding	6	14.63414634	0.11135858	AHRH, HEY1, SDX2, CUJX2, ZBTB43, PITX1	38	1004	22880	2.529270454	0.999595726	0.974992577	74.92871933
UP_KEYWORDS	GO:0003682-DNA-binding	3	7.317073171	0.122859356	SDX2, CUJX2, PITX1	38	346	20594	4.712583812	0.999599939	0.937200894	73.13990606
UP_KEYWORDS	GO:0003682-DNA-binding	3	7.317073171	0.132754103	SDX2, CUJX2, PITX1	28	206	10425	4.522122614	0.996131463	0.937802354	72.61775539
GOTERM_BP_DIRECT	GO:0001022--negative regulation of transcription from RNA polymerase II promoter	4	9.756097561	0.137043255	AHRH, HEY1, CUJX2, CRYM1	33	729	18082	3.005226197	1	0.999932934	86.34178512
GOTERM_BP_DIRECT	GO:0009787-RNA polymerase II core promoter proximal region	3	7.317073171	0.140162556	SDX2, CUJX2, PITX1	33	389	17446	4.417827238	0.999999965	0.974313808	81.10957722
UP_KEYWORDS	GO:0003682-DNA-binding	6	14.63414634	0.160332359	PITX1	38	1799	22880	1.960579502	0.999999985	0.749884597	86.06005682
UP_KEYWORDS	GO:0003682-DNA-binding	6	14.63414634	0.162411922	PITX1	38	1859	22880	1.920532777	0.999999988	0.736233208	89.32182196
GOTERM_BP_DIRECT	GO:0006355--regulation of transcription, DNA-templated	7	17.07317073	0.209084984	PITX1	33	2279	18082	1.683008231	1	0.999920537	95.79108715
GOTERM_BP_DIRECT	GO:0006351--transcription, DNA-templated	6	14.63414634	0.230739837	PITX1	33	1885	18082	1.744104172	1	0.999999571	97.39838082
GOTERM_BP_DIRECT	GO:0003677-DNA binding	6	14.63414634	0.246679002	AHRH, HEY1, SDX2, ZBTB43, PITX1	33	1847	17446	1.717379534	1	0.98973928	96.61070414
GOTERM_BP_DIRECT	GO:0045944--positive regulation of transcription from RNA polymerase II promoter	4	9.756097561	0.266942381	HEY1, SDX2, GDNF, PITX1	33	995	18082	2.202771433	1	0.999929705	98.18915721
UP_KEYWORDS	GO:0003700--transcription factor activity, sequence-specific DNA binding	9	21.95121951	0.46621104	NAP1L2, CUJX2, ZBTB43, PITX1	38	4534	22880	1.184732895	1	0.982143783	99.9051772
GOTERM_MF_DIRECT	GO:0003700--transcription factor activity, sequence-specific DNA binding	3	7.317073171	0.487716285	HEY1, SDX2, PITX1	33	893	17446	1.79614949	1	0.989244931	99.93637821
GOTERM_CC_DIRECT	GO:0005934-nucleus	12	29.28829288	0.566591379	PITX1	37	6019	19662	1.059455687	1	0.988509693	99.97841604
Annotation Cluster 5	Enrichment Score: 0.4589159505189517	Count %	PValue	Genes	List Total	Pop Hits	Pop Total	Fold Enrichment	Bonferroni	Benjamini	FDR	
UP_KEYWORDS	GO:0003682-DNA-binding	3	7.317073171	0.280061682	MPO, CYP2E1, CRYM1	38	639	22880	2.802075012	1	0.852444665	97.37536304
GOTERM_BP_DIRECT	GO:0016491--oxidoreductase activity	3	7.317073171	0.304456933	MPO, CYP2E1, CRYM1	33	604	17446	2.625827815	1	0.993479237	98.18309544
GOTERM_BP_DIRECT	GO:005114--oxidation-reduction process	3	7.317073171	0.337425171	MPO, CYP2E1, CRYM1	33	676	18082	2.431683701	1	0.999994151	98.61505996
GOTERM_CC_DIRECT	GO:0005739-mitochondrion	4	9.756097561	0.621230375	PFM1E, MPO, CYP2E1, CRYM1	37	1721	19662	1.235108438	1	0.988881529	98.99461996
Annotation Cluster 6	Enrichment Score: 0.29253511593598636	Count %	PValue	Genes	List Total	Pop Hits	Pop Total	Fold Enrichment	Bonferroni	Benjamini	FDR	
UP_KEYWORDS	GO:0003682-DNA-binding	12	29.28829288	0.138688856	KCNIP4	38	4779	22880	1.498601909	0.999999914	0.707874348	80.84193025
UP_KEYWORDS	GO:0003682-DNA-binding	11	26.82928293	0.38593028	TAC1, CNTN4, NPY1R, LRFN5, GDNF, KCNIP4	35	4891	18012	1.206760696	1	0.999999997	99.79103217
GOTERM_CC_DIRECT	GO:0002885--plasma membrane	8	19.51219512	0.824589195	NPY1R, KCNIP4	37	4874	19662	0.872228815	1	0.999982707	99.99999778
GOTERM_CC_DIRECT	GO:0018020-membrane	11	26.82928293	0.877287834	KCNIP4	37	6988	19662	0.835304295	1	0.989983617	99.99999994
UP_KEYWORDS	GO:0003682-DNA-binding	5	12.195121956	0.8831331	CNTN6, TANC1, CNTN4, NPY1R, KCNIP4	38	3759	22880	0.793884152	1	0.989798737	100
Annotation Cluster 7	Enrichment Score: 0.020243619168367223	Count %	PValue	Genes	List Total	Pop Hits	Pop Total	Fold Enrichment	Bonferroni	Benjamini	FDR	
UP_KEYWORDS	GO:0003682-DNA-binding	13	31.70731707	0.815786168	NPY1R, LRFN5, KCNIP4	38	8883	22880	0.893791905	1	0.999311387	99.99999927
UP_KEYWORDS	GO:0003682-DNA-binding	3	7.317073171	0.938144684	ITGA4, NPY1R, LRFN5	35	2256	18012	0.684546605	1	0.999999999	100
UP_KEYWORDS	GO:0003682-DNA-binding	3	7.317073171	0.96093507	ITGA4, NPY1R, LRFN5	35	2850	18012	0.593071429	1	0.999999999	100
UP_KEYWORDS	GO:0003682-DNA-binding	7	17.07317073	0.985745548	NPY1R, LRFN5	38	6938	22880	0.602179691	1	0.999999901	100
UP_KEYWORDS	GO:0003682-DNA-binding	7	17.07317073	0.986080759	NPY1R, LRFN5	38	6995	22880	0.600703772	1	0.999999922	100
UP_KEYWORDS	GO:0003682-DNA-binding	4	9.756097561	0.99390742	OTOF2, ITGA4, NPY1R, LRFN5	35	4312	18012	0.477391996	1	0.999999999	100
GOTERM_CC_DIRECT	GO:0018021--integral component of membrane	7	17.07317073	0.995705247	NPY1R, LRFN5	37	6878	19662	0.540831323	1	0.999999999	100

**Table S4B. Clustering of functional annotations of genes with increased expression in the microarray of E18.5 Rbpj-cKO ureters.** Functional clustering was performed on functional annotation terms by DAVID 6.8 web software (<https://david.ncifcrf.gov>) for 45 genes with increased expression in the microarray of E18.5 Rbpj-cKO ureters. Shown are the top 10 clusters.



Part – 3 Notch signaling in SMC differentiation

gene	genotype	biological replicates				standard deviation	normalized biological replicates				standard deviation	Student's t-test-unpaired
		#1	#2	#3	mean		#1	#2	#3	mean		
<i>Ckm</i>	control	1,421	1,039	1	1,15333333	0,189937417	1,23208092	0,90086705	0,86705202	1	0,16468562	p = 0,0029
	<i>Rbpj-cKO</i>	0,283	0,27	0,292	0,28166667	0,009030811	0,24537572	0,23410405	0,25317919	0,24421965	0,00783018	
<i>Pcp4</i>	control	1,458	1,482	1	1,31333333	0,221776664	1,11015228	1,1284264	0,76142132	1	0,16886548	p = 0,0045
	<i>Rbpj-cKO</i>	0,329	0,444	0,394	0,389	0,04708149	0,25050761	0,33807107	0,3	0,29619289	0,03584885	
<i>Pcp4l1</i>	control	1,286	1,323	1	1,203	0,144335258	1,06899418	1,09975062	0,8312552	1	0,11997943	p = 0,0017
	<i>Rbpj-cKO</i>	0,421	0,433	0,441	0,43166667	0,008219219	0,34995844	0,3599335	0,36658354	0,35882516	0,00683227	
<i>Tagln</i>	control	1,059	0,995	1	1,018	0,02906315	1,04027505	0,97740668	0,98231827	1	0,02854926	p = 0,0019
	<i>Rbpj-cKO</i>	0,874	0,863	0,857	0,86466667	0,007039571	0,85854617	0,84774067	0,84184676	0,84937787	0,0069151	
<i>Tnn2</i>	control	1,165	1,16	1	1,10833333	0,076630426	1,05112782	1,04661654	0,90225564	1	0,06914023	p = 0,0040
	<i>Rbpj-cKO</i>	0,661	0,721	0,525	0,63566667	0,08199729	0,59639098	0,65052632	0,47368421	0,57353384	0,07398252	
<i>Tpm2</i>	control	1,021	1,027	1	1,016	0,011575837	1,00492126	1,01082677	0,98425197	1	0,01139354	p = 0,0394
	<i>Rbpj-cKO</i>	0,947	0,754	0,836	0,84566667	0,079087856	0,93208661	0,74212598	0,82283465	0,83234908	0,07784238	

**Table S5A. qRT-PCR analysis of SMC gene expression in control and *Rbpj-cKO* ureters at E18.5 (relates to Fig. 2I).**

gene	genotype	biological replicates				standard deviation	normalized biological replicates				standard deviation	Student's t-test-unpaired
		#1	#2	#3	mean		#1	#2	#3	mean		
<i>Ckm</i>	control	0,068	0,109	0,075	0,084	0,017907168	0,80952381	1,29761905	0,89285714	1	0,21318057	p = 0,0427
	<i>Rbpj-cKO</i>	0,034	0,047	0,009	0,03	0,015769168	0,4047619	0,55952381	0,10714286	0,35714286	0,18772819	
<i>Pcp4</i>	control	2,21	2,232	2,828	2,42333333	0,286283465	0,91196699	0,92104539	1,16698762	1	0,11813623	p = 0,0730
	<i>Rbpj-cKO</i>	1,141	0,398	2,023	1,18733333	0,664211981	0,47083906	0,16423659	0,83480055	0,48995873	0,27409023	
<i>Pcp4l1</i>	control	0,31	0,421	0,257	0,32933333	0,068334146	0,94129555	1,27834008	0,78036437	1	0,20749235	p = 0,0224
	<i>Rbpj-cKO</i>	0,165	0,039	0,123	0,109	0,052383203	0,50101215	0,11842105	0,37348178	0,33097166	0,15905831	
<i>Tagln</i>	control	0,594	0,434	0,555	0,52766667	0,068119177	1,12571068	0,82248895	1,05180038	1	0,12909509	p = 0,1682
	<i>Rbpj-cKO</i>	0,458	0,396	0,463	0,439	0,030474033	0,8679722	0,75047378	0,87744788	0,83196462	0,05775243	
<i>Tnn2</i>	control	0,213	0,26	0,245	0,23933333	0,019601587	0,88997214	1,08635097	1,02367688	1	0,08190078	p = 0,0091
	<i>Rbpj-cKO</i>	0,131	0,032	0,098	0,087	0,041158231	0,54735376	0,13370474	0,40947075	0,36350975	0,17197032	
<i>Tpm2</i>	control	0,351	0,38	0,449	0,39333333	0,041104204	0,89237288	0,96610169	1,14152542	1	0,10450221	p = 0,0180
	<i>Rbpj-cKO</i>	0,267	0,232	0,147	0,21533333	0,050387388	0,67881356	0,58983051	0,37372881	0,54745763	0,12810353	

**Table S5B. qRT-PCR analysis of SMC gene expression in mRNA of control and E18.5 *Rbpj-cKO* ureters cultured for 6 days (relates to Fig. 3E).**

gene	genotype	biological replicates				standard deviation	Student's t-test-unpaired	
		#1	#2	#3	mean			
<i>Foxf1</i>	control	0,70885242	1,14307404	1,02726259	0,95972968	0,21	p=0,7431	
	<i>Rbpj-cKO</i>	0,76369365	0,95605874	1,05422583	0,92465941			
<b>technical replicates</b>								
gene	genotype	#1	#2	#3	#4	mean	standard deviation	Student's t-test-unpaired
<i>Myocd</i>	control	0,9565335	1	1,01883316	1,17108711	1,036613443	0,09	p=0,0000119
	<i>Rbpj-cKO</i>	0,25836976	0,37364131	0,23516852	0,3214145	0,297148521	0,06	

**Table S5C. RT-PCR analysis of *Foxf1* and *Myocd* expression in mRNA of E14.5 control and *Rbpj-cKO* ureters (relates to Fig. 5D). For *Foxf1* analysis 3 pools of control and mutant ureters (n=10) were tested. For *Myocd* expression 1 pool of control and mutant ureters (n=10) were tested with 4 technical replicates.**

Part – 3 Notch signaling in SMC differentiation

gene	genotype	biological replicates				standard deviation	normalized biological replicates				standard deviation	Student's t-test-unpaired	
		#1	#2	#3	mean		#1	#2	#3	mean			
<i>Myocd</i>	control	1,28	1,025	1	1,10166667	0,126513065	1,16187595	0,93040847	0,90771558	1	0,11483788	p = 0,3635	E18.5
	<i>Rbpj-cKO</i>	1,206	1,095	1,377	1,226	0,115991379	1,09470499	0,99394856	1,24992436	1,1128593	0,10528718		
<i>Myocd</i>	control	0,061	0,089	0,051	0,067	0,016083117	0,91044776	1,32835821	0,76119403	1	0,24004653	p = 0,1717	E18.5 + 6 d
	<i>Rbpj-cKO</i>	0,065	0,026	0,018	0,03633333	0,020531818	0,26865672	0,97014925	0,3880597	0,54228856	0,30644504		

**Table S5D.** qRT-PCR analysis of SMC gene expression in control and *Rbpj-cKO* ureters at E18.5 (relates to Fig. 5E).

gene	genotype	biological replicates				standard deviation	normalized biological replicates				standard deviation	Student's t-test-unpaired	
		#1	#2	#3	mean		#1	#2	#3	mean			
<i>Ckm</i>	control	0,258	0,314	0,321	0,29766667	0,028193774	0,866741321	1,054871221	1,07838746	1	0,09471593	p = 0,0427	
	1 $\mu$ M DAPT	0,227	0,229	0,25	0,23533333	0,010402991	0,762597984	0,769316909	0,83986562	0,79059351	0,03494846		
<i>Myocd</i>	control	1,17	0,793	1,527	1,16333333	0,299691323	1,005730659	0,681661891	1,31260745	1	0,25761432	p = 0,5219	
	1 $\mu$ M DAPT	1,061	0,784	1,144	0,99633333	0,153918449	0,912034384	0,673925501	0,98338109	0,85644699	0,13230812		
<i>Pcp4</i>	control	1,444	2,106	1,337	1,629	0,340106846	0,886433395	1,29281768	0,82074893	1	0,20878259	p = 0,7432	
	1 $\mu$ M DAPT	1,45	1,917	1,18	1,51566667	0,304440835	0,890116636	1,17679558	0,72437078	0,93042767	0,18688817		
<i>Pcp4l1</i>	control	0,948	0,887	1,364	1,06633333	0,211950204	0,889027821	0,831822445	1,27914973	1	0,19876543	p = 0,1091	
	1 $\mu$ M DAPT	0,581	0,789	0,804	0,72466667	0,101772077	0,544857768	0,739918725	0,75398562	0,67958737	0,09544115		
<i>Tagln</i>	control	0,468	0,497	0,796	0,587	0,148258783	0,797274276	0,846678024	1,3560477	1	0,25257033	p = 0,7647	
	1 $\mu$ M DAPT	0,559	0,539	0,562	0,55333333	0,010208929	0,95229983	0,918228279	0,95741056	0,94264622	0,0173917		
<i>Tnnt2</i>	control	0,907	1,07	0,934	0,97033333	0,071331776	0,934730333	1,102713844	0,96255582	1	0,07351265	p = 0,0091	
	1 $\mu$ M DAPT	0,687	0,559	0,702	0,64933333	0,064168182	0,708004122	0,57609069	0,72346273	0,66918585	0,06613004		
<i>Tpm2</i>	control	1,189	0,718	1,179	1,02866667	0,219712438	1,155865198	0,697990927	1,14614388	1	0,21358954	p = 0,1526	
	1 $\mu$ M DAPT	0,743	0,592	0,843	0,726	0,103172994	0,722294232	0,575502268	0,81950745	0,70576798	0,10029779		

**Table S5E.** qRT-PCR analysis of SMC gene expression in mRNA of E18.5 ureters cultured for 18h in presence of DMSO or 1  $\mu$ M DAPT (relates to Fig. 6C).

gene	genotype	biological replicates				standard deviation	normalized biological replicates				standard deviation	Student's t-test-unpaired	
		#1	#2	#3	mean		#1	#2	#3	mean			
<i>Ckm</i>	control	0,099	0,066	0,058	0,07433333	0,017745109	1,331838565	0,887892377	0,78026906	1	0,23872344	p = 0,0241	
	1 $\mu$ M DAPT	0,037	0,02	0,02	0,02566667	0,008013877	0,497757848	0,269058296	0,2690583	0,34529148	0,10781		
<i>Myocd</i>	control	0,064	0,048	0,058	0,05666667	0,006599663	1,129411765	0,847058824	1,02352941	1	0,11646465	p = 0,0182	
	1 $\mu$ M DAPT	0,039	0,024	0,019	0,02733333	0,008498366	0,688235294	0,423529412	0,33529412	0,48235294	0,14997116		
<i>Pcp4</i>	control	1,57	1,41	1,362	1,44733333	0,088924437	1,08475357	0,974205435	0,94104099	1	0,06144019	p = 0,0210	
	1 $\mu$ M DAPT	1,166	0,926	0,754	0,94866667	0,168960219	0,80561953	0,639797328	0,52095808	0,65545831	0,11673898		
<i>Pcp4l1</i>	control	0,371	0,181	0,241	0,26433333	0,079302515	1,403530895	0,684741488	0,91172762	1	0,30000951	p = 0,0392	
	1 $\mu$ M DAPT	0,118	0,076	0,075	0,08966667	0,020038851	0,446406053	0,287515763	0,28373266	0,33921816	0,07580902		
<i>Tagln</i>	control	0,439	0,394	0,537	0,45666667	0,059701107	0,961313869	0,862773723	1,17591241	1	0,13073235	p = 0,0110	
	1 $\mu$ M DAPT	0,286	0,233	0,213	0,244	0,030800433	0,626277372	0,510218978	0,46642336	0,53430657	0,0674462		
<i>Tnnt2</i>	control	0,146	0,152	0,09	0,12933333	0,027920522	1,128865979	1,175257732	0,69587629	1	0,21588033	p = 0,0337	
	1 $\mu$ M DAPT	0,072	0,062	0,029	0,05433333	0,018372685	0,556701031	0,479381443	0,2242268	0,42010309	0,14205684		
<i>Tpm2</i>	control	0,276	0,332	0,206	0,27133333	0,051545018	1,017199017	1,223587224	0,75921376	1	0,18996935	p = 0,4684	
	1 $\mu$ M DAPT	0,236	0,298	0,138	0,224	0,065868556	0,86977887	1,098280098	0,50859951	0,82555283	0,24275881		

**Table S5F.** qRT-PCR analysis of SMC gene expression in mRNA of E18.5 ureters cultured for 6 days in presence of DMSO or 1  $\mu$ M DAPT (relates to Fig. 6D).

## Part – 3 Notch signaling in SMC differentiation

Control specimens (1 and 2 refer to the left and right ureter)	day 1 of culture		day 2 of culture		day 3 of culture		day 4 of culture		day 5 of culture		day 6 of culture	
	contractions of one ureter in 1 min	average contraction of left and right ureter	contractions of one ureter in 1 min	average contraction of left and right ureter	contractions of one ureter in 1 min	average contraction of left and right ureter	contractions of one ureter in 1 min	average contraction of left and right ureter	contractions of one ureter in 1 min	average contraction of left and right ureter	contractions of one ureter in 1 min	average contraction of left and right ureter
#13_1	2		1,5		1		1		1,5		1,5	
#13_2	1	1,5	1,5	1,5	2	1,5	1	1	0,5	1	2	1,75
#15_1	1,5		2		2,5		2,5		3,5		2,5	
#15_2	1,5	1,5	1	1,5	1	1,75	1	1,75	1	2,25	1	1,75
#16_1	2		1,5		1,5		2		1,5		1,5	
#16_2	1,5	1,75	1,5	1,5	1	1,25	3,5	2,75	2,5	2	1	1,25
#20_1	1		1,5		2		1		1		1	
#20_2	0,5	0,75	0,5	1	1	1,5	1	1	2,5	1,75	1	1
#22_1	2		1,5		1		1		1		1	
#22_2	1	1,5	0,5	1	1	1	1	1	1	1	1,5	1,25
#25_1	2		1		1		1,5		1		1	
#25_2	1,5	1,75	1,5	1,25	2,5	1,75	2	1,75	1,5	1,25	1,5	1,25
#29_1	1		1		2		1,5		1,5		1	
#29_2	1,5	1,25	2	1,5	2	2	1,5	1,5	1	1,25	1	1
#30_1	1		1		1		1,5		1		2	
#30_2	2	1,5	1,5	1,25	1,5	1,25	1,5	1,5	2	1,5	1	1,5
#32_1	2		1		1		1		2		1	
#32_2	0,5	1,25	2	1,5	1,5	1,25	2	1,5	1	1,5	1,5	1,25
#34_1	1,5		1,5		1		1,5		1		1	
#34_2	1	1,25	1	1,25	2	1,5	1	1,25	1	1	1	1
#37_1	2		2		2		1		1,5		1	
#37_2	2	2	2	2	2,5	2,25	2,5	1,75	1,5	1,5	2,5	1,75
#40_1	1,5		2,5		1		1,5		1		1	
#40_2	2	1,75	1	1,75	1,5	1,25	2	1,75	2	1,5	2	1,5
#42_1	2		1,5		1,5		2		1		2	
#42_2	2,5	2,25	2,5	2	2,5	2	1,5	1,75	2,5	1,75	1	1,5
#47_1	1		2,5		1,5		3,5		3		2	
#47_2	2	1,5	2	2,25	1,5	1,5	2	2,75	2	2,5	2	2
#50_1	3,5		3,5		1,5		2		2		2	
#50_2	2	2,75	2,5	3	2	1,75	2,5	2,25	3	2,5	2,5	2,25
#54_1	1,5		2		2		2		1,5		1	
#54_2	2	1,75	3	2,5	2,5	2,25	2	2	2,5	2	3	2
#55_1	2		2,5		1		1		1,5		1	
#55_2	1	1,5	2,5	2,5	1,5	1,25	1,5	1,25	1,5	1,5	1,5	1,25
#57_1	2		2				2		1		1	
#57_2	2	2	2,5	2,25	2,5	2,5	2	2	2	1,5	1,5	1,25
#59_1	1		1		1,5		1		1		1	
#59_2	1,5	1,25	2,5	1,75	3	2,25	2,5	1,75	2	1,5	1	1
#60_1	1		2		1,5		1		1,5		3,5	
#60_2	1	1	2	2	2	1,75	1	1	1	1,25	2	2,75
#61_1	1		2		1		1		4,5		1	
#61_2	1	1	2	2	4	2,5	2	1,5	2,5	3,5	2,5	1,75
#62_1	3		3		2,5		2,5		3		1,5	
#62_2	3	3	3	3	2	2,25	2	2,25	2	2,5	1,5	1,5
#63_1	2		2		3		2,5		2		2,5	
#63_2	2,5	2,25	2	2	2	2,5	1,5	2	1,5	1,75	1	1,75
#64_1	3		2		0,5		2		1,5		1,5	
#64_2	2	2,5	2	2	2	1,25	2	2	1	1,25	1,5	1,5
#68_1	2		2		2		2		1		1,5	
#68_2	2,5	2,25	2	2	2	2	3	2,5	1,5	1,25	1,5	1,5
#69_1	3		2,5		2,5		2,5		2		2	
#69_2	2	2,5	2	2,25	2,5	2,5	2	2,25	1,5	1,75	2,5	2,25

<i>Rbpj</i> -cKO specimens (1 and 2 refer to the left and right ureter)	day 1 of culture		day 2 of culture		day 3 of culture		day 4 of culture		day 5 of culture		day 6 of culture	
	contractions of one ureter in 1 min	average contraction of left and right ureter	contractions of one ureter in 1 min	average contraction of left and right ureter	contractions of one ureter in 1 min	average contraction of left and right ureter	contractions of one ureter in 1 min	average contraction of left and right ureter	contractions of one ureter in 1 min	average contraction of left and right ureter	contractions of one ureter in 1 min	average contraction of left and right ureter
#14_1	1		1		3		1,5		1,5		1	
#14_2	1	1	2	1,5	2	2,5	2	1,75	2	1,75	3	2
#17_1	1		1,5		1		4		1,5		1	
#17_2	0,5	0,75	2	1,75	2	1,5	2,5	3,25	1,5	1,5	1,5	1,25
#18_1	0,5		1		1		1,5		1		1,5	
#18_2	0,5	0,5	1	1	1,5	1,25	1,5	1,5	1	1	1	1,25
#19_1	1		0,5		2		2,5		4,5		4,5	
#19_2	0,5	0,75	1	0,75	1,5	1,75	1,5	2	1,5	3	2	3,25
#24_1	1		1,5		2		2		1,5		1	
#24_2	1,5	1,25	2,5	2	2	2	1	1,5	1	1,25	1	1
#31_1	0,5		0,5		1,5		2		1,5		1	
#31_2	0,5	0,5	0,5	0,5	1	1,25	0,5	1,25	3	2,25	2,5	1,75
#33_1	1		1,5		1		1		1		1	
#33_2	0,5	0,75	1	1,25	1,5	1,25	1	1	1	1	1	1
#35_1	1		1,5		4		1,5		2		1	
#35_2	1	1	1	1,25	1	2,5	2,5	2	1,5	1,75	1	1
#36_1	1		1,5		1,5		2		1		1,5	
#36_2	2	1,5	1	1,25	1	1,25	1	1,5	1	1	1	1,25
#39_1	1		1		2,5		2		2,5		2,5	
#39_2	1	1	1	1	2	2,25	2	2	3	2,75	1	1,75
#41_1	1		1		1		1,5		1		1	
#41_2	1	1	1	1	1	1	2	1,75	1	1	1	1
#43_1	1		2,5		2		1,5		1		1	
#43_2	0,5	0,75	1	1,75	1,5	1,75	2	1,75	2,5	1,75	1,5	1,25
#45_1	0,5		1		1		1,5		1		1	
#45_2	0,5	0,5	1	1	1	1	1,5	1,5	1	1	1	1
#49_1	1		2,5		2,5		2,5		1,5		1,5	
#49_2	2	1,5	2,5	2,5	3	2,75	4,5	3,5	4,5	3	2,5	2
#53_1	1		1		2,5		1		1		1	
#53_2	1	1	2,5	1,75	2,5	2,5	2	1,5	1,5	1,25	1	1
#67_1	1		3		4,5		2		1,5		2,5	
#67_2	1	1	2,5	2,75	1	2,75	1	1,5	1	1,25	1	1,75

	day 1 of culture	day 2 of culture	day 3 of culture	day 4 of culture	day 5 of culture	day 6 of culture
<b>Control average (n=23)</b>	1,74	1,87	1,79	1,76	1,69	1,56
<b>Rbpjk cKO average (n=16)</b>	0,92	1,44	1,83	1,83	1,66	1,47
<b>Control stdev</b>	0,57	0,54	0,48	0,51	0,58	0,44
<b>Rbpjk cKO stdev</b>	0,31	0,62	0,64	0,66	0,72	0,60
<b>t-test</b>	4,8497E-06	0,022957219	0,81940761	0,708869426	0,85968586	0,583781274

**Table S6A. Statistical analysis of the peristaltic frequency of E18.5 control (n=26) and Rbpj-cKO (n=16) ureters over 6 days of culture (relates to Figure 3B).** Shown are the average and corresponding standard deviations of peristaltic contractions per minute after 1 to 6 days after ureter explantation at E18.5. One minute was video-monitored. The statistical significance was calculated by a two-tailed Student's t-test. \*:  $p \leq 0.05$ ; \*\*:  $p \leq 0.01$ ; \*\*\*:  $p \leq 0.001$ .

## Part – 3 Notch signaling in SMC differentiation

Day 1 proximal						Day 3 proximal					
Time	Control average	Control stdev	Rbpj-cKO average	Rbpj-cKO stdev	t-test	Time	Control average	Control stdev	Rbpj-cKO average	Rbpj-cKO stdev	t-test
0	0,00027525	0,00095565	0	0	0,26756869	0	0,002277309	0,0054192	0,002918955	0,006291365	0,730658688
1	0,45813082	0,19077348	0,27537906	0,172742547	0,00372291	1	0,598296874	0,17246748	0,483467279	0,151070578	0,036502833
2	0,64175340	0,13510043	0,51164199	0,194528255	0,01518951	2	0,694215781	0,15456277	0,659325867	0,114606266	0,447128152
3	0,65556137	0,13854860	0,59062374	0,173781446	0,19279709	3	0,699648758	0,17625909	0,677543114	0,125215621	0,668889767
4	0,64437768	0,13394654	0,62080573	0,146297079	0,59993037	4	0,684915015	0,18389509	0,643940542	0,149464207	0,463557483
5	0,58706858	0,14100650	0,59060847	0,128477562	0,93617611	5	0,630269054	0,18027432	0,55537769	0,168813145	0,193845483
6	0,49677433	0,16407376	0,53219249	0,136768207	0,48062491	6	0,512203032	0,16482944	0,422630396	0,158990123	0,094789173
7	0,42048470	0,17979472	0,45443477	0,158843846	0,54395639	7	0,37164506	0,12959444	0,286005093	0,107940988	0,035202311
8	0,36020551	0,18837770	0,37539067	0,160923661	0,79315773	8	0,27593852	0,09710123	0,216543554	0,075812128	0,046573958
9	0,30916313	0,18228868	0,31717832	0,16581005	0,88840904	9	0,221239433	0,08672965	0,16728923	0,063588522	0,040129365
10	0,25382510	0,16157484	0,27068730	0,159879081	0,74637829	10	0,181558928	0,08073572	0,146437967	0,058712064	0,145005914
11	0,20574701	0,13983667	0,22702108	0,146846329	0,64496807	11	0,151308423	0,0701205	0,131606255	0,052587352	0,346293537
12	0,17714770	0,11495469	0,19520351	0,129624476	0,64397176	12	0,131892581	0,05855051	0,115689828	0,051758665	0,375171918
13	0,14924769	0,09365595	0,16101064	0,101491994	0,7070294	13	0,118916869	0,05495345	0,099461275	0,048129434	0,256699857
14	0,12970652	0,07854779	0,13710018	0,084103312	0,7770615	14	0,112461382	0,04740619	0,086162244	0,046351592	0,093200636
15	0,11156816	0,06209172	0,11951127	0,069756571	0,70605355	15	0,101215213	0,04627507	0,075185537	0,044451327	0,092808377
16	0,09768265	0,04773416	0,10382525	0,057709859	0,71333824	16	0,094594319	0,04561216	0,06770423	0,04270787	0,076243059
17	0,08560472	0,03766944	0,09306682	0,052206204	0,59726636	17	0,090575804	0,05095602	0,061497869	0,04073368	0,072304086
18	0,08640923	0,06473763	0,08573457	0,047102159	0,97177368	18	0,085717877	0,04936653	0,0492821331	0,037815461	0,03532831
19	0,07768900	0,06919190	0,07610392	0,041226945	0,93547391	19	0,077931344	0,04649741	0,049124521	0,035159055	0,048824975
20	0,05744224	0,03225041	0,06850005	0,038141014	0,32538045	20	0,074197346	0,04527571	0,047201416	0,031458812	0,053024298

Day 1 medial						Day 3 medial					
Time	Control average	Control stdev	Rbpj-cKO average	Rbpj-cKO stdev	t-test	Time	Control average	Control stdev	Rbpj-cKO average	Rbpj-cKO stdev	t-test
0	0,00120482	0,00322755	0	0	0,15287176	0	0,002256075	0,00447259	0,004408806	0,008638656	0,293370159
1	0,52435162	0,19711253	0,23513400	0,101137376	4,028E-06	1	0,679520089	0,16418879	0,526112406	0,159237493	0,00496464
2	0,68509314	0,13977453	0,48254948	0,178470037	0,00022144	2	0,734447107	0,14469287	0,699219567	0,160459356	0,466505131
3	0,70652538	0,12866941	0,57347842	0,16738548	0,00650835	3	0,725175194	0,15549182	0,729586972	0,154070054	0,929050998
4	0,69417965	0,12995078	0,60365465	0,149749271	0,0473499	4	0,70850935	0,17055561	0,731847461	0,145744323	0,652113456
5	0,65822580	0,13327660	0,60528537	0,134276502	0,22536293	5	0,678112497	0,18144886	0,67704862	0,152286949	0,984484361
6	0,58073398	0,14521275	0,57359910	0,125228509	0,87333918	6	0,57805983	0,19571405	0,549851921	0,15455537	0,627195459
7	0,48097317	0,17801381	0,51341304	0,123699839	0,53285344	7	0,433433381	0,21451415	0,389743856	0,159205696	0,486184837
8	0,40492412	0,19829959	0,43735851	0,139327668	0,57638307	8	0,328607998	0,18539863	0,274614421	0,12382968	0,309331685
9	0,34612367	0,20258161	0,36851533	0,155231089	0,71118535	9	0,245660821	0,14713838	0,199083306	0,076211995	0,24910097
10	0,28793582	0,19719245	0,32052328	0,157950622	0,58462128	10	0,190255562	0,11026942	0,153845956	0,050075035	0,222211293
11	0,24137453	0,17698500	0,27906933	0,14858528	0,48735845	11	0,160758393	0,09291409	0,125690103	0,037948476	0,159763549
12	0,20213559	0,14534400	0,24363760	0,135944209	0,3689622	12	0,141272039	0,0793963	0,107317669	0,03665962	0,116805719
13	0,16873901	0,11285580	0,21163151	0,120080763	0,25539169	13	0,123597216	0,06550761	0,095549552	0,036069082	0,124801029
14	0,14135896	0,08631661	0,18112133	0,102892366	0,19007073	14	0,112689147	0,05736255	0,082783979	0,033043677	0,072759089
15	0,11868637	0,06754842	0,14525397	0,082322463	0,26658215	15	0,107010657	0,05702017	0,07783438	0,035413774	0,08163704
16	0,10422506	0,05644103	0,12368945	0,070868625	0,33581732	16	0,100868408	0,05761927	0,072409815	0,038518425	0,096797733
17	0,09112969	0,05345650	0,10721086	0,063208133	0,38750984	17	0,09467232	0,05755686	0,066243586	0,038586783	0,096971462
18	0,09815418	0,08133938	0,09879213	0,05674577	0,97855226	18	0,086312962	0,05363759	0,06428499	0,046560375	0,192334386
19	0,08994873	0,08226213	0,08795132	0,051807501	0,93228718	19	0,080399402	0,05683069	0,05894842	0,046632177	0,222728173
20	0,06977041	0,04804739	0,08259165	0,044815303	0,40040166	20	0,074922235	0,05882858	0,056022629	0,044600916	0,288365717

Day 1 distal						Day 3 distal					
Time	Control average	Control stdev	Rbpj-cKO average	Rbpj-cKO stdev	t-test	Time	Control average	Control stdev	Rbpj-cKO average	Rbpj-cKO stdev	t-test
0	0,00056260	0,00208277	0	0	0,29800768	0	0,0005495	0,00225758	0,002603138	0,008910564	0,266967301
1	0,52440847	0,20367635	0,25827585	0,173647394	0,00011289	1	0,68760679	0,14232025	0,509585751	0,153993666	0,000460322
2	0,70604749	0,13098769	0,45923748	0,190381316	1,4426E-05	2	0,778822621	0,09026241	0,706941897	0,117100571	0,030984774
3	0,75667714	0,09260805	0,55564152	0,176802807	2,1598E-05	3	0,779830078	0,10047214	0,757538658	0,0982508	0,485479393
4	0,76581572	0,08409615	0,60295223	0,162383241	0,00012099	4	0,782635614	0,09889544	0,747491946	0,108921933	0,288275872
5	0,75384944	0,07674702	0,61359188	0,152357984	0,0003157	5	0,754454866	0,10156325	0,697818733	0,113974019	0,101650958
6	0,69367989	0,10004267	0,60103799	0,13766138	0,01666046	6	0,666965949	0,13528386	0,581382288	0,147398893	0,06141312
7	0,60696893	0,15372473	0,55800566	0,119261326	0,29050163	7	0,531499084	0,16185301	0,440687147	0,12423822	0,062026388
8	0,52107396	0,19230767	0,49822537	0,117658732	0,67629893	8	0,398711946	0,15847752	0,329790948	0,097272524	0,125800576
9	0,44669046	0,21719515	0,42540187	0,138823596	0,73250114	9	0,302185153	0,13744779	0,248413477	0,071162737	0,156112396
10	0,38206864	0,21894645	0,36768752	0,148135519	0,82076906	10	0,237940217	0,10287929	0,202550554	0,054479241	0,212497492
11	0,32908248	0,20451805	0,32311406	0,153059524	0,92160451	11	0,194646985	0,0836278	0,176155746	0,050489454	0,429955997
12	0,28233875	0,18039964	0,28217235	0,152323224	0,99759673	12	0,170269781	0,07565935	0,155005753	0,045476966	0,470801114
13	0,23819757	0,15427484	0,24389446	0,143146684	0,90679528	13	0,151455388	0,06769122	0,138496602	0,041488386	0,495139272
14	0,19956847	0,12634201	0,21222404	0,129840844	0,75950519	14	0,137145335	0,0592563	0,129285504	0,039256034	0,641056897
15	0,16687034	0,09965587	0,18071970	0,119966549	0,69102244	15	0,121523985	0,05293823	0,115620513	0,03727464	0,7072407
16	0,13916543	0,08261280	0,16206166	0,102680132	0,43609476	16	0,110106764	0,04723543	0,103838032	0,032392674	0,662002037
17	0,11739434	0,06978465	0,14621755	0,086562687	0,24753593	17	0,098207552	0,04341111	0,095514937	0,032401941	0,840859945
18	0,11435666	0,07734746	0,13173023	0,074740005	0,4837507	18	0,089317691	0,03944436	0,090459958	0,031460898	0,926489483
19	0,10182712	0,07653698	0,11840581	0,066922924	0,48528529	19	0,079965101	0,03695865	0,085513251	0,031496519	0,638967652
20	0,07567418	0,04393104	0,10758670	0,059166498	0,05435358	20	0,072212476	0,03591294	0,077407125	0,030254578	0,65015464



Part – 3 Notch signaling in SMC differentiation

Day 6 proximal						Day 6 medial					
Time	Control average	Control stdev	Rbpj-cKO average	Rbpj-cKO stdev	t-test	Time	Control average	Control stdev	Rbpj-cKO average	Rbpj-cKO stdev	t-test
0	0,01405435	0,02223799	0,00740533	0,02739539	0,39915386	0	0,00844387	0,01946865	0,00524994	0,01582922	0,58359747
1	0,543429	0,18657847	0,50975586	0,18858414	0,57939994	1	0,67086553	0,17095206	0,64298952	0,10647209	0,56206092
2	0,62294685	0,1659331	0,67077467	0,15444532	0,3637357	2	0,72946792	0,15462149	0,7784823	0,08881208	0,25576817
3	0,63315483	0,15570103	0,69440852	0,15040572	0,2228726	3	0,74341676	0,13597097	0,80008388	0,0742857	0,13440836
4	0,6196521	0,16716445	0,68664721	0,16413261	0,21708359	4	0,73912111	0,14415213	0,80536865	0,07508783	0,09754297
5	0,60650183	0,17304881	0,65889335	0,19076129	0,37028655	5	0,71909144	0,14905808	0,80253591	0,07305585	0,04364304
6	0,56716731	0,19422136	0,63364254	0,20386329	0,30244019	6	0,67055558	0,15969886	0,78780237	0,0790841	0,0093998
7	0,49066389	0,21597486	0,58391069	0,21604371	0,18717671	7	0,57887286	0,17024426	0,73865508	0,11479017	0,00197279
8	0,41237566	0,2122837	0,51305152	0,22541783	0,15736799	8	0,49340472	0,17292633	0,66091684	0,16341347	0,00342614
9	0,33555464	0,17684835	0,42827667	0,21718255	0,14233811	9	0,40962871	0,1526232	0,57512355	0,18005715	0,00279228
10	0,26750674	0,14058873	0,3615772	0,21506878	0,09617324	10	0,33658031	0,13320295	0,47334124	0,189807	0,00903695
11	0,22227416	0,12572994	0,31311054	0,20585869	0,08480989	11	0,26342364	0,1229359	0,3901552	0,18940262	0,01188945
12	0,19290591	0,11446379	0,27956028	0,19660204	0,07975724	12	0,21236909	0,11156676	0,32573682	0,19419847	0,02065533
13	0,17099391	0,10501962	0,24214073	0,18041162	0,11555831	13	0,18699875	0,09654909	0,28711239	0,189878	0,02898372
14	0,14964087	0,09045346	0,21105649	0,16135668	0,12338884	14	0,1651175	0,08597366	0,25792409	0,17863285	0,02880468
15	0,13412254	0,08313757	0,18993179	0,15056497	0,13122944	15	0,14886724	0,07731469	0,23307404	0,11438579	0,03733546
16	0,12378492	0,08195862	0,17225325	0,14104517	0,17409004	16	0,1365179	0,06456381	0,2066006	0,16220651	0,05918502
17	0,11174951	0,07701222	0,15272211	0,12314205	0,19993117	17	0,12815282	0,06303013	0,18035726	0,14184772	0,11419301
18	0,10079152	0,07429375	0,13827122	0,11029817	0,20415764	18	0,1210171	0,0633948	0,16238704	0,12684352	0,17288015
19	0,08833328	0,07216451	0,12658675	0,09770816	0,16642608	19	0,10601911	0,06306492	0,14931429	0,11433402	0,13134473
20	0,08470456	0,07206543	0,12937779	0,09035976	0,09964353	20	0,09742489	0,06361476	0,13147471	0,10964209	0,23168668

Day 6 distal					
Time	Control average	Control stdev	Rbpj-cKO average	Rbpj-cKO stdev	t-test
0	0,00461066	0,00982767	0,00988468	0,03786295	0,5011896
1	0,70367447	0,13310234	0,54573409	0,17643606	0,0020629
2	0,78938867	0,1278408	0,7476073	0,10543993	0,27945944
3	0,78624552	0,12794172	0,78515935	0,08221927	0,97601415
4	0,779782	0,13086262	0,79867105	0,07215781	0,60011903
5	0,76130099	0,14039095	0,80361526	0,07166679	0,27116842
6	0,73575899	0,15786767	0,79226279	0,07642952	0,18971217
7	0,67592936	0,16961886	0,75141213	0,1041957	0,11753621
8	0,59729427	0,18848338	0,68963521	0,14341633	0,10071506
9	0,50931799	0,19135901	0,59132002	0,17226135	0,1694247
10	0,40947693	0,17520225	0,498245	0,16564167	0,11153206
11	0,32970105	0,14233949	0,40908151	0,14195935	0,08658929
12	0,26969069	0,12132487	0,3351724	0,12100907	0,09684565
13	0,2271935	0,10645025	0,28627254	0,10468852	0,08648219
14	0,19139664	0,09248669	0,24345004	0,08895091	0,07993023
15	0,16427221	0,08050491	0,21457045	0,07679156	0,05227677
16	0,14637319	0,06856399	0,19505641	0,07919004	0,04340036
17	0,1323249	0,06000689	0,1777388	0,07312281	0,03614786
18	0,11929175	0,05665707	0,15780864	0,05831228	0,04228339
19	0,10346885	0,04554403	0,13898259	0,05351073	0,0301283
20	0,09572319	0,04143796	0,1303107	0,05243185	0,02788482

**Table S6B. Statistical analysis of contraction intensities of E18.5 ureters from control and Rbpj-cKO embryos after 1,3 and 6 days of culture (relates to Figure 3C).** Shown is the average intensity and corresponding standard deviations (STDV) in one sec intervals of one peristaltic contraction at day 1,3 and 6 of culture after ureter explantation at E18.5. n=26 (control), n=16 (Rbpj-cKO). The proximal level equals to 25%, medial to 50% and distal to 75% of the entire ureter length. One minute was video-monitored. Contraction intensity equals to Multi-Kymograph grey value ratios (grey value at “t” / maximum grey value). The statistical significance was calculated by a two-tailed Student’s t-test. \*: p ≤ 0.05; \*\*: p ≤ 0.01; \*\*\*: p ≤ 0.001.

	day 1 of culture	day 2 of culture	day 3 of culture	day 4 of culture	day 5 of culture	day 6 of culture
Control (n=46 ureter)	0	0	16 (35%)	44 (96%)	46 (100%)	46 (100%)
Rbpjk cKO (n=32 ureter)	0	0	0	4 (12,5%)	23 (72%)	32 (100%)

**Table S7A. Statistical analysis of onset of peristaltic contractions in E14.5 control and Rbpj-cKO ureters over 6 days of culture (relates to Figure 4D).**

## Part – 3 Notch signaling in SMC differentiation

Control specimens (1 and 2 refer to the left and right ureter)	day 1 of culture		day 2 of culture		day 3 of culture		day 4 of culture		day 5 of culture		day 6 of culture		day 7 of culture		day 8 of culture	
	contractions of one ureter in 1 min	average contraction of left and right ureter	contractions of one ureter in 1 min	average contraction of left and right ureter	contractions of one ureter in 1 min	average contraction of left and right ureter	contractions of one ureter in 1 min	average contraction of left and right ureter	contractions of one ureter in 1 min	average contraction of left and right ureter	contractions of one ureter in 1 min	average contraction of left and right ureter	contractions of one ureter in 1 min	average contraction of left and right ureter	contractions of one ureter in 1 min	average contraction of left and right ureter
#72_1	0		0,5		1		1		2		2,5		2,5		2,5	
#72_2	0	0	0,5	0,5	1	1	1,5	1,25	2,5	2,25	2,5	2,5	2,5	2,5	2,5	2,5
#73_1	0		0		1		1		1		1		1		2,5	
#73_2	0	0	0,5	0,25	1	1	1	1	1,5	1,25	1,5	1,25	2,5	2	1,5	2
#79_1	0		0		1		1,5		1		1,5		2		2	
#79_2	0	0	0	0	1	1	1	1,25	1,5	1,25	1,5	1,5	1,5	1,75	1,5	1,75
#80_1	0		0		1		1		1		1,5		1,5		2	
#80_2	0	0	0	0	1	1	1,5	1,25	1	1	1,5	1,5	1,5	1,5	2	2
#81_1	0		0		1		1		1		1		2		1,5	
#81_2	0	0	0	0	1	1	1	1	1	1	1,5	1,25	1,5	1,75	1,5	1,5
#84_1	0		0		1		1,5		1,5		2		2,5		3,5	
#84_2	0	0	0	0	1	1	1,5	1,5	1,5	1,5	1,5	1,75	1,5	2	2,5	3
#85_1	0		0		1		1		2,5		2		2,5		2,5	
#85_2	0	0	0,5	0,25	1	1	1,5	1,25	2,5	2,5	2,5	2,25	3	2,75	3,5	3
#86_1	0		0		1		1,5				2,5		2		2,5	
#86_2	0	0	0	0	1	1	1	1,25	1,5	1,5	2	2,25	2,5	2,25	2,5	2,5
#87_1	0		0,5		1,5		1		1,5		1,5		2		2,5	
#87_2	0	0	0,5	0,5	1	1,25	1	1	1,5	1,5	2,5	2	2,5	2,25	2,5	2,5
#88_1	0		0		1		1		1,5		2,5		2,5		2,5	
#88_2	0	0	0,5	0,25	1	1	1,5	1,25	2,5	2	2,5	2,5	1,5	2	2,5	2,5
#90_1	0		0		1		0,5		1		2,5		2,5		2,5	
#90_2	0	0	0	0	1	1	0,5	0,5	1,5	1,25	1,5	2	2	2,25	2,5	2,5
#93_1	0		0		1		1,5		2		3,5		3,5		3,5	
#93_2	0	0	0,5	0,25	1	1	1,5	1,5	1,5	1,75	2,5	3	3,5	3,5	2,5	3
#94_1	0		0		1,5		1		1,5		2		2,5		2,5	
#94_2	0	0	0,5	0,25	1,5	1,5	1	1	2	1,75	2,5	2,25	2,5	2,5	2,5	2,5
#95_1	0		0		1		1		1,5		1,5		2,5		2,5	
#95_2	0	0	0,5	0,25	1	1	0,5	0,75	2	1,75	2	1,75	2,5	2,5	2,5	2,5
#101_1	0		0,5		1,5		1		1,5		2		2		2,5	
#101_2	0	0	0	0,25	1	1,25	1	1	2	1,75	1,5	1,75	2,5	2,25	1,5	2
#108_1	0		0,5		1		1,5		2,5		1,5		2,5		2,5	
#108_2	0	0	0	0,25	1	1	1,5	1,5	2,5	2,5	2,5	2	3,5	3	2,5	2,5
#110_1	0		0,5		1		1,5		2,5		1,5		3,5		2,5	
#110_2	0	0	0,5	0,5	1	1	1	1,25	2,5	2,5	2	1,75	3,5	3,5	3,5	3
#113_1	0		0		1		1		1		2		2,5		2,5	
#113_2	0	0	0	0	1	1	1	1	1,5	1,25	1,5	1,75	2	2,25	1,5	2
#114_1	0		0		1		1		2		2,5		2,5		2,5	
#114_2	0	0	0	0	1	1	1	1	1	1,5	1	1,75	2	2,25	2,5	2,5
#116_1	0		0		0		1		1		2		2,5		1,5	
#116_2	0	0	0	0	1	0,5	1	1	1	1	1,5	1,75	2	2,25	2,5	2
#117_1	0		0		1		1		2		2		1,5		2	
#117_2	0	0	0	0	1	1	1	1	1,5	1,75	2	2	2	1,75	2,5	2,25
#119_1	0		0,5		1,5		1,5		2		2		2,5		2,5	
#119_2	0	0	0,5	0,5	1,5	1,5	1,5	1,5	1,5	1,75	2,5	2,25	2	2,25	3,5	3
#120_1	0		0		0		1		1		1		1		2	
#120_2	0	0	0	0	1,5	0,75	1	1	1	1	1,5	1,25	2	1,5	2,5	2,25

<i>Rbpj</i> -cKO specimens (1 and 2 refer to the left and right ureter)	day 1 of culture		day 2 of culture		day 3 of culture		day 4 of culture		day 5 of culture		day 6 of culture		day 7 of culture		day 8 of culture	
	contractions of one ureter in 1 min	average contraction of left and right ureter	contractions of one ureter in 1 min	average contraction of left and right ureter	contractions of one ureter in 1 min	average contraction of left and right ureter	contractions of one ureter in 1 min	average contraction of left and right ureter	contractions of one ureter in 1 min	average contraction of left and right ureter	contractions of one ureter in 1 min	average contraction of left and right ureter	contractions of one ureter in 1 min	average contraction of left and right ureter	contractions of one ureter in 1 min	average contraction of left and right ureter
#70_1	0		0		0,5		1		1		1		2		3,5	
#70_2	0	0	0	0	0	0,25	0,5	0,75	1	1	1	1	2,5	2,25	0,5	2
#74_1	0		0		0		0		0,5		1		2		2,5	
#74_2	0	0	0	0	0	0	0,5	0,25	1	0,75	1	1	2	2	2	2,25
#75_1	0		0		0		0,5		1		1		2		1,5	
#75_2	0	0	0	0	0	0	1	0,75	1	1	1	1	2	2	2,5	2
#77_1	0		0		0		0,5		1		1		2,5		1,5	
#77_2	0	0	0	0	0	0	0	0,25	1	1	1	1	2	2,25	2	1,75
#83_1	0		0		0		0,5		1,5		1,5		2		3,5	
#83_2	0	0	0	0	0,5	0,25	0,5	0,5	1	1,25	2,5	2	3	2,5	3	3,25
#96_1	0		0		0		1		1		1		2		2,5	
#96_2	0	0	0	0	0	0	0	0,5	1	1	2	1,5	2,5	2,25	3	2,75
#98_1	0		0		0,5		0,5		1		2		2,5		3,5	
#98_2	0	0	0	0	0	0,25	1	0,75	1	1	2	2	2	2,25	3	3,25
#99_1	0		0		1		0,5		1		3		2		3	
#99_2	0	0	0	0	0	0,5	0,5	0,5	2	1,5	1,5	2,25	2	2	3	3
#102_1	0		0		0		0,5		1		1		2		3,5	
#102_2	0	0	0	0	0	0	0	0,25	1	1	1	1	2	2	2,5	3
#103_1	0		0		0		0,5		1,5		1		2		2	
#103_2	0	0	0	0	0	0	0	0,25	1	1,25	1	1	1,5	1,75	2,5	2,25
#104_1	0		0		0		0,5		1		2		2		3	
#104_2	0	0	0	0	0	0	0	0,25	1	1	1	1,5	1,5	1,75	3	3
#105_1	0		0		0,5		0,5		1		2		4		2,5	
#105_2	0	0	0	0	0	0,25	0,5	0,5	1	1	1,5	1,75	4,5	4,25	3	2,75
#107_1	0		0		0		0,5		1		2		3		3	
#107_2	0	0	0	0	0	0	0,5	0,5	1	1	1	1,5	2	2,5	3,5	3,25
#109_1	0		0		0		0,5		1		1		2		3	
#109_2	0	0	0	0	0	0	0	0,25	1,5	1,25	1,5	1,25	2	2	3	3
#111_1	0		0		0		0,5		1		1,5		2,5		2,5	
#111_2	0	0	0	0	0	0	0	0,25	1	1	1	1,25	2	2,25	3	2,75
#115_1	0		0		0		0,5		1		1,5		2		2	
#115_2	0	0	0	0	0	0	0	0,25	0,5	0,75	1	1,25	2	2	1	1,5

Part – 3 Notch signaling in SMC differentiation

	day 1 of culture	day 2 of culture	day 3 of culture	day 4 of culture	day 5 of culture	day 6 of culture	day 7 of culture	day 8 of culture
Control average (n=26)	0	0,17	1,03	1,13	1,62	1,91	2,28	2,40
Rbpjk cKO average (n=16)	0	0	0,09	0,42	1,05	1,39	2,25	2,61
Control stdev	0	0,19	0,20	0,25	0,48	0,44	0,53	0,42
Rbpjk cKO stdev	0	0,00	0,15	0,20	0,19	0,42	0,58	0,57
t-test	0	0,000868562	8,24809E-18	1,90288E-11	6,38638E-05	0,000626761	0,856294078	0,492319052

**Table S7B. Statistical analysis of the peristaltic frequency of E14.5 control (n=23) and Rbpj-cKO (n=16) ureters over 8 days of culture (relates to Figure 4E).** Shown are the average and corresponding standard deviations of peristaltic contractions per minute after 1 to 6 days after ureter explantation at E14.5. One minute was video-monitored. The statistical significance was calculated by a two-tailed Student's t-test. \*:  $p \leq 0.05$ ; \*\*:  $p \leq 0.01$ ; \*\*\*:  $p \leq 0.001$ . The onset of peristaltic activity is shown in the amount of ureters that contract and the percentage of contracting ureters out of all ureters at day 1 to 6 days of culture.

Part – 3 Notch signaling in SMC differentiation

Day 4 proximal						Day 8 proximal					
Time	Control average	Control stdev	Rbpj-cKO average	Rbpj-cKO stdev	t-test	Time	Control average	Control stdev	Rbpj-cKO average	Rbpj-cKO stdev	t-test
0	0.000364371	0.001114027	0	0	0.210497538	0	0.000666731	0.00832262	0.001638142	0.003610675	0.057978907
1	0.152956292	0.10037105	0.075839618	0.043688248	0.0007594025	1	0.165589092	0.07174453	0.21490099	0.118737378	0.117159332
2	0.366297155	0.185983741	0.155080633	0.058691922	0.000123985	2	0.403143982	0.11340369	0.434584631	0.11340369	0.471896799
3	0.50509992	0.203548584	0.229447931	0.075472281	1.19743E-05	3	0.545133194	0.12253595	0.530839056	0.127699995	0.730014291
4	0.576797237	0.188487776	0.271060037	0.082652879	7.17594E-07	4	0.577476667	0.13677876	0.531005917	0.0432258	0.266974196
5	0.613903502	0.168219255	0.29174026	0.08995678	4.49415E-08	5	0.535727207	0.19073956	0.466720245	0.112214691	0.219091546
6	0.618136863	0.158264207	0.292636964	0.091128888	1.25736E-08	6	0.480409122	0.19767634	0.354385157	0.150013421	0.040974469
7	0.594826288	0.153857376	0.282510355	0.088843823	1.69673E-08	7	0.406420503	0.18151207	0.281315328	0.147700221	0.030890916
8	0.55512233	0.146562214	0.25850753	0.089847073	2.3126E-08	8	0.345419986	0.1558164	0.201543454	0.112878951	0.003638586
9	0.496694195	0.138917436	0.236575696	0.086464029	1.25299E-07	9	0.264643042	0.13834161	0.141637527	0.081533825	0.003423244
10	0.435636028	0.128643041	0.212944763	0.076863059	4.98093E-07	10	0.205500924	0.11523263	0.118041682	0.064604557	0.010555794
11	0.369705021	0.124069699	0.189352545	0.071525091	9.30705E-06	11	0.167203508	0.09354092	0.109327776	0.054859885	0.035860924
12	0.307110458	0.117671032	0.16751342	0.066394121	0.000158302	12	0.14246695	0.07680802	0.097232901	0.041869206	0.042604166
13	0.250099281	0.100715944	0.145490752	0.061015954	0.000840172	13	0.115413545	0.05862902	0.086582745	0.036530603	0.095370592
14	0.20288501	0.086773696	0.125161716	0.055749953	0.003712914	14	0.105667844	0.05158376	0.081928817	0.052358576	0.1182096
15	0.175763061	0.075032788	0.108353711	0.049011421	0.003729853	15	0.092896112	0.04461877	0.066268641	0.028430531	0.045740641
16	0.157710265	0.066379548	0.093483041	0.044739329	0.002081801	16	0.079469859	0.04558607	0.055781349	0.021608758	0.075640855
17	0.140542038	0.059905251	0.082321155	0.043559228	0.002360628	17	0.069994741	0.04111151	0.047111252	0.013137625	0.068794621
18	0.118960566	0.053948293	0.072308579	0.04213742	0.007111943	18	0.068898159	0.03537708	0.043513114	0.02523861	0.043001799
19	0.1097787	0.055036049	0.064868998	0.039788529	0.009269818	19	0.06430952	0.0329377	0.038643981	0.030763275	0.077946236
20	0.095305884	0.054575013	0.057561229	0.038908556	0.025065542	20	0.061612913	0.03376413	0.036258805	0.0250255	0.074351219

Day 4 medial						Day 8 medial					
Time	Control average	Control stdev	Rbpj-cKO average	Rbpj-cKO stdev	t-test	Time	Control average	Control stdev	Rbpj-cKO average	Rbpj-cKO stdev	t-test
0	0	0	0.003000748	0.012002994	0.235431144	0	0.00369287	0.01020004	0.000675882	0.010919156	0.252167162
1	0.170915697	0.083612594	0.087978259	0.034724958	0.000773217	1	0.227018267	0.10756743	0.22013954	0.135456832	0.860798389
2	0.389128854	0.125067293	0.199583851	0.059023351	2.82699E-06	2	0.452113201	0.13356403	0.417808831	0.162006188	0.474276958
3	0.486461209	0.124816829	0.288029851	0.084111301	3.59434E-06	3	0.568460426	0.13748869	0.496308904	0.163108395	0.143811415
4	0.529106946	0.128249529	0.338522215	0.095923636	1.61658E-05	4	0.605167283	0.13872507	0.511830579	0.167678132	0.065643688
5	0.549442718	0.121392151	0.362367238	0.104358612	1.73959E-05	5	0.577691453	0.16581129	0.479797979	0.17524413	0.087011287
6	0.5503167	0.125867117	0.369391686	0.111719344	5.58064E-05	6	0.522968559	0.16377675	0.402674728	0.176128053	0.035070627
7	0.535090856	0.139526444	0.363939875	0.116246626	0.000322996	7	0.470682693	0.15453638	0.315704237	0.152025509	0.003680366
8	0.507358117	0.15920672	0.343106803	0.123027485	0.001583407	8	0.388747076	0.15878054	0.236282304	0.113093915	0.002162521
9	0.464424965	0.174802833	0.317733838	0.126437657	0.007611031	9	0.318397252	0.14599579	0.181963066	0.085208989	0.001851367
10	0.416860875	0.176635529	0.288819235	0.124728128	0.018984956	10	0.256515605	0.12992551	0.153683594	0.067273718	0.006309337
11	0.366386001	0.168071498	0.256490794	0.118557172	0.033106808	11	0.221383669	0.10251997	0.138162491	0.060878637	0.006188829
12	0.324480705	0.15256678	0.227542122	0.113226103	0.040474973	12	0.197741733	0.08352506	0.126757408	0.057692351	0.005616166
13	0.284096286	0.137262186	0.202169137	0.104258271	0.054916298	13	0.175644908	0.07816353	0.117823953	0.053372622	0.014437726
14	0.249900776	0.124964304	0.179669343	0.094569361	0.069646573	14	0.160725667	0.0744017	0.105951093	0.053587747	0.016154629
15	0.217803082	0.113029116	0.160156853	0.083561828	0.096369492	15	0.14911032	0.07002001	0.09678586	0.051024245	0.015019512
16	0.193952407	0.10099577	0.140046526	0.070225167	0.077733872	16	0.134526368	0.07115314	0.08436193	0.047029554	0.018452841
17	0.172632458	0.08956961	0.125744755	0.059358862	0.080311898	17	0.126990549	0.06204654	0.073684106	0.042588728	0.005102532
18	0.156270314	0.081366773	0.113259767	0.052065274	0.075372699	18	0.124334552	0.05176605	0.061215789	0.033168123	0.000121844
19	0.138992505	0.072376405	0.104734084	0.045510365	0.10858486	19	0.122698081	0.04951969	0.053566798	0.032050711	7.29284E-05
20	0.129798645	0.068191873	0.103575836	0.040492045	0.196719071	20	0.120040774	0.05350193	0.047885328	0.030523559	9.56826E-05

Day 4 distal						Day 8 distal					
Time	Control average	Control stdev	Rbpj-cKO average	Rbpj-cKO stdev	t-test	Time	Control average	Control stdev	Rbpj-cKO average	Rbpj-cKO stdev	t-test
0	0	0	0	0	0	0	0.009841688	0.03831049	0.001706232	0.002976082	0.403974182
1	0.162524956	0.062540706	0.067687145	0.03904095	6.00296E-06	1	0.214256299	0.11441214	0.13861986	0.069469468	0.023980465
2	0.339257031	0.131011349	0.145429519	0.087803153	1.13849E-05	2	0.43623326	0.17356707	0.266114684	0.141079193	0.002514859
3	0.452168614	0.151309601	0.196581405	0.111464591	1.83628E-06	3	0.542438914	0.1639151	0.319147397	0.162282038	0.000160473
4	0.501905576	0.149274754	0.225925042	0.119730758	5.44595E-07	4	0.58783434	0.16886221	0.330812289	0.160269858	2.84318E-05
5	0.524947118	0.147806302	0.242327534	0.12136358	3.27695E-07	5	0.579729493	0.17676563	0.286875035	0.154500594	4.73895E-06
6	0.533726134	0.143893493	0.248282905	0.12396309	2.14923E-07	6	0.533150874	0.18919852	0.231267899	0.137665301	3.50566E-06
7	0.528198835	0.150398107	0.246934013	0.123656886	5.04791E-07	7	0.478190412	0.18702522	0.18239143	0.118510191	2.3085E-06
8	0.504731927	0.156992647	0.23764761	0.119176095	1.86547E-06	8	0.420094093	0.18252329	0.142612779	0.089004534	2.06793E-06
9	0.470874419	0.160759263	0.220762746	0.110685666	5.60451E-06	9	0.352268891	0.16944589	0.11758308	0.068823464	6.88242E-06
10	0.429787015	0.158279256	0.202862824	0.103178	1.68346E-05	10	0.294752169	0.1513747	0.100022146	0.056609431	1.94156E-05
11	0.377989788	0.159277758	0.182119834	0.092673912	0.000107108	11	0.248915569	0.12904561	0.084229464	0.045993714	2.06125E-05
12	0.332470065	0.144838076	0.162703135	0.086314172	0.000207599	12	0.212576444	0.11149436	0.076756185	0.039675745	4.06179E-05
13	0.292727314	0.135570305	0.146759918	0.076947543	0.000502985	13	0.18163842	0.08875296	0.066796273	0.034888962	1.90385E-05
14	0.261161411	0.128734983	0.130741883	0.068216459	0.000855106	14	0.157642648	0.0710674	0.061723874	0.029957075	1.10863E-05
15	0.235489174	0.115111386	0.115539165	0.059969144	0.000617929	15	0.142058703	0.0633625	0.055605603	0.02770442	9.9626E-06
16	0.205205508	0.097273382	0.101873939	0.055912002	0.000597169	16	0.129015624	0.05942867	0.052837491	0.022527081	2.08541E-05
17	0.181001602	0.095767843	0.091655643	0.049564364	0.001851045	17	0.12033844	0.0582528	0.048608941	0.02192419	3.72507E-05
18	0.15984233	0.086123006	0.083718614	0.044897546	0.003024926	18	0.110009485	0.05168983	0.043779764	0.021568915	2.41342E-05
19	0.143905085	0.079344415	0.072810503	0.041021894	0.00265939	19	0.099332505	0.04935983	0.038562637	0.020500355	0.000173128
20	0.131280604	0.076344961	0.066942754	0.038513086	0.004522892	20	0.088408167	0.05025277	0.040721262	0.016721905	0.002340055

**Table S7C. Statistical analysis of contraction intensities of E14.5 ureters from control and Rbpj-cKO embryos after 4 and 8 days of culture (relates to Figure 4F).** Shown is the average intensity and corresponding standard deviations (STDV) in one sec intervals of one peristaltic contraction at day 1 and 6 of culture after ureter explantation at E14.5. n=23 (control), n=16 (Rbpj-cKO). The proximal level equals to 25%, medial to 50% and distal to 75% of the entire ureter length. One minute was video-monitored. Contraction intensity equals to Multi-Kymograph grey value ratios (grey value at “t” / maximum grey value). The statistical significance was calculated by a two-tailed Student’s t-test. \*: p ≤ 0.05; \*\*: p ≤ 0.01; \*\*\*: p ≤ 0.001.

Gene Symbol	control 1	mutant 1	control 2	mutant 2	FC 1	FC 2	avgFC
<i>Gsdmc3</i>	53	155	44	331	2,9	7,5	5,2
<i>Chgb</i>	4091	29950	2855	4901	7,3	1,7	4,5
<i>Fos</i>	166	258	161	1083	1,6	6,7	4,1
<i>Chga</i>	1350	5900	567	1152	4,4	2,0	3,2
<i>Ren2</i>	2361	6209	162	542	2,6	3,3	3,0
<i>A930009L07Rik</i>	805	2482	379	921	3,1	2,4	2,8
<i>Resp18</i>	195	495	65	188	2,5	2,9	2,7
<i>Slc18a1</i>	259	796	128	298	3,1	2,3	2,7
<i>Dbh</i>	3402	12254	2011	3348	3,6	1,7	2,6
<i>ENSMUST00000085379</i>	147	361	150	406	2,5	2,7	2,6
<i>Insm1</i>	646	1364	385	942	2,1	2,4	2,3
<i>Dgkk</i>	840	2521	499	775	3,0	1,6	2,3
<i>Fam92b</i>	114	257	72	155	2,3	2,2	2,2
<i>Gnas</i>	676	1674	405	765	2,5	1,9	2,2
<i>Hey1</i>	1534	2651	1301	3423	1,7	2,6	2,2
<i>Dusp26</i>	612	1235	365	827	2,0	2,3	2,1
<i>LOC102636514</i>	532	847	293	789	1,6	2,7	2,1
<i>Hey2</i>	99	205	134	293	2,1	2,2	2,1
<i>Phox2a</i>	2456	3867	1436	3496	1,6	2,4	2,0
<i>Hand2</i>	715	1067	437	1109	1,5	2,5	2,0
<i>Scg3</i>	363	562	230	512	1,5	2,2	1,9
<i>Smpd3</i>	175	281	96	205	1,6	2,1	1,9
<i>Lrriq1</i>	81	142	95	188	1,8	2,0	1,9
<i>Rab3c</i>	143	308	109	174	2,2	1,6	1,9
<i>Pcp4</i>	315	569	227	405	1,8	1,8	1,8
<i>Ttyh1</i>	165	249	97	194	1,5	2,0	1,8
<i>Sytl4</i>	1249	2196	891	1502	1,8	1,7	1,7
<i>Glrb</i>	761	1163	692	1169	1,5	1,7	1,6
<i>Rims3</i>	387	590	273	441	1,5	1,6	1,6
<i>Fabp7</i>	670	1058	535	808	1,6	1,5	1,5

**Table S8A. Genes with increased expression in microarrays of E14.5 Rbpj-cKO ureters.** Shown are gene names, individual intensities of the two control and mutant samples and the individual and average fold change.

Gene Symbol	control 1	mutant 1	control 2	mutant 2	FC 1	FC 2	avgFC
<i>Anp32a</i>	4584	1862	11954	2342	-2,5	-5,1	-3,8
<i>Mdfi</i>	15782	6639	18107	7468	-2,4	-2,4	-2,4
<i>Aspn</i>	413	195	364	136	-2,1	-2,7	-2,4
<i>Traf2</i>	228	110	238	89	-2,1	-2,7	-2,4
<i>Car3</i>	14935	8300	14350	5024	-1,8	-2,9	-2,3
<i>Pi4k2b</i>	1377	641	1363	699	-2,1	-1,9	-2,0
<i>Myocd</i>	583	337	366	157	-1,7	-2,3	-2,0
<i>C1ql3</i>	256	146	208	100	-1,8	-2,1	-1,9
<i>Dffa</i>	261	156	355	164	-1,7	-2,2	-1,9
<i>Wif1</i>	176	107	214	98	-1,6	-2,2	-1,9
<i>Rbpj</i>	3088	1395	2314	1474	-2,2	-1,6	-1,9
<i>Shisa2</i>	3273	1770	2713	1436	-1,8	-1,9	-1,9
<i>Cyp26a1</i>	209	112	191	108	-1,9	-1,8	-1,8
<i>Colq</i>	1365	766	1254	710	-1,8	-1,8	-1,8
<i>Nyap1</i>	1283	680	1155	723	-1,9	-1,6	-1,7
<i>Cldn4</i>	682	454	616	403	-1,5	-1,5	-1,5

**Table S8B. Genes with decreased expression in microarrays of E14.5 Rbpj-cKO ureters.** Shown are gene names, individual intensities of the two control and mutant samples and the individual and average fold change



Part – 3 Notch signaling in SMC differentiation

Term	Coun %	PValue	Genes	List Tot Pop	Hit Pop	Tot Fold	Enrichm	Bonterroni	Benjamini	FDR
GOTERM_CC_DIRECT	4	14.3	CHGA, SGC3, SYTL4, DBH	24	27	19662	121,3703704	2.97E-04	2.97E-04	0.00420267
UP_KEYWORDS	6	21.4	CHGA, RESP18, REN2, SGC3, GNAS, CHGB, CHGA, SGC3, SYTL4	26	248	22680	21,10421836	5.74E-04	5.74E-04	0.00719351
UP_KEYWORDS	6	21.4	1,70E-04 GNAS, SLC18A1, DBH	26	489	22680	10,70316187	0,01449319	0,00727304	0,18288846
GOTERM_CC_DIRECT	4	14.3	2,93E-04 CHGA, RESP18, SYTL4, CHGA, SGC3, SYTL4	24	112	19662	29,25892857	0,02146913	0,01079281	0,30649956
GOTERM_CC_DIRECT	6	21.4	7,75E-04 GNAS, SLC18A1, DBH	24	646	19662	7,609133127	0,0557892	0,01896336	0,80867051
KEGG_PATHWAY	3	10.7	0,00202378 FOS, GNAS, SLC18A1	9	67	7691	38,26368159	0,12515172	0,12515172	2,04989495
GOTERM_BP_DIRECT	2	7.14	0,00232147 HEY1, HEY2	22	2	18082	821,9090909	0,48915241	0,48915241	3,0408966
GOTERM_BP_DIRECT	2	7.14	0,00232147 HEY1, HEY2	22	2	18082	821,9090909	0,48915241	0,48915241	3,0408966
INTERPRO	2	7.14	0,00232947 CHGA, CHGB	25	2	20594	823,76	0,15062409	0,15062409	2,38472438
INTERPRO	2	7.14	0,00232947 CHGA, CHGB	25	2	20594	823,76	0,15062409	0,15062409	2,38472438
GOTERM_MF_DIRECT	2	7.14	0,00343544 HEY1, HEY2	21	3	17446	553,8412698	0,26886943	0,26886943	3,68223012
GOTERM_BP_DIRECT	2	7.14	0,00348028 HEY1, HEY2	22	3	18082	547,9393939	0,634889	0,39575584	4,52661305
INTERPRO	2	7.14	0,00349226 CHGA, CHGB	25	3	20594	549,1733333	0,2172063	0,1152437	3,55575997
UP_SEQ_FEATURE	2	7.14	0,00399223 HEY1, HEY2	25	3	18012	480,32	0,33503624	0,33503624	4,35869265
GOTERM_BP_DIRECT	2	7.14	0,0046378 HEY1, HEY2	22	4	18082	410,9545455	0,73905414	0,36097654	5,98964402
GOTERM_BP_DIRECT	2	7.14	0,0046378 HEY1, HEY2	22	4	18082	410,9545455	0,73905414	0,36097654	5,98964402
GOTERM_MF_DIRECT	2	7.14	0,00685966 HEY1, HEY2	21	6	17446	276,9206349	0,46547689	0,26888913	7,22947105
KEGG_PATHWAY	3	10.7	0,00787613 FOS, GNAS, SLC18A1	9	134	7691	19,1318408	0,40659751	0,22967378	7,76656107
GOTERM_BP_DIRECT	2	7.14	0,0081027 INSM1, DBH	22	7	18082	234,8311688	0,90474705	0,44445453	10,2460496
GOTERM_BP_DIRECT	2	7.14	0,0081027 HEY1, HEY2	22	7	18082	234,8311688	0,90474705	0,44445453	10,2460496
GOTERM_BP_DIRECT	2	7.14	0,0081027 HEY1, HEY2	22	7	18082	234,8311688	0,90474705	0,44445453	10,2460496
SMART	2	7.14	0,00841295 HEY1, HEY2	12	8	10425	217,1875	0,11902685	0,1902685	5,70474189
GOTERM_BP_DIRECT	2	7.14	0,00925511 HEY1, HEY2	22	8	18082	205,4772727	0,93192751	0,41575591	11,6217383
GOTERM_BP_DIRECT	2	7.14	0,00925511 HEY1, HEY2	22	8	18082	205,4772727	0,93192751	0,41575591	11,6217383
GOTERM_BP_DIRECT	2	7.14	0,01040625 HEY1, HEY2	22	9	18082	182,6464646	0,95135292	0,39580639	12,9764158
GOTERM_BP_DIRECT	2	7.14	0,01040625 HEY1, HEY2	22	9	18082	182,6464646	0,95135292	0,39580639	12,9764158
GOTERM_BP_DIRECT	2	7.14	0,0127047 PCP4, SLC18A1	22	11	18082	149,4380165	0,97515707	0,41014774	15,6240114
GOTERM_BP_DIRECT	2	7.14	0,0127047 HEY1, HEY2	22	11	18082	149,4380165	0,97515707	0,41014774	15,6240114
INTERPRO	2	7.14	0,01389906 HEY1, HEY2, INSM1, FOS, RAB3C	25	12	20594	137,2933333	0,62459829	0,27861781	13,4849641
GOTERM_CC_DIRECT	7	25	0,01447796 PCP4, GSDMC3, GNAS,	24	1784	19662	3,214545964	0,66013281	0,23646788	14,1564703
GOTERM_MF_DIRECT	2	7.14	0,01480611 HEY1, HEY2	21	13	17446	127,8095238	0,74267874	0,36394907	15,0087488
GOTERM_BP_DIRECT	2	7.14	0,01498807 HEY1, HEY2	22	13	18082	126,4475524	0,98731424	0,42068529	18,1913367
GOTERM_BP_DIRECT	2	7.14	0,01498807 HEY1, HEY2	22	13	18082	126,4475524	0,98731424	0,42068529	18,1913367
GOTERM_BP_DIRECT	2	7.14	0,01498807 HEY1, HEY2	22	13	18082	126,4475524	0,98731424	0,42068529	18,1913367
UP_SEQ_FEATURE	2	7.14	0,0158775 HEY1, HEY2	25	12	18012	120,08	0,80455947	0,55791343	16,331371
UP_SEQ_FEATURE	3	10.7	0,01815666 FOS, HEY1, HEY2	25	156	18012	13,85538462	0,84572197	0,46366679	18,4649641
GOTERM_BP_DIRECT	2	7.14	0,01956596 HEY1, HEY2, PHOX2A, INSM1, HEY1,	22	17	18082	96,69518717	0,9966929	0,46986927	23,0948043
UP_KEYWORDS	5	17.9	0,02096206 HEY2, SMPD3	26	976	22680	4,468789407	0,83828175	0,45518004	20,4228402
GOTERM_BP_DIRECT	2	7.14	0,02525559 GLRB, FABP7	22	22	18082	74,71900825	0,99938422	0,52253364	28,8142936
GOTERM_BP_DIRECT	2	7.14	0,02525559 HEY1, HEY2	22	22	18082	74,71900825	0,99938422	0,52253364	28,8142936

GOTERM_BP_DIRECT	GO:0045672~positive regulation of osteoclast differentiation	2	7, 14	0.0286521	FOS, GNAS	22	25	18082	65.75272727	0.99977545	0.53409029	32.0404325
GOTERM_BP_DIRECT	GO:0007275~multicellular organism development	5	17, 9	0.02873061	PHOX2A, INSM1, HEY1, SMYD3	22	1029	18082	3.993727361	0.99978063	0.50443822	32.1133852
GOTERM_BP_DIRECT	GO:0060716~labyrinthine layer blood	2	7, 14	0.02978176	HEY1, HEY2	22	26	18082	63.22377622	0.99983958	0.48938042	33.0831024
GOTERM_CC_DIRECT	GO:0030667~secretory granule	2	7, 14	0.02999221	SYTL4, DBH	24	26	19662	63.01923077	0.89495715	0.36280362	27.2923043
GOTERM_BP_DIRECT	GO:0048791~calcium ion-regulated exocytosis of neurotransmitter	2	7, 14	0.03203733	SYTL4, RIMS3	22	28	18082	58.70779221	0.99991813	0.48939944	35.1208629
GOTERM_MF_DIRECT	GO:0043565~sequence-specific DNA binding	4	14, 3	0.03422663	PHOX2A, FOS, HEY1, CHGA, RESP18, REN2, SCG3, GNAS, CHGB	21	633	17446	5.249680283	0.95796165	0.5471948	31.5913584
UP_KEYWORDS	Secreted	6	21, 4	0.03427808	SCG3, GNAS, CHGB	26	1685	22680	3.106140151	0.95019422	0.52758907	31.347646
GOTERM_BP_DIRECT	GO:0045746~negative regulation of Notch signaling pathway	2	7, 14	0.03541132	HEY1, HEY2	22	31	18082	53.02639296	0.99997015	0.50074136	38.0621431
UP_KEYWORDS	Neurotransmitter transport	2	7, 14	0.04001706	SLC18A1, RIMS3	26	37	22680	47.15176715	0.97016938	0.50462686	35.6213259
GOTERM_MF_DIRECT	GO:0001102~RNA polymerase II activating transcription factor binding	2	7, 14	0.04269602	DUSP26, HEY2	21	38	17446	43.72431078	0.98114017	0.54803215	37.9548573
GOTERM_BP_DIRECT	GO:0060412~ventricular septum	2	7, 14	0.04324048	HEY1, HEY2	22	38	18082	43.25837321	0.99999717	0.54996068	44.4186536
GOTERM_BP_DIRECT	GO:1902476~chloride transmembrane transport	2	7, 14	0.04768707	GLRB, TTYH1	22	42	18082	39.13852814	0.99999926	0.56423273	47.7545792
GOTERM_CC_DIRECT	GO:0005576~extracellular region	6	21, 4	0.04859551	SCG3, GNAS, CHGB	24	1753	19662	2.8040502	0.97493749	0.45903302	40.6316129
UP_KEYWORDS	Chloride channel	2	7, 14	0.04951591	GLRB, TTYH1	26	46	22680	37.9264214	0.98731598	0.5170789	42.1674239
KEGG_PATHWAY	mmu05030:Cocaine addiction	2	7, 14	0.04986869	GNAS, SLC18A1	9	49	7691	34.87981859	0.96582412	0.67548118	40.7277948
UP_KEYWORDS	Notch signaling pathway	2	7, 14	0.05056576	HEY1, HEY2	26	47	22680	37.11947627	0.98846598	0.47138425	42.9525303
GOTERM_BP_DIRECT	GO:0000122~negative regulation of transcription from RNA polymerase II	4	14, 3	0.05056596	HEY2	22	729	18082	4.509789251	0.99999969	0.56530485	49.8145864
GOTERM_BP_DIRECT	GO:0006836~neurotransmitter transport	2	7, 14	0.05100909	SLC18A1, RIMS3	22	45	18082	36.52929293	0.99999973	0.54903391	50.1249098
					FOS, GLRB, HEY1, DUSP26, PCP4, HEY2, GSDMC3, SYTL4,							
GOTERM_CC_DIRECT	GO:0005737~cytoplasm	13	46, 4	0.05222948	GNAS, SLC18A1, DBH,	24	6631	19662	1.606130297	0.98111849	0.43282182	42.9626124
GOTERM_CC_DIRECT	GO:0034707~chloride channel complex	2	7, 14	0.05247563	GLRB, TTYH1	24	46	19662	35.61956522	0.98147796	0.39261913	43.1174699
UP_KEYWORDS	Transport	6	21, 4	0.05330897	SLC18A1, FBP7, RIMS3	26	1901	22680	2.753206814	0.99100687	0.4450692	44.6080833
GOTERM_BP_DIRECT	GO:0006810~transport	6	21, 4	0.0534982	SLC18A1, FBP7, RIMS3	22	1822	18082	2.706616106	0.99999987	0.54819098	51.8353323
GOTERM_BP_DIRECT	GO:0003151~outflow tract	2	7, 14	0.06090905	HEY1, HEY2	22	54	18082	30.44107744	0.99999999	0.5788805	56.6119691
GOTERM_CC_DIRECT	GO:0017053~transcriptional repressor	2	7, 14	0.06572549	INSM1, HEY2	24	58	19662	28.25	0.99346699	0.42821232	50.9130771
GOTERM_CC_DIRECT	GO:0030424~axon	3	10, 7	0.06892818	PCP4, TTYH1, DBH	24	370	19662	6.64267568	0.99493295	0.41051122	52.6460053
GOTERM_MF_DIRECT	GO:0005254~chloride channel activity	2	7, 14	0.0698348	GLRB, TTYH1	21	63	17446	26.3733938	0.99862289	0.66644973	54.58026
GOTERM_BP_DIRECT	GO:0007399~nervous system chloride	3	10, 7	0.07017732	INSM1, FOS, GLRB	22	377	18082	6.540390644	1	0.61550321	61.9691108
UP_KEYWORDS	Chloride	2	7, 14	0.07133029	GLRB, TTYH1	26	67	22680	26.03903559	0.99827785	0.50694352	54.9765984
KEGG_PATHWAY	mmu04924:Remin secretion	2	7, 14	0.07154141	REN2, GNAS	9	71	7691	24.07198748	0.99254706	0.70617964	53.1843049
UP_SEQ_FEATURE	domain:JQ	2	7, 14	0.0720533	LRR1Q, PCP4	25	56	18012	25.73142857	0.9995132	0.8514621	56.5306568
GOTERM_BP_DIRECT	GO:0045669~positive regulation of osteoblast differentiation	2	7, 14	0.07611374	HEY1, GNAS	22	68	18082	24.17379679	1	0.6301811	65.0717095
GOTERM_BP_DIRECT	GO:0001570~vasculogenesis	2	7, 14	0.07611374	HEY1, HEY2	22	68	18082	24.17379679	1	0.6301811	65.0717095
GOTERM_BP_DIRECT	GO:0006357~regulation of transcription from RNA polymerase II promoter	3	10, 7	0.07676899	FOS, HEY2, GNAS	22	397	18082	6.210899931	1	0.61781009	65.3994253
BIOCARTA	m_gpcrPathway:Signaling Pathway from GPCR	2	7, 14	0.07712049	FOS, GNAS	4	34	1289	18.95588235	0.97298996	0.97298996	52.9876676
GOTERM_MF_DIRECT	GO:0003700~transcription factor activity, sequence-specific DNA binding	4	14, 3	0.07758315	HEY2	21	883	17446	3.763360837	0.99935675	0.65001134	58.539023
GOTERM_BP_DIRECT	GO:0001568~blood vessel development	2	7, 14	0.07934124	HEY1, HEY2	22	71	18082	23.15236876	1	0.61542517	66.6586124
UP_SEQ_FEATURE	mutagenesis site	4	14, 3	0.08142028	FOS, HEY2, SYTL4,	25	772	18012	3.733056995	0.99982705	0.82315865	61.1764634
GOTERM_BP_DIRECT	GO:0006821~chloride transport	2	7, 14	0.08895944	GLRB, TTYH1	22	80	18082	20.54772727	1	0.6449855	71.0010354
UP_KEYWORDS	DNA-binding	5	17, 9	0.09625546	HEY1, HEY2	26	1604	22680	27.19163629	0.99983407	0.58121327	66.4241408
KEGG_PATHWAY	mmu04915:Estrogen signaling pathway	2	7, 14	0.09754763	FOS, GNAS	9	98	7691	17.4399093	0.99885711	0.74201135	64.9861118
KEGG_PATHWAY	mmu04713:Circadian entrainment	2	7, 14	0.09754763	FOS, GNAS	9	98	7691	17.4399093	0.99885711	0.74201135	64.9861118

**Table S9A. Functional annotation of genes with increased expression in the microarray of E14.5 Rbpj-cKO ureters.** Functional annotation was performed by DAVID 6.8 web software (<https://david.ncicrf.gov>) for 30 genes with increased expression in the microarray of E14.5 Rbpj-cKO ureters.

	Term	Coun %	PValue	Genes	List Tot:Pop Hit Pop Tot:Fold Enrichm	Bonferroni	Benjamini	FDR			
GOTERM_BP_DIRECT	GO:0030178~negative regulation of Wnt signaling pathway	3	18,8	9,64E-04 MDFI, SHISA2, WIF1	16	18082	60,54241071	0,16097479	0,16097479	1,18299428	
GOTERM_MF_DIRECT	GO:0008134~transcription factor binding	3	18,8	0,02984718 MDFI, MYOCD, RBPJ	15	342	17446	10,20233918	0,85619644	0,6207856	26,4963882
BIOCARTA	m_setPathway:Granzyme A mediated Apoptosis Pathway	2	12,5	0,0420108 DFFA, ANP32A	6	11	1289	39,06060606	0,627356	0,627356	28,8364755
KEGG_PATHWAY	mmu04210:Apoptosis	2	12,5	0,05336803 TRAF2, DFFA	8	60	7691	32,04583333	0,75972404	0,75972404	36,2225691
UP_KEYWORDS	Cytoplasm	7	43,8	0,05378316 CAR3	16	4404	22680	2,253065395	0,95949962	0,95949962	42,3070276
INTERPRO	IPR008160:Collagen triple helix repeat	2	12,5	0,05396642 COLQ, C1QL3	16	76	20594	33,87171053	0,93025478	0,93025478	41,1071873
UP_KEYWORDS	Collagen	2	12,5	0,05478226 COLQ, C1QL3	16	85	22680	33,35294118	0,96190674	0,80482505	42,9102598
GOTERM_CC_DIRECT	GO:0005581~collagen trimer	2	12,5	0,06150409 COLQ, C1QL3	16	83	19662	29,61144578	0,94606265	0,94606265	45,1172133
UP_KEYWORDS	Alternative splicing	7	43,8	0,0758332 RBPJ	16	4779	22680	2,076271186	0,98968377	0,78230908	54,3712572
GOTERM_MF_DIRECT	GO:0001228~transcriptional activator activity, RNA polymerase II transcription regulatory region sequence-specific binding	2	12,5	0,08032835 MYOCD, RBPJ	15	104	17446	22,36666667	0,99529565	0,83244152	57,2885338
GOTERM_BP_DIRECT	GO:0051091~positive regulation of sequence-specific DNA binding	2	12,5	0,08520982 TRAF2, MYOCD	16	107	18082	21,12383178	0,99999991	0,99999991	66,680453
GOTERM_MF_DIRECT	GO:0042802~identical protein binding	3	18,8	0,08775853 MDFI, TRAF2, CLDN4	15	625	17446	5,58272	0,99720084	0,76998458	60,6672505

**Table S9B. Functional annotation of genes with decreased expression in the microarray of E14.5 Rbpj-cKO ureters.** Functional annotation was performed by DAVID 6.8 web software (<https://david.ncicrf.gov>) for 16 genes with decreased expression in the microarray of E14.5 Rbpj-cKO ureters.

Part – 3 Notch signaling in SMC differentiation

Experiment with 1 $\mu$ M DAPT													
Contractions NMRI, DMSO-treated specimen (n=19)	contractions of one ureter in 1 min						Contractions NMRI, DAPT-treated specimen (n=19)	contractions of one ureter in 1 min					
	day 5 of culture	day 6 of culture	day 7 of culture	day 8 of culture	day 9 of culture	day 10 of culture		day 5 of culture	day 6 of culture	day 7 of culture	day 8 of culture	day 9 of culture	day 10 of culture
#45	0	0	0	3	2	2	#45	0	0	0	2,5	2,5	2
#48	0	0	0	0	1,5	1	#48	0	0	0	0	0	1
#49	0	0	0	0	2	2,5	#49	0	0	0	0	2	1
#50	0	0	1,5	3	1,5	1,5	#50	0	0	2	2	1	1,5
#51	0	0	0	0	1	2	#51	0	0	2	1	1	1
#52	0	0	2	2,5	1	2,5	#52	0	0	1	1,5	1	1,5
#53	0	0	1	2,5	2	2,5	#53	0	0	0	1	2,5	1,5
#54	0	0,5	1	2	2	2	#54	0	0	2,5	1	1	1,5
#55	0	0	1,5	2	1	1,5	#55	0	0	1	1,5	2	2
#57	0	0	2	2	1,5	2,5	#57	0	0	3,5	2	2	2
#58	0	0	0	3,5	2	1,5	#58	0	0	0	1,5	1,5	1
#59	0	0	0	1	3	3	#59	0	0	0	0	1	1,5
#60	0	0	0	2	1,5	1	#60	0	0	0	0	1,5	1
#61	0	0	0	1	1	1,5	#61	0	0	0	0	0	1
#62	0	0	1	2	2	1,5	#62	0	0	0	1	1,5	1,5
#63	0	0	1,5	1	2	2	#63	0	0	0	1	2,5	2
#66	0	0	2	2	1	1	#66	0	0	0	1	2	2
#72	0	0	1	2	1,5	2	#72	0	0	1	1	1	1
#73	0	0,5	0,5	2	1,5	1,5	#73	0	0	0	1	1,5	1,5
<b>Frequency</b>	<b>day 5 of culture</b>	<b>day 6 of culture</b>	<b>day 7 of culture</b>	<b>day 8 of culture</b>	<b>day 9 of culture</b>	<b>day 10 of culture</b>	<b>Onset of peristaltic activity</b>	<b>day 5 of culture</b>	<b>day 6 of culture</b>	<b>day 7 of culture</b>	<b>day 8 of culture</b>	<b>day 9 of culture</b>	<b>day 10 of culture</b>
average of all DMSO- treated NMRI	0	0,05	0,79	1,76	1,63	1,84	DMSO-treated NMRI (n=19)	0	2 (10,5%)	34 (57,9%)	16 (84,2%)	19 (100%)	19 (100%)
average of all DAPT- treated NMRI	0	0,00	0,68	1,00	1,45	1,45	DAPT-treated NMRI (n=19)	0	0	7 (36,8%)	14 (73,7%)	17 (98,5%)	19 (100%)
stdev of all DMSO- treated NMRI	0,00	0,16	0,79	1,02	0,52	0,58							
stdev of all DMSO- treated NMRI	0,00	0,00	1,07	0,75	0,74	0,40							
t-test of DMSO- treated vs. DAPT- treated NMRI	0	0,1542753	0,7318007	0,012326	0,3828409	0,0198872							

Experiment with 2.5 $\mu$ M DAPT													
contractions NMRI, DMSO-treated specimen (n=20)	contractions of one ureter in 1 min						contractions NMRI, DAPT-treated specimen (n=19)	contractions of one ureter in 1 min					
	day 5 of culture	day 6 of culture	day 7 of culture	day 8 of culture	day 9 of culture	day 10 of culture		day 5 of culture	day 6 of culture	day 7 of culture	day 8 of culture	day 9 of culture	day 10 of culture
#112	0	0	2	2	2	1	#112	0	0	0,5	2,5	1,5	2,5
#113	0	0,5	2	3,5	2,5	3,5	#113	0	0	0	0,5	1	1,5
#114	0	0	1,5	3	4,5	4	#114	0	0	0	1	1	2
#115	0	0	0	0	1	1	#115	0	0	0	0,5	1	1
#116	0	0	1,5	2	2	3,5	#116	0	0	0	1	1,5	1
#117	0	1	3	4	3,5	3	#117	0	0	0	0,5	0,5	1
#119	0	0	2	3	3,5	1,5	#119	0	0	0,5	1	1	1,5
#120	0	1	1	2	2	2	#120	0	0	1	1	2,5	1,5
#122	0	0	1	2	2	1,5	#122	0	0	0	0	0,5	1
#123	0	0,5	2	2	2	2,5							
#124	0	0	2,5	3	2,5	3,5	#124	0	0	1	2	1,5	2
#125	0	0	0	0,5	0,5	1	#125	0	0	0	0,5	1	1
#126	0	0	0	1	1,5	1	#126	0	0	0	1	2,5	1
#128	0	0	0,5	1	1	2	#128	0	0	0	1	2	1,5
#129	0	0	0	2	4,5	3	#129	0	0	0	0	0,5	1
#132	0	0,5	2	2	2,5	2,5	#132	0	0	0	1	1	1
#133	0	1	2	3,5	2	2	#133	0	0	1,5	1	2	2,5
#134	0	0	0	0	1	1	#134	0	0	0	0	0	0
#135	0	0	0,5	2	2	2	#135	0	0	0	1,5	1	1
#136	0	0	1	1	1,5	2	#136	0	0	0	0	0,5	1
<b>Frequency</b>	<b>day 5 of culture</b>	<b>day 6 of culture</b>	<b>day 7 of culture</b>	<b>day 8 of culture</b>	<b>day 9 of culture</b>	<b>day 10 of culture</b>	<b>Onset of peristaltic activity</b>	<b>day 5 of culture</b>	<b>day 6 of culture</b>	<b>day 7 of culture</b>	<b>day 8 of culture</b>	<b>day 9 of culture</b>	<b>day 10 of culture</b>
average of all DMSO- treated NMRI	0	0,23	1,23	1,98	2,20	2,18	DMSO-treated NMRI (n=40)	0	6 (30%)	15 (75%)	18 (90%)	20 (100%)	20 (100%)
average of all DAPT- treated NMRI	0	0,00	0,24	0,84	1,18	1,32	DAPT-treated NMRI (n=40)	0	0	5 (26,3%)	15 (78,9%)	18 (94,7%)	18 (94,7%)
stdev of all DMSO- treated NMRI	0,00	0,38	0,95	1,14	1,09	0,98							
stdev of all DMSO- treated NMRI	0,00	0,00	0,45	0,67	0,69	0,61							
T-test of DMSO- treated vs. DAPT- treated NMRI	0	0,0139153	0,0002158	0,0005904	0,0014278	0,0022688							

**Table S10. Statistical analysis of ureter contraction frequency in contralateral explanted E12.5 ureters treated with either DMSO or 1  $\mu$ M DAPT or 2.5  $\mu$ M DAPT over 10 days of culture (relates to Figure 6A).** Shown are the contractions of one contralateral explanted ureter in one minute after 5 days until 10 days after explantation as well as the average frequency and corresponding standard deviations (stdev). The statistical significance was calculated by a two-tailed Student's t-test. \*  $p \leq 0.05$ ; \*\*  $p \leq 0.01$ ; \*\*\*  $p \leq 0.001$ .

	contractions of one ureter in 1 min			
NMRI, DMSO-treated specimen (n=8)	day 1 of culture	day 2 of culture	day 4 of culture	day 6 of culture
1	2	2	2	1
2	3	2	3	1
3	2	2	2	2
4	2	3	1	3
5	2	2	3	2
6	1	1	2	1
7	2	1	1	2
8	2	1	2	1
<b>Average</b>	<b>2</b>	<b>1,75</b>	<b>2</b>	<b>1,625</b>
<b>STDV</b>	<b>0,534522484</b>	<b>0,707106781</b>	<b>0,755928946</b>	<b>0,744023809</b>
	contractions of one ureter in 1 min			
NMRI, DAPT-treated specimen (n=8)	day 1 of culture	day 2 of culture	day 4 of culture	day 6 of culture
1	2	1	1	2
2	1	1	2	1
3	1	2	2	1
4	1	1	1	1
5	1	2	3	3
6	1	1	2	2
7	1	2	2	3
8	1	1	1	1
<b>Average</b>	<b>1,125</b>	<b>1,375</b>	<b>1,75</b>	<b>1,75</b>
<b>STDV</b>	<b>0,353553391</b>	<b>0,51754917</b>	<b>0,707106781</b>	<b>0,88640526</b>
<b>t-test</b>	<b>0,001727111</b>	<b>0,246157665</b>	<b>0,505673234</b>	<b>0,764476762</b>
Onset of peristaltic activity	day 1 of culture	day 2 of culture	day 4 of culture	day 6 of culture
DMSO-treated NMRI (n=8)	8 (100%)	8 (100%)	8 (100%)	8 (100%)
DAPT-treated NMRI (n=8)	8 (100%)	8 (100%)	8 (100%)	8 (100%)

**Table S11. Statistical analysis of ureter contraction frequency in contralateral explanted E18.5 ureters treated with either DMSO or 1  $\mu$ M DAPT over 6 days of culture (relates to Figure 6B).** Shown are the contractions of one contralateral explanted ureter in one minute after 1 days until 6 days after explantation as well as the average frequency and corresponding standard deviations (stdev). The statistical significance was calculated by a two-tailed Student's t-test. \*  $p \leq 0.05$ ; \*\*  $p \leq 0.01$ ; \*\*\*  $p \leq 0.001$ . The onset of peristaltic activity is shown in the amount of ureters that contract and the percentage of contracting ureters out of all ureters at day 1 to 6 days of culture.



## Concluding remarks

### **GATA6, GATA2 and RBPJ-dependent Notch signaling are independent players of SMC differentiation in the murine ureter**

SMC differentiation in the ureter is controlled by a complex network of signals emanating both from the UM and UE. Previous work has shown that epithelial SHH and WNT signaling are positive regulators of *Myocd* expression and SMC differentiation. SHH activates FOXF1 and BMP4 expression in the UM and both together regulate SMC differentiation [53]. WNT signaling from the epithelium promotes SMC differentiation mainly via TBX2 and TBX3 by maintaining WNT signaling and BMP4 expression in the inner layer of the UM [49]. In contrast, RA signaling provides a negative input on SMC differentiation of the UM possibly through modulation of the WNT signaling pathway [48], [50]. The work in this thesis identified GATA2 as a downstream target of RA signaling in the UM, whereas GATA6 in the UM is mainly regulated by BMP4. NOTCH signaling seems to be independent of the other signaling pathways involved in SMC differentiation. All three factors have a diverse and independent impact on the onset of *Myocd* expression and SMC differentiation.

### **GATA6, GATA2 and Notch signaling have different molecular functions in SMC differentiation**

The expression analysis of *Gata6*/GATA6 revealed strong expression in the UM until E12.5 and downregulation at E14.5, showing that it is active until SMC differentiation starts, reminiscent of the situation found for RA signaling activity and *Bmp4* expression in this domain. Conditional *Gata6*-mutant ureters showed delayed SMC differentiation leading to hydroureter formation at birth and severe hydroureteronephrosis at postnatal stages. The functional analysis of the ureter in *ex vivo* culture studies at E14.5, shortly before the onset of urine production, showed a two-day delay in the onset of the peristaltic activity, recapitulating the two-day delay in the onset of expression of SMC differentiation markers. Additional *ex vivo* culture experiments, performed with E18.5 explants, when hydroureter formation had already occurred, rescued the contraction intensities after 6 days at the medial and distal part of the ureter, but not at the proximal level. A good option for humans with such a defect, where SMC differentiation is only delayed and not completely abrogated, could therefore be an implantation of a temporal artificial bypass from the kidney to the bladder, thereby releasing the ureter from

the hydrostatic pressure of the urine so that SMC differentiation can occur and peristaltic activity can recover. Microarray analysis and signaling pathway component analysis using RNA in situ hybridization in the *Gata6cKO* mutant ureter revealed upregulation of the RA synthesizing genes *Aldh1a2* and *Aldh1a3* as well as of the target genes *Wt1* and *Ecm1*. To investigate if increased RA signaling in the *GATA6cKO* contributes to the delayed onset of peristaltic activity, *ex vivo* cultures of E13.5 ureter explants with pharmacological inhibition of RA signaling were performed. The onset of peristaltic activity in the *Gata6cKO* mutant ureter was even more delayed and the peristaltic frequency was lower in the BMS treated ureters compared to the untreated ones, showing that increased RA does not contribute to the delayed peristaltic activity in the *Gata6cKO* ureters. The most interesting downregulated genes, which have been found in the microarray analysis were *Car3*, *Shisa2* and *Myocd*. *Car3* was previously found as a downstream target of SOX9 in the UM, but its function in SMC differentiation is unclear [92]. *Shisa2* is a WNT signaling antagonist and it is directly repressed by TBX2/TBX3, indicating that WNT signaling is reduced in the *Gata6cKO* mutant. However, WNT signaling components such as *Wnt7b*, *Wnt9b*, *Axin2* and TBX2/TBX3 were unchanged [49]. Components of other signaling pathways involved in SMC differentiation, SHH and BMP4 signaling, were also unchanged. In contrast, expression of the master regulator of SMC differentiation, *Myocd*, was strongly downregulated at E14.5; at late fetal and postnatal time points expression was still reduced. *Foxf1* expression was normal, suggesting that GATA6 is not necessary to establish the SMC lineage, but for the timely onset before urine production starts. Since GATA6 was described as a pioneer factor in cardiac mesoderm, it may open the chromatin around the *Myocd* locus for subsequent activation of *Myocd* transcription by FOXF1. Assay for Transposase-Accessible Chromatin using sequencing (ATAC-seq) and chromatin immunoprecipitation (ChIP-Seq) experiments should investigate this possibility in the future [70], [93], [94].

Notch signaling components are strongly expressed in the undifferentiated UM and UE but persist in later fetal and postnatal ureter development. In conditional *Rbpj* mutant ureters SMC differentiation and peristaltic activity occurred with a delay of one day. *Ex vivo* culture experiments performed with E18.5 explants revealed more intense and lasting contractions especially in the medial position. *Myocd* expression was one-day delayed in the *RbpjcKO* ureters, but this did not result in any phenotypical changes at

birth. In postnatal stages hydroureter formation was observed and “late” SMC genes such as *Tnnt2*, *Ckm*, *Pcp4* and *Pcp4l1* were strongly downregulated at this time point. This identifies two different molecular functions for NOTCH signaling. Early in development Notch signaling plays a (minor) role in the timely activation of *Myocd* expression and SMC differentiation; at later time-points it functions by activating “late” SMC genes. Pharmacological *ex vivo* experiments using the Notch signaling inhibitor DAPT validated the *in vivo* results. Misexpression of NICD did not lead to premature onset of SMC differentiation indicating that Notch signaling modulates rather than induces the SMC program.

Interestingly, *Gata6cKO* and *RbpjcKO* ureters showed similar changes of expression of *Tnnt2*, *Car3* and *Shisa2* (Inhibitor of WNT signaling, but also FGF signaling [95]). Moreover, activation of *Myocd* expression was delayed suggesting some kind of molecular interaction in the UM. Interestingly, in the intestinal epithelium GATA6 and GATA4 modulate NOTCH signaling by regulation of *Dll1* [96]; in vascular SMCs it was described that GATA6 directly activates *Myocd* and *Jag1* expression [70]. In preliminary experiments, we did not find changes of *Gata6* expression in *Rbpj-cKO* ureters, and of Notch components in *Gata6cKO* ureters making it unlikely that GATA6 and NOTCH signaling act in an epistatic relation. However, further work including genetic interaction studies are required to further investigate this possibility.

GATA2 is expressed in the UM during ureter development with decreasing levels over time. *Gata2cKO* ureters exhibited a two-day delay in SMC differentiation and peristaltic activity, leading to hydroureter formation at birth. Relieving the ureter of urine hydrostatic pressure in *ex vivo* cultures, led to a partial recovery of contraction intensities in *Gata2cKO* ureters as in *Gata6cKO* ureters. Microarray analysis of *Gata2cKO* ureters identified altered expression of genes, which are members of RA signaling pathway. *Rarb*, the RA-synthesizing gene *Aldh1a3* and the target gene *Ecm1* were upregulated, whereas the RA-degrading enzyme *Cyp26a1* was downregulated. *Cyp26a1* was characterized as a direct target of GATA2 in an *in vivo* CHIP-seq analysis in E14.5 ureters. Reduction of RA signaling in *Gata2cKO* mutant ureters using pharmacological inhibition experiments increased the peristaltic contractions, indicating that increased RA contributes to the delay in peristaltic activity in the mutant. Overall, this shows that GATA2 acts as a feedback inhibitor of RA signaling participating in the timed onset of SMC differentiation.

Since *Gata2* and *Gata6* loss-of-function mutants showed delayed onset of SMC differentiation and increased RA signaling when deleted in the ureter, a possible cooperation in the regulation of SMC differentiation was investigated. However, ureters conditional double heterozygous for *Gata2* and *Gata6* did not show increased hydroureter formation compared to the single mutants, arguing against a cooperation of the two GATA factors. At present, GATA2 and GATA6 seem not to interact but regulate independent subprograms in ureteric SMC differentiation.

### ***GATA6*, *GATA2* and *RBPJ* are possible CAKUT-causing genes in humans**

Dilatation of the ureter is one of the frequent defects in human newborns. Causes of this defect can be physical obstruction along the ureter and its junctions and dysfunction of the peristaltic machinery [37]. Our phenotypic characterizations revealed that the degree of ureter dilatation varied greatly in *Gata6cKO*, *Gata2cKO* and *RbpjcKO* mice. *Gata2cKO*-mutants show very strong hydroureter to megaureter formation due to two independent defects in ureter development: a delay of SMC differentiation resulting in functional obstruction and mispositioning of the ureteric bud leading to physical obstruction [61], [62]. *Sostdc1*, which was identified in the *Gata2cKO* mutant, is found regularly upregulated in human CAKUT patients [97]. *Rbpj-cKO* mice developed proximal ureter dilatation only at postnatal stages probably due to lack of activation of late SMC genes. The mild to strong hydroureter formation in *Gata6cKO* mutants also resulted from a delay in SMC differentiation. These results propose that these genes are possible CAKUT-causing genes, but so far mutations in the human orthologues have not been found in CAKUT patients.

Taken together, this thesis has identified and characterized three novel molecular players in the SMC differentiation program of the murine ureter. The findings advance the understanding of the molecular circuits that impinge on the expression of *Myocd*, and thus provide insight into the etiology of congenital ureter anomalies in mice and men.

## References

- [1] N. Zhou, S. Stoll, C. Leimena, and H. Qiu, "Vascular Smooth Muscle Cell," in *Muscle Cell and Tissue - Current Status of Research Field*, InTech, 2018.
- [2] D. C. Hill-Eubanks, M. E. Werner, T. J. Heppner, and M. T. Nelson, "Calcium signaling in smooth muscle," *Cold Spring Harb. Perspect. Biol.*, vol. 3, no. 9, pp. 1–20, 2011, doi: 10.1101/cshperspect.a004549.
- [3] E. M. Rzucidlo, K. A. Martin, and R. J. Powell, "Regulation of vascular smooth muscle cell differentiation," *J. Vasc. Surg.*, vol. 45, no. 6 SUPPL., pp. A25–A32, 2007, doi: 10.1016/j.jvs.2007.03.001.
- [4] M. W. Majesky, "Developmental basis of vascular smooth muscle diversity," *Arterioscler. Thromb. Vasc. Biol.*, vol. 27, no. 6, pp. 1248–1258, 2007, doi: 10.1161/ATVBAHA.107.141069.
- [5] M. Donadon and M. M. Santoro, "The origin and mechanisms of smooth muscle cell development in vertebrates," pp. 1–17, 2021, doi: 10.1242/dev.197384.
- [6] C. S. Le Lievre and N. M. Le Douarin, "Mesenchymal derivatives of the neural crest: analysis of chimaeric quail and chick embryos," *J. Embryol. Exp. Morphol.*, vol. 34, no. 1, pp. 125–154, 1975.
- [7] P. M. Kulesa and S. E. Fraser, "In ovo time-lapse analysis of chick hindbrain neural crest cell migration shows cell interactions during migration to the branchial arches," *Development*, vol. 127, no. 6, pp. 1161–1172, 2000.
- [8] A. Lumsden, N. Sprawson, and A. Graham, "Segmental origin and migration of neural crest cells in the hindbrain region of the chick embryo," *Development*, vol. 113, no. 4, pp. 1281–1291, 1991.
- [9] X. Jiang, D. H. Rowitch, P. Soriano, A. P. McMahon, and H. M. Sucov, "Jiang et al. - 2000 - Fate of the mammalian cardiac neural crest," vol. 1616, pp. 1607–1616, 2000.
- [10] P. Wasteson *et al.*, "Developmental origin of smooth muscle cells in the descending aorta in mice," *Development*, vol. 135, no. 10, pp. 1823–1832, 2008, doi: 10.1242/dev.020958.
- [11] K. L. Waldo *et al.*, "Secondary heart field contributes myocardium and smooth muscle to the arterial pole of the developing heart," *Dev. Biol.*, vol. 281, no. 1, pp. 78–90, 2005, doi: 10.1016/j.ydbio.2005.02.012.
- [12] Y. P. Yang, H. R. Li, X. M. Cao, Q. X. Wang, C. J. Qiao, and J. Ya, "Second heart field and the development of the outflow tract in human embryonic heart," *Dev. Growth Differ.*, vol. 55, no. 3, pp. 359–367, 2013, doi: 10.1111/dgd.12050.
- [13] A. C. Gittenberger-de Groot, M. P. F. M. Vrancken Peeters, M. M. T. Mentink, R. G. Gourdie, and R. E. Poelmann, "Epicardium-derived cells contribute a novel population to the myocardial wall and the atrioventricular cushions," *Circ. Res.*, vol. 82, no. 10, pp. 1043–1052, 1998, doi: 10.1161/01.RES.82.10.1043.
- [14] T. Mikawa and R. G. Gourdie, "Pericardial mesoderm generates a population of coronary smooth muscle cells migrating into the heart along with ingrowth of



- the epicardial organ," *Dev. Biol.*, vol. 174, no. 2, pp. 221–232, 1996, doi: 10.1006/dbio.1996.0068.
- [15] B. Wilm, A. Ipenberg, N. D. Hastie, J. B. E. Burch, and D. M. Bader, "The serosal mesothelium is a major source of smooth muscle cells of the gut vasculature," *Development*, vol. 132, no. 23, pp. 5317–5328, 2005, doi: 10.1242/dev.02141.
- [16] D. J. Roberts, "Molecular Mechanisms of Development of the," vol. 120, no. June, pp. 109–120, 2000.
- [17] N. Uetani and M. Bouchard, "Plumbing in the embryo: Developmental defects of the urinary tracts," *Clin. Genet.*, vol. 75, no. 4, pp. 307–317, 2009, doi: 10.1111/j.1399-0004.2009.01175.x.
- [18] A. Minty and L. Kedes, "Upstream regions of the human cardiac actin gene that modulate its transcription in muscle cells: presence of an evolutionarily conserved repeated motif.," *Mol. Cell. Biol.*, vol. 6, no. 6, pp. 2125–2136, 1986, doi: 10.1128/mcb.6.6.2125.
- [19] C. L. Browning *et al.*, "The developmentally regulated expression of serum response factor plays a key role in the control of smooth muscle-specific genes," *Dev. Biol.*, vol. 194, no. 1, pp. 18–37, 1998, doi: 10.1006/dbio.1997.8808.
- [20] D. Z. Wang *et al.*, "Potentiation of serum response factor activity by a family of myocardin-related transcription factors," *Proc. Natl. Acad. Sci. U. S. A.*, vol. 99, no. 23, pp. 14855–14860, 2002, doi: 10.1073/pnas.222561499.
- [21] T. Yoshida *et al.*, "Myocardin is a key regulator of CArG-dependent transcription of multiple smooth muscle marker genes," *Circ. Res.*, vol. 92, no. 8, pp. 856–864, 2003, doi: 10.1161/01.RES.0000068405.49081.09.
- [22] S. Li, D. Z. Wang, Z. Wang, J. A. Richardson, and E. N. Olson, "The serum response factor coactivator myocardin is required for vascular smooth muscle development," *Proc. Natl. Acad. Sci. U. S. A.*, vol. 100, no. 16, pp. 9366–9370, 2003, doi: 10.1073/pnas.1233635100.
- [23] S. Chen and R. J. Lechleider, "Transforming growth factor- $\beta$ -induced differentiation of smooth muscle from a neural crest stem cell line," *Circ. Res.*, vol. 94, no. 9, pp. 1195–1202, 2004, doi: 10.1161/01.RES.0000126897.41658.81.
- [24] P. Qiu, X. H. Feng, and L. Li, "Interaction of Smad3 and SRF-associated complex mediates TGF- $\beta$ 1 signals to regulate SM22 transcription during myofibroblast differentiation," *J. Mol. Cell. Cardiol.*, vol. 35, no. 12, pp. 1407–1420, 2003, doi: 10.1016/j.yjmcc.2003.09.002.
- [25] T. Yoshida, Q. Gan, Y. Shang, and G. K. Owens, "Platelet-derived growth factor-BB represses smooth muscle cell marker genes via changes in binding of MKL factors and histone deacetylases to their promoters," *Am. J. Physiol. - Cell Physiol.*, vol. 292, no. 2, pp. 886–895, 2007, doi: 10.1152/ajpcell.00449.2006.
- [26] Y. Liu, S. Sinha, O. G. McDonald, Y. Shang, M. H. Hoofnagle, and G. K. Owens, "Kruppel-like factor 4 abrogates myocardin-induced activation of

- smooth muscle gene expression," *J. Biol. Chem.*, vol. 280, no. 10, pp. 9719–9727, 2005, doi: 10.1074/jbc.M412862200.
- [27] M. Ramalho-Santos, D. A. Melton, and A. P. McMahon, "Hedgehog signals regulate multiple aspects of gastrointestinal development," *Development*, vol. 127, no. 12, pp. 2763–2772, 2000.
- [28] Y. Shiroyanagi *et al.*, "Urothelial sonic hedgehog signaling plays an important role in bladder smooth muscle formation," *Differentiation*, vol. 75, no. 10, pp. 968–977, 2007, doi: 10.1111/j.1432-0436.2007.00187.x.
- [29] L. A. D. Miller, S. E. Wert, J. C. Clark, Y. Xu, A. K. T. Perl, and J. A. Whitsett, "Role of Sonic hedgehog in patterning of tracheal-bronchial cartilage and the peripheral lung," *Dev. Dyn.*, vol. 231, no. 1, pp. 57–71, 2004, doi: 10.1002/dvdy.20105.
- [30] A. A. Mailloux *et al.*, "Fgf10 expression identifies parabronchial smooth muscle cell progenitors and is required for their entry into the smooth muscle cell lineage," *Development*, vol. 132, no. 9, pp. 2157–2166, 2005, doi: 10.1242/dev.01795.
- [31] E. D. Cohen, K. Ihida-Stansbury, M. M. Lu, R. A. Panettieri, P. L. Jones, and E. E. Morrisey, "Wnt signaling regulates smooth muscle precursor development in the mouse lung via a tenascin C/PDGFR pathway," *J. Clin. Invest.*, vol. 119, no. 9, pp. 2538–2549, 2009, doi: 10.1172/JCI38079.
- [32] R. M. Ilagan *et al.*, "Smooth muscle phenotypic diversity is mediated through alterations in Myocardin gene splicing," *J. Cell. Physiol.*, vol. 226, no. 10, pp. 2702–2711, 2011, doi: 10.1002/jcp.22622.
- [33] W. Jiang *et al.*, "Wnt-GSK3 $\beta$ / $\beta$ -catenin regulates the differentiation of dental pulp stem cells into bladder smooth muscle cells," *Stem Cells Int.*, vol. 2019, 2019, doi: 10.1155/2019/8907570.
- [34] J. T. Velardo, *The Ureter*. New York, NY: Springer New York, 1981.
- [35] R. Hurtado, G. Bub, and D. Herzlinger, "The pelvis-kidney junction contains HCN3, a hyperpolarization-activated cation channel that triggers ureter peristalsis," *Kidney Int.*, vol. 77, no. 6, pp. 500–508, 2010, doi: 10.1038/ki.2009.483.
- [36] T. Bohnenpoll and A. Kispert, "Ureter growth and differentiation," *Seminars in Cell and Developmental Biology*. 2014, doi: 10.1016/j.semcdb.2014.07.014.
- [37] I. V. Yosypiv, "Congenital anomalies of the kidney and urinary tract: A genetic disorder?," *Int. J. Nephrol.*, vol. 2012, 2012, doi: 10.1155/2012/909083.
- [38] M. M. Rodriguez, "Congenital anomalies of the kidney and the urinary tract (CAKUT)," *Fetal Pediatr. Pathol.*, vol. 33, no. 5–6, pp. 293–320, 2014, doi: 10.3109/15513815.2014.959678.
- [39] T. Bohnenpoll *et al.*, "Diversification of Cell Lineages in Ureter Development," *J Am Soc Nephrol*, vol. 28, 2016, doi: 10.1681/ASN.2016080849.
- [40] J. Yu, T. J. Carroll, and A. P. McMahon, "Sonic hedgehog regulates proliferation and differentiation of mesenchymal cells in the mouse metanephric kidney," *Development*, vol. 129, no. 22, pp. 5301–5312, 2002.

- [41] R. Haraguchi *et al.*, “The hedgehog signal induced modulation of bone morphogenetic protein signaling: An essential signaling relay for urinary tract morphogenesis,” *PLoS One*, vol. 7, no. 7, 2012, doi: 10.1371/journal.pone.0042245.
- [42] A. Raatikainen-Ahokas, M. Hytönen, A. Tenhunen, K. Sainio, and H. Sariola, “BMP-4 affects the differentiation of metanephric mesenchyme and reveals an early anterior-posterior axis of the embryonic kidney,” *Dev. Dyn.*, vol. 217, no. 2, pp. 146–158, 2000, doi: 10.1002/(SICI)1097-0177(200002)217:2<146::AID-DVDY2>3.0.CO;2-I.
- [43] Y. Miyazaki, K. Oshima, A. Fogo, B. L. M. Hogan, and I. Ichikawa, “Bone morphogenetic protein 4 regulates the budding site and elongation of the mouse ureter,” *J. Clin. Invest.*, vol. 105, no. 7, pp. 863–873, 2000, doi: 10.1172/JCI8256.
- [44] T. M. Mamo, A. B. Wittern, M.-J. Kleppa, T. Bohnenpoll, A.-C. Weiss, and A. Kispert, “BMP4 uses several different effector pathways to regulate proliferation and differentiation in the epithelial and mesenchymal tissue compartments of the developing mouse ureter,” *Hum. Mol. Genet.*, 2017, doi: 10.1093/hmg/ddx242.
- [45] G. Winnier, M. Blessing, P. A. Labosky, and B. L. M. Hogan, “Bone morphogenetic protein-4 is required for mesoderm formation and patterning in the mouse,” *Genes Dev.*, vol. 9, no. 17, pp. 2105–2116, 1995, doi: 10.1101/gad.9.17.2105.
- [46] Y. Miyazaki, K. Oshima, A. Fogo, and I. Ichikawa, “Evidence that bone morphogenetic protein 4 has multiple biological functions during kidney and urinary tract development,” *Kidney Int.*, vol. 63, no. 3, pp. 835–844, 2003, doi: 10.1046/j.1523-1755.2003.00834.x.
- [47] V. Brault *et al.*, “Inactivation of the  $\beta$ -catenin gene by Wnt1-Cre-mediated deletion results in dramatic brain malformation and failure of craniofacial development,” *Development*, vol. 128, no. 8, pp. 1253–1264, 2001.
- [48] M. O. Trowe *et al.*, “Canonical wnt signaling regulates smooth muscle precursor development in the mouse ureter,” *Dev.*, vol. 139, no. 17, pp. 3099–3108, 2012, doi: 10.1242/dev.077388.
- [49] N. Aydođdu *et al.*, “TBX2 and TBX3 act downstream of canonical WNT signaling in patterning and differentiation of the mouse ureteric mesenchyme,” *Dev.*, vol. 145, no. 23, 2018, doi: 10.1242/dev.171827.
- [50] T. Bohnenpoll, A. C. Weiss, M. Labuhn, T. H. Lüdtkke, M. O. Trowe, and A. Kispert, “Retinoic acid signaling maintains epithelial and mesenchymal progenitors in the developing mouse ureter,” *Sci. Rep.*, vol. 7, no. 1, pp. 1–13, 2017, doi: 10.1038/s41598-017-14790-2.
- [51] M. Murone, A. Rosenthal, and F. J. De Sauvage, “Sonic hedgehog signaling by the patched-smoothened receptor complex,” *Curr. Biol.*, vol. 9, no. 2, pp. 76–84, 1999, doi: 10.1016/S0960-9822(99)80018-9.
- [52] Z. Wang, D. Z. Wang, G. C. T. Pipes, and E. N. Olson, “Myocardin is a master regulator of smooth muscle gene expression,” *Proc. Natl. Acad. Sci. U. S. A.*, vol. 100, no. 12, pp. 7129–7134, 2003, doi: 10.1073/pnas.1232341100.

- [53] T. Bohnenpoll *et al.*, “A SHH-FOXF1-BMP4 signaling axis regulating growth and differentiation of epithelial and mesenchymal tissues in ureter development,” *PLoS Genet.*, vol. 13, no. 8, pp. 1–28, 2017, doi: 10.1371/journal.pgen.1006951.
- [54] R. Airik, M. Bussen, M. K. Singh, M. Petry, and A. Kispert, “Tbx18 regulates the development of the ureteral mesenchyme,” *J. Clin. Invest.*, 2006, doi: 10.1172/JCI26027.
- [55] E. Martin *et al.*, “TSHZ3 and SOX9 Regulate the Timing of Smooth Muscle Cell Differentiation in the Ureter by Reducing Myocardin Activity,” *PLoS One*, 2013, doi: 10.1371/journal.pone.0063721.
- [56] Y. Aoki *et al.*, “Id2 haploinsufficiency in mice leads to congenital hydronephrosis resembling that in humans,” *Genes to Cells*, vol. 9, no. 12, pp. 1287–1296, 2004, doi: 10.1111/j.1365-2443.2004.00805.x.
- [57] M. Tremblay, O. Sanchez-Ferras, and M. Bouchard, “Gata transcription factors in development and disease,” *Dev.*, vol. 145, no. 20, 2018, doi: 10.1242/dev.164384.
- [58] M. Khandekar, N. Suzuki, J. Lewton, M. Yamamoto, and J. D. Engel, “Multiple, Distant Gata2 Enhancers Specify Temporally and Tissue-Specific Patterning in the Developing Urogenital System,” *Mol. Cell. Biol.*, vol. 24, no. 23, pp. 10263–10276, 2004, doi: 10.1128/mcb.24.23.10263-10276.2004.
- [59] L. Yu *et al.*, “GATA2 Regulates Body Water Homeostasis through Maintaining Aquaporin 2 Expression in Renal Collecting Ducts,” *Mol. Cell. Biol.*, vol. 34, no. 11, pp. 1929–1941, 2014, doi: 10.1128/mcb.01659-13.
- [60] F. Y. Tsai *et al.*, “An early haematopoietic defect in mice lacking the transcription factor GATA-2,” *Nature*, vol. 371, no. 6494, pp. 221–226, 1994, doi: 10.1038/371221a0.
- [61] Y. Zhou *et al.*, “Rescue of the embryonic lethal hematopoietic defect reveals a critical role for GATA-2 in urogenital development,” *EMBO J.*, vol. 17, no. 22, pp. 6689–6700, 1998, doi: 10.1093/emboj/17.22.6689.
- [62] T. Hoshino *et al.*, “Reduced BMP4 abundance in Gata2 hypomorphic mutant mice result in uropathies resembling human CAKUT,” *Genes to Cells*, vol. 13, no. 2, pp. 159–170, 2008, doi: 10.1111/j.1365-2443.2007.01158.x.
- [63] K. Ainoya *et al.*, “UG4 Enhancer-Driven GATA-2 and Bone Morphogenetic Protein 4 Complementation Remedies the CAKUT Phenotype in Gata2 Hypomorphic Mutant Mice,” *Mol. Cell. Biol.*, vol. 32, no. 12, pp. 2312–2322, 2012, doi: 10.1128/mcb.06699-11.
- [64] E. E. Morrissey *et al.*, “GATA6 regulates HNF4 and is required for differentiation of visceral endoderm in the mouse embryo,” *Genes Dev.*, vol. 12, no. 22, pp. 3579–3590, 1998, doi: 10.1101/gad.12.22.3579.
- [65] M. Koutsourakis, A. Langeveld, R. Patient, R. Beddington, and F. Grosveld, “The transcription factor GATA6 is essential for early extraembryonic development,” *Development*, vol. 126, no. 4, pp. 723–732, 1999.
- [66] E. E. Morrissey, H. S. Ip, M. M. Lu, and M. S. Parmacek, “GATA-6: A Zinc Finger Transcription Factor That Is Expressed in Multiple Cell Lineages

- Derived from Lateral Mesoderm," *Dev. Biol.*, vol. 177, no. 0165, pp. 309–322, 1996.
- [67] E. Suzuki *et al.*, "The Human GATA-6 Gene: Structure, Chromosomal Location, and Regulation of Expression by Tissue-Specific and Mitogen-Responsive Signals," *Genomics*, vol. 38, pp. 283–290, 1996.
- [68] H. Perlman, E. Suzuki, M. Simonson, R. C. Smith, and K. Walsh, "GATA-6 Induces p21 Cip1 Expression and G 1 Cell Cycle Arrest\*."
- [69] F. Yin and B. P. Herring, "GATA-6 can act as a positive or negative regulator of smooth muscle-specific gene expression," *J. Biol. Chem.*, 2005, doi: 10.1074/jbc.M411585200.
- [70] M. Losa *et al.*, "A tissue-specific, Gata6-driven transcriptional program instructs remodeling of the mature arterial tree," *Elife*, vol. 6, pp. 1–22, 2017, doi: 10.7554/eLife.31362.
- [71] A. Kanematsu, A. Ramachandran, and R. M. Adam, "GATA-6 mediates human bladder smooth muscle differentiation: involvement of a novel enhancer element in regulating -smooth muscle actin gene expression," *AJP Cell Physiol.*, 2007, doi: 10.1152/ajpcell.00225.2007.
- [72] S. Kiiveri *et al.*, "Differential expression of GATA-4 and GATA-6 in fetal and adult mouse and human adrenal tissue," *Endocrinology*, vol. 143, no. 8, pp. 3136–3143, 2002, doi: 10.1210/endo.143.8.8939.
- [73] M. Pihlajoki *et al.*, "Conditional mutagenesis of Gata6 in SF1-positive cells causes gonadal-like differentiation in the adrenal cortex of mice," *Endocrinology*, vol. 154, no. 5, pp. 1754–1767, 2013, doi: 10.1210/en.2012-1892.
- [74] R. Kopan and M. X. G. Ilagan, "The Canonical Notch Signaling Pathway: Unfolding the Activation Mechanism," *Cell*, vol. 137, no. 2, pp. 216–233, 2009, doi: 10.1016/j.cell.2009.03.045.
- [75] W. R. Gordon *et al.*, "Mechanical Allosterity: Evidence for a Force Requirement in the Proteolytic Activation of Notch," *Dev. Cell*, vol. 33, no. 6, pp. 729–736, 2015, doi: 10.1016/j.devcel.2015.05.004.
- [76] K. Tiyanont, T. E. Wales, M. Aste-Amezaga, J. C. Aster, J. R. Engen, and S. C. Blacklow, "Evidence for increased exposure of the notch1 metalloprotease cleavage site upon conversion to an activated conformation," *Structure*, vol. 19, no. 4, pp. 546–554, 2011, doi: 10.1016/j.str.2011.01.016.
- [77] J. S. Mumm *et al.*, "A ligand-induced extracellular cleavage regulates  $\gamma$ -secretase-like proteolytic activation of Notch1," *Mol. Cell*, vol. 5, no. 2, pp. 197–206, 2000, doi: 10.1016/S1097-2765(00)80416-5.
- [78] G. Struhl and A. Adachi, "Requirements for Presenilin-dependent cleavage of notch and other transmembrane proteins," *Mol. Cell*, vol. 6, no. 3, pp. 625–636, 2000, doi: 10.1016/S1097-2765(00)00061-7.
- [79] G. Struhl and A. Adachi, "Nuclear access and action of Notch in vivo," *Cell*, vol. 93, no. 4, pp. 649–660, 1998, doi: 10.1016/S0092-8674(00)81193-9.
- [80] Y. Sasai, R. Kageyama, Y. Tagawa, R. Shigemoto, and S. Nakanishi, "Two



- mammalian helix-loop-helix factors structurally related to *Drosophila* hairy and Enhancer of split,” *Genes Dev.*, vol. 6, no. 12 B, pp. 2620–2634, 1992, doi: 10.1101/gad.6.12b.2620.
- [81] T. Gridley, “Notch signaling in vascular development and physiology,” *Development*, vol. 134, no. 15, pp. 2709–2718, 2007, doi: 10.1242/dev.004184.
- [82] H. Liu, S. Kennard, and B. Lilly, “NOTCH3 expression is induced in mural cells through an autoregulatory loop that requires Endothelial-expressed JAGGED1,” *Circ. Res.*, vol. 104, no. 4, pp. 466–475, 2009, doi: 10.1161/CIRCRESAHA.108.184846.
- [83] F. A. High, M. L. Min, W. S. Pear, K. M. Loomes, K. H. Kaestner, and J. A. Epstein, “Endothelial expression of the Notch ligand Jagged1 is required for vascular smooth muscle development,” *Proc. Natl. Acad. Sci. U. S. A.*, vol. 105, no. 6, pp. 1955–1959, 2008, doi: 10.1073/pnas.0709663105.
- [84] P. Varadkar, M. Kraman, D. Despres, G. Ma, J. Lozier, and B. McCright, “Notch2 is required for the proliferation of cardiac neural crest-derived smooth muscle cells,” *Dev. Dyn.*, vol. 237, no. 4, pp. 1144–1152, 2008, doi: 10.1002/dvdy.21502.
- [85] X. Feng, L. T. Krebs, and T. Gridley, “Patent ductus arteriosus in mice with smooth muscle-specific Jag1 deletion,” *Development*, vol. 137, no. 24, pp. 4191–4199, 2010, doi: 10.1242/dev.052043.
- [86] M. Monet *et al.*, “The archetypal R90C CADASIL-NOTCH3 mutation retains NOTCH3 function in vivo,” *Hum. Mol. Genet.*, vol. 16, no. 8, pp. 982–992, 2007, doi: 10.1093/hmg/ddm042.
- [87] N. Boulos *et al.*, “Notch3 is essential for regulation of the renal vascular tone,” *Hypertension*, vol. 57, no. 6, pp. 1176–1182, 2011, doi: 10.1161/HYPERTENSIONAHA.111.170746.
- [88] K. Kurpinski *et al.*, “Transforming growth factor- $\beta$  and notch signaling mediate stem cell differentiation into smooth muscle cells,” *Stem Cells*, vol. 28, no. 4, pp. 734–742, 2010, doi: 10.1002/stem.319.
- [89] T. Grieskamp, C. Rudat, T. H. W. Lüdtkke, J. Norden, and A. Kispert, “Notch signaling regulates smooth muscle differentiation of epicardium-derived cells,” *Circ. Res.*, vol. 108, no. 7, pp. 813–823, 2011, doi: 10.1161/CIRCRESAHA.110.228809.
- [90] S. Jin *et al.*, “Notch signaling regulates platelet-derived growth factor receptor- $\beta$  expression in vascular smooth muscle cells,” *Circ. Res.*, vol. 102, no. 12, pp. 1483–1491, 2008, doi: 10.1161/CIRCRESAHA.107.167965.
- [91] Y. Tang *et al.*, “Notch and transforming growth factor- $\beta$ (TGF $\beta$ ) signaling pathways cooperatively regulate vascular smooth muscle cell differentiation,” *J. Biol. Chem.*, vol. 285, no. 23, pp. 17556–17563, 2010, doi: 10.1074/jbc.M109.076414.
- [92] R. Airik *et al.*, “Hydronephrosis due to loss of Sox9-regulated smooth muscle cell differentiation of the ureteric mesenchyme,” *Hum. Mol. Genet.*, 2010, doi: 10.1093/hmg/ddq426.

- [93] A. Sharma *et al.*, “GATA6 mutations in hiPSCs inform mechanisms for maldevelopment of the heart, pancreas, and diaphragm,” *Elife*, vol. 9, pp. 1–28, 2020, doi: 10.7554/eLife.53278.
- [94] J. Buenrostro, B. Wu, H. Chang, and W. Greenleaf, “ATAC-seq method,” *Curr. Protoc. Mol. Biol.*, vol. 2015, pp. 1–10, 2016, doi: 10.1002/0471142727.mb2129s109.ATAC-seq.
- [95] T. A. Hedge and I. Mason, “Expression of Shisa2, a modulator of both Wnt and Fgf signaling, in the chick embryo,” *Int. J. Dev. Biol.*, vol. 52, no. 1, pp. 81–85, 2008, doi: 10.1387/ijdb.072355th.
- [96] E. M. Walker, C. A. Thompson, and M. A. Battle, “GATA4 and GATA6 regulate intestinal epithelial cytodifferentiation during development,” *Dev. Biol.*, vol. 392, no. 2, pp. 283–294, 2014, doi: 10.1016/j.ydbio.2014.05.017.
- [97] I. Jovanovic *et al.*, “Transcriptome-driven integrative exploration of functional state of ureter tissue affected by CAKUT,” *Life Sci.*, vol. 212, no. September, pp. 1–8, 2018, doi: 10.1016/j.lfs.2018.09.042.

## Appendix

The appendix contains the license agreement for the copyright protected material used in this work.

### JOHN WILEY AND SONS LICENSE TERMS AND CONDITIONS

May 21, 2021

This Agreement between Jennifer Kurz ("You") and John Wiley and Sons ("John Wiley and Sons") consists of your license details and the terms and conditions provided by John Wiley and Sons and Copyright Clearance Center.

License Number	5071320891102
License date	May 17, 2021
Licensed Content Publisher	John Wiley and Sons
Licensed Content Publication	Wiley Books
Licensed Content Date	Dec 31, 1969
Licensed Content Volume	248
Licensed Content Issue	4
Licensed Content Pages	12
Type of use	Dissertation/Thesis
Requestor type	Author of this Wiley article
Format	Print
Portion	Full article
Will you be translating?	No
Title	Transcriptional regulation of smooth muscle cell differentiation in the murine ureter
Institution name	Medizinische Hochschule Hannover
Expected presentation date	May 2021
Requestor Location	Jennifer Kurz Vahrenheider Markt 2 Hannover, 30179 Germany Attn: Jennifer Kurz
Publisher Tax ID	EU826007151
Total	0.00 USD

## Acknowledgement

First and foremost, I want to thank Prof. Dr. Andreas Kispert for giving me the opportunity to work in his lab and providing me with this challenging projects. Also for the helpful discussions, the critical feedback and his kind support during the time of my thesis, also during hard times.

I also want to thank Prof. Dr. Hansjörg Küster for accepting the duty as chair of my disputation and Prof. Dr. Ngezahayo for taking over the duty as chair of my disputation on very short notice. Prof. Dr. Gerardy-Schahn I want to thank for her kind acceptance to be referee of my dissertation and for providing me lab space and a nice work environment after the water damage in my institute.

I would like to thank Prof. Dr. Achim Gossler, the head of the IFM, for proving nice environment in the institute to work and for giving his best for us after the water damage.

Thank you to all past and present lab members for helpful discussions, support, fantastic team-work, nice lunchtimes and conversations. Especially, I want to thank Dr. Timo Lüdtke for supervising me in the very beginning and introducing me into the lab work and Dr. Anna-Carina Weiss for the supervision and introduction into the ureter methods.

I also want to thank the members from the department of clinical biochemistry for their nice welcome, help and support during my time in worked there after the water damage.

Finally, I would like to thank my parents, my brother and Tobias for their constant support and for cheering and backing me up, especially during bad times. Without them, this work would not have been possible.

## Curriculum vitae

### Personal information

Name: Jennifer Kurz  
Date of birth: 24.04.1989  
Place of birth: Schwäbisch Hall  
Citizenship: German  
Email: kurz.jennifer@mh-hannover.de; kurz.jenny89@gmail.com

### School education

1996-2000 Grundschule (GHRs), Obersontheim  
2000-2005 Realschule, Bühlertann  
2005-2008 Sibilla-Egen-Schule, Berufliches Gymnasium mit biotechnologischer Richtung, Schwäbisch Hall

### University studies

2008-2011 Undergraduate studies (B.Sc.) in Biology at the Karlsruhe Institute of Technology  
Bachelor's degree thesis at the ITG at the KIT under the supervision of Dr. Clemens Grabher:  
„Identification and Characterization of Molecular Markers for Leukocyte Subpopulations in Zebrafish“

2011-2014 Graduate studies (M.Sc.) in Biology at the Karlsruhe Institute of Technology  
Master's degree thesis at the Institute for Toxicology und Genetics (ITG) at the Karlsruhe Institute of Technology (KIT) under the supervision of Dr. Steffen Scholpp:  
„Regulation of Wnt-Signaling by Frizzled-Endocytosis in Zebrafish Embryogenesis“

### Professional activity

2014-2015 Temporary employment as waitress at event service:  
„Hubers-Veranstaltungsservice“

**Language skills** English: fluent (written and spoken)  
French: basic knowledge



## List of publications

Weiss, Anna Carina, Tobias Bohnenpoll, **Jennifer Kurz**, Patrick Blank, Rannar Airik, Timo H. Lüdtkke, Marc Jens Kleppa, et al. 2019. "Delayed Onset of Smooth Muscle Cell Differentiation Leads to Hydroureter Formation in Mice with Conditional Loss of the Zinc Finger Transcription Factor Gene *Gata2* in the Ureteric Mesenchyme." *Journal of Pathology* 248 (4). John Wiley and Sons Ltd: 452–63. doi:10.1002/path.5270.

Lüdtkke, Timo H., Carsten Rudat, **Jennifer Kurz**, Regine Häfner, Franziska Greulich, Irina Wojahn, Nurullah Aydoğdu, et al. 2019. "Mesothelial Mobilization in the Developing Lung and Heart Differs in Timing, Quantity, and Pathway Dependency." *American Journal of Physiology - Lung Cellular and Molecular Physiology* 316 (5). American Physiological Society: L767–83. doi:10.1152/ajplung.00212.2018.

Lüdtkke, Timo H., Carsten Rudat, Irina Wojahn, Anna Carina Weiss, Marc Jens Kleppa, **Jennifer Kurz**, Henner F. Farin, Anne Moon, Vincent M. Christoffels, and Andreas Kispert. 2016. "Tbx2 and Tbx3 Act Downstream of Shh to Maintain Canonical Wnt Signaling during Branching Morphogenesis of the Murine Lung." *Developmental Cell* 39 (2). Cell Press: 239–53. doi:10.1016/j.devcel.2016.08.007.

Hagemann, Anja I.H., **Jennifer Kurz**, Silke Kauffeld, Qing Chen, Patrick M. Reeves, Sabrina Weber, Simone Schindler, Gary Davidson, Tomas Kirchhausen, and Steffen Scholpp. 2014. "Correction to In Vivo Analysis of Formation and Endocytosis of the Wnt/ $\beta$ -Catenin Signaling Complex in Zebrafish Embryos [J. Cell Sci. 127, (2014) 3970-3982]." *Journal of Cell Science*. Company of Biologists Ltd. doi:10.1242/jcs.165704.